

Auckland's Exposure to Coastal Inundation by Storm-tides and Waves

December 2020

Technical Report 2020/024



Auckland's exposure to coastal inundation by storm-tides and waves

December 2020

Auckland Council technical report

TR2020/024

ISSN 2230-4525 (Print)

ISSN 2230-4533 (Online)

ISBN 978-1-99-002280-7 (Print)

ISBN 978-1-99-002281-4 (PDF)

Reviewed and recommended for publication by:

Name: Branko Veljanovski

Position: Head of Engineering Design & Asset Management

Approved for publication by:

Name: Sarah Sinclair

Position: Chief Engineer

Recommended citation:

Roberts, R., N Carpenter and P Klinac (2020). Auckland's exposure to coastal inundation by storm-tides and waves. Auckland Council technical report, TR2020/24

© 2020 Auckland Council

Auckland Council disclaims any liability whatsoever in connection with any action taken in reliance of this document for any error, deficiency, flaw or omission contained in it.

This document is licensed for re-use under the [Creative Commons Attribution 4.0 International licence](https://creativecommons.org/licenses/by/4.0/).

In summary, you are free to copy, distribute and adapt the material, as long as you attribute it to Auckland Council and abide by the other licence terms.

Acknowledgements

This document was prepared with technical input from Auckland Council and industry experts including, but not limited to, the following individuals:

Authors (Overview)

Natasha Carpenter, Ross Roberts, Paul Klinac (Auckland Council)

Authors / Contributors (Part 1, NIWA)

Scott Stephens, Sanjay Wadhwa, Richard Gorman, Nigel Goodhue, Mark Pritchard, Ron Ovenden, Glen Reeve

Authors / Contributors (Part 2, NIWA)

Scott Stephens, Sanjay Wadhwa

Authors / Contributors (Part 3, NIWA)

Michael Allis, Richard Gorman, Scott Stephens, Ron Ovenden, Chris Eager

Authors / Contributors (Part 4, DHI)

DHI Water and Environmental

Editor

Ross Roberts (Auckland Council)

Peer Reviewers

Nick Brown (Healthy Waters, Auckland Council)

Auckland Council Overview

Table of contents

| | | |
|------------|---|----------|
| 1.0 | Introduction | 1 |
| 1.1 | Background..... | 1 |
| 1.2 | Purpose..... | 1 |
| 2.0 | Reports | 2 |
| 2.1 | Part 1: NIWA (2013) | 2 |
| 2.2 | Part 2: Small East Coast Estuaries Update (NIWA, 2016)..... | 3 |
| 2.3 | Part 3: Addition of Great Barrier and Little Barrier Islands (NIWA, 2019) | 3 |
| 2.4 | Part 4: Kaipara Harbour: Parakai/Helensville (DHI, 2020) | 4 |
| 3.0 | How this data is being used | 5 |
| 3.1 | Extreme water levels and habitable floor calculations..... | 5 |
| 3.2 | Update of Inundation Mapping on GeoMaps..... | 6 |

Part 1: Coastal inundation by storm tides and waves in the Auckland region, NIWA 2013

Part 2: Coastal-storm inundation in the Auckland region, supplementary information: Updated coastal-storm exposure at Parakai and re-mapping of East Coast estuaries, NIWA 2016

Part 3: Coastal Inundation levels by storm-tides and waves at Great Barrier Islands, NIWA 2019

Part 4: Technical Report: Parakai/Helensville Coastal Flood Inundation, DHI 2020

1.0 Introduction

1.1 Background

Bounded on the east by the South Pacific Ocean and on the west by the Tasman Sea, Auckland has 3,200 km of dynamic coastline that includes three major harbours. As well as a long and diverse coastline, Auckland has the largest population density to coastline ratio in New Zealand which means that the city has a high exposure to coastal hazards including coastal inundation.

Coastal inundation is the flooding of normally dry, low-lying coastal land due to extreme high water levels. Extreme sea levels can result from several processes including astronomical tides, monthly mean sea level anomalies, and storm-surge. In areas of open coast, waves during certain conditions can also raise the effective sea level.

Coastal inundation is a natural process which becomes a hazard when valuable assets, such as houses and infrastructure, are flooded. The risk from inundation is increasing over time because of climate change induced sea-level rise and because of increasing development in low-lying coastal areas. Under the Resource Management Act and NZ Coastal Policy Statement (2010), Auckland Council is tasked with identifying and managing this hazard. The Auckland Unitary Plan (Chapter E36, Activity Control A12), which sets out controls on land-use in the Auckland region, also contains specific requirements for developments located within the flooding zone for a 1-in-100 year plus 1 m sea level rise inundation event.

1.2 Purpose

Auckland Council has commissioned a series of studies focusing on understanding extreme high-water values across the region along the city's coastline to provide:

- A better understanding of the potential extent of coastal flooding and the risk extreme events pose to Auckland
- Data to inform the calculation of appropriate habitable floor levels for developments within the inundation zone
- Data to inform coastal asset management including renewals, replacements, or potential relocations.

2.0 Reports

This technical report collates four separate pieces of work, completed between 2013, 2019, 2020 which are included as Parts 1, 2, 3, and 4. This Auckland Council Overview provides context for each of the studies commissioned and gives detail on how this information is used.

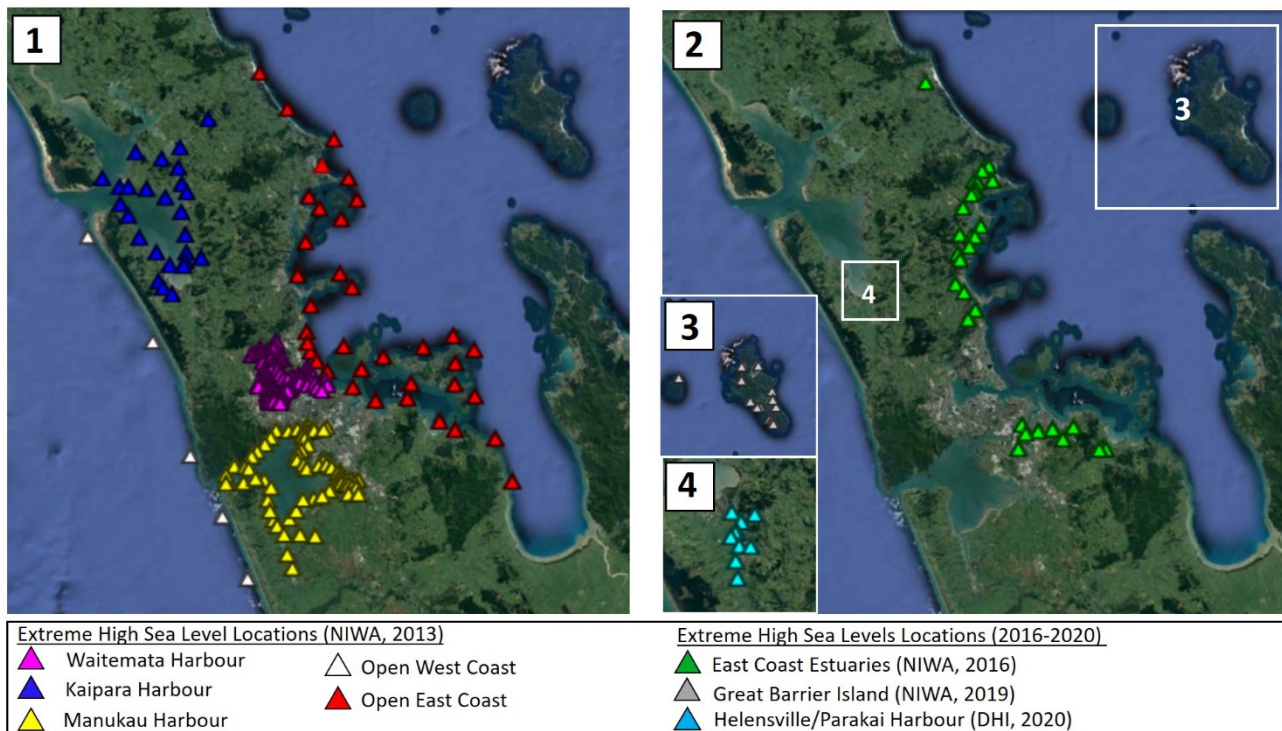


Figure 1: Locations of calculated extreme high-water values

1) Harbours and open coasts (Part 1, NIWA 2013); 2) East Coast estuaries (Part 2, NIWA 2016); 3) Helensville/Parakai area (Part 3, DHI 2020); and Great Barrier Island (Part 4, NIWA, 2019)

2.1 Part 1: NIWA (2013)

In 2013, Auckland Council's Civil Defence & Emergency Management Department commissioned NIWA to calculate and model coastal-storm inundation elevations for the entire Auckland region, primarily for emergency management purposes. This work identified areas that could potentially be affected by coastal hazards, as required by the New Zealand Coastal Policy Statement (2010), and provided an appropriate, region-wide, consistent basis for delineating areas exposed to both present-day and future coastal storm inundation.

NIWA calculated extreme high-water level values at fixed locations across the region (see Figure 1) using data from tide gauges (which capture detailed information on tide levels), monthly mean sea level anomalies, and historical storm surge heights. Where tide gauge information was not available, hydrodynamic models were created for specific areas to simulate tides, storm surge, and wave set-up. For Auckland's harbours (i.e. Waitemata, Manukau and Kaipara), both tide gauge data and hydrodynamic models were used to determine potential extreme sea levels.

Predicted flood areas were then mapped using the static level (otherwise known as the 'bathtub') inundation mapping technique; whereby all land lying below the calculated extreme water level (with a direct flow path to the coast) is assumed to be flooded in its entirety. For this modelling, NIWA mapped a series of scenarios at average recurrence intervals (ARI) of 1, 2, 5, 10, 20, 50 and 100-years excluding climate change effects. As sea levels are increasing due to climate change, they included additional scenarios adding 1 m and 2 m sea level rise to the 50 and 100-year scenarios.

Results of the inundation modelling were presented in GIS format on Auckland Council GeoMaps. The dataset provided a high-level yes/no approach to whether a property would be likely to be flooded during a 100-year ARI event. If a location fell within a "wetted" area (indicated as coverage by blue water in GIS), it was expected to experience flooding and was therefore subject to development controls specified in the Auckland Unitary Plan.

2.2 Part 2: Small East Coast Estuaries Update (NIWA, 2016)

Modelling extreme high-water values within estuaries is complex. The 2013 modelling assumed that wave setup elevations (the increase in mean water level due to the influence of waves) at estuary mouths could travel throughout the estuary. However, this assumption was later revised based on feedback from the Unitary Plan submission process. Mean high sea-level values for the East Coast estuaries (Figure 1) were recalculated without wave-setup, and the 'GeoMaps' inundation layer was updated accordingly. These updates are detailed in Part 2 of this report.

2.3 Part 3: Addition of Great Barrier and Little Barrier Islands (NIWA, 2019)

Great Barrier Island – Aotea and Little Barrier Island were not included in the original regional study (Part 1) as appropriate datasets were not available to accurately map coastal inundation extents at the time. In 2019, an additional study was commissioned utilising Auckland Council's 2016-2018 LiDAR dataset and supported by the provision of additional field data. The methodology and results of this study are presented in Part 4 of this Technical Report.

Taking the approach of the original Regional Report (Part 1), extreme sea level elevations for Great Barrier and Little Barrier were calculated for 16 on-shore sites (see Figure 1) at ARI scenarios of 1, 2, 5, 10, 20, 50 and 100 years.

2.4 Part 4: Kaipara Harbour: Parakai/Helensville (DHI, 2020)

Static inundation mapping provides an appropriate, region-wide and consistent basis for delineating areas exposed to both present-day and future coastal storm inundation. However, the technique is conservative and does not fully capture the dynamic and time-variant processes that occur during a coastal-storm event along some of Auckland's coasts such as the Parakai/Helensville area to the south of the Kaipara Harbour.

At this location, potential inundation is particularly complex due to the wide, low lying coastal plains sitting above the confluence of the Kaipara river within the harbour. Using new tide gauge information for Helensville, a site-specific hydrodynamic model was developed in 2016 to represent the more complex flood processes in this area in more detail. In the model, coastal inundation areas were considered independent of the presence of fixed structures such as stopbanks because of their dynamic nature and potential to change over time. In 2020, the model was updated to incorporate Auckland Council's 2016-2018 LiDAR dataset.

Part 4 of this Technical Report presents the updated extreme sea level values for the area (see Figure 1 for locations).

3.0 How this data is being used

3.1 Extreme water levels and habitable floor calculations

For properties located within the 1% Annual Exceedance Probability (100-year ARI) Coastal Inundation Zone plus 1 m of sea-level rise, the Auckland Unitary Plan specifies that habitable floor levels must be above the 1% AEP plus 1 m sea level rise.

A freeboard allowance is added to the calculated flood level to result in a minimum ground and/or floor level to account for any uncertainties associated with historical data and hydraulic assessments.

To calculate habitable floor levels, freeboard plus 1 m (representing sea level rise) is added to the nearest high sea level value. High sea level values vary by area, with the open coast values including wave-set up heights, and are split across the 2013, 2016, and 2019 reports as detailed in Section 2 and Table 1.

Table 1: Location of calculated high-water level values across all four reports, broken down by area.

| Report Part | Area | Table containing extreme sea level values | Includes wave set-up? | Includes sea level rise? |
|-----------------------|--|---|-----------------------|--------------------------|
| Part 1 (NIWA 2013) | Waitemata Harbour | Part 1 Table 3-3 | No | No |
| | Manukau Harbour | Part 1 Table 3-6 | No | No |
| | Kaipara Harbour (<i>one data point superseded by Part 4</i>) | Part 1 Table 3-9 | No | No |
| | Open East Coast | Part 1 Table 4-3 | Yes | No |
| | Open West Coast | Part 1 Table 4-7 | Yes | No |
| Part 2 (NIWA 2016) | East Coast Estuaries | Part 2 Table 3-2 | No | No |
| Part 3 (NIWA 2019) | Great Barrier and Little Barrier Island | Part 3 Table 3-1 | Yes | No |
| Part 4 (DHI 2020) | Parakai/Helensville | Part 4 Table 6-1 | No | Yes |

3.2 Update of Inundation Mapping on GeoMaps

Due to the addition of new and updated high sea level values and the availability of region-wide LiDAR, the inundation zone was remapped in 2020. The updated inundation map supersedes the previous modelling and is available on GeoMaps.



Part 1: Coastal inundation by storm-
tides and waves in the Auckland region,
NIWA 2013





Coastal inundation by storm-tides and waves in the Auckland region

Prepared for Auckland Council

September 2013

Authors / Contributors

Scott Stephens
Sanjay Wadhwa
Richard Gorman
Nigel Goodhue
Mark Pritchard
Ron Ovenden
Glen Reeve

For any information regarding this report please contact:

Scott Stephens
Coastal Scientist
Coastal and Estuarine Processes Group
+64-7-856 7026
scott.stephens@niwa.co.nz

National Institute of Water & Atmospheric Research Ltd

Gate 10, Silverdale Road
Hillcrest, Hamilton 3216
PO Box 11115, Hillcrest
Hamilton 3251
New Zealand
Phone: +64 7 856 7026
Fax +64-7-856 0151

NIWA Client Report No: HAM2013-059
Report date: September 2013
NIWA Project: ARC13216

© All rights reserved. This publication may not be reproduced or copied in any form without the permission of the copyright owner(s). Such permission is only to be given in accordance with the terms of the client's contract with NIWA. This copyright extends to all forms of copying and any storage of material in any kind of information retrieval system.

Whilst NIWA has used all reasonable endeavours to ensure that the information contained in this document is accurate, NIWA does not give any express or implied warranty as to the completeness of the information contained herein, or that it will be suitable for any purpose(s) other than those specifically contemplated during the Project or agreed by NIWA and the Client.

Table of Contents

| | |
|--|-----|
| Technical summary..... | 8 |
| 1 Introduction and project scope..... | 9 |
| 2 How inundation areas were calculated and mapped..... | 12 |
| 3 Extreme sea levels in the Waitemata, Manukau and Kaipara Harbours..... | 22 |
| 4 Extreme sea-level elevations from storm-tides and waves on the open coasts of the Auckland region..... | 55 |
| 5 Glossary of abbreviations and terms..... | 82 |
| 6 References..... | 85 |
| Appendix A – How extreme sea-levels were calculated – details..... | 89 |
| Appendix B – Mapping inundation areas..... | 105 |

Figures

| | |
|--|----|
| Figure 2-1: Schematic illustrating the various processes that contribute to coastal inundation. | 15 |
| Figure 3-1: Ports of Auckland hourly sea-level record 26 Oct 1903 – 31 May 2012..... | 23 |
| Figure 3-3: Decomposed Ports of Auckland Ltd tide-gauge sea-level record, 26 July 2008 storm surge. | 23 |
| Figure 3-5: Waitemata Harbour MIKE-3 FM hydrodynamic model grid (Oldman et al. 2007). | 27 |
| Figure 3-6: Locations of extreme storm-tide predictions in the Waitemata Harbour. | 28 |
| Figure 3-7: Simulated extreme storm-tide frequency-magnitude distributions in the Waitemata Harbour. | 29 |
| Figure 3-8: Storm-tide elevations in the Waitemata Harbour, simulated for 23 January 2011 storm-tide..... | 30 |
| Figure 3-9: Elevation difference (cm) between 23 January 2011 storm-tide simulations and 100-year ARI estimates in the Waitemata Harbour. | 31 |
| Figure 3-10: Onehunga sea-level record used for this study..... | 36 |
| Figure 3-11: Hydrodynamic model MIKE3FM flexible mesh grid of the Manukau Harbour. | 37 |
| Figure 3-12: Hydrodynamic model bathymetry, with output locations marked. | 37 |
| Figure 3-13: Extreme sea-level frequency–magnitude distribution at the Onehunga tide gauge in the Manukau Harbour. . | 39 |
| Figure 3-14: Extreme sea-level frequency–magnitude distribution at selected locations in the Manukau Harbour. | 40 |
| Figure 3-15: Locations of extreme sea-level calculations in the Manukau Harbour. | 41 |
| Figure 3-16: Pouto Point sea-level record 2001-2012. | 45 |
| Figure 3-17: Aerial photo of the Kaipara Harbour and tidal inlet with Delft3d model grid overlaid..... | 46 |
| Figure 3-18: Location of sea-level records and bathymetry collection (black lines) in 2011 for hydrodynamic model calibration..... | 47 |
| Figure 3-19: Reconstructed wind time-series used for modelling of wind-driven storm surge in the Kaipara Harbour..... | 48 |
| Figure 3-20: Rose plot of reconstructed wind series used for modelling of wind-driven storm surge in the Kaipara Harbour. | 49 |
| Figure 3-21: Locations of storm-tide model output from the central and southern Kaipara Harbour. | 50 |
| Figure 3-22: Predicted tide at Pouto Point and Kaipara River entrance..... | 50 |
| Figure 3-23: Kaipara mean sea-level pressure record and calculated inverse-barometer sea level. | 51 |
| Figure 3-24: Extreme sea-level curves for Pouto Point tide-gauge. | 52 |
| Figure 4-1: Locations of storm-tide and wave simulation output along the east open coast of the Auckland region. | 55 |
| Figure 4-2: Time-series of storm surge at Port of Auckland from tide gauge and WASP model. | 56 |
| Figure 4-3: Scatter plot of measured (tide gauge) and modelled (WASP) storm surge at Port of Auckland (Waitemata), with quantile-quantile comparison. | 57 |
| Figure 4-4: Distribution of extreme appendon the open-coast of the Auckland region. | 57 |
| Figure 4-5: Outer and inner SWAN wave model grids of the Hauraki Gulf..... | 60 |
| Figure 4-6: Comparison of significant wave height (H_{m0}) values predicted by the outer Hauraki Gulf SWAN model with measurements from the Mokohinau Islands Waverider buoy..... | 62 |
| Figure 4-7: Comparison of peak wave period (T_{peak}) values predicted by the outer Hauraki Gulf SWAN model with measurements from the Mokohinau Islands Waverider buoy..... | 63 |
| Figure 4-8: Comparison of peak wave direction (θ_{peak}) values predicted by the outer Hauraki Gulf SWAN model with measurements from the Mokohinau Islands Waverider buoy..... | 63 |
| Figure 4-9: Comparison of significant wave height (H_{m0}) values predicted by the outer Hauraki Gulf SWAN model with measurements from the Mangawhai wave buoy. | 64 |
| Figure 4-10: Comparison of peak wave period (T_{peak}) values predicted by the outer Hauraki Gulf SWAN model with measurements from the Mangawhai wave buoy. | 64 |
| Figure 4-11: Comparison of peak wave direction (θ_{peak}) values predicted by the outer Hauraki Gulf SWAN model with measurements from the Mangawhai wave buoy. | 65 |

| | |
|--|-----|
| Figure 4-12: Distribution of extreme significant wave height on the eastern open-coast of the Auckland region. | 66 |
| Figure 4-13: 1% annual exceedance probability storm-tide plus wave setup elevations on the eastern open-coast. | 70 |
| Figure 4-14: Difference between 1% annual exceedance probability storm-tide plus wave setup and storm-tide-only elevations on the eastern open-coast. | 71 |
| Figure 4-15: Location of combined storm-tide plus wave setup elevation calculations along the western open-coast..... | 74 |
| Figure 4-16: Quantile-quantile comparison of storm surge derived from the Anawhata tide gauge and the WASP model. . | 75 |
| Figure 4-17: Quantile-quantile comparison of monthly mean sea-level anomaly derived from the Anawhata tide gauge and the WASP model. | 76 |
| Figure 4-18: Extreme storm-tide distributions at Anawhata. | 76 |
| Figure 4-19: Storm-tide frequency–magnitude distributions along western open-coast. | 77 |
| Figure 4-20: Comparison of significant wave height values predicted by the WASP rcm_9_era model with measurements from the Taharoa wave buoy. | 78 |
| Figure 4-21: Comparison of significant wave height values predicted by the WASP rcm_9_era model with measurements off Mangonui Bluff, near Hokianga Harbour..... | 79 |
| Figure 4-22: Extreme significant wave height (m) along the western open-coast at the 5 sites. | 79 |
| Figure 7-1: Joint-probability of storm-tide and significant wave height at Mangawhai Beach. | 96 |
| Figure 7-2: Pakiri Beach profiles, at site P6. | 103 |
| Figure 7-3: Pakiri Beach profiles near the high-tide line; profile P6. | 103 |
| Figure 8-1: Map of the Auckland Region with 0.01 AEP storm-tide elevations marked at model-output locations..... | 106 |
| Figure 8-2: Map of the Auckland Region with interpolated elevations on the lines connecting model output locations, and elevations transferred from offshore lines to points along the coastline. | 107 |
| Figure 8-3: Map of Waitemata Harbour with interpolated elevation values on the simplified coastline. | 108 |
| Figure 8-4: Map of Auckland region with interpolated elevation values on simplified coastline. | 110 |
| Figure 8-5: 600,000 random points in the analysis area..... | 111 |
| Figure 8-6: Map of Auckland region with water surface for 0.01 AEP (100-year ARI) elevations..... | 112 |
| Figure 8-7: Inundation area from 0.01 AEP (100-year ARI) extreme sea-level scenario, including present-day +0.15 m mean sea-level offset to AVD-46, in Whangateau Harbour..... | 113 |
| Figure 8-8: Inundation area from 0.01 AEP (100-year ARI) extreme sea-level scenario, including present-day +0.15 m mean sea-level offset to AVD-46 + 2.0 m sea-level rise, in Whangateau Harbour..... | 114 |
| Figure 8-9: Verification of present-day 0.01 AEP (100-year ARI) storm-tide line against surveyed location of maximum flood incursion during 23 Jan 2011 storm-tide, at Kohimarama. | 116 |
| Figure 8-10: Verification of present-day 0.01 AEP (100-year ARI) storm-tide line against surveyed location of maximum flood incursion during 23 Jan 2011 storm-tide, at Half-Moon Bay. | 117 |
| Figure 8-11: Verification of present-day 0.01 AEP (100-year ARI) storm-tide line against surveyed location of maximum flood incursion during 23 Jan 2011 storm-tide, at St Heliers Bay. | 118 |
| Figure 8-12: Verification of present-day 0.01 AEP (100-year ARI) storm-tide line against surveyed location of maximum flood incursion during 23 Jan 2011 storm-tide, at St Heliers Bay (east). | 119 |
| Figure 8-13: Verification of present-day 0.01 AEP (100-year ARI) storm-tide line against surveyed location of maximum flood incursion during 23 Jan 2011 storm-tide, at St Marys Bay. | 120 |
| Figure 8-14: Verification of present-day 0.01 AEP (100-year ARI) storm-tide line against photograph of observed flooding on the north-western motorway during the 23 Jan 2011 storm-tide. | 121 |
| Figure 8-15: Verification of present-day 0.01 AEP (100-year ARI) storm-tide line against photograph of observed flooding on the Northern motorway during the 23 Jan 2011 storm-tide. | 122 |

Tables

| | |
|---|-----------|
| Table 1-1: Coastal extreme sea-level elevation and inundation map outputs. | 10 |
| Table 2-1: Sea-level gauges with known offsets to local vertical datum used in this study. | 17 |
| Table 2-2: Mean sea-level offsets to AVD-46 datum used in this study, at several locations in the Auckland region. | 18 |
| Figure 3-2: Decomposed Ports of Auckland Ltd tide-gauge sea-level record 2006–2011..... | 23 |
| Table 3-1: Ten largest sea-level annual maxima at Port of Auckland, in descending order. | 24 |
| Figure 3-4: Extreme sea-level curves using Port of Auckland tide-gauge data. | 25 |
| Table 3-2: Extreme sea-level at Port of Auckland tide-gauge. | 26 |
| Table 3-3: Extreme sea-level in the Waitemata Harbour. | 32 |
| Table 3-4: The seven largest storm-tide annual maxima since 1926 recorded at Onehunga..... | 39 |
| Table 3-5: Extreme sea-level at Onehunga. | 41 |
| Table 3-6: Extreme sea-level in the Manukau Harbour. | 42 |
| Table 3-7: Wind records used for Kaipara Harbour wind-driven storm surge modelling. | 48 |
| Table 3-8: Extreme sea-level at Pouto Point. | 53 |
| Table 3-9: Extreme sea-level in the Kaipara Harbour. | 53 |
| Table 4-1: Storm-tide elevations on the eastern open-coast. | 58 |
| Table 4-2: Extreme significant wave heights offshore from the eastern open coast at same sites as Table 4-1 and Figure 4-1. | 66 |
| Table 4-3: Maximum storm-tide plus wave setup elevations along the eastern open-coast..... | 68 |
| <i>Table 4-3: Maximum storm-tide plus wave setup elevations in small east-coast estuaries.</i> | <i>72</i> |
| Table 4-5: Storm-tide elevations along the western open-coast..... | 77 |
| Table 4-6: Extreme significant wave height (m) along the western open-coast..... | 80 |
| Table 4-7: Maximum storm-tide plus wave setup elevations along the western open-coast. | 80 |
| Table 4-8: Elevation difference (m) between storm-tide + wave setup and storm-tide-only along the western open-coast. | 81 |
| Table 7-1: Relationship between annual exceedance probability (AEP) and average recurrence interval (ARI). | 89 |
| Table 7-2: Likelihood of at least one exceedance event occurring within planning lifetimes. | 90 |
| Table 7-3: Average number of exceedances occurring within planning lifetimes, for event magnitudes with a specified probability of occurrence. | 91 |
| Table 7-4: Summary of extreme value techniques used here for estimating the probabilities of extreme still water levels. | 93 |
| Table 7-5: Representative beach profile slopes at MHWs elevation for Auckland east-coast beaches. | 102 |

Reviewed by



Dr Emily Lane

Approved for release by



Dr Rob Bell

Formatting checked by



Technical summary

Auckland Council commissioned NIWA in March 2013 to calculate extreme sea level elevations and their likelihood around the entire coastline of the Auckland region, and to map selected inundation areas.

Coastal extreme sea-level elevations resulting from storm-tides and wave setup were calculated for annual exceedance probabilities of 39%, 18%, 10%, 5%, 2%, 1% and 0.5% (corresponding to 2, 5, 10, 20, 50, 100 and 200-year average recurrence intervals, respectively). These extreme storm-generated sea levels are likely to persist for only short periods of 1–2 hours around the coincident high tide.

The study used hydrodynamic models calibrated against tide-gauge and wave buoy measurements to calculate storm-tide and wave setup along the coastline, and applied robust joint-probability modelling techniques to calculate the occurrence likelihood of the extreme sea-level elevations. The modelling was divided into the major harbours (Waitemata, Manukau and Kaipara), the beaches of the east and west coasts, and inside the small east-coast estuaries, according to geographical influences on models and the processes controlling extreme sea level.

The extreme sea-level elevations were spatially interpolated along the coastline, and intersected with a digital elevation model of the land surface produced from LiDAR, to produce maps of inundation associated with a subset of annual exceedance probabilities of 18%, 5%, 2% and 1% (5, 20, 50 and 100-year average recurrence intervals).

The inundation levels and inundation maps were calculated relative to Auckland Vertical Datum 1946 (AVD-46), and they include the present-day mean sea-level offset added to AVD-46 (e.g., +0.15 m at Auckland). Further inundation maps were produced for additional sea-level rise scenarios of +1 m and +2 m above present-day mean sea-level, added to the 1% annual exceedance probability elevation.

This report presents tables that include the coastal extreme sea-level elevations used to generate the coastal storm inundation maps, and presents the data, models and methods that were employed in the study.

1 Introduction and project scope

Coastal hazards are a significant issue within the Auckland region and Auckland Council is tasked with managing such hazards under the RMA and associated NZ Coastal Policy Statement (e.g., Policies 24–27). Coastal hazards include tsunamis, storm erosion and storm-tide inundation.

Added to these are the increasing effects of climate change and especially, the prospect of a projected rise in sea level of 0.5–0.8 m (or greater) by the 2090s (Ministry for the Environment 2008) or 0.7–1.0 m (or greater) in the next 100 years, by 2115 (Britton et al. 2011).

Auckland Council requires estimates of extreme sea level elevations and their likelihood around the whole coastline of the Auckland region that are well-founded on robust and defensible science. Auckland Council requested that the coastal inundation elevations be translated into inundation maps within a geographic information system (GIS) for some scenarios.

High storm-tides and large waves contribute to storm erosion and flooding on the open coast of the Auckland region. There are a number of meteorological and astronomical phenomena involved in the development of a combined extreme storm-tide and wave event, and these processes can combine in a number of ways to inundate low-lying coastal margins, or cause coastal erosion. Storm-tide is defined as the sea-level peak reached during a storm event, from a combination of monthly mean sea-level anomaly + tide + storm surge. Waves also further raise the effective storm-tide level at the coastline. Wave setup is the increase in the sea level within the surf zone from the release of wave energy. Flooding, from rivers, streams and stormwater, is another contributor to coastal inundation when the flood discharge is constrained inside narrower sections of estuaries. Flooding from rivers was not considered in this phase of the project. Coastal inundation by tsunami and coastal erosion were also not considered in this study.

Mean sea level (MSL) is rising, which will raise the base level for wave attack on the coastline and storm-tide inundation of low-lying land. Estimates of long-term sea-level rise are required, along with methods to include sea-level rise into coastal hazard assessments. Climate change will also cause acceleration in long-term trends of sea-level rise, but recent research in New Zealand shows only minor increases will occur in the drivers (winds, barometric pressure) that produce storm surges (Mullan et al. 2011).

Coastal extreme sea-level elevations were calculated previously for parts of the Auckland region now under Auckland Council's jurisdiction. Former Manukau City Council (MCC) and Auckland City Council (ACC) respectively commissioned NIWA to assess extreme sea levels for the coastlines under their jurisdiction (Ramsay et al. 2008a; Ramsay et al. 2008b). Likewise, former North Shore City Council and Rodney District Council commissioned Tonkin and Taylor to calculate sea inundation levels for their coastlines (Andrews 2004; Reinen-Hamill & Shand 2005). Projections of future sea-level rise were under constant debate and review over the period spanning these studies, and the studies applied different sea-level rise estimates for different planning timeframes. Also, the NIWA and Tonkin and Taylor studies used different techniques to calculate extreme storm-tide levels. NIWA rationalised these four studies to the common datum of 1980–99 mean sea level in Auckland Vertical datum 1946 (AVD–46) (Stephens et al. 2011c). The rationalisation study dealt only with storm-tides, and not waves, since NIWA's studies inside the Waitemata and Manukau Harbours did not consider wave setup. Since those

studies, new techniques have become available to calculate the joint probabilities (frequency–magnitude relationships) of large storm-tides and large waves occurring together, and these techniques are applied here. Previous coastal inundation studies were undertaken individually for Territorial Local Authorities, so they only covered the coastline under the individual TLA jurisdictions. The present study provides complete coverage of the entire Auckland region using recent developments in dynamic and probabilistic modelling.

NIWA’s Waves and Storm Surge Prediction (WASP), project has provided a regionally consistent set of wave and storm surge predictions, both a 40-year hindcast and projections of future climate-induced changes. The WASP project allows both the magnitude and joint probability of storm surges and waves to be calculated, offshore of the open coast, and has been used here for open-coast locations, after cross-checking and calibrating against available tide-gauge and wave-buoy data.

1.1 Study output

Coastal extreme sea-level elevations resulting from storm-tides and wave setup were calculated for annual exceedance probabilities of 39%, 18%, 10%, 5%, 2%, 1% and 0.5% (which correspond to 2, 5, 10, 20, 50, 100 and 200-year average recurrence intervals). These elevations were calculated at intervals along the entire coastline of the Auckland region, including the major harbours (Waitemata, Manukau and Kaipara), the beaches of the east and west coasts, and inside the small east-coast estuaries.

The extreme sea-level elevations were spatially interpolated along the coastline, and intersected with a digital elevation model of the land surface produced from LiDAR, to produce inundation area maps. Inundation areas were mapped for annual exceedance probabilities of 18%, 5%, 2% and 1% (5, 20, 50 and 100-year average recurrence intervals).

The inundation levels and inundation area maps were calculated relative to AVD-46, and they include the present-day mean sea-level offset added to AVD-46. Auckland Council requested that further inundation area maps be produced for additional sea-level rise scenarios of +1 m and +2 m above present-day mean sea-level, added to the 1% and 2% annual exceedance probability elevations. Table 1-1 summarises the study output.

Table 1-1: Coastal extreme sea-level elevation and inundation map outputs.

| Annual exceedance probability | 0.39 | 0.18 | 0.1 | 0.05 | 0.02 | 0.01 | 0.005 |
|--|------|------|-----|------|------|------|-------|
| Average recurrence interval (years) | 2 | 5 | 10 | 20 | 50 | 100 | 200 |
| Present-day extreme sea-level elevations | | | | | | | |
| Present-day inundation maps | | | | | | | |
| +1 m SLR inundation maps | | | | | | | |
| +2 m SLR inundation maps | | | | | | | |

The GIS inundation maps supplied to Auckland Council are the primary output of this study (e.g., Figure 8-7). This report presents tables that include the coastal extreme sea-level elevations used to generate the inundation area maps. The report also presents the data, models and methods used to calculate the extreme sea-level elevations and generate the inundation area maps.

The report is structured as follows: Section 2 presents the methods used to generate the extreme sea-level elevations and the inundation area maps; Sections 3 and 4 present location-specific information on the data and models used, and calculated extreme sea-level elevations.

2 How inundation areas were calculated and mapped

This section outlines the methods used to calculate extreme storm-tide plus wave setup elevations around the coastline of the Auckland region. It also describes the process used to convert the elevations into inundation area maps, within GIS. The method description in this section is designed to be generic. Location-specific details, such as data and models relevant to the application of these methods, are given in later sections.

2.1 Processes contributing to sea-level variability (and extreme sea levels)

Extreme sea levels in the Waitemata, Manukau and Kaipara Harbours were estimated from calculations of storm-tide elevations within the harbours, whereas extreme sea levels on the open coast were estimated from calculations of combined storm-tide plus wave setup elevations. The “open coast” is coastline located outside of sheltered harbours and estuaries, in locations subject to ocean swell. In this study we have modelled wave effects at all locations outside from harbours and estuaries, including the inner Hauraki Gulf, which is treated as open coast.

2.1.1 Sea level (excluding waves)

There are a number of meteorological and astronomical phenomena involved in the development of extreme sea level events. These processes can combine to inundate low-lying coastal margins. The processes involved are:

- Astronomical tides
- Storm surge
- Monthly mean sea level (MMSL), which can vary up or down over time periods of months up to decades
- Climate-change effects including sea-level rise. Sea-level rise was considered in this study as +1 m, and +2 m above present-day mean sea level
- Tsunami – not considered in this study.

The astronomical tides are caused by the gravitational attraction of solar-system bodies, primarily the Sun and the Earth’s moon, which then propagate as forced long waves in the ocean interacting in a complex way with continental shelves. In New Zealand, the astronomical tides have by far the largest influence on sea level, followed by storm surge (in most locations).

Low-pressure weather systems and/or adverse winds cause a rise in water level known as storm surge. Storm surge results from two processes:

- Low atmospheric pressure relaxes the pressure on the ocean surface causing a temporary rise in sea level, and
- Wind stress on the ocean surface pushes water down-wind, or alternatively, to the left of an alongshore wind (in the southern hemisphere) from a persistent wind field, piling up against any adjacent coast e.g., for the Auckland east coast, this would occur for onshore winds (from NE quadrant) and alongshore winds from SE respectively, and for the Auckland west coast, onshore winds from south-west and alongshore winds from north-west. Wind setup within harbours varies according to the fetch present at various tide states, but at high tide can be several cm.

Storm-tide is defined as the sea-level peak reached during a storm event, from a combination of **MMSL + tide + storm surge** (see below for description of MMSL). It is the storm-tide that is primarily measured by sea-level gauges such as the Ports of Auckland Ltd gauges analysed here. Throughout this report, we refer to storm-tide as the sea-level quantity relevant to coastal inundation.

The mean sea level describes the variation of the non-tidal sea level on longer time scales ranging from a monthly basis, through an annual sea-level cycle, up to decades due to climate variability, including the effects of El Niño–Southern Oscillation (ENSO) and the Interdecadal Pacific Oscillation (IPO) patterns on sea level, winds and sea temperatures, and seasonal effects. The following bullet points describe mean sea level definitions and how mean sea level measurements were obtained from sea-level gauge records:

- Tidal harmonic analysis was used to resolve the astronomical tide from the sea-level measurement record. The tide was then subtracted to produce a non-tidal residual sea-level record.
- The non-tidal residual sea-level record was then low-pass filtered (using a wavelet filter) to remove variability with periods of less than 1 month. The remaining sea-level time-series contained only sea-level variations with periods of motion of one month or greater, and this low-frequency time-series is termed the “Monthly Mean Sea Level” (MMSL). A simple way to obtain MMSL is to remove the tidal component of sea-level variability from the sea-level record, and then average the non-tidal residual on a monthly basis.
- When MMSL is averaged over a defined time period (usually several years), the Mean Sea Level (MSL) is obtained. New Zealand’s local vertical datums were obtained in this way. Auckland Vertical Datum 1946 (AVD-46) was established as the mean sea level (MSL) at Port of Auckland (Waitemata) from 7 years of sea level measurements collected in 1909, 1917–1919 and 1921–1923. MSL (AVD-46) is +1.743 m relative to tide gauge zero at Port of Auckland, which equals Chart Datum (CD) for Waitemata Harbour. Thus, for the purposes of this report, MSL is the average sea level over a defined time period. The mean sea level changes in time, due to climate variability and long-term sea-level rise. Therefore the mean sea-level offset to AVD-46 changes depending on the sea-level averaging epoch used. Sea level has risen since the years of measurements used to establish AVD-46 datum, at a long-term rate of 1.5 mm/yr at Auckland relative to the land (Auckland Regional Council 2010). Thus, the mean sea level from 1999–2008 was 1.89 m CD, which is +0.15 relative to AVD-46.
- The Mean Monthly Sea Level Anomaly (MMSLA) was obtained by detrending MMSL time-series and removing the time-series mean (mean of zero). MMSLA defines the monthly (and greater) sea-level anomaly due to climate variability such as seasonal effects, ENSO and IPO.
- All storm-tide plus wave setup and runup elevations were calculated relative to a zero MSL. Thus a MSL offset is subsequently required to relate the results to AVD-46.

Climate change will also cause acceleration in long-term trends of sea-level rise (Ministry for the Environment 2008) and could cause minor increases in the drivers (winds, barometric pressure) that produce storm surges (Mullan et al. 2011).

Tidal hysteresis is an additional setup in mean sea level in harbours relative to the open coast, caused by the differential speed of the tidal wave between low and high tides in shallow harbours.

2.1.2 Wave setup and runup

Waves also raise the effective sea level at the coastline (Figure 2-1). Wave setup describes an average raised elevation of sea level when breaking waves are present. Wave runup is the maximum vertical extent of wave “up-rush” on a beach or structure above the instantaneous still water level (that would occur without waves), and thus constitutes only a short-term fluctuation in water level relative to wave setup, tidal and storm-surge time scales. Wave runup includes the wave setup component. When offshore waves are large, wave setup and runup can raise the water level at the beach substantially.

Which of wave setup or wave runup is most important to widespread inundation? Wave runup elevations are considerably higher than wave setup elevations, being about 2.5 larger for a steep beach and about 10 larger for a dissipative beach. The two processes are important for different reasons. Wave setup is an integral component of the total water level that potentially could cause direct inundation of coastal margins. The combined storm-tide plus wave setup level is important for large-scale inundation. The combined storm-tide plus wave runup level is important to any overtopping of dunes and seawalls, beach erosion and wave impact on seawalls. Generally, overtopping by wave runup will not cause substantial flooding, compared to more direct inundation from wave setup, but this also depends on the capacity of the drainage system behind the overtopped barrier, and the safety of vehicles and pedestrians if close to a road. For seawalls, formulae exist to calculate the number of waves overtopping in one hour, the probability of overtopping per wave, and the mean overtopping discharge that enables estimates of damage to buildings and seawalls (EurOtop 2007). Note: this approach was used for the design of the north-western motorway causeway at Waterview.

In this study, calculated extreme sea-level elevations and inundation maps include wave setup (in open coast locations) but do not include wave runup elevations.

There are a number of different approaches to calculating wave setup. The Stockdon et al. (2006) formula was developed from empirical measurements made on 10 sandy beaches on USA and Netherlands coastline with different morphologies; so it is expected to be appropriate for sandy beaches along the coastline of the Auckland region. Depending on the nature of the coastline at each location, it may be more appropriate to use empirical formulae designed for gravel beaches, rock revetments or sea walls (e.g., EurOtop 2007; HR Wallingford; Van Rijn 2010). The Stockdon et al. (2006) formula (Equation 2-1) estimates wave setup using the offshore significant wave height and wavelength and the slope of the upper beach face.

Wave setup is highly sensitive to the beach profile shape (Stephens et al. 2011b) and likewise, calculations made using the empirical wave setup equation (Equation 2-1) are also sensitive to the beach slope parameter. Thus there is considerable uncertainty around the use of empirical wave setup calculations, because beach profiles are in a constant state of evolution, and it is often difficult to pick a representative beach slope from a profile.

What beach slope should be used in the wave setup equation?

For future planning purposes, a sound approach is to use historical beach profiles where available, locate the upper beach face near the high tide mark, examine the beach slope variability and choose a relatively steep beach slope to be conservative (steep beach = larger setup). For sandy beaches, the calculated wave setup is more sensitive to choice of beach slope than to calibration factors or the particular equation chosen. Choice of beach slope for this study is described in Section 7.4.

Equation -: Empirical wave setup formula (Stockdon et al. 2006). H_0 = Deep-water significant wave height (m). L_0 = Deep-water wave length (m). β_s = Beach slope (m/m = dimensionless).

Wave setup (m) =

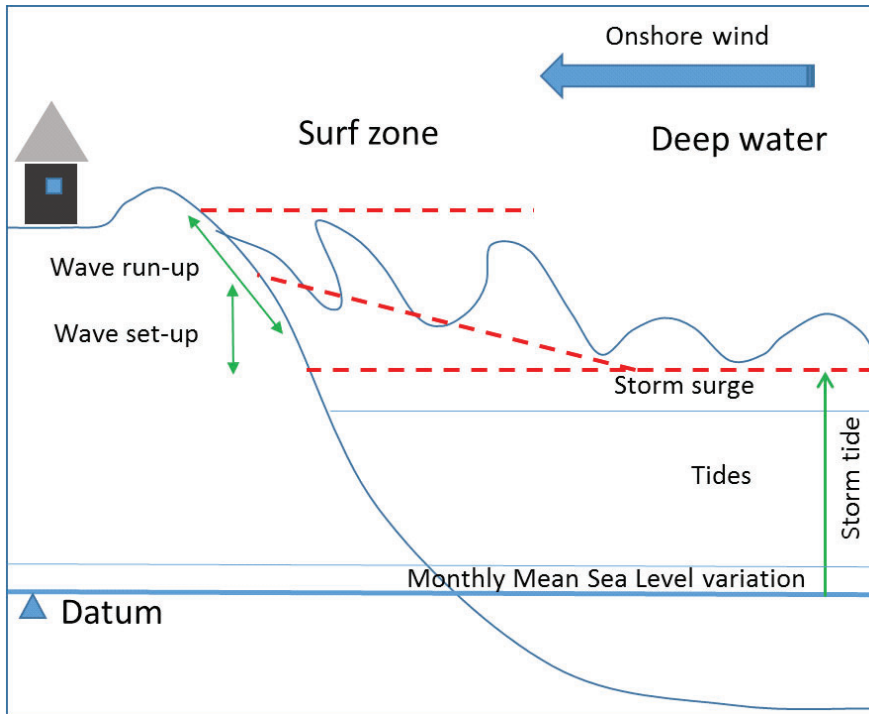


Figure 2-1: Schematic illustrating the various processes that contribute to coastal inundation.

2.2 Sea-level datum and mean sea level (MSL)

All data in this report are referenced relative to Auckland Vertical Datum–1946 (AVD-46), unless otherwise stated.

Before the introduction of New Zealand Vertical Datum 2009 (NZVD2009) in September 2009, land heights in New Zealand were referred to one of 13 local vertical datums, two of which are applicable to the Auckland region, being Auckland Vertical Datum–1946 and One Tree Point Datum–1964.

These local datums were established historically by determining mean sea level (MSL) at a tide-gauge and then transferring this level by precise levelling to benchmarks in the surrounding hinterland.

Sea level is known to vary around the coast of New Zealand and the local datums were set a different times during last century. This means that the level of MSL determined at each datum's tide-gauge will be different and that offsets will occur between adjacent datums. Also, in most cases the level of MSL for the vertical datums was determined many decades ago (apart from One Tree Point in the 1960s) and has not been officially updated since then to include the effect of sea level rise. Recent MSL values relative to these local vertical datums have been reported by Hannah and Bell (2012).

At a particular port, the level of the water is expressed as a height above a local datum which is also the datum used for the depths of the sea on nautical charts, known as Chart Datum (CD). This datum is defined with reference to permanent benchmarks ashore and the zero of the tide gauge. The Chart

Datum adopted usually approximates Lowest Astronomical Tide (LAT) which is the lowest tide predicted to occur under normal meteorological conditions.

2.2.1 Auckland Vertical Datum 1946

Auckland Vertical Datum 1946 (AVD-46) was established as the mean sea level (MSL) at Port of Auckland from 7 years of sea level measurements collected in 1909, 1917–1919 and 1921–1923 (Hannah & Bell 2012). Based on these historical measurements, the MSL for Auckland Vertical Datum-1946 (AVD-46) was set in 1946 to +1.743 m relative to the present tide gauge zero at Port of Auckland, which equals Chart Datum. For the Manukau Harbour, Chart Datum at the Port of Onehunga is 2.201 m below AVD-46, being lower than the Waitemata Harbour because of the larger tide range (i.e., lower low tides).

2.2.2 One Tree Point Datum 1964

One Tree Point Datum-1964 (OTP-64) was established as the mean sea level (MSL) at Marsden Point from 4 years of sea level measurements collected between 1960 and 1963. The historic MSL set in 1964 was +1.676 m relative to local Chart Datum at Marsden Point.

2.2.3 Offset between datums

From the official offsets of the two local vertical datums from NZVD2009, LINZ implies that OTP-64 is 0.28 m higher than AVD-46 on average, based on several benchmarks in both local datums. There is uncertainty however, because the New Zealand geoid varies spatially, therefore it is difficult to define the offset as it depends on where it is measured, and the accuracy of past precise surveying levels. Also, the offset between local vertical datums depends on the relative accuracy between the two surveys. For example, the offset between datums at benchmark ABHL at Wellsford is 0.206 m, and in earlier research on developing a geoid model for New Zealand, Amos (2007) shows a 0.25 m offset between the two local vertical datums. Overall, OTP-64 is about 25 cm higher than AVD-46, but its exact value at any location is unknown and could differ by about ± 4 cm. Note: a progressive move towards using NZVD2009 for land elevations will eventually eliminate these cross-boundary issues with the offsets between adjoining local vertical datums. NZVD2009 is based on a New Zealand-wide geoid model – the geoid varies spatially. We have adopted a +0.25 m offset (OTP-64 = AVD-46 + 0.25 m) for this study. The estimated ± 4 cm uncertainty is not significant in the comparison of extreme sea levels between coasts.

2.2.4 Defining present mean sea level

The aforementioned local vertical datums were established from the mean sea level, averaged over several years during different historical periods. Sea level has risen since the AVD-46 datum was established, at a long-term rate of 1.5 mm/yr at Auckland relative to the land (Auckland Regional Council 2010). Thus, mean sea level is now higher than when the local vertical datum were established. The OTP-64 datum is somewhat of an anomaly as present MSL is still below the OTP-64 datum zero at Marsden Point (partly due to the short record used from the 1960s and the way it was defined – not known).

To define MSL in the Auckland region, we need to calculate recent MSL by averaging modern sea-level gauge records, referenced to local vertical datum, as shown in Table 2-1. These tide-gauges are all surveyed to local vertical datum. For an exact comparison, the averaging periods used in Table 2-1 should be identical. We were reliant on quality-assured data that was available and so the averaging periods are a little different, but are mostly post-2001, whereas the two local vertical datums were set

several decades earlier. Small (± 1 cm) uncertainties introduced from using slightly different averaging periods are insignificant for the purposes of establishing extreme sea-level inundation area maps.

Table 2-1: Sea-level gauges with known offsets to local vertical datum used in this study.

Shown in italics is a MSL derived from Hannah and Bell (2012)* for a longer half nodal-tide period (10 years) which confirms the Auckland value. The local gauge-zero level for Pouto Point was obtained from Northland Regional Council (Dale Hansen, pers. com.); a corrected MSL offset (explained in the text) is also given.

| Sea-level gauge location | Local vertical datum | Chart datum (or gauge zero) | Mean sea level | Averaging period |
|--------------------------|----------------------|-----------------------------|--------------------------|------------------|
| Auckland | AVD-46 | -1.743 (AVD-46) | +0.15 m (AVD-46) | 2006–2011 |
| | | | <i>+0.15 m* (AVD-46)</i> | <i>1999–2008</i> |
| Marsden Point | OTP-64 | -1.676 (OTP-64) | -0.09 m (OTP-64) | 2001–2011 |
| Onehunga | AVD-46 | -2.201 (AVD-46) | +0.22 m (AVD-46) | 2001–2009 |
| Pouto Point | OTP-64 | -1.687 (OTP-64) | +0.16 m (OTP-64) | 2001–2011 |
| | | | <i>-0.02 m (OTP-64)</i> | <i>Corrected</i> |

The sea-level records and their associated assigned datum level indicate that mean sea level in the Kaipara Harbour at Pouto Point is about 26 cm higher than at Auckland (Waitemata) and 19 cm higher than at Port Onehunga (Manukau). The Pouto Point level is higher than we would expect from tidal shoaling theory, and we suspect that the Pouto Point gauge level offset may need re-surveying. The Pouto Point gauge was buried by a sand wave in about September 2012, so at the time of writing it is not possible to re-survey the gauge offset. The gauge zero for the sea-level gauge that NIWA operated at Anawhata (now closed) is also likely to be inaccurate (appears to be lower than expected) due to the open-coast wave environment which makes it difficult to establish a datum without the use of a tide-board. Thus we have lower confidence in the mean sea-level offsets for the Kaipara Harbour and the open west coast of the Auckland region.

The mean sea level for the open west coast was derived by subtracting 6 cm of tidal hysteresis from the mean sea level at the Onehunga sea-level gauge. Bell et al. (1998) calculated a rise in the mean tide level between the harbour entrance (Paratutae Island) and Onehunga Wharf of 4.5 cm using an M2 tidal harmonic hydrodynamic model simulation, which is similar to an estimate of 6 cm derived from survey measurements (Tonkin & Taylor Ltd 1986).

Given our uncertainty in the levelling of the Pouto Point tide gauge, the mean sea level for the Kaipara Harbour was derived as follows. A hydrodynamic model of the Kaipara Harbour was used to calculate an approximate tidal hysteresis rate, giving an expected tidal hysteresis rise from Pouto Point to Ruawai of +0.083 m. An archived 1969–74 sea-level record from Ruawai (northern Kaipara Harbour) with known datum levelling (not shown), suggests Ruawai mean sea level is about +0.1 \pm 0.045 m OTP-64 after accounting for sea-level rise of +0.15 mm/yr in the intervening period. This suggests Pouto Point MSL \approx OTP-64, rather than +0.16 m as shown in Table 2-1 (which is very high relative to MSL at Auckland). MSL at Onehunga is +0.22 m AVD-46, with tidal hysteresis of 6 cm to entrance (Bell et al. 1998), that suggests +0.16 m AVD-46 for open west coast. The expected tidal hysteresis from open coast to Pouto Point (based on hydrodynamic model of upper harbour, but through larger

entrance) is 7 cm. So Pouto Point MSL expected to be about +0.23 AVD-46, or similar to Onehunga, which makes sense dynamically. This is also similar to the 25 cm OTP-64 to AVD-46 offset. In conclusion, for the purposes of this study we estimate that the present-day mean sea-level offset from AVD-46 is +0.23 m at Pouto Point, and -0.02 m from OTP-64 (Table 2-1).

Table 2-2 gives the mean sea-level offsets to AVD-46 that were used in this study, based on the averaging epochs given in Table 2-1. For the purposes of this study, the values in Table 2-2 are taken as representative of “present-day” mean sea level.

Table 2-2: Mean sea-level offsets to AVD-46 datum used in this study, at several locations in the Auckland region.

| Location | Mean sea-level offset relative to AVD-46 |
|---------------------------------------|--|
| Waitemata Harbour at Port of Auckland | + 0.15 m |
| Open east coast | + 0.15 m |
| Kaipara Harbour at Pouto Point | + 0.23 m |
| Manukau Harbour at Onehunga | + 0.22 m |
| Open west coast | + 0.16 m |

2.3 How extreme sea-levels were calculated – overview

This section gives an overview of the calculation of extreme sea-levels around the Auckland coastline. This overview is designed to enable the reader to understand what was done and why, with a minimum of technical detail. Details are provided in Appendix A.

Extreme sea levels are, by definition, rare events. Only by observing a system for a long period of time can an understanding of the frequency and magnitude of extreme sea levels be attained. For the calculation of extreme sea levels, a sea-level record would ideally meet the following criteria:

- Sea-level gauge surveyed to datum
- Accurate: no long-term drift or sensor subsidence, no siltation or blockage of the gauge. Known tectonic movement or subsidence at gauge site
- ≥ 50-years length to incorporate approximately two IPO and multiple ENSO climate variability cycles
- Sample at least hourly to capture storm-tide peak
- Include all extreme sea-levels that occurred (no data gaps at crucial times).

Because this is generally not the case, techniques have been developed to overcome the lack of long-term records and calculate extreme events from shorter records. The method used for this project is the Monte Carlo joint-probability (MCJP) technique (Goring et al. 2010), which is explained further in Section 7.2.3. This method makes best use of short, but regularly sampled (e.g., hourly or better), data records.

The MCJP method uses component parts of a storm-tide: tide, storm surge and MMSLA, by assuming they are independent and reassembling them into a storm-tide sequence. Therefore, for each location where extreme storm-tides are required, we need to first obtain time-series for each of the three sea-level components, tide, storm surge and MMSLA.

Tide-gauge records at Ports of Auckland Ltd, Port of Onehunga, Pouto Point and Anawhata provide the required data within the Waitemata, Manukau and Kaipara Harbours, and the open west coast. These gauge records are crucial to the study because they allow extreme sea-level analyses to be made that are founded on actual sea-level measurements. These are then used to validate extreme sea-level estimates based on modelled data.

Extreme sea-level estimates are needed throughout the Auckland region, not just at the tide-gauge locations. Extreme sea-levels change with location as the tide, storm surges, MMSLA and wave setup all interact in different ways with the local environment such as the underwater bathymetry, topographic constriction, and wind and wave exposure.

Numerical hydrodynamic models, calibrated against sea-level measurements, were used to simulate tides, storm surges and wave setup at locations around the Auckland region. Extreme sea-levels were then modelled from the simulated time-series, at “model-output locations” around the coastline.

Sea-level components were calculated differently for locations in three different regions: the major harbours Waitemata, Manukau and Kaipara – which each have at least one sea level gauge for validation; the open coast; and the minor harbours/estuaries. This is because of the different physical environment between the open coast and the harbours, and the need to deal with multiple small estuaries in an efficient way.

Open coast sites occasionally experience high wave energy as well as large storm-tides, so joint-probability methods were used to calculate the combined likelihood of large waves and storm-tides occurring simultaneously. The joint-probability method accounts for any dependence between waves and storm-tide.

2.3.1 Major harbours

The following steps were used to calculate extreme sea-levels inside the Waitemata, Manukau and Kaipara Harbours:

- Tide-gauge data was decomposed into sea-level components: tide, storm-surge and MMSLA.
- Extreme sea levels were calculated from measured sea-level components at tide gauge sites
- For model output locations away from tide gauge sites, time-series of sea-level components were simulated using hydrodynamic models, as follows:
 - Tides were simulated for a full lunar cycle (1-month). From this, scaling relationships were developed between the tide at the tide-gauge site and those at the model-output locations. Tides were predicted at the tide-gauge site (from tidal harmonic analysis) for > 45 years, to match available meteorological records, used for winds (see next bullet). The spatial scaling relationships from the 1-month tidal simulation were applied to the predicted tide-gauge time-series to simulate tidal time-series at the model-output locations.
 - The wind-driven component of storm-surge was simulated by matching the > 45-year meteorological records (1965–2011 for Waitemata and Manukau; 1960–2010 for Kaipara) to a wind setup response matrix, for each model-output location. The wind setup response matrices were created using hydrodynamic models to simulate wind setup along different fetches from a variety of wind speeds and directions. The wind response was simulated at high spring tide, when fetch is maximum.

- The inverse-barometer component of storm-surge from low-pressure weather systems was calculated from the barometric pressure record, by applying Equation 71 (Section 7.3.1).
- MMSLA was taken directly from the tide-gauge record, and assumed to be of uniform magnitude throughout the harbour. The MMSLA record does not need to match in time the simulated tide and storm-surge, because the cumulative distribution function of MMSLA is used in the MCJP extreme sea-level technique. MMSLA generally follows a normal (Gaussian) distribution above and below MSL.
- Tidal hysteresis relative to the tide-gauge location was calculated for all model-output locations, using the 1-month tidal simulation.

2.3.2 Open Coast

The following steps were used to calculate extreme sea-levels along the open coastlines of the Auckland region:

- Time-series of storm surge, tides and waves were extracted directly from WASP model simulations, for the 30-year hindcast period 1970–2000. For the east coast (Hauraki Gulf) where there are several islands, a SWAN wave model was used to transform the WASP offshore wave time-series (from the northern Gulf region) inshore to the coast
- Storm-tide and wave height and period statistics were combined in a joint probability analysis, for each model-output location
- Beach profile data were examined to establish a representative beach slope with which to calculate wave setup, using Equation 2-1
- The maximum storm-tide plus wave setup elevation was calculated for various annual exceedance probabilities, at each model-output location.

The WASP programme was intended to provide long-term time-series and statistics for both waves and storm surge around the New Zealand, based on (30 years or more) numerical simulations of historic conditions ('hindcasts'), as well as of conditions expected towards the end of this century ('projections') based on expected climate change. Results of the WASP modelling project are available at <http://wrenz.niwa.co.nz/webmodel/coastal>.

2.3.3 Small east-coast harbours and estuaries

Storm-tide elevations in the numerous relatively small east-coast harbours and estuaries were calculated as follows:

- The maximum storm-tide plus wave setup elevations calculated for the open east coast were applied to the harbour entrances
- The storm-tide component is expected to amplify inside the harbours. An amplification factor that increased with distance from the harbour entrance was applied to the storm-tide component.

The applied amplification rate, in lieu of tidal height measurements inside these harbours, was equivalent to the tidal amplification between the Ports of Auckland Ltd and Salthouse Jetty (Lucas Creek) gauges in the Waitemata Harbour, being 4.2 mm of elevation per km of horizontal distance. There remains uncertainty in the amplification rates used for the smaller estuaries that have no sea-level records. The wave setup component at the entrance was assumed to translate inside the estuary without dissipation, so was added to the amplified storm-tide elevations inside the estuary.

2.4 Inundation mapping

Inundation maps were created within GIS, for the scenarios outlined in Table 1-1. Extreme sea-level elevations from the sea-level modelling were input to GIS at model-output locations around the Auckland coastline. These were interpolated along the coastline and intersected with a digital elevation model of the land topography, to create GIS polygons that map the areas where extreme sea-level was higher than land level. For low-lying land areas that were not connected to the sea by rivers or drains, the “inundation” areas were removed from the maps. The GIS inundation mapping process is described, using examples, in Section 8.

The major assumption in the GIS mapping procedure was the use of a “bathtub” flooding approach, whereby every land area below the extreme sea-level is mapped as instantly flooded in its entirety. In reality, the peak of a storm-tide only lasts for about 1–2 hours centred around high tide, and this may not be enough time to flood a large area of the wider hinterland if the flow rate of the storm-tide is restricted by a narrow connection to the sea.

An example of this occurred at the Waitemata Golf Course near the suburb of Narrowneck, during the 23 January 2011 storm-tide, which is the highest storm-tide on record in the Waitemata Harbour. The modelled present-day 0.01 AEP extreme sea-level elevation closely matched the extreme sea-levels that were both simulated and measured during the 23 January 2011 storm-tide. The modelling agreed with observations of storm-tide breaching Lake Road into the golf course. However, whereas the bathtub mapping procedure predicted the entire golf course was inundated due to that breach, the storm-tide actually flowed over Lake Road for only an hour or so at the peak of the tide, and this did not cause substantial inundation in the golf course. In this instance, the present-day 0.01 AEP inundation map was hand-edited to remove excess flooding in the golf course.

The bathtub inundation mapping approach is conservative in that it tends to over-predict rather than under-predict inundation by storm-tides, although can be tempered by delays in inundation subsiding if drainage to the sea is inadequate. The bathtub mapping approach is best suited to locations where the topography rises approximately continuously with distance from the coast, and without large low-lying areas behind coastal barriers. This is the case for most parts of Auckland city.

3 Extreme sea levels in the Waitemata, Manukau and Kaipara Harbours

In this section we provide location-specific information, such as data and models, required to explain how the methods from Section 2 and Appendix A (Section 7.3) were applied in the Waitemata, Manukau and Kaipara Harbours.

3.1 Waitemata Harbour

3.1.1 Tide-gauge analysis

Figure 3-1 plots the most up-to-date quality-analysed sea-level record for the Ports of Auckland Ltd gauge. This hourly sea-level record was digitised from archived records and has undergone considerable quality analysis as part of three studies of long-term sea-level rise in New Zealand (Hannah 1990; Hannah 2004; Hannah & Bell 2012), and has recently become available for analysis in this study. It provides an excellent record for extreme-sea-level analysis using direct extreme-value techniques (Table 7-4).

Two examples of the decomposition of the sea-level record are shown for 2006–2011 (Figure 3-2) and for the large (~0.6 m) storm surge that peaked on 26 July 2008 (Figure 3-3).

Previous extreme sea-level analyses conducted by Stephens et al. (2011c) used a digital sea-level record from 1974–May 2011, supplemented by a graph of annual maxima from 1925 onward from Auckland Harbour Board records (Auckland Harbour Board 1974). Subtle differences in the processing of the datasets has led to differences, generally of ± 1 cm in the elevations of sea-level maxima between the two records, which are insignificant for the extreme sea-level analyses. Of more importance to the extreme sea-level analysis is the length and coverage of the dataset. We consider the following extreme sea-level analyses to be more robust than those of Stephens et al. (2011c) owing to longer and more complete record used here.

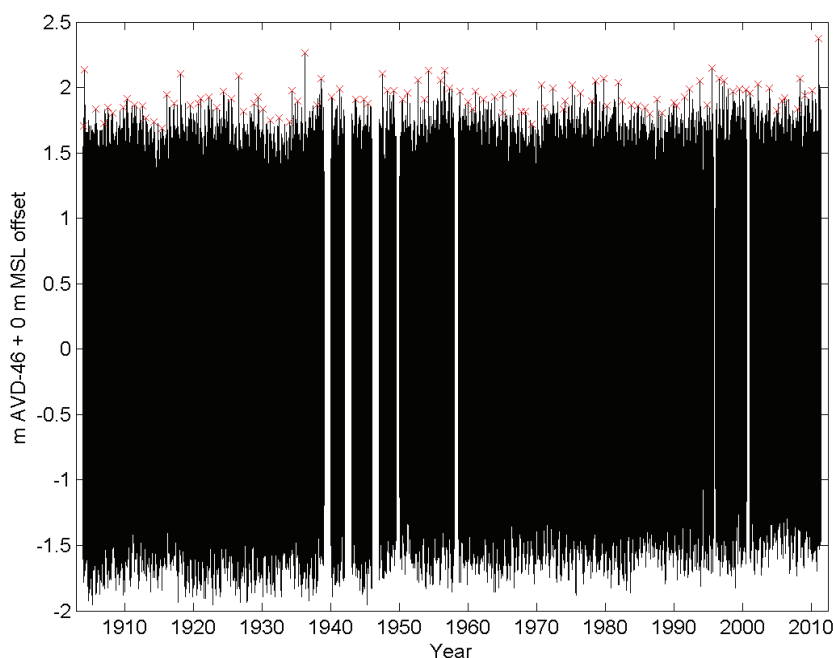


Figure 3-1: Ports of Auckland hourly sea-level record 26 Oct 1903 – 31 May 2012.

Data is relative to AVD-46, with no (0 m) mean sea-level offset applied. Crosses mark annual maxima.

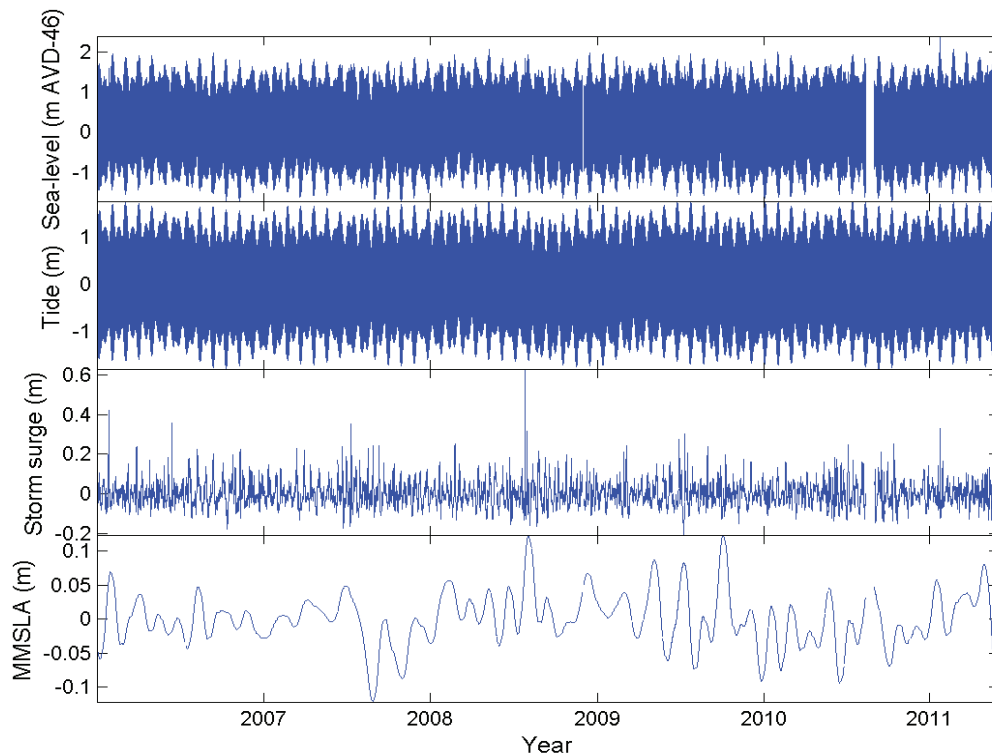


Figure 3-2: Decomposed Ports of Auckland Ltd tide-gauge sea-level record 2006–2011.

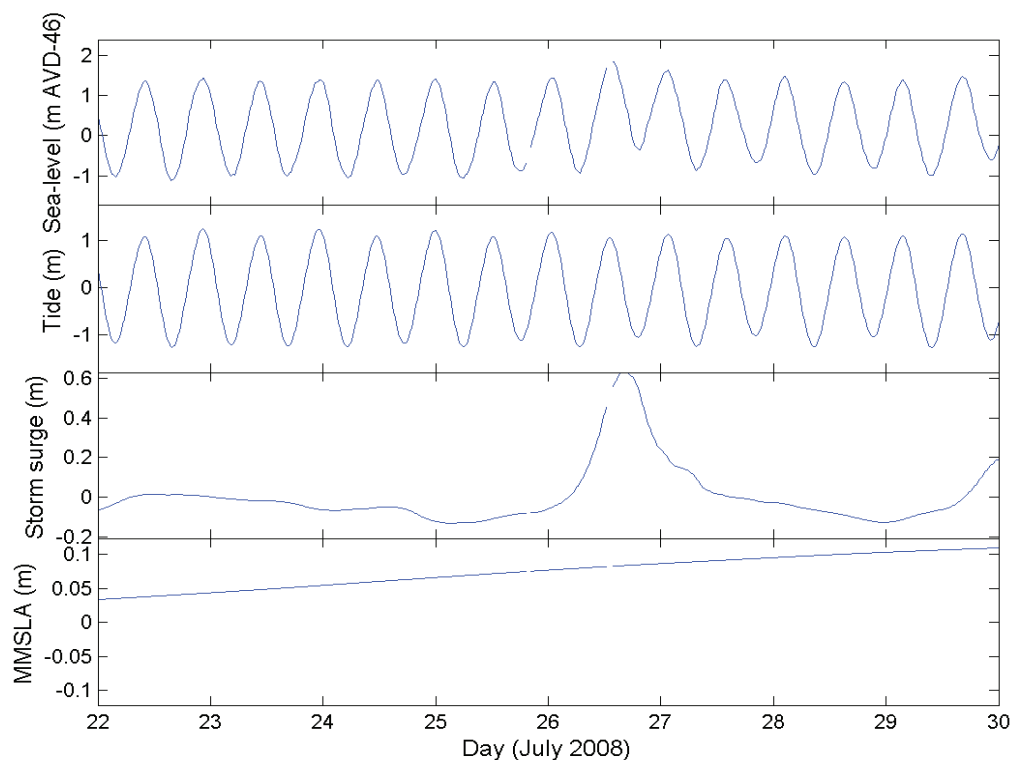


Figure 3-3: Decomposed Ports of Auckland Ltd tide-gauge sea-level record, 26 July 2008 storm surge.

Before undertaking extreme sea-level analyses, the raw sea-level time-series was detrended by removing a linear long-term sea-level rise trend of 1.5 mm/year (Hannah & Bell 2012). This was done using 2004 (1999–2008) as the pivot year, to make subsequent extreme-value analyses relative to present-day (1999–2008) MSL = +0.15 m AVD-46 (Table 2-1).

Table 3-1 shows the ten largest sea-level annual maxima, with their rank based on the de-trended sea-level time-series. This differs from Table 2-3 of Stephens et al. (2011c) owing to the more complete record available here. Interestingly, the large storm-surge event of 26 July 2008 (Figure 3-3) doesn't appear in the top-ten list of storm-tides because it only coincided with an average tide.

Table 3-1: Ten largest sea-level annual maxima at Port of Auckland, in descending order.

Elevations are specified in AVD-46. Detrended annual maxima have been adjusted using a linear long-term sea-level rise rate of 1.5 mm/year (Hannah & Bell 2012). Annual exceedance probabilities (AEP) are provided by interpolating the event magnitudes onto the three extreme-sea-level curves shown in Figure 3-4, using the Monte-Carlo joint-probability technique (MCJP), generalised Pareto distribution (GPD) and generalised extreme-value distribution (GEV). These data differ by ± 1 cm from Table 2-3 of Stephens et al. (2011c) due to subtle differences in the processing of the datasets.

| Year | Raw sea level (m AVD-46) | Detrended sea level (1.5 mm/year), adjusted to present-day MSL = +0.15 m AVD-46 | AEP (MCJP) | AEP (GPD) | AEP (GEV) |
|-----------|--------------------------|---|------------|-----------|-----------|
| 23-Jan-11 | 2.38 | 2.41 | 0.007 | 0.008 | 0.005 |
| 26-Mar-36 | 2.27 | 2.41 | 0.006 | 0.008 | 0.005 |
| 14-Jul-95 | 2.15 | 2.20 | 0.069 | 0.079 | 0.083 |
| 4-Feb-04 | 2.14 | 2.33 | 0.018 | 0.019 | 0.018 |
| 7-Mar-54 | 2.13 | 2.25 | 0.044 | 0.048 | 0.053 |
| 14-Jul-56 | 2.13 | 2.24 | 0.045 | 0.05 | 0.054 |
| 14-Feb-18 | 2.11 | 2.28 | 0.03 | 0.037 | 0.037 |
| 20-Jun-47 | 2.11 | 2.24 | 0.049 | 0.056 | 0.06 |
| 11-Jul-26 | 2.09 | 2.25 | 0.044 | 0.048 | 0.052 |
| 27-Jul-38 | 2.07 | 2.21 | 0.069 | 0.078 | 0.083 |

Figure 3-4 shows results of three extreme sea-level analyses based on the Port of Auckland gauge measurements. The peaks-over-threshold (POT) data are plotted using their Gringorten (1963) plotting positions. If the empirical distribution of the data exactly matched the Gumbel extreme-value distribution (similar to the GEV and GPD distributions), then they would form a straight line when plotted in their Gringorten plotting positions. The GPD and GEV distributions were fitted following (Coles 2001) using the extRemes software in R (Stephenson & Gilleland 2006). A 1.915 m (AVD-46) threshold was used for the POT data, selected using extRemes analysis tools. The MCJP technique was applied by Stephens et al. (2011c) using data from only 2006–2011. A longer dataset from 1970–2000 was analysed in this study to produce a storm surge comparison with the WASP storm surge hindcast for the same time period. The inclusion of additional years of storm surge annual maxima makes the MCJP more robust than the analysis by Stephens et al. (2011c) that used only 2006–2011 data.

The three techniques give similar results (Figure 3-4). The average recurrence interval for the January 2011 event lies between 126 and 205 years, depending on the method used. It is worth noting that the difference between a 100-year and a 200-year ARI event is only 6 cm, due to the rather flat extreme sea-level distribution. Thus small differences in the extreme-value curves make considerable differences to the frequency estimates for these large events. This illustrates that extreme-value modelling is not a precise science, and the occurrence likelihoods for these large events are not precise estimates. However, the use of a very robust dataset, three extreme sea-level modelling techniques, and the degree of agreement between the models, provides confidence in the estimates.

The March 1936 storm-tide has a similar magnitude and exceedance probability to the 2011 event after removal of the sea-level trend. Following the Gringorten (1963) plotting position, the 1936 event plots as a large outlier compared to the extreme sea-level models. This illustrates that if the empirical distribution of the annual maxima approximately conforms to an extreme-value distribution, then we would not expect to see, on average, two events as large as the 1936 and 2011 events within the 108-year observation period. This illustrates the concept that although the average recurrence interval (over a very long timeframe) might be considerable between the largest events, there is a (small) probability of more than one large storm-tide occurring at close intervals, as tides and storm surges randomly combine. The term annual exceedance probability conveys that (small) likelihood.

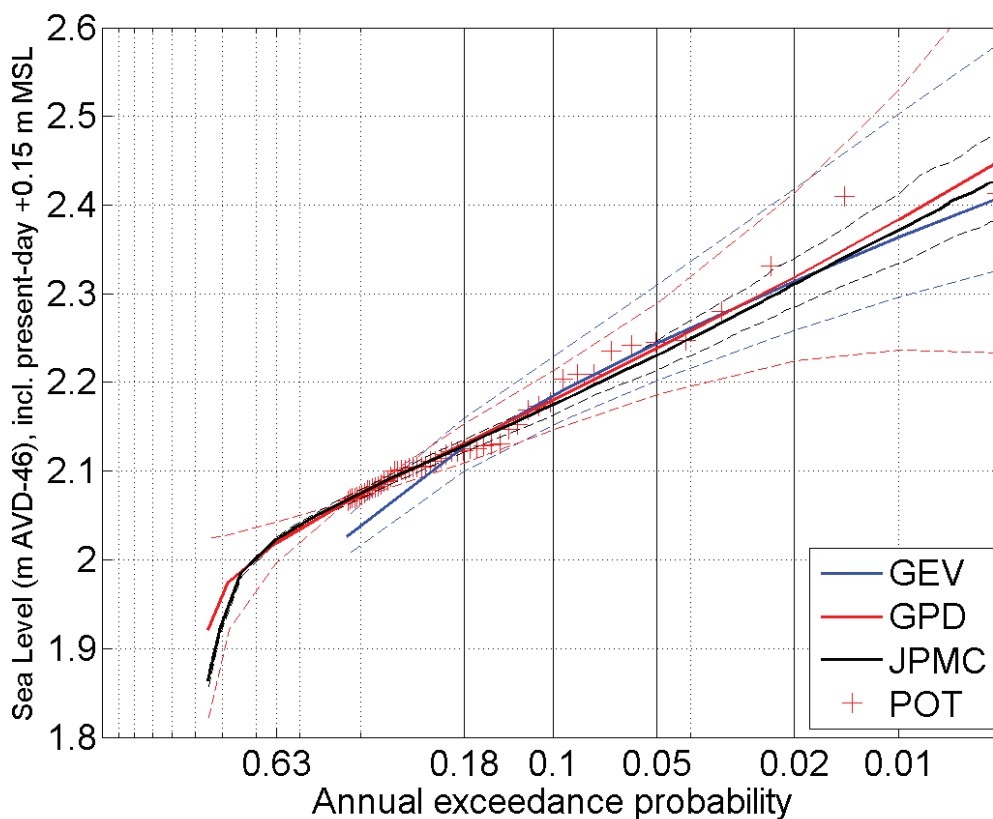


Figure 3-4: Extreme sea-level curves using Port of Auckland tide-gauge data.

(Three techniques were used: the Monte-Carlo joint-probability technique (MCJP), generalised Pareto distribution (GPD) fitted to peaks-over-threshold (POT) data and generalised extreme-value distribution (GEV) fitted to annual maxima (AM). Bold lines indicate central fit, dashed lines indicate 95% confidence intervals. The POT data have also been plotted using Gringorten (1963) plotting positions. Elevations are relative to AVD-46 including +0.15 m offset for baseline mean sea level (present-day estimate).

The extreme sea-level elevations from the three extreme sea-level models are given in Table 3-2. Elevations are specified relative to AVD-46 and include a +0.15 m offset for present-day MSL (Table 2-1).

Table 3-2: Extreme sea-level at Port of Auckland tide-gauge.

Elevations are relative to AVD-46 including +0.15 m offset for baseline mean sea level (present-day estimate).

| AEP | ARI | MCJP | | | POT / GPD | | | AM / GEV | | |
|-------|-----|--------|-----------------|-----------------|-----------|-----------------|-----------------|----------|-----------------|-----------------|
| | | Median | Lower 95th C.I. | Upper 95th C.I. | Median | Lower 95th C.I. | Upper 95th C.I. | Median | Lower 95th C.I. | Upper 95th C.I. |
| 0.39 | 2 | 2.07 | 2.06 | 2.07 | 2.07 | 2.07 | 2.07 | 2.03 | 2 | 2.05 |
| 0.18 | 5 | 2.13 | 2.12 | 2.14 | 2.13 | 2.11 | 2.15 | 2.13 | 2.1 | 2.16 |
| 0.10 | 10 | 2.18 | 2.17 | 2.19 | 2.18 | 2.15 | 2.22 | 2.19 | 2.16 | 2.23 |
| 0.05 | 20 | 2.23 | 2.22 | 2.25 | 2.24 | 2.19 | 2.29 | 2.25 | 2.2 | 2.31 |
| 0.02 | 50 | 2.31 | 2.29 | 2.34 | 2.32 | 2.22 | 2.41 | 2.31 | 2.26 | 2.42 |
| 0.01 | 100 | 2.37 | 2.33 | 2.41 | 2.38 | 2.24 | 2.53 | 2.36 | 2.3 | 2.5 |
| 0.005 | 200 | 2.43 | 2.38 | 2.48 | 2.45 | 2.23 | 2.67 | 2.41 | 2.33 | 2.59 |

3.1.2 Hydrodynamic model

Simulations of tide and the wind-driven component of storm surge were undertaken using the DHI MIKE 3 FM modelling suite. The hydrodynamic model domain for the Waitemata Harbour is shown in Figure 3-5. This model was originally developed and calibrated as part of the Central Waitemata Contaminant Study (Oldman et al. 2007). The model was calibrated against sea-level measurements located at the entrance to the upper Waitemata, in the upper Whau River, the approach to the Whau River, the middle Waitemata, Shoal Bay and Watchman Island. The model closely reproduced the tidal wave at all sites, demonstrating accurate representation of tidal wave shoaling and amplification.

Tidal simulations for a full lunar month were forced at the open boundary using NIWA's New Zealand regional tide model (Stanton et al. 2001; Walters et al. 2001). The Waitemata Harbour model was also forced with winds of various speeds and directions to create wind response matrices. These results were used as discussed in Section 2.3.1.

A simulation of the 23 Jan 2011 storm-tide was forced at the open boundary using Port of Auckland tide gauge measurements with an appropriate phase-lag applied. Simulated storm-tide elevations on the 23 Jan 2011 were compared to predicted 100-year ARI storm-tide levels.

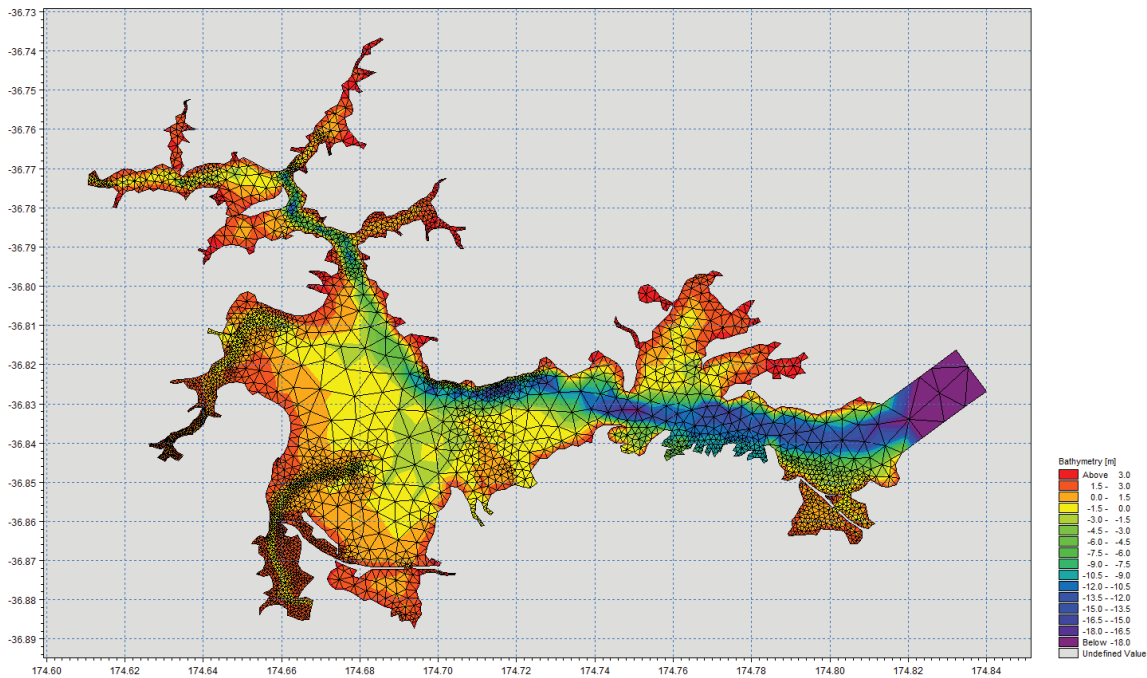


Figure 3-5: Waitemata Harbour MIKE-3 FM hydrodynamic model grid (Oldman et al. 2007).
 (Note: idealised channel created for eastern boundary condition)

3.1.3 Modelling storm surge

The Auckland Airport (located adjacent to the Manukau Harbour) wind and mean sea-level pressure records were obtained from 8 Nov 1965 – 11 May 2011. The isthmus between the Manukau and Waitemata Harbours is relatively flat so the airport weather station (located adjacent to the Manukau Harbour) should reasonably approximate the wind field in both harbours. The wind-driven component of storm surge was calculated as described in Section 7.3 by using the wind record to interpolate storm surge from the simulated wind-surge response matrix from the hydrodynamic model. The wind-driven component of storm surge differs depending on the output location within the harbour due to the available wind fetch.

The inverse-barometer component of sea level arising from low-pressure weather systems was calculated as described in Section 7.3.1.

3.1.4 Modelling storm-tide

Storm-tide time-series were simulated using the methods described in Sections 2.3.1 and 7.3, at 114 locations within the Waitemata Harbour (Figure 3-6), for later extreme sea-level analysis.

The three sea-level components required for extreme sea-level analysis are tide + storm surge + monthly mean sea-level anomaly (MMSLA). The tide and storm surge are affected by harbour geography, but MMSLA is a slowly varying sea-level component that we assumed to be ubiquitous throughout the harbour. Simulated storm-tide time-series consisted of tide plus storm surge. A time-series of MMSLA derived from the Port of Auckland tide gauge was used in the Monte Carlo joint-probability extreme sea-level modelling. For each model-output location the tidal time-series, the storm surge time-series, and MMSLA time-series were input to the MCJP extreme sea-level analysis.

Tidal hysteresis was calculated from the hydrodynamic model using the mean sea-level over the simulated lunar month; enabling a mean sea-level offset to be calculated for each location, relative to

the Port of Auckland tide-gauge location. This mean sea-level offset due to tidal hysteresis was added to the extreme storm-tide distribution at each output location.

Figure 3-7 compares the extreme sea-level frequency–magnitude distributions derived from the Port of Auckland gauge data (Figure 3-1, Figure 3-4), and from simulated data at the gauge site, and, for comparison, at selected sites located further toward the upper Waitemata Harbour. Using the IBfactor as a calibration parameter (Section 7.3.1), the extreme sea-level distributions from both measured and simulated data were closely matched at the Port of Auckland tide-gauge site. The other curves demonstrate how the simulated extreme sea-level magnitudes magnify toward the estuary head, due to amplification of the tide and storm surge. Extreme storm-tide elevations for 114 locations in the Waitemata Harbour are presented in Table 3-3.

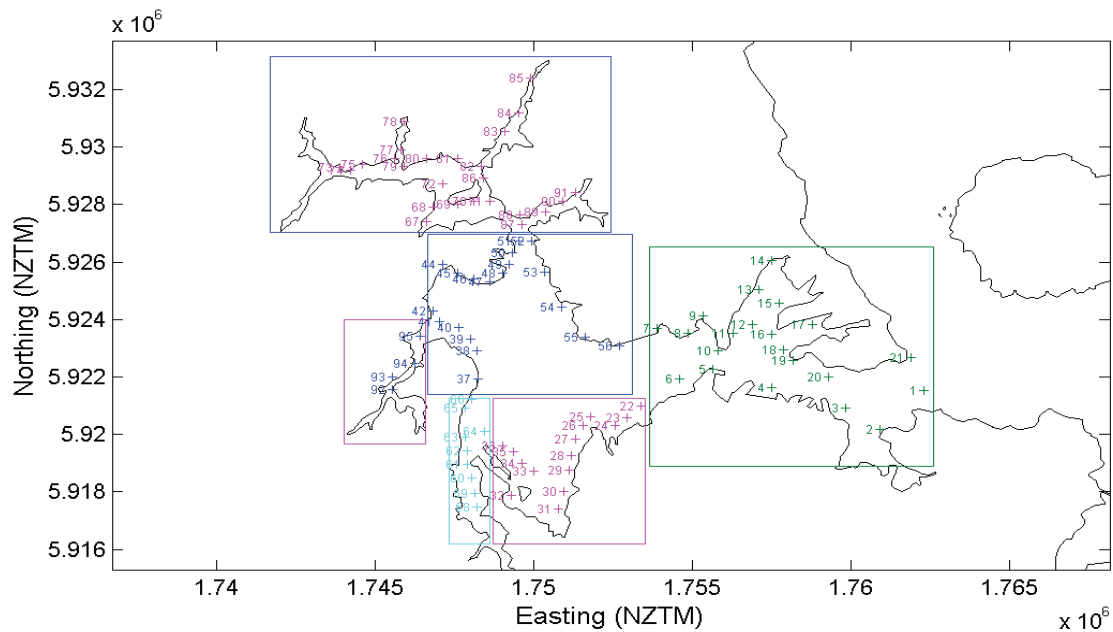


Figure 3-6: Locations of extreme storm-tide predictions in the Waitemata Harbour.
(Colour-coding corresponds to Table 3-3.)

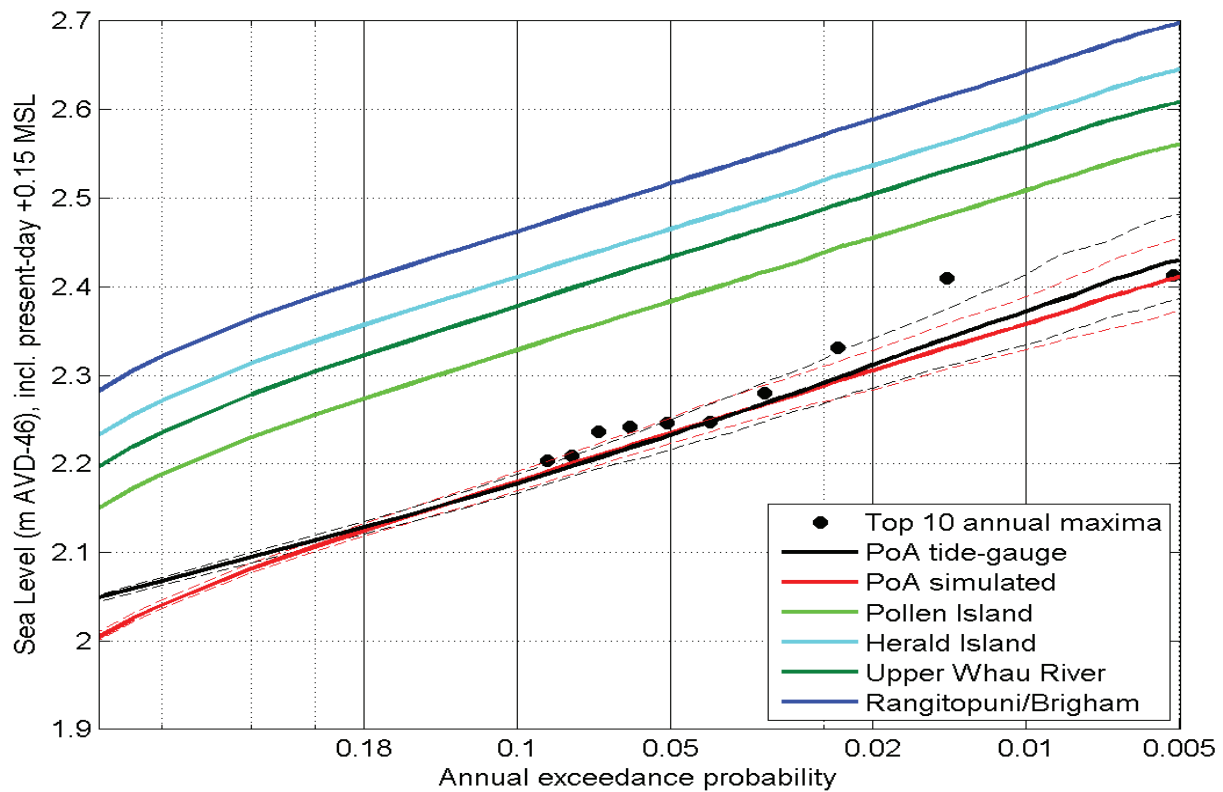


Figure 3-7: Simulated extreme storm-tide frequency-magnitude distributions in the Waitemata Harbour.

(Largest 10 annual maxima (Table 3-1) plotted in Gringorten plotting positions (rate of 10 events in 108-years). A selection of output locations plotted for comparison with Port of Auckland tide-gauge site. Elevations are relative to AVD-46 including +0.15 m offset for baseline mean sea level (present-day estimate).

Figures 3-8 and 3-9 compare the simulated 100-year ARI storm-tide elevations to the simulation of the 23 January 2011 storm-tide. From extreme sea-level analyses at the Port of Auckland tide-gauge location we estimate that the average recurrence interval for the 23 January 2011 storm-tide was 88–205 years, and so the simulated elevations for 23 January 2011 are expected to lie close to, or a few cm above, the predicted 100-year ARI storm-tide levels (Figure 3-4). Figure 3-9 shows that this is generally the case at most locations throughout the harbour. The most noticeable discrepancy occurs at the three sites located behind the north-western motorway causeway near Pollen Island, where the 23 January 2011 storm-tide simulation is 17 cm above the predicted 100-year ARI levels. The bathymetric resolution of causeway channel in the hydrodynamic model was insufficient to correctly transfer tidal flow (on which the 100-year ARI elevations are based), whereas the combined influence of tide plus storm surge in the 23 January storm-tide simulation was sufficiently high to overcome this limitation in the simulation.

Further validation of the model was provided by the comparison of the simulated present-day 0.01 AEP inundation elevations and maps, against observed flooding during the 2011 storm-tide (Figure 8-9 – Figure 8-15).

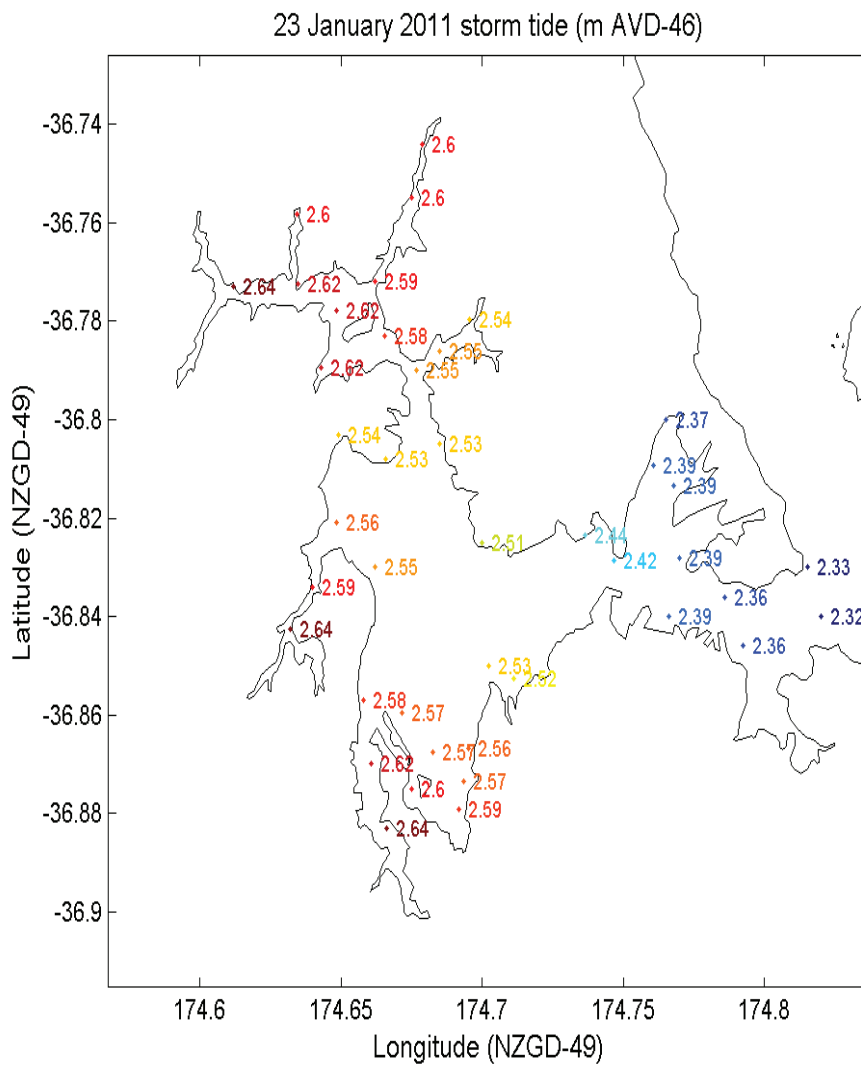


Figure 3-8: Storm-tide elevations in the Waitemata Harbour, simulated for 23 January 2011 storm-tide.
 Elevations are relative to AVD-46 and include +0.15 m (present-day) offset for baseline mean sea-level rise

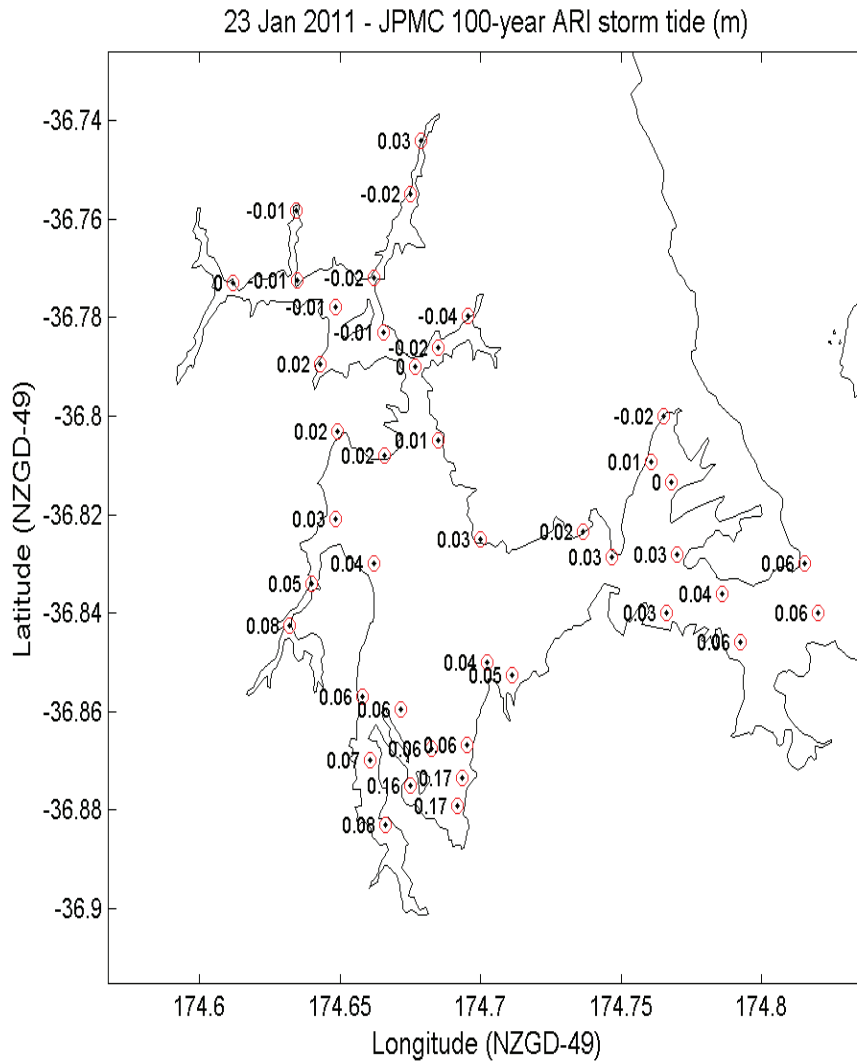


Figure 3-9: Elevation difference (cm) between 23 January 2011 storm-tide simulations and 100-year ARI estimates in the Waitemata Harbour.

(Positive values = 23 January 2011 storm-tide is above 100-year ARI storm-tide estimate, and vice versa.)

Table 3-3: Extreme sea-level in the Waitemata Harbour.

Elevations are relative to AVD-46 including +0.15 m offset for baseline mean sea level (present-day estimate). Elevations calculated from simulated data. Colour-coding corresponds to Figure 3-6.

| Site | Easting (NZTM) | Northing (NZTM) | AEP: | 0.39 | 0.18 | 0.1 | 0.05 | 0.02 | 0.01 | 0.005 |
|------|----------------|-----------------|------|------|------|-------|-------|-------|--------|--------|
| | | | ARI: | 2 yr | 5 yr | 10 yr | 20 yr | 50 yr | 100 yr | 200 yr |
| | | | | | | | | | | |
| 1 | 1762303 | 5921531 | | 1.94 | 2.03 | 2.08 | 2.14 | 2.21 | 2.26 | 2.31 |
| 2 | 1760922 | 5920192 | | 1.98 | 2.06 | 2.12 | 2.17 | 2.24 | 2.30 | 2.35 |
| 3 | 1759830 | 5920934 | | 1.99 | 2.07 | 2.13 | 2.18 | 2.25 | 2.30 | 2.35 |
| 4 | 1757487 | 5921632 | | 2.04 | 2.12 | 2.18 | 2.23 | 2.31 | 2.36 | 2.41 |
| 5 | 1755640 | 5922256 | | 2.08 | 2.16 | 2.22 | 2.27 | 2.34 | 2.40 | 2.45 |
| 6 | 1754603 | 5921918 | | 2.11 | 2.19 | 2.25 | 2.30 | 2.37 | 2.43 | 2.48 |
| 7 | 1753867 | 5923685 | | 2.12 | 2.20 | 2.26 | 2.31 | 2.38 | 2.44 | 2.49 |
| 8 | 1754872 | 5923511 | | 2.10 | 2.18 | 2.24 | 2.29 | 2.36 | 2.42 | 2.47 |
| 9 | 1755321 | 5924125 | | 2.10 | 2.18 | 2.23 | 2.29 | 2.36 | 2.41 | 2.46 |
| 10 | 1755798 | 5922917 | | 2.08 | 2.16 | 2.22 | 2.27 | 2.34 | 2.40 | 2.45 |
| 11 | 1756273 | 5923530 | | 2.06 | 2.15 | 2.20 | 2.26 | 2.33 | 2.38 | 2.43 |
| 12 | 1756876 | 5923808 | | 2.06 | 2.14 | 2.20 | 2.25 | 2.32 | 2.38 | 2.43 |
| 13 | 1757077 | 5925036 | | 2.07 | 2.15 | 2.20 | 2.26 | 2.33 | 2.38 | 2.43 |
| 14 | 1757480 | 5926061 | | 2.07 | 2.15 | 2.21 | 2.26 | 2.33 | 2.39 | 2.44 |
| 15 | 1757720 | 5924558 | | 2.07 | 2.15 | 2.20 | 2.26 | 2.33 | 2.38 | 2.43 |
| 16 | 1757504 | 5923474 | | 2.05 | 2.13 | 2.19 | 2.24 | 2.31 | 2.37 | 2.42 |
| 17 | 1758777 | 5923817 | | 2.05 | 2.13 | 2.19 | 2.24 | 2.32 | 2.37 | 2.42 |
| 18 | 1757869 | 5922946 | | 2.04 | 2.13 | 2.18 | 2.24 | 2.31 | 2.36 | 2.41 |
| 19 | 1758183 | 5922574 | | 2.03 | 2.12 | 2.17 | 2.23 | 2.30 | 2.35 | 2.40 |
| 20 | 1759279 | 5922009 | | 2.01 | 2.09 | 2.14 | 2.20 | 2.27 | 2.32 | 2.37 |
| 21 | 1761896 | 5922670 | | 1.95 | 2.03 | 2.09 | 2.14 | 2.21 | 2.26 | 2.31 |
| 22 | 1753394 | 5920977 | | 2.14 | 2.22 | 2.28 | 2.33 | 2.41 | 2.46 | 2.51 |
| 23 | 1752927 | 5920576 | | 2.15 | 2.23 | 2.29 | 2.34 | 2.41 | 2.47 | 2.52 |
| 24 | 1752568 | 5920305 | | 2.16 | 2.24 | 2.30 | 2.35 | 2.42 | 2.47 | 2.52 |
| 25 | 1751774 | 5920613 | | 2.17 | 2.25 | 2.31 | 2.36 | 2.43 | 2.49 | 2.54 |
| 26 | 1751548 | 5920296 | | 2.17 | 2.26 | 2.31 | 2.37 | 2.44 | 2.49 | 2.54 |

| Site | Easting (NZTM) | Northing (NZTM) | AEP: | 0.39 | 0.18 | 0.1 | 0.05 | 0.02 | 0.01 | 0.005 |
|------|----------------|-----------------|------|------|------|-------|-------|-------|--------|--------|
| | | | ARI: | 2 yr | 5 yr | 10 yr | 20 yr | 50 yr | 100 yr | 200 yr |
| | | | | | | | | | | |
| 27 | 1751319 | 5919843 | | 2.18 | 2.26 | 2.32 | 2.37 | 2.44 | 2.50 | 2.55 |
| 28 | 1751176 | 5919250 | | 2.18 | 2.27 | 2.32 | 2.38 | 2.45 | 2.50 | 2.55 |
| 29 | 1751101 | 5918756 | | 2.19 | 2.27 | 2.33 | 2.38 | 2.45 | 2.51 | 2.56 |
| 30 | 1750937 | 5918027 | | 2.08 | 2.16 | 2.22 | 2.27 | 2.34 | 2.40 | 2.45 |
| 31 | 1750777 | 5917400 | | 2.10 | 2.19 | 2.24 | 2.30 | 2.37 | 2.42 | 2.47 |
| 32 | 1749304 | 5917884 | | 2.12 | 2.20 | 2.26 | 2.31 | 2.39 | 2.44 | 2.49 |
| 33 | 1749997 | 5918709 | | 2.19 | 2.27 | 2.33 | 2.38 | 2.45 | 2.51 | 2.56 |
| 34 | 1749646 | 5919012 | | 2.19 | 2.27 | 2.33 | 2.38 | 2.45 | 2.51 | 2.56 |
| 35 | 1749355 | 5919387 | | 2.19 | 2.27 | 2.33 | 2.38 | 2.45 | 2.51 | 2.56 |
| 36 | 1749031 | 5919620 | | 2.19 | 2.27 | 2.33 | 2.38 | 2.45 | 2.51 | 2.56 |
| 37 | 1748233 | 5921920 | | 2.19 | 2.27 | 2.33 | 2.38 | 2.45 | 2.51 | 2.56 |
| 38 | 1748224 | 5922919 | | 2.19 | 2.27 | 2.33 | 2.38 | 2.46 | 2.51 | 2.56 |
| 39 | 1748025 | 5923311 | | 2.19 | 2.28 | 2.33 | 2.39 | 2.46 | 2.51 | 2.57 |
| 40 | 1747622 | 5923718 | | 2.20 | 2.28 | 2.34 | 2.39 | 2.46 | 2.52 | 2.57 |
| 41 | 1747028 | 5923917 | | 2.20 | 2.29 | 2.34 | 2.40 | 2.47 | 2.52 | 2.58 |
| 42 | 1746820 | 5924309 | | 2.20 | 2.29 | 2.34 | 2.40 | 2.47 | 2.52 | 2.58 |
| 43 | 1750882 | 5924426 | | 2.18 | 2.26 | 2.32 | 2.37 | 2.44 | 2.50 | 2.55 |
| 44 | 1747124 | 5925913 | | 2.20 | 2.28 | 2.34 | 2.39 | 2.46 | 2.52 | 2.57 |
| 45 | 1747619 | 5925615 | | 2.20 | 2.28 | 2.34 | 2.39 | 2.46 | 2.52 | 2.57 |
| 46 | 1748124 | 5925418 | | 2.20 | 2.28 | 2.34 | 2.39 | 2.46 | 2.52 | 2.57 |
| 47 | 1748622 | 5925321 | | 2.19 | 2.28 | 2.33 | 2.39 | 2.46 | 2.51 | 2.57 |
| 48 | 1749020 | 5925613 | | 2.20 | 2.28 | 2.34 | 2.39 | 2.46 | 2.52 | 2.57 |
| 49 | 1749222 | 5925920 | | 2.21 | 2.29 | 2.35 | 2.40 | 2.47 | 2.53 | 2.58 |
| 50 | 1749318 | 5926318 | | 2.22 | 2.30 | 2.35 | 2.41 | 2.48 | 2.53 | 2.59 |
| 51 | 1749521 | 5926714 | | 2.23 | 2.31 | 2.37 | 2.42 | 2.49 | 2.55 | 2.60 |
| 52 | 1749923 | 5926718 | | 2.23 | 2.31 | 2.37 | 2.42 | 2.49 | 2.54 | 2.60 |
| 53 | 1750332 | 5925635 | | 2.20 | 2.28 | 2.34 | 2.39 | 2.46 | 2.52 | 2.57 |
| 54 | 1750882 | 5924426 | | 2.18 | 2.26 | 2.32 | 2.37 | 2.44 | 2.50 | 2.55 |

| Site | Easting (NZTM) | Northing (NZTM) | AEP: | 0.39 | 0.18 | 0.1 | 0.05 | 0.02 | 0.01 | 0.005 |
|------|----------------|-----------------|------|------|------|-------|-------|-------|--------|--------|
| | | | ARI: | 2 yr | 5 yr | 10 yr | 20 yr | 50 yr | 100 yr | 200 yr |
| | | | | | | | | | | |
| 55 | 1751631 | 5923392 | | 2.16 | 2.24 | 2.30 | 2.35 | 2.42 | 2.48 | 2.53 |
| 56 | 1752696 | 5923084 | | 2.14 | 2.22 | 2.28 | 2.33 | 2.40 | 2.45 | 2.51 |
| 57 | 1748140 | 5917965 | | 2.23 | 2.32 | 2.37 | 2.43 | 2.50 | 2.55 | 2.60 |
| 58 | 1748221 | 5917482 | | 2.23 | 2.32 | 2.38 | 2.43 | 2.50 | 2.55 | 2.60 |
| 59 | 1748140 | 5917965 | | 2.23 | 2.32 | 2.37 | 2.43 | 2.50 | 2.55 | 2.60 |
| 60 | 1748031 | 5918485 | | 2.23 | 2.31 | 2.37 | 2.42 | 2.49 | 2.55 | 2.60 |
| 61 | 1747920 | 5918968 | | 2.22 | 2.31 | 2.36 | 2.42 | 2.49 | 2.54 | 2.59 |
| 62 | 1747898 | 5919449 | | 2.21 | 2.29 | 2.35 | 2.41 | 2.48 | 2.53 | 2.58 |
| 63 | 1747833 | 5919919 | | 2.20 | 2.28 | 2.34 | 2.39 | 2.47 | 2.52 | 2.57 |
| 64 | 1748434 | 5920119 | | 2.19 | 2.28 | 2.33 | 2.39 | 2.46 | 2.51 | 2.56 |
| 65 | 1747832 | 5920917 | | 2.19 | 2.28 | 2.33 | 2.39 | 2.46 | 2.51 | 2.56 |
| 66 | 1748033 | 5921213 | | 2.19 | 2.27 | 2.33 | 2.38 | 2.46 | 2.51 | 2.56 |
| 67 | 1746620 | 5927412 | | 2.28 | 2.36 | 2.42 | 2.47 | 2.54 | 2.60 | 2.65 |
| 68 | 1746820 | 5927915 | | 2.28 | 2.36 | 2.42 | 2.47 | 2.54 | 2.60 | 2.65 |
| 69 | 1747616 | 5928013 | | 2.27 | 2.36 | 2.42 | 2.47 | 2.54 | 2.59 | 2.64 |
| 70 | 1748118 | 5928115 | | 2.27 | 2.36 | 2.41 | 2.47 | 2.54 | 2.59 | 2.64 |
| 71 | 1748618 | 5928117 | | 2.27 | 2.35 | 2.41 | 2.46 | 2.53 | 2.59 | 2.64 |
| 72 | 1747119 | 5928709 | | 2.30 | 2.39 | 2.44 | 2.50 | 2.57 | 2.62 | 2.68 |
| 73 | 1743880 | 5929297 | | 2.32 | 2.41 | 2.46 | 2.52 | 2.59 | 2.64 | 2.70 |
| 74 | 1744235 | 5929180 | | 2.32 | 2.41 | 2.46 | 2.52 | 2.59 | 2.64 | 2.70 |
| 75 | 1744613 | 5929407 | | 2.32 | 2.41 | 2.46 | 2.51 | 2.59 | 2.64 | 2.69 |
| 76 | 1745617 | 5929612 | | 2.32 | 2.40 | 2.46 | 2.51 | 2.58 | 2.64 | 2.69 |
| 77 | 1745809 | 5929908 | | 2.29 | 2.38 | 2.43 | 2.49 | 2.56 | 2.62 | 2.67 |
| 78 | 1745909 | 5930885 | | 2.30 | 2.38 | 2.44 | 2.49 | 2.56 | 2.61 | 2.66 |
| 79 | 1745915 | 5929318 | | 2.31 | 2.40 | 2.45 | 2.51 | 2.58 | 2.63 | 2.69 |
| 80 | 1746617 | 5929606 | | 2.31 | 2.39 | 2.45 | 2.50 | 2.57 | 2.63 | 2.68 |
| 81 | 1747617 | 5929611 | | 2.30 | 2.38 | 2.44 | 2.49 | 2.56 | 2.62 | 2.67 |
| 82 | 1748344 | 5929332 | | 2.29 | 2.37 | 2.43 | 2.48 | 2.55 | 2.61 | 2.66 |

| Site | Easting (NZTM) | Northing (NZTM) | AEP: | 0.39 | 0.18 | 0.1 | 0.05 | 0.02 | 0.01 | 0.005 |
|------|----------------|-----------------|------|------|------|-------|-------|-------|--------|--------|
| | | | ARI: | 2 yr | 5 yr | 10 yr | 20 yr | 50 yr | 100 yr | 200 yr |
| | | | | | | | | | | |
| 83 | 1749079 | 5930540 | | 2.31 | 2.39 | 2.45 | 2.50 | 2.57 | 2.62 | 2.68 |
| 84 | 1749537 | 5931198 | | 2.31 | 2.40 | 2.45 | 2.50 | 2.57 | 2.63 | 2.68 |
| 85 | 1749907 | 5932412 | | 2.25 | 2.33 | 2.39 | 2.44 | 2.51 | 2.56 | 2.61 |
| 86 | 1748417 | 5928920 | | 2.28 | 2.37 | 2.42 | 2.47 | 2.55 | 2.60 | 2.65 |
| 87 | 1749621 | 5927312 | | 2.24 | 2.32 | 2.38 | 2.43 | 2.50 | 2.56 | 2.61 |
| 88 | 1749565 | 5927646 | | 2.24 | 2.33 | 2.38 | 2.44 | 2.51 | 2.56 | 2.61 |
| 89 | 1750370 | 5927743 | | 2.25 | 2.34 | 2.39 | 2.44 | 2.52 | 2.57 | 2.62 |
| 90 | 1750923 | 5928128 | | 2.26 | 2.34 | 2.40 | 2.45 | 2.52 | 2.58 | 2.63 |
| 91 | 1751319 | 5928425 | | 2.26 | 2.35 | 2.40 | 2.45 | 2.52 | 2.58 | 2.63 |
| 92 | 1745533 | 5921567 | | 2.24 | 2.32 | 2.38 | 2.43 | 2.50 | 2.56 | 2.61 |
| 93 | 1745541 | 5922011 | | 2.23 | 2.32 | 2.37 | 2.43 | 2.50 | 2.55 | 2.60 |
| 94 | 1746262 | 5922487 | | 2.22 | 2.31 | 2.36 | 2.42 | 2.49 | 2.54 | 2.59 |
| 95 | 1746430 | 5923416 | | 2.21 | 2.30 | 2.35 | 2.41 | 2.48 | 2.53 | 2.59 |

3.2 Manukau Harbour

The methods used to simulate storm-tide time-series and frequency-magnitude distributions are explained in Section 7.3; this section provides information and examples specific to the application of those methods in the Manukau Harbour.

3.2.1 Tide-gauge

The modern digital Onehunga tide-gauge record (1 Jan 2001 – 31 May 2011) was used as the base dataset for storm-tide modelling in the Manukau Harbour (Figure 3-10). Note: this is much shorter than the lengthy record that was available for the Ports of Auckland Waitemata Harbour gauge, which will result in more uncertainty in upper extreme storm-tide values.

Fortunately, a historical analysis of the higher storm-tide levels measured at the Port of Onehunga is available (Auckland Harbour Board 1974) for the period 1926 to 1973.

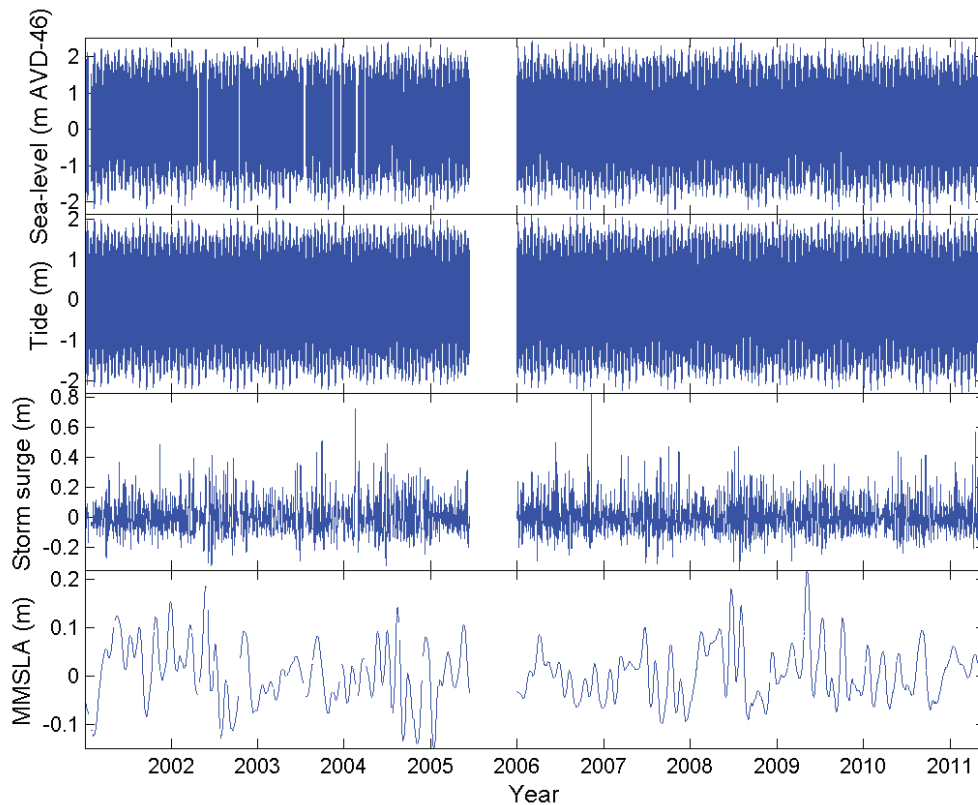


Figure 3-10: Onehunga sea-level record used for this study.

(The raw sea-level is plotted relative to AVD-46. Three sea-level components are also plotted: astronomical tide, storm surge and monthly mean sea-level anomaly (MMSLA). Source: measurements from Ports of Auckland Ltd.)

3.2.2 Hydrodynamic model

An existing calibrated hydrodynamic model, Figure 3-11, Figure 3-12 (Reeve & Pritchard 2010) was used to simulate tides and the wind-driven component of storm surge in the Manukau Harbour. The bathymetry is much better resolved in the shallow upper reaches of the Manukau Harbour in this hydrodynamic model, compared to model used by Stephens et al. (2011c). This, together with the simulation and scaling of tide over a full lunar month, means that the levels simulated here are considered to supersede those of Stephens et al. (2011c).

The hydrodynamic model was calibrated and validated against sea-level and current measurements at Onehunga Wharf, Paratutae Island, Waiuku, Papakura, Purakau and Wairopa Channels, Karore Bank, and Pahurehure Inlet. Water level calibrations indicated root-mean-square errors in the range 7–19 cm, relative-root-mean-square errors of $\leq 5\%$ and bias of 1–9 cm, meaning that the model slightly over-predicted sea-level heights. This means that simulated storm-tide levels in the harbour will be conservatively high.

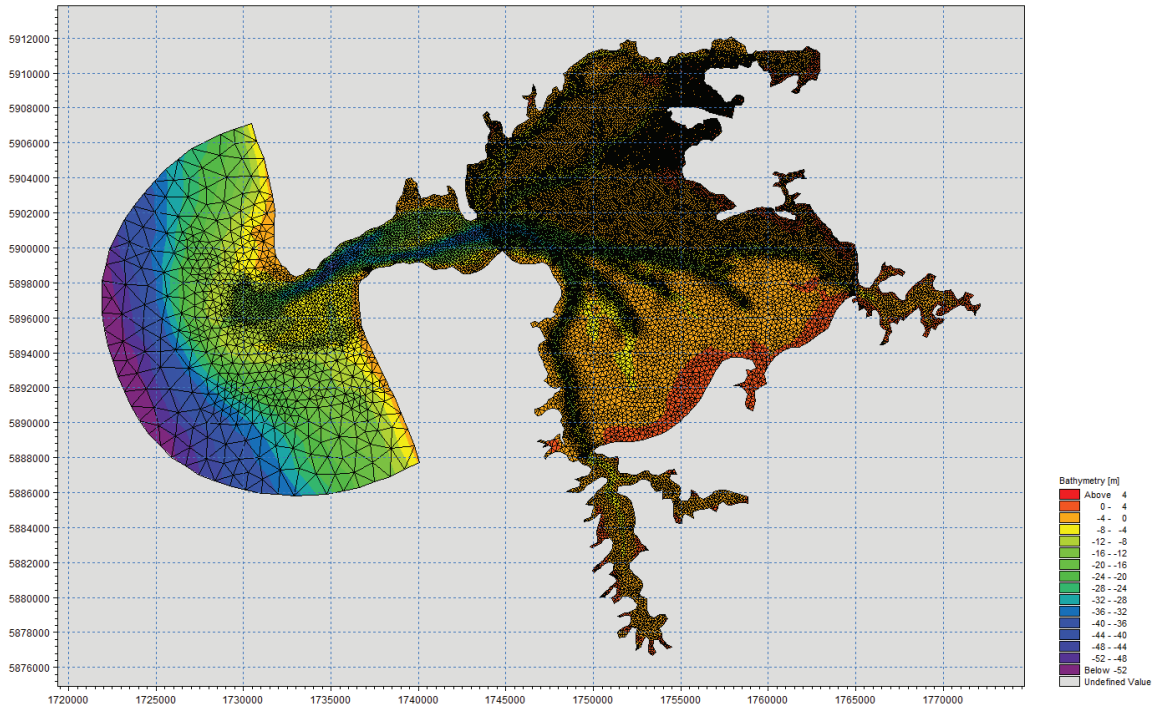


Figure 3-11: Hydrodynamic model MIKE3FM flexible mesh grid of the Manukau Harbour.

(Colour scale indicates depth.)

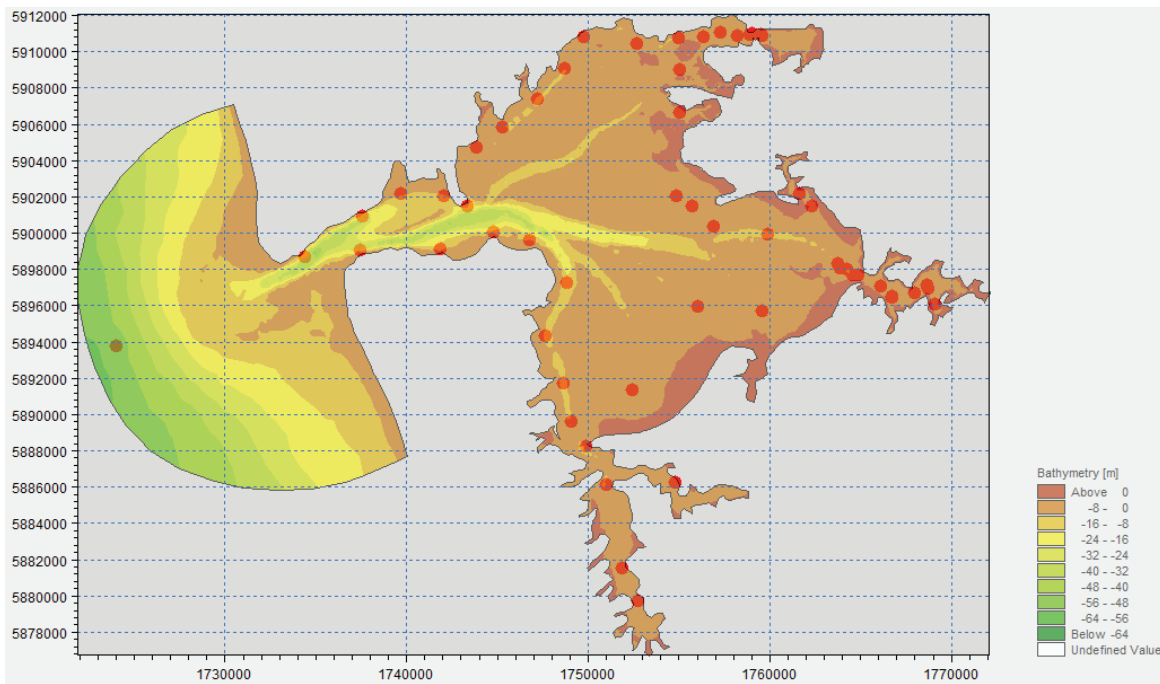


Figure 3-12: Hydrodynamic model bathymetry, with output locations marked.

3.2.3 Modelling storm surge

The Auckland Airport (located adjacent to the Manukau Harbour) wind and mean sea-level pressure records were obtained from 8 Nov 1965 – 11 May 2011. The wind-driven component of storm surge was calculated as described in Section 7.3 by using the wind record to interpolate storm surge from the

simulated wind-surge response matrix from the hydrodynamic model. The wind-driven component of storm surge differs depending on the output location within the harbour due to the available wind fetch.

The inverse-barometer component of sea level was calculated as described in Section 7.3.1.

3.2.4 Modelling storm-tide

Storm-tide time-series were simulated using the methods described in Sections 2.3.1 and 7.3, at 68 locations within the Manukau Harbour (Figure 3-12), for later extreme sea-level analysis.

Time-series of monthly MMSLA were not simulated in the Manukau Harbour model, but the empirical cumulative exceedance distribution of MMSLA, derived from the Onehunga tide gauge (location in Figure 3-12), was included in the Monte Carlo joint-probability extreme sea-level modelling.

For each output location, the tidal time-series were added to the storm surge time-series, and combined with MMSLA in a MCJP extreme sea-level analysis

Tidal hysteresis was calculated from the hydrodynamic model using the mean sea level over the simulated lunar month; enabling a mean sea-level offset to be calculated for each location, relative to the Onehunga tide-gauge location. This mean sea-level offset due to tidal hysteresis was added to the extreme storm-tide distribution at each output location.

Figure 3-13 plots extreme storm-tide peaks and extreme sea-level distributions predicted for the Onehunga tide gauge. There are two extreme sea-level curves plotted – the MCJP curve is reliable, but the GPD fit to POT curve is unreliable, as follows:

Seven large historical events

The seven largest recorded historical storm-tides (Table 3-4) are plotted in their Gringorten plotting positions, with six of these events from the analysis of 1926 to 1973 by the Auckland Harbour Board (1974). The Gringorten plotting positions assume that the empirical distribution of the data follows a Gumbel extreme-value distribution. An assumption has been made that these are the 7 largest storm-tides in the 86 years since the earliest in 1926. However they could be the largest events in a longer timeframe, or there may have been sizeable events in the data gap between 1974 and the start of the modern record, and this would affect their plotting positions on Figure 3-13. Nevertheless, they provide a useful comparison for the fit of the two extreme-value models.

Unreliable GPD fit to modern digital data

A GPD model was fitted to the largest 5 storm-tides per year from the modern 2001–2011 digital record. The 2001–2011 record is not long enough (insufficient extreme events) to get reliable extreme sea-level estimates using the POT/GPD technique, hence the very flat distribution at low exceedance probabilities that under-predicts the historical storm-tide peak magnitudes.

Reliable MCJP fit to modern data

The extreme sea-level frequency–magnitude distribution from the MCJP technique, fitted using 2001–2011 data, is also plotted. The MCJP technique considers all possible combinations of tides, storm surges and MMSLA (even if the numerous possible combinations did not occur within the measured record), and so it compares better with the Gringorten estimates of the historical storm-tides. The MCJP technique is upward biased at higher AEPs (left side of Figure 3-13) by ≤ 5 cm.

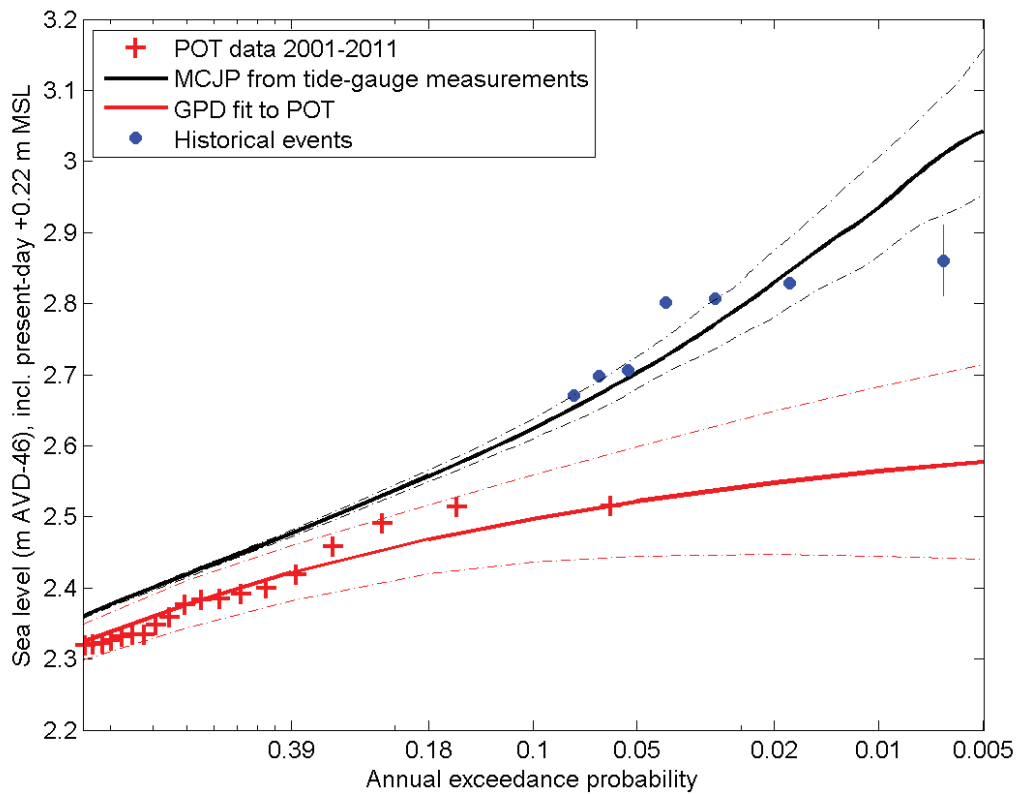


Figure 3-13: Extreme sea-level frequency–magnitude distribution at the Onehunga tide gauge in the Manukau Harbour.

Elevations are relative to AVD-46 including +0.22 m offset for baseline mean sea level (present-day estimate). Historical events in Table 3-4.

Table 3-4: The seven largest storm-tide annual maxima since 1926 recorded at Onehunga.

Excludes a gap from 1974 to start of modern record in 2001.

| Date | Metres above AVD-46; raw data with no sea-level rise adjustment | Metres above AVD-46 adjusted to present-day MSL = +0.22 m AVD-46, adjusted for 1.5mm/yr SLR |
|----------------------------|---|---|
| 22-Jun-47 | 2.74 | 2.80 |
| 7-Sep-48 | 2.72 | 2.81 |
| 1949 | 2.62 | 2.71 |
| 1954 | 2.62 | 2.70 |
| 31-Aug-65 | 2.74 | 2.83 |
| 1972 | 2.62 | 2.67 |
| 17-Apr-99 (lower estimate) | 2.80 | 2.81 |
| 17-Apr-99 (upper estimate) | 2.90 | 2.91 |

Figure 3-14 compares the extreme sea-level frequency–magnitude distributions derived from the Onehunga gauge data (Figure 3-10), and from simulated data at the gauge site, and, for comparison, at sites located in the upper Pahurehure inlet and in the tidal inlet channel near the harbour entrance. Using the IBfactor as a calibration parameter, the extreme sea-level distributions from both measured and simulated data were closely matched at the Onehunga tide-gauge site. The other curves demonstrate how the simulated extreme sea-level magnitudes decrease toward the harbour entrance and increase toward the head of the harbour, due to amplification of the tide and storm surge. Note also how the slope of extreme sea-level curve steepens at lower frequencies. This represents a change in storm–tide characteristics between smaller and larger events. Although tides are the major component of all storm-tides, moderate to large storm surges play an increasingly important role in the very largest storm-tides. Traditional direct extreme-value techniques (POT/GPD, AM/GEV Table 7-4) cannot account for this change in storm-tide characteristics across all of the recorded storm-tides. Instead, a long enough data record is required that the direct techniques be fitted only to the largest storm-tide population (represented by the steeper, lower-frequency part of the MCJP curve). For short data records, where few or no large storm-tides are expected, the direct techniques fit to the smallest storm-tide population (represented by the shallower, lower, higher-frequency part of the MCJP curve), and a result is obtained like that shown in Figure 3-13.

Table 3-5 provides the estimated extreme sea-level frequency–magnitude relationship at Onehunga based on the MCJP technique applied to the Onehunga tide-gauge record. Table 3-6 provides the estimated extreme sea-level frequency–magnitude relationship at locations throughout the harbour.

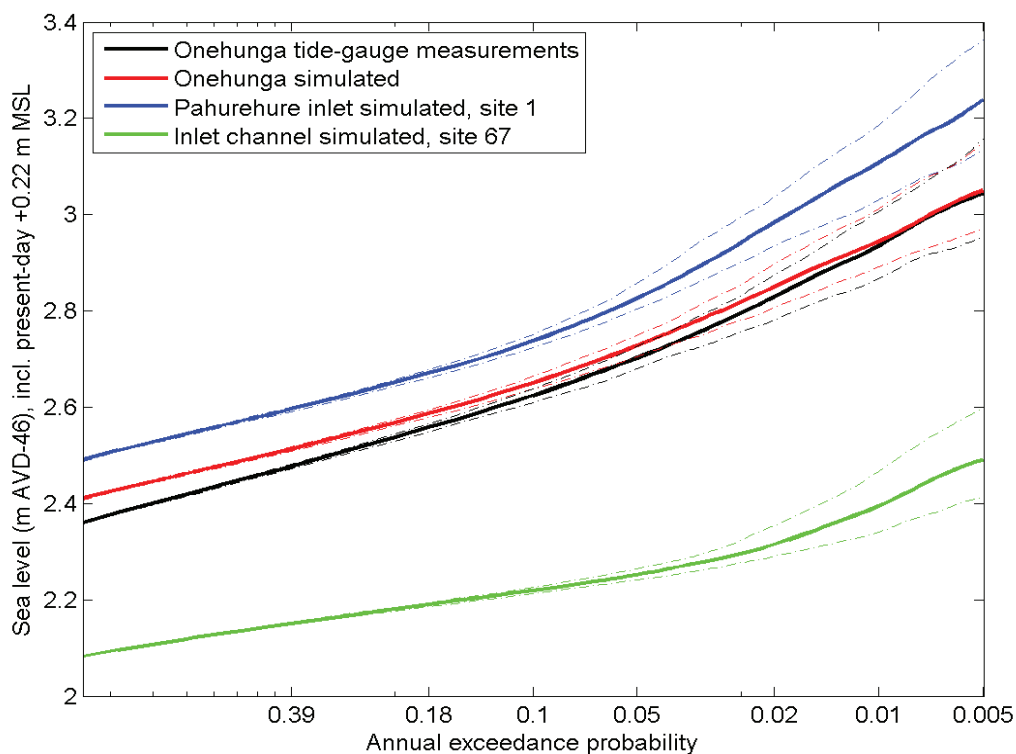


Figure 3-14: Extreme sea-level frequency–magnitude distribution at selected locations in the Manukau Harbour.

(Elevations are relative to AVD-46 including +0.22 m offset for baseline mean sea level (present-day estimate). The black line is identical to that in Figure 3-13.)

Table 3-5: Extreme sea-level at Onehunga.

Elevations are relative to AVD-46 including +0.22 m offset for baseline mean sea level (present-day estimate). C.I. = confidence interval. Elevations calculated from tide-gauge data.

| AEP | 0.39 | 0.18 | 0.10 | 0.05 | 0.02 | 0.01 | 0.005 |
|-----------------|------|------|------|------|------|------|-------|
| ARI | 2 | 5 | 10 | 20 | 50 | 100 | 200 |
| Median | 2.48 | 2.56 | 2.62 | 2.70 | 2.83 | 2.93 | 3.04 |
| Lower 95th C.I. | 2.47 | 2.55 | 2.61 | 2.68 | 2.78 | 2.87 | 2.95 |
| Upper 95th C.I. | 2.48 | 2.57 | 2.64 | 2.73 | 2.87 | 3.01 | 3.16 |

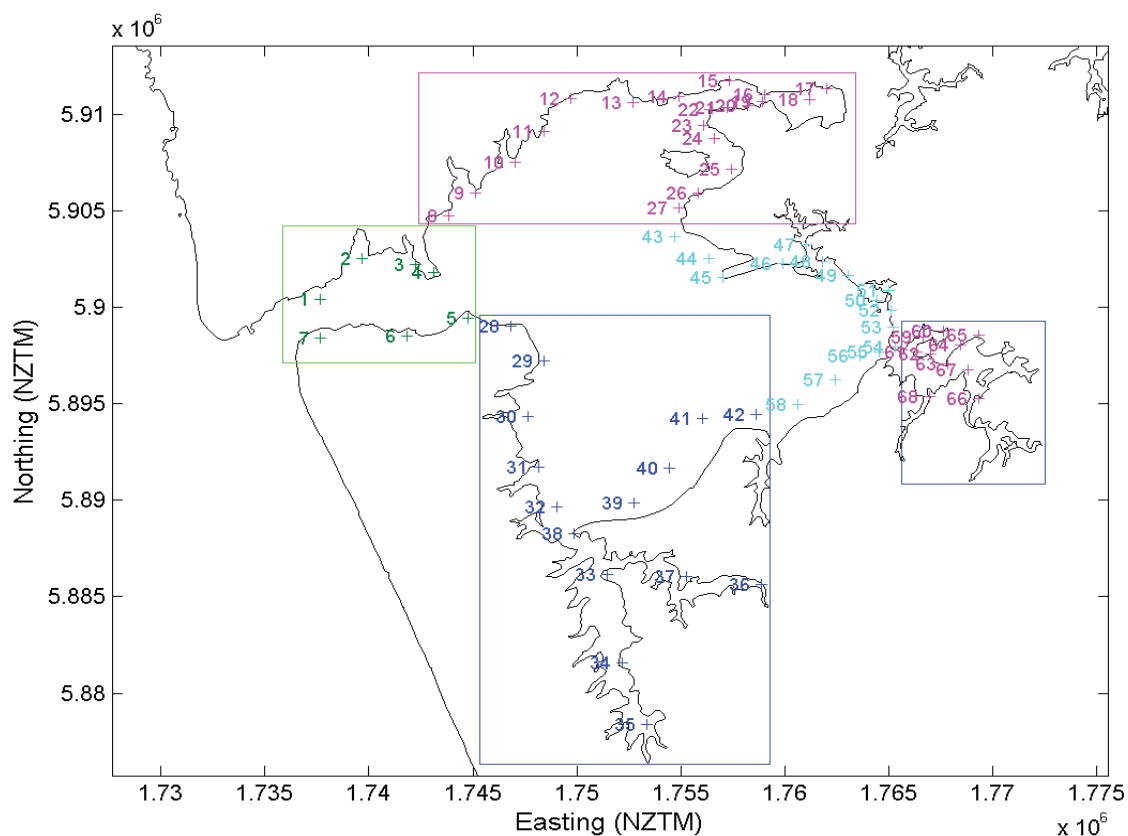


Figure 3-15: Locations of extreme sea-level calculations in the Manukau Harbour.

(Colour-coding corresponds to Table 3-6.)

Table 3-6: Extreme sea-level in the Manukau Harbour.

Elevations are relative to AVD-46 including +0.22 m offset for baseline mean sea level (present-day estimate). Elevations calculated from simulated data. Colour-coding corresponds to Figure 315.

| Site | Easting (NZTM) | Northing (NZTM) | AEP: | 0.39 | 0.18 | 0.1 | 0.05 | 0.02 | 0.01 | 0.005 |
|------|----------------|-----------------|------|------|------|-------|-------|-------|--------|--------|
| | | | ARI: | 2 yr | 5 yr | 10 yr | 20 yr | 50 yr | 100 yr | 200 yr |
| 1 | 1737645 | 5900426 | | 2.15 | 2.18 | 2.21 | 2.25 | 2.31 | 2.39 | 2.48 |
| 2 | 1739641 | 5902530 | | 2.23 | 2.27 | 2.31 | 2.34 | 2.40 | 2.47 | 2.55 |
| 3 | 1742241 | 5902235 | | 2.20 | 2.24 | 2.27 | 2.31 | 2.38 | 2.47 | 2.56 |
| 4 | 1743142 | 5901836 | | 2.34 | 2.39 | 2.42 | 2.46 | 2.52 | 2.57 | 2.64 |
| 5 | 1744746 | 5899440 | | 2.28 | 2.32 | 2.35 | 2.39 | 2.46 | 2.55 | 2.65 |
| 6 | 1741848 | 5898534 | | 2.19 | 2.23 | 2.26 | 2.30 | 2.36 | 2.45 | 2.55 |
| 7 | 1737649 | 5898426 | | 2.13 | 2.17 | 2.21 | 2.24 | 2.30 | 2.37 | 2.46 |
| 8 | 1743836 | 5904737 | | 2.29 | 2.33 | 2.36 | 2.40 | 2.47 | 2.56 | 2.65 |
| 9 | 1745134 | 5905940 | | 2.33 | 2.37 | 2.40 | 2.44 | 2.51 | 2.60 | 2.69 |
| 10 | 1747030 | 5907543 | | 2.34 | 2.39 | 2.42 | 2.46 | 2.54 | 2.63 | 2.73 |
| 11 | 1748427 | 5909146 | | 2.35 | 2.40 | 2.43 | 2.48 | 2.57 | 2.66 | 2.75 |
| 12 | 1749723 | 5910848 | | 2.39 | 2.44 | 2.49 | 2.54 | 2.63 | 2.71 | 2.79 |
| 13 | 1752724 | 5910654 | | 2.42 | 2.48 | 2.53 | 2.60 | 2.69 | 2.77 | 2.85 |
| 14 | 1754923 | 5910958 | | 2.47 | 2.53 | 2.59 | 2.66 | 2.76 | 2.84 | 2.93 |
| 15 | 1757321 | 5911763 | | 2.50 | 2.57 | 2.63 | 2.71 | 2.83 | 2.92 | 3.02 |
| 16 | 1759022 | 5911066 | | 2.54 | 2.62 | 2.68 | 2.76 | 2.88 | 2.97 | 3.08 |
| 17 | 1762021 | 5911372 | | 2.56 | 2.64 | 2.72 | 2.80 | 2.92 | 3.00 | 3.09 |
| 18 | 1761223 | 5910771 | | 2.51 | 2.58 | 2.66 | 2.76 | 2.91 | 3.02 | 3.12 |
| 19 | 1758923 | 5910666 | | 2.54 | 2.61 | 2.67 | 2.75 | 2.87 | 2.97 | 3.07 |
| 20 | 1758223 | 5910465 | | 2.52 | 2.59 | 2.65 | 2.73 | 2.85 | 2.95 | 3.05 |
| 21 | 1757224 | 5910363 | | 2.50 | 2.57 | 2.63 | 2.71 | 2.83 | 2.93 | 3.03 |
| 22 | 1756424 | 5910261 | | 2.50 | 2.57 | 2.63 | 2.70 | 2.82 | 2.92 | 3.02 |
| 23 | 1756126 | 5909461 | | 2.48 | 2.55 | 2.61 | 2.69 | 2.82 | 2.91 | 3.02 |
| 24 | 1756627 | 5908762 | | 2.48 | 2.55 | 2.62 | 2.70 | 2.83 | 2.92 | 3.03 |
| 25 | 1757430 | 5907164 | | 2.45 | 2.52 | 2.58 | 2.67 | 2.81 | 2.91 | 3.03 |
| 26 | 1755832 | 5905960 | | 2.43 | 2.49 | 2.54 | 2.62 | 2.77 | 2.88 | 2.99 |

| Site | Easting (NZTM) | Northing (NZTM) | AEP: | 0.39 | 0.18 | 0.1 | 0.05 | 0.02 | 0.01 | 0.005 |
|------|----------------|-----------------|------|------|------|-------|-------|-------|--------|--------|
| | | | ARI: | 2 yr | 5 yr | 10 yr | 20 yr | 50 yr | 100 yr | 200 yr |
| 27 | 1754934 | 5905159 | | 2.42 | 2.48 | 2.53 | 2.61 | 2.75 | 2.86 | 2.97 |
| 28 | 1746847 | 5899044 | | 2.32 | 2.36 | 2.39 | 2.43 | 2.51 | 2.61 | 2.71 |
| 29 | 1748450 | 5897247 | | 2.37 | 2.41 | 2.45 | 2.49 | 2.58 | 2.68 | 2.78 |
| 30 | 1747655 | 5894346 | | 2.38 | 2.42 | 2.46 | 2.50 | 2.60 | 2.71 | 2.82 |
| 31 | 1748160 | 5891747 | | 2.44 | 2.48 | 2.53 | 2.58 | 2.71 | 2.83 | 2.95 |
| 32 | 1749064 | 5889649 | | 2.49 | 2.55 | 2.61 | 2.68 | 2.83 | 2.95 | 3.08 |
| 33 | 1751470 | 5886154 | | 2.53 | 2.58 | 2.63 | 2.72 | 2.89 | 3.03 | 3.17 |
| 34 | 1752179 | 5881555 | | 2.63 | 2.70 | 2.77 | 2.86 | 3.04 | 3.18 | 3.32 |
| 35 | 1753385 | 5878358 | | 2.67 | 2.74 | 2.82 | 2.93 | 3.12 | 3.26 | 3.42 |
| 36 | 1758871 | 5885667 | | 2.68 | 2.75 | 2.82 | 2.93 | 3.12 | 3.26 | 3.41 |
| 37 | 1755270 | 5886061 | | 2.67 | 2.72 | 2.78 | 2.88 | 3.05 | 3.20 | 3.34 |
| 38 | 1749867 | 5888251 | | 2.49 | 2.54 | 2.59 | 2.67 | 2.84 | 2.97 | 3.11 |
| 39 | 1752763 | 5889856 | | 2.44 | 2.49 | 2.55 | 2.64 | 2.81 | 2.95 | 3.08 |
| 40 | 1754460 | 5891659 | | 2.45 | 2.50 | 2.56 | 2.65 | 2.82 | 2.95 | 3.09 |
| 41 | 1756055 | 5894262 | | 2.43 | 2.48 | 2.54 | 2.62 | 2.79 | 2.93 | 3.06 |
| 42 | 1758654 | 5894467 | | 2.43 | 2.49 | 2.55 | 2.64 | 2.82 | 2.95 | 3.09 |
| 43 | 1754737 | 5903659 | | 2.41 | 2.46 | 2.51 | 2.56 | 2.65 | 2.73 | 2.82 |
| 44 | 1756339 | 5902562 | | 2.42 | 2.48 | 2.52 | 2.58 | 2.67 | 2.76 | 2.86 |
| 45 | 1757041 | 5901563 | | 2.43 | 2.48 | 2.52 | 2.57 | 2.68 | 2.77 | 2.87 |
| 46 | 1759939 | 5902269 | | 2.49 | 2.55 | 2.60 | 2.66 | 2.77 | 2.87 | 2.96 |
| 47 | 1761037 | 5903271 | | 2.55 | 2.61 | 2.66 | 2.72 | 2.83 | 2.92 | 3.02 |
| 48 | 1761839 | 5902372 | | 2.55 | 2.61 | 2.67 | 2.73 | 2.85 | 2.95 | 3.05 |
| 49 | 1763040 | 5901675 | | 2.54 | 2.61 | 2.67 | 2.74 | 2.87 | 2.97 | 3.07 |
| 50 | 1764443 | 5900377 | | 2.56 | 2.62 | 2.69 | 2.77 | 2.90 | 3.01 | 3.12 |
| 51 | 1765042 | 5900879 | | 2.57 | 2.64 | 2.71 | 2.79 | 2.92 | 3.02 | 3.13 |
| 52 | 1765144 | 5899879 | | 2.56 | 2.63 | 2.69 | 2.78 | 2.92 | 3.03 | 3.14 |
| 53 | 1765246 | 5898979 | | 2.56 | 2.62 | 2.69 | 2.77 | 2.92 | 3.05 | 3.17 |
| 54 | 1765347 | 5897979 | | 2.55 | 2.62 | 2.68 | 2.77 | 2.92 | 3.05 | 3.18 |

| Site | Easting (NZTM) | Northing (NZTM) | AEP: | 0.39 | 0.18 | 0.1 | 0.05 | 0.02 | 0.01 | 0.005 |
|------|----------------|-----------------|------|------|------|-------|-------|-------|--------|--------|
| | | | ARI: | 2 yr | 5 yr | 10 yr | 20 yr | 50 yr | 100 yr | 200 yr |
| 55 | 1764548 | 5897678 | | 2.55 | 2.61 | 2.67 | 2.75 | 2.91 | 3.03 | 3.17 |
| 56 | 1763648 | 5897476 | | 2.54 | 2.60 | 2.66 | 2.75 | 2.90 | 3.03 | 3.16 |
| 57 | 1762451 | 5896274 | | 2.53 | 2.59 | 2.65 | 2.74 | 2.91 | 3.04 | 3.18 |
| 58 | 1760653 | 5894970 | | 2.46 | 2.52 | 2.58 | 2.68 | 2.85 | 2.98 | 3.12 |
| 59 | 1766646 | 5898482 | | 2.59 | 2.66 | 2.72 | 2.81 | 2.97 | 3.09 | 3.22 |
| 60 | 1767646 | 5898784 | | 2.60 | 2.67 | 2.73 | 2.82 | 2.98 | 3.11 | 3.22 |
| 61 | 1766348 | 5897681 | | 2.59 | 2.66 | 2.72 | 2.81 | 2.97 | 3.10 | 3.22 |
| 62 | 1767048 | 5897583 | | 2.61 | 2.68 | 2.74 | 2.83 | 2.98 | 3.12 | 3.25 |
| 63 | 1767849 | 5897084 | | 2.63 | 2.70 | 2.77 | 2.86 | 3.02 | 3.15 | 3.27 |
| 64 | 1768447 | 5898085 | | 2.64 | 2.71 | 2.78 | 2.87 | 3.02 | 3.15 | 3.28 |
| 65 | 1769346 | 5898587 | | 2.65 | 2.72 | 2.79 | 2.88 | 3.04 | 3.16 | 3.29 |
| 66 | 1769353 | 5895287 | | 2.95 | 3.03 | 3.10 | 3.20 | 3.37 | 3.51 | 3.66 |
| 67 | 1768850 | 5896786 | | 2.64 | 2.71 | 2.78 | 2.87 | 3.03 | 3.16 | 3.30 |
| 68 | 1766952 | 5895382 | | 2.60 | 2.67 | 2.73 | 2.83 | 2.99 | 3.13 | 3.27 |

3.3 Kaipara Harbour

The methods used to simulate storm-tide time-series and frequency-magnitude distributions are explained in Section 7.3; this section provides information and examples specific to the application of those methods in the Kaipara Harbour.

3.3.1 Tide-gauge analysis¹

The Pouto Point sea-level record from 18 April 2001 to 1 September 2012 is plotted in Figure 3-16. The Pouto Point sea-level gauge is located on a wave-exposed sandy shoreline inside the Kaipara Harbour. Occasionally, sand waves bury the bubbler orifice, affecting the tide-gauge readings for several months. For example, a burial occurred beginning around the start of September 2012. In 2011 the bubbler orifice had broken free of its mooring block (Dale Hansen, Northland Regional Council, pers. comm.), so those data have been omitted from our analysis. As outlined in Section 2.2, we suspect that the relationship between tide-gauge zero and One-Tree-Point 1964 datum needs re-surveying. Despite these difficulties, the gauge record is invaluable as a reference point for hydrodynamic modelling, for tidal harmonic analysis, and for extreme sea-level modelling. Although too short for extreme sea-level analysis using direct techniques (Table 7-4), it is suitable for analysis using the indirect MCJP technique.

¹ Please refer to the NIWA report 2016 (Part 2, Section 2.2) for an additional tide gauge dataset for Helensville.

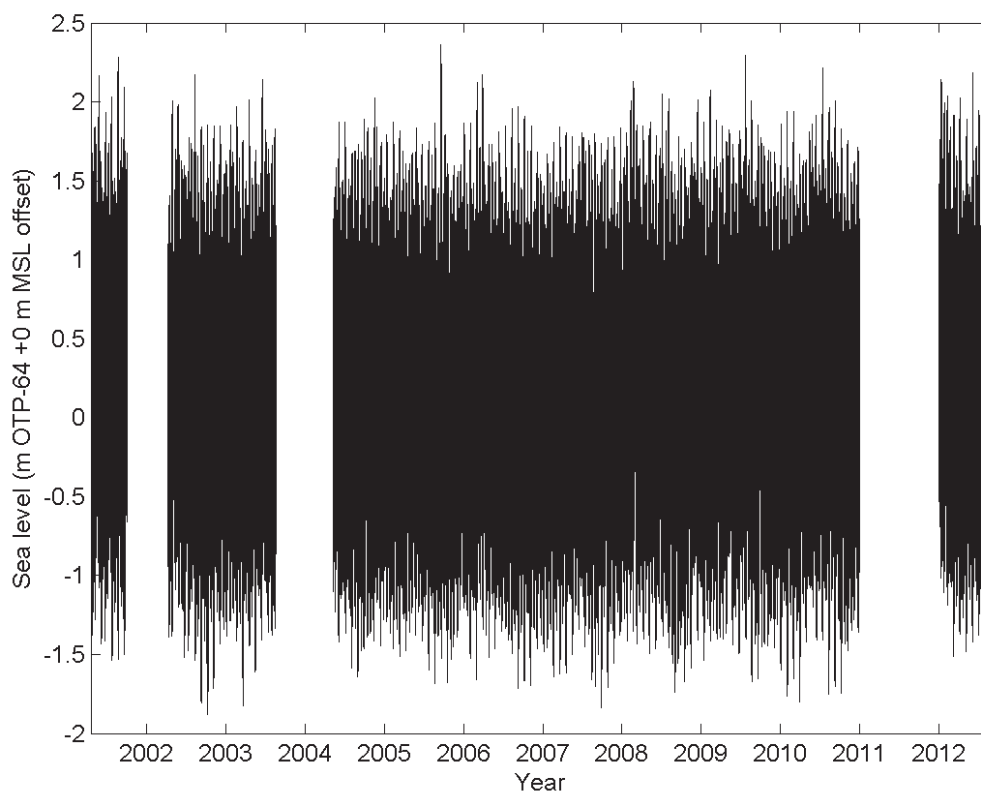


Figure 3-16: Pouto Point sea-level record 2001-2012.

(Source: Northland Regional Council.)

3.3.2 Hydrodynamic model

A Deltares Delft3d 2-dimensional depth averaged hydrodynamic model was developed for the Kaipara Harbour during a previous study for Auckland Council (Pritchard et al. 2012). Three curvi-linear model grids that covered the Northern, Central and Southern areas of the harbour were designed to be online coupled (dynamically nested) and simultaneously run to resolve tidal elevations and hydrodynamic flows through the entire Kaipara Harbour (Figure 3-17). New and archived depth survey data were used to construct the bathymetric grid for the model. The model grid resolved the deeper sub-tidal channels and inter-tidal flats that interact with currents to control the hydrodynamics of the harbour.

A series of calibration and validation simulations were undertaken for a fortnight in March 2011 that coincided with the timing of observations of sea surface elevation and current flow measured around the harbour during an extensive fieldwork program in 2011 and additional bathymetric surveys, Figure 3-18 (Stephens et al. 2011a). The model was driven at an offshore open boundary by tidal sea-level elevations and a wind stress was imposed at the sea surface.

The predicted values were then compared to observational data. The error between predicted and observed data was then assessed using several statistical skill tests. The skill tests for predicted sea surface heights indicated root mean square errors of 10–20 cm, relative root mean square errors ~5%, and bias 1–2 cm indicating excellent agreement with observations. The generation of over-tide harmonics in the model demonstrated that the shallow water effects within the model domain are predicted.

Inclusion of surface wind stress in simulations showed that there was less than 5% improvement introduced by the wind across all skill measures, when compared to the tide-only simulations.

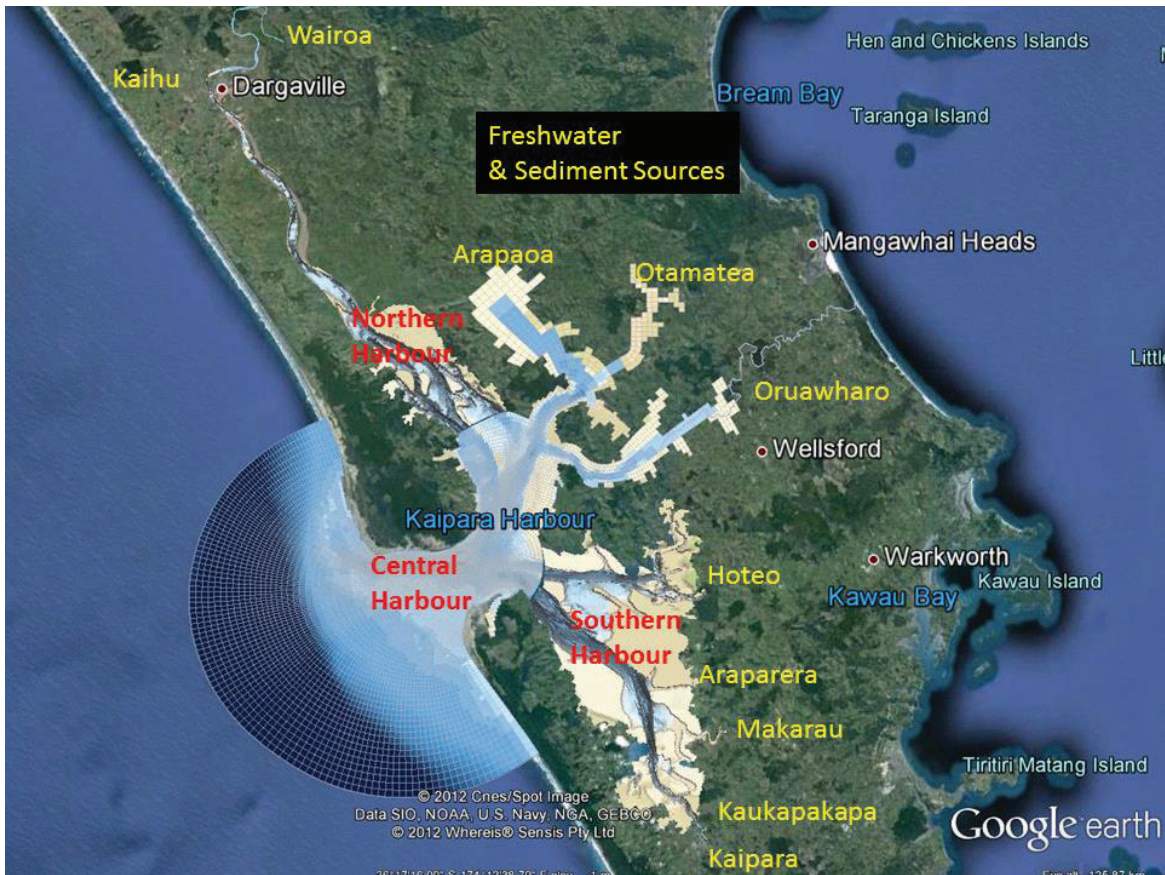


Figure 3-17: Aerial photo of the Kaipara Harbour and tidal inlet with Delft3d model grid overlaid.
 The three coupled model domains are labelled in red. The freshwater sources are labelled in yellow.

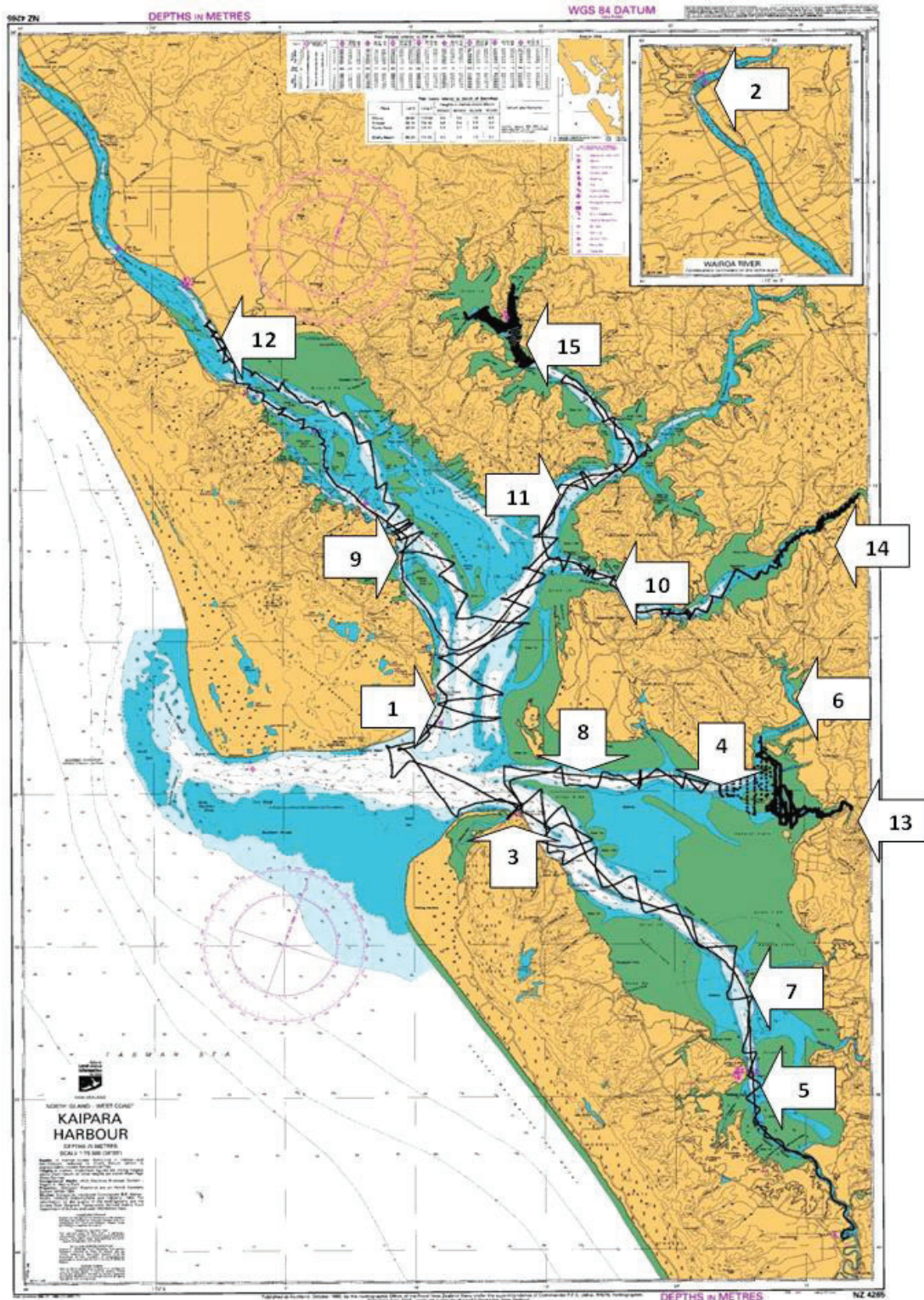


Figure 3-18: Location of sea-level records and bathymetry collection (black lines) in 2011 for hydrodynamic model calibration.

3.3.3 Meteorological record

There are no long-term wind records located directly adjacent to the Kaipara Harbour. A representative wind record for modelling wind-driven storm surge in the Kaipara Harbour was reconstructed from several wind records (Table 3-7).

Table 3-7: Wind records used for Kaipara Harbour wind-driven storm surge modelling.

| Name | Agent and Network Number | Latitude, Longitude | Record Start | Record Finish | Record used in reconstruction | Scaling factor |
|-----------------------------|--------------------------|---------------------|--------------|---------------|-------------------------------|----------------|
| Kaipara South Head N.Z.F.S. | 1368, A64422 | -36.459, 174.256 | 1 Jun 1966 | 30 Apr 1968 | Not used | 1 |
| Auckland, Whenuapai Aero | 1410, A64761 | -36.793, 174.624 | 1 Jan 1960 | 22 Jul 2007 | 1 Jan 1960 – 31 Mar 1997 | 1.26 |
| Whangarei Aero AWS | 1287, A54737 | -35.769, 174.364 | 1 Jan 1994 | 1 Jan 2013 | 1 Apr 1997 – 30 May 2005 | 1.73 |
| Auckland, Whenuapai AWS | 23976, A64762 | -36.793, 174.624 | 30 May 2005 | 1 Jan 2013 | 30 May 2005 – 8 Jun 2010 | 1.26 |

The Kaipara South Head wind record was perfectly located to represent wind near the Kaipara Harbour entrance, but the 1966–68 record is too short to use for reconstructing wind-driven storm surge over the ~30 years required. Instead, the Kaipara South Head record was used to scale the Whenuapai wind speeds, from a linear comparison between the overlapping parts of the record. The scaling factor was Whenuapai wind speed 1.26. The 1960–2007 Whenuapai record has significant gaps after 1997, so the Whangarei record was used to fill the gap between 1997 and the modern Whenuapai record beginning in 2005 (Table 3-7). The reconstructed time-series are plotted in Figure 3-19 and a wind rose in Figure 3-20. The highest frequency of winds is from the south-west quadrant.

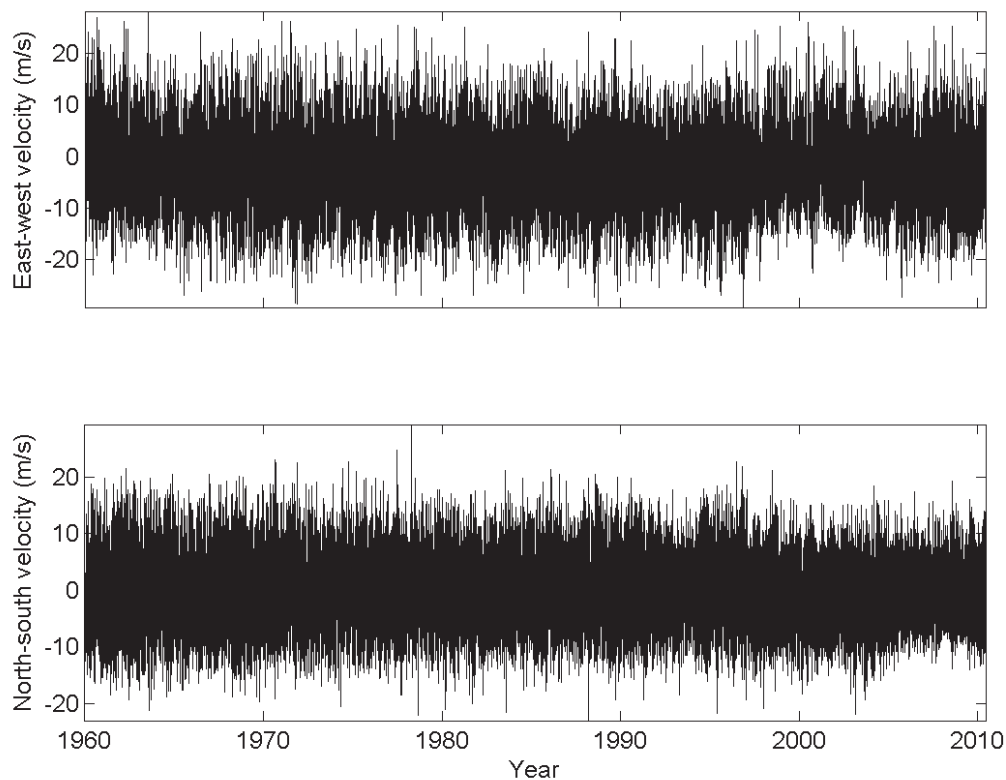


Figure 3-19: Reconstructed wind time-series used for modelling of wind-driven storm surge in the Kaipara Harbour.

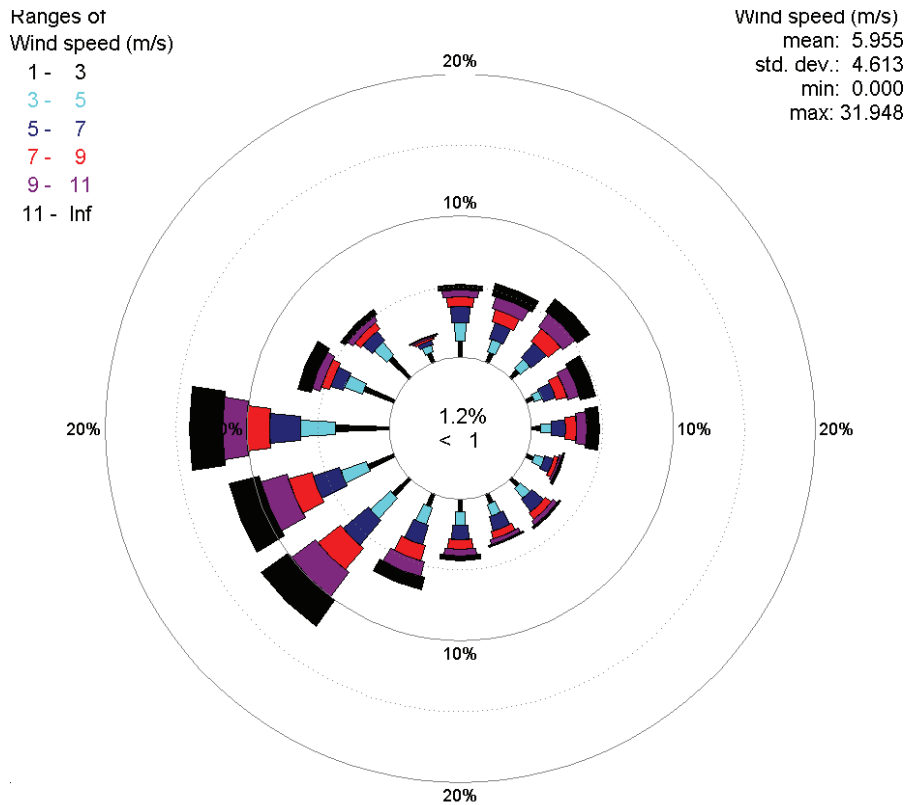


Figure 3-20: Rose plot of reconstructed wind series used for modelling of wind-driven storm surge in the Kaipara Harbour.

(Wind direction relates to where wind blows from)

3.3.4 Modelling storm-tide

Storm-tide time-series were simulated at 27 locations within the central and southern Kaipara Harbour, for later extreme sea-level analysis (Figure 3-21). The three sea-level components required are tide + storm surge + monthly mean sea-level anomaly. Time-series of monthly MMSLA were not simulated, but the empirical cumulative exceedance distribution of MMSLA, derived from tide gauges, was included in the extreme sea-level analysis.

The hydrodynamic model was used to predict tide elevations at these locations for a full perigean lunar cycle (1-month). The 1-month tidal time-series were each compared to the Pouto Point tide-gauge location (Site 7, Figure 3-21), and scaling factors were derived for each location, for the full range of the tide. Tidal time-series were then predicted for the duration of the available meteorological record. For example, Figure 3-22 shows the tide predictions for the Pouto Point tide-gauge location, and site 16 at the Kaipara River entrance. Tidal amplification occurs due to topographic constriction of the tidal wave and due to the generation of compound over tides inside the shallowing estuary basins.

Tidal hysteresis was calculated from the hydrodynamic model using the mean sea-level over the simulated lunar month; enabling a mean sea-level offset to be calculated for each location, relative to a location outside the harbour entrance. This mean sea-level offset due to tidal hysteresis was added to the extreme storm-tide distribution at each output location.

The wind-driven component of storm surge was calculated as described in Sections 2.3.1 and 7.3 by using the wind record to interpolate storm surge from the simulated wind-surge response matrix. The wind-driven component of storm surge differs depending on the output location within the harbour due to the available wind fetch.

The inverse-barometer component of sea level was calculated using the Whenuapai mean sea-level pressure record (Figure 3-23) and Equation 71. The inverse-barometer component of sea level was calculated as described in Section 7.3.1, and is shown in Figure 3-23.

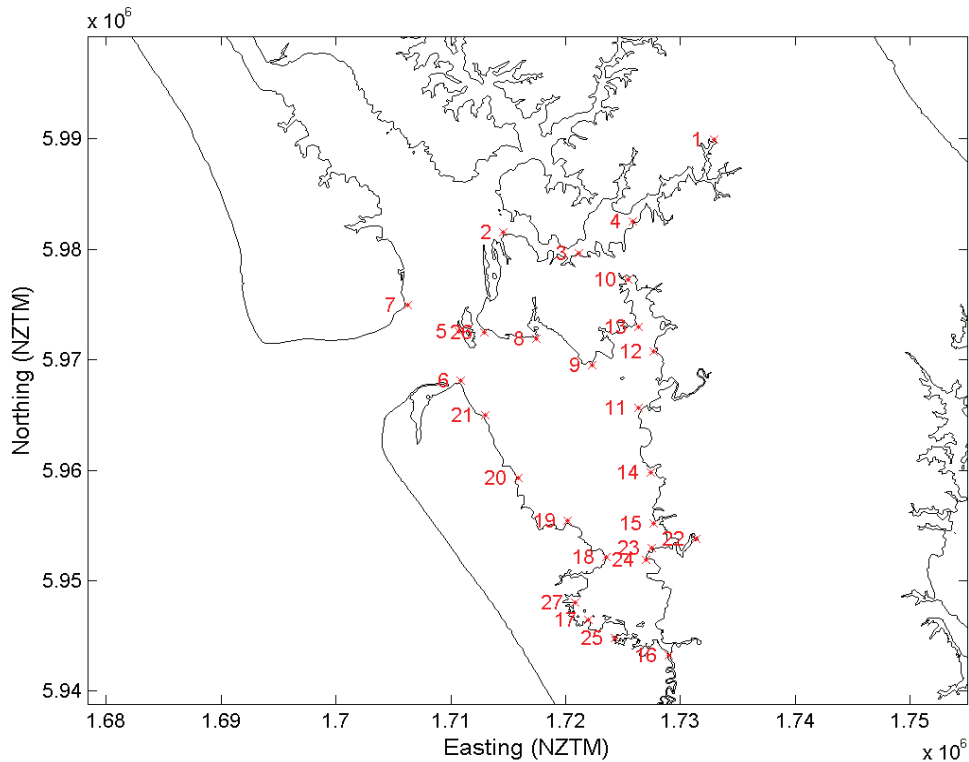


Figure 3-21: Locations of storm-tide model output from the central and southern Kaipara Harbour.
The northern Harbour lies within the Northland region.

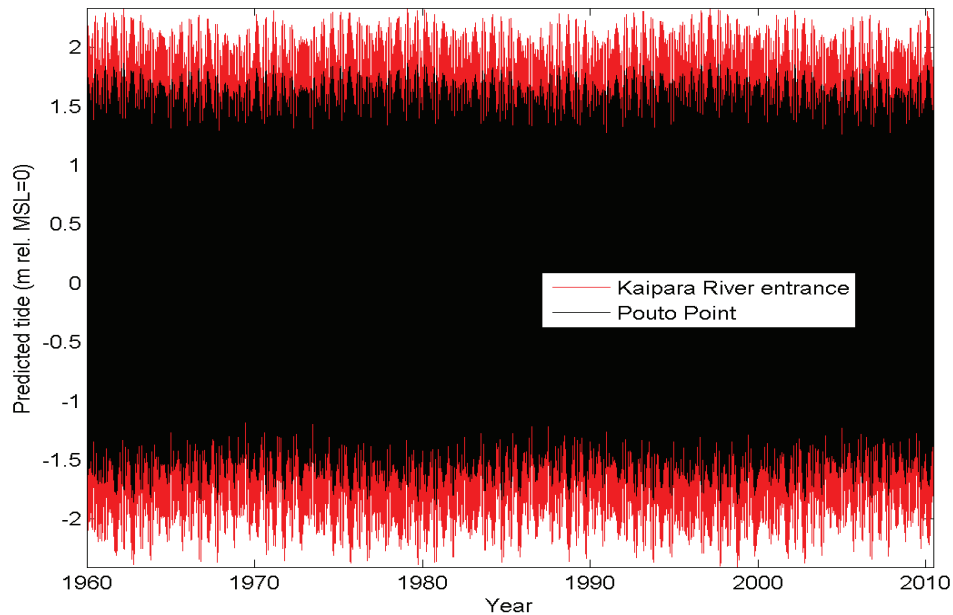


Figure 3-22: Predicted tide at Pouto Point and Kaipara River entrance.
(Pouto Point tide, site 7 is predicted directly from harmonic analysis of Pouto Point tide-gauge measurements. Tides at Kaipara River entrance, site 16 (and other locations not shown) were predicted by scaling the Pouto Point predictions using hydrodynamic model results. Tides were predicted for the duration of the available wind record.)

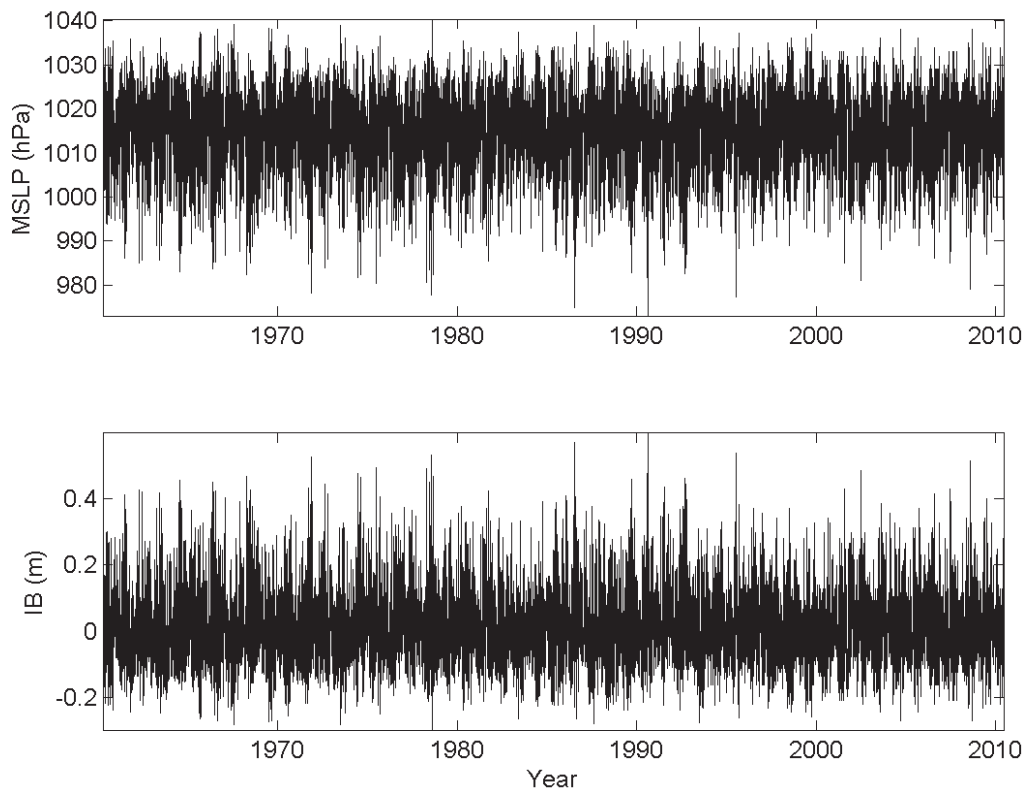


Figure 3-23: Kaipara mean sea-level pressure record and calculated inverse-barometer sea level.

MSLP = mean sea-level pressure measured at Whenuapai. IB = inverse-barometer sea level.

Storm-tide time-series were simulated using the methods described in Sections 2.3.1 and 7.3, at 27 locations within the Kaipara Harbour (Figure 3-21), for later extreme sea-level analysis.

Three extreme sea-level frequency–magnitude distributions are shown in Figure 3-24 for Pouto Point and one for the Kaipara River mouth. The black and red lines compare the extreme sea-level distributions calculated using the Pouto Point tide-gauge measurements, using the Monte-Carlo joint-probability (MCJP) technique and a peaks-over-threshold (POT/GPD) technique (see Section 7.2 for more information about these techniques). The record is not long enough (not enough extreme events) to get reliable extreme sea-level estimates using the POT/GPD technique, hence the very flat distribution at low exceedance probabilities; the POT/GPD is shown for comparison purposes.

The black and green lines compare extreme sea-level distributions at Pouto Point derived from measured and simulated data. The IBfactor was used as a calibration parameter to ensure that the modelled extreme storm-tide distribution matched that derived from the tide-gauge. The technique was then applied to other locations in the harbour (Figure 3-21). An example is shown in Figure 3-24 (blue line) for the Kaipara River mouth (site 16; Figure 3-21). This demonstrates the significant increase in extreme storm-tide magnitude higher in the estuary arms, due primarily to topographic amplification of the tide (e.g., Figure 3-22), but also to storm surge amplification.

Table 3-8 provides the estimated extreme sea-level frequency–magnitude relationship at Pouto Point based on the MCJP technique applied to the Pouto Point tide-gauge record. Table 3-9 provides the estimated extreme sea-level frequency–magnitude relationship at locations throughout the southern arm of the harbour.

The MCJP technique randomly samples from several sea-level component time-series and empirical cumulative exceedance distributions. In most tide-gauge records, the monthly mean sea-level anomaly is normally distributed. However, the Pouto Point tide-gauge record had a positively skewed MMSLA distribution, which we attribute to the episodic burial of the bubbler orifice by sand for several months on occasion. The sand burial increases the back-pressure in the bubbler tube, causing the gauge to read higher than normal pressures, and this affects the MMSLA component of sea level. As a workaround, we instead used the (normally-distributed) empirical cumulative exceedance distribution of MMSLA from the open-west-coast gauge record located at Anawhata, located 58 km south of the Kaipara Harbour entrance.

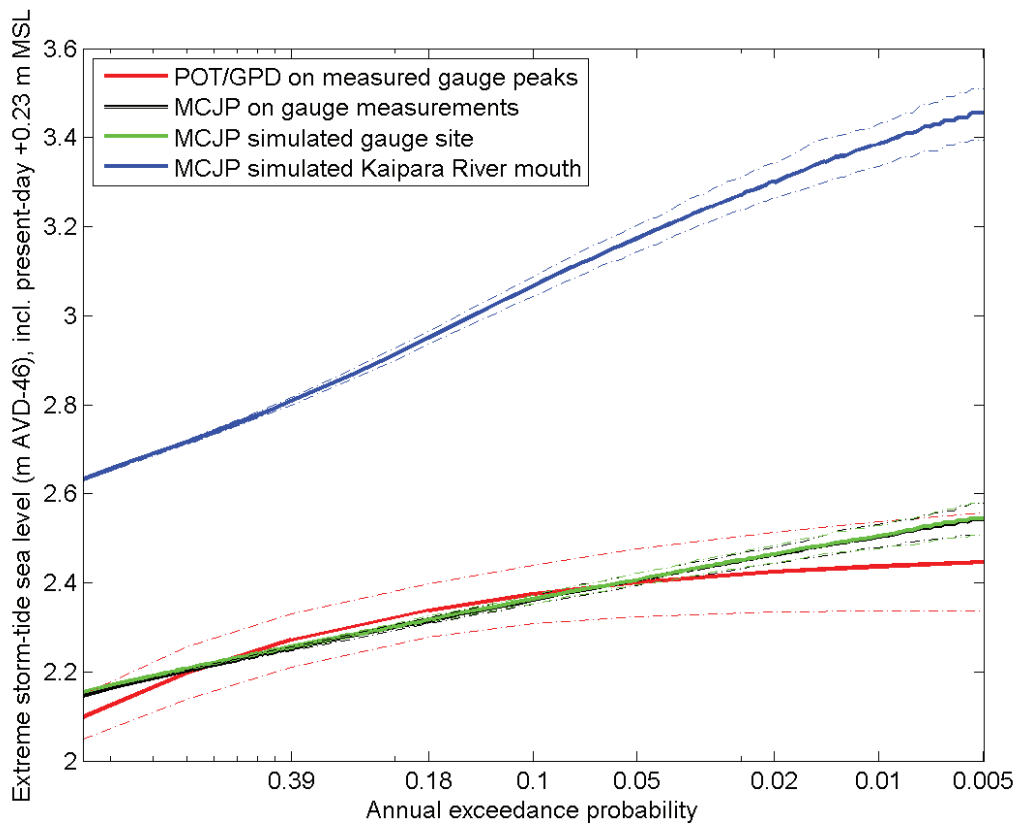


Figure 3-24: Extreme sea-level curves for Pouto Point tide-gauge.

Elevations are relative to AVD-46 including +0.23 m offset for baseline mean sea level (present-day estimate). Bold lines marks median values, dashed lines mark 95th percentile confidence intervals.

Table 3-8: Extreme sea-level at Pouto Point.

Elevations are relative to AVD-46 including +0.23 m offset for baseline mean sea level (present-day estimate). C.I. = confidence interval. Elevations calculated from tide-gauge data.

| AEP | 0.39 | 0.18 | 0.10 | 0.05 | 0.02 | 0.01 | 0.005 |
|-----------------|------|------|------|------|------|------|-------|
| ARI | 2 | 5 | 10 | 20 | 50 | 100 | 200 |
| Median | 2.25 | 2.31 | 2.36 | 2.41 | 2.46 | 2.50 | 2.54 |
| Lower 95th C.I. | 2.25 | 2.31 | 2.35 | 2.39 | 2.44 | 2.48 | 2.51 |
| Upper 95th C.I. | 2.26 | 2.32 | 2.37 | 2.42 | 2.48 | 2.53 | 2.58 |

Table 3-9: Extreme sea-level in the Kaipara Harbour.

Elevations are relative to AVD-46 including +0.23 m offset for baseline mean sea level (present-day estimate). Elevations calculated from simulated data. Locations given in Figure 3-21.

| Site number | Easting (NZTM) | Northing (NZTM) | AEP: | 0.39 | 0.18 | 0.10 | 0.05 | 0.02 | 0.01 | 0.005 |
|-----------------------|----------------|-----------------|------|-------------|-------------|-------------|-------------|-------------|-------------|-------------|
| | | | ARI: | 2 yr | 5 yr | 10 yr | 20 yr | 50 yr | 100 yr | 200 yr |
| | | | | | | | | | | |
| 1 | 1732914 | 5989908 | | 2.80 | 2.87 | 2.92 | 2.98 | 3.04 | 3.09 | 3.14 |
| 2 | 1714569 | 5981549 | | 2.35 | 2.41 | 2.45 | 2.50 | 2.56 | 2.60 | 2.64 |
| 3 | 1721187 | 5979670 | | 2.53 | 2.60 | 2.64 | 2.69 | 2.75 | 2.79 | 2.84 |
| 4 | 1725821 | 5982551 | | 2.65 | 2.72 | 2.77 | 2.82 | 2.88 | 2.92 | 2.97 |
| 5 | 1710704 | 5972533 | | 2.24 | 2.30 | 2.34 | 2.39 | 2.44 | 2.49 | 2.52 |
| 6 | 1710904 | 5968074 | | 2.28 | 2.34 | 2.39 | 2.43 | 2.49 | 2.53 | 2.57 |
| 7 | 1706237 | 5974952 | | 2.28 | 2.34 | 2.38 | 2.43 | 2.48 | 2.52 | 2.56 |
| 8 | 1717470 | 5971893 | | 2.41 | 2.47 | 2.51 | 2.56 | 2.62 | 2.66 | 2.70 |
| 9 | 1722273 | 5969479 | | 2.50 | 2.56 | 2.61 | 2.66 | 2.72 | 2.76 | 2.81 |
| 10 | 1725440 | 5977226 | | 2.55 | 2.62 | 2.68 | 2.74 | 2.82 | 2.89 | 2.95 |
| 11 | 1726302 | 5965647 | | 2.59 | 2.66 | 2.72 | 2.78 | 2.86 | 2.91 | 2.97 |
| 12 | 1727640 | 5970779 | | 2.59 | 2.66 | 2.72 | 2.77 | 2.85 | 2.90 | 2.96 |
| 13 | 1726306 | 5972938 | | 2.64 | 2.71 | 2.76 | 2.81 | 2.88 | 2.93 | 2.99 |
| 14 | 1727398 | 5959766 | | 2.65 | 2.73 | 2.79 | 2.86 | 2.95 | 3.01 | 3.07 |
| 15 | 1727676 | 5955207 | | 2.72 | 2.81 | 2.88 | 2.96 | 3.05 | 3.12 | 3.19 |
| 16² | 1728962 | 5943240 | | 2.95 | 3.10 | 3.21 | 3.32 | 3.44 | 3.53 | 3.60 |

² The results for Site 16 have been superseded by more detailed modelling undertaken by the DHI report (Part 3), and also summarised in the NIWA 2016 report (Part 2)

| Site number | Easting (NZTM) | Northing (NZTM) | AEP: | 0.39 | 0.18 | 0.10 | 0.05 | 0.02 | 0.01 | 0.005 |
|-------------|----------------|-----------------|------|------|------|-------|-------|-------|--------|--------|
| | | | ARI: | 2 yr | 5 yr | 10 yr | 20 yr | 50 yr | 100 yr | 200 yr |
| | | | | | | | | | | |
| 17 | 1721949 | 5946471 | | 2.85 | 2.95 | 3.03 | 3.11 | 3.22 | 3.29 | 3.36 |
| 18 | 1723547 | 5952115 | | 2.76 | 2.84 | 2.91 | 2.98 | 3.07 | 3.14 | 3.20 |
| 19 | 1720204 | 5955418 | | 2.65 | 2.72 | 2.78 | 2.83 | 2.91 | 2.96 | 3.01 |
| 20 | 1715889 | 5959302 | | 2.55 | 2.62 | 2.67 | 2.71 | 2.77 | 2.82 | 2.86 |
| 21 | 1712991 | 5965012 | | 2.38 | 2.45 | 2.49 | 2.54 | 2.59 | 2.64 | 2.68 |
| 22 | 1731343 | 5953771 | | 2.75 | 2.86 | 2.96 | 3.05 | 3.16 | 3.24 | 3.31 |
| 23 | 1727503 | 5952984 | | 2.73 | 2.83 | 2.91 | 2.99 | 3.10 | 3.17 | 3.23 |
| 24 | 1727028 | 5951911 | | 2.78 | 2.87 | 2.95 | 3.04 | 3.14 | 3.22 | 3.28 |
| 25 | 1724252 | 5944778 | | 2.86 | 2.97 | 3.06 | 3.15 | 3.27 | 3.34 | 3.41 |
| 26 | 1712894 | 5972482 | | 2.34 | 2.40 | 2.45 | 2.49 | 2.55 | 2.59 | 2.63 |
| 27 | 1720787 | 5948055 | | 2.83 | 2.91 | 2.98 | 3.05 | 3.15 | 3.21 | 3.28 |

4 Extreme sea-level elevations from storm-tides and waves on the open coasts of the Auckland region

In this section we provide location-specific information, such as data and models, required to explain how the methods from Section 2 were applied to the open coastlines in the Auckland region.

4.1 The open east coast

Section 7.4 outlines the general procedure for calculating extreme sea-level elevations for open-coast locations. To briefly recap, both wave and storm-tide conditions were simulated for the 1970–2000 period, at 37 locations along the eastern open-coast (Figure 4-1). A joint-probability analysis was undertaken (Section 7.2.5) to calculate the likelihood of various coincident storm-tide and wave combinations. Wave setup was then calculated and added to storm-tide elevations to calculate the total combined storm-tide plus wave setup elevation.

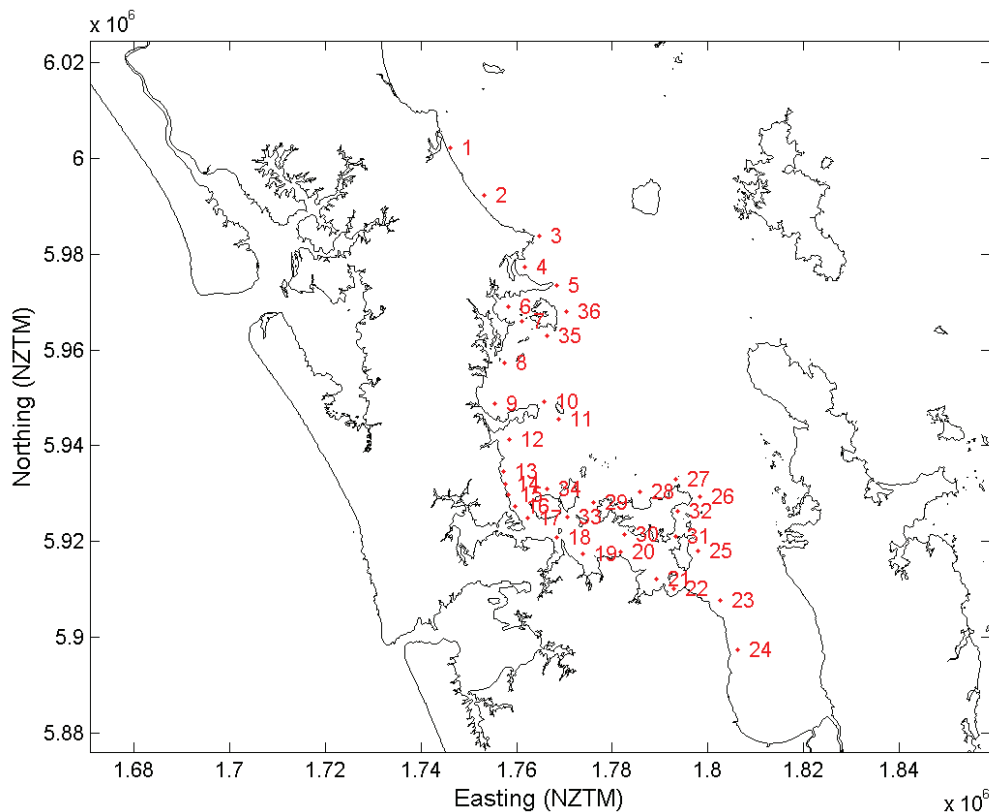


Figure 4-1: Locations of storm-tide and wave simulation output along the east open coast of the Auckland region.

4.1.1 Storm-tide on the eastern open-coast

Time-series of storm-tide sea-level for 1970–2000 were estimated by adding the following three sea-level components:

- Astronomical tide – predicted using NIWA’s New Zealand tide model (Stanton et al. 2001; Walters et al. 2001).

- Storm surge – hindcast by the WASP models (<http://wrenz.niwa.co.nz/webmodel/coastal>).
- Monthly mean sea-level anomaly – derived from the Port of Auckland (Waitemata) tide gauge (e.g., Figure 3-2, Figure 3-3).
- Figure 4-2 shows an example of the WASP storm surge prediction at the Port of Auckland tide-gauge location, compared to that derived from the tide-gauge measurements. Although not an exact match, it can be seen that the WASP model generally reproduced the magnitude and timing of the storm surges. Figure 4-3 shows the scatter between the measured and modelled storm surges at the tide-gauge location. While there is considerable scatter (at times), the quantile-quantile relationship lies close to the 1:1 line, indicating that the probability distributions of the measured and modelled storm surges are similar. For example, the magnitude of the largest modelled storm surges matches those of the largest measured storm surges.
- From the re-constructed storm-tide time-series (tide + storm surge), extreme storm-tide distributions were calculated using the MCJP technique (Table 7-4) for each location, and the distribution of these is shown in Figure 4-4. Storm-tide elevations are shown in Table 4-1.

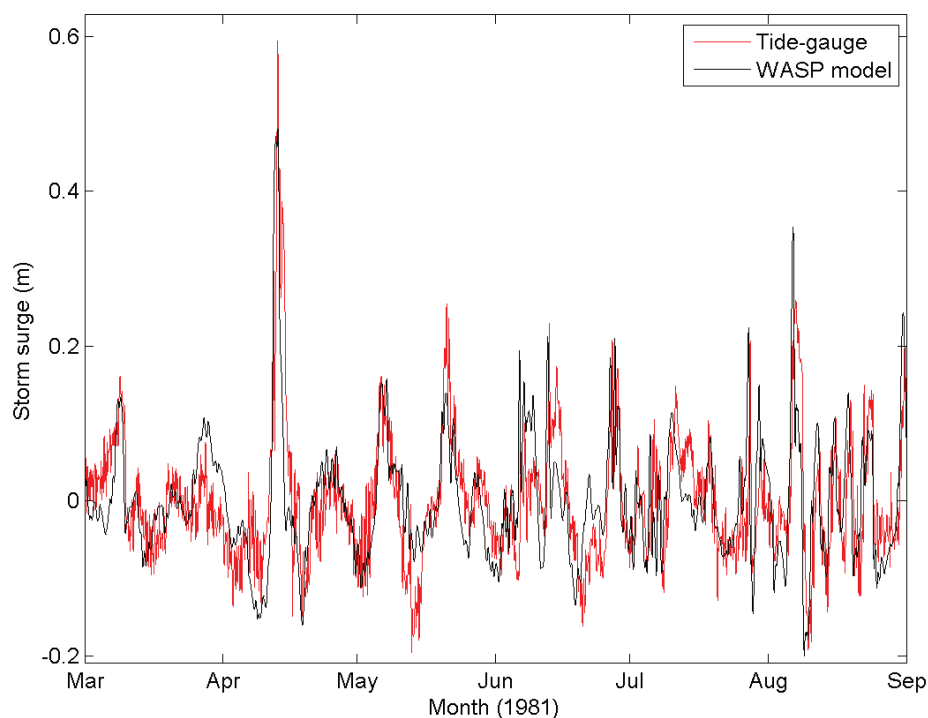


Figure 4-2: Time-series of storm surge at Port of Auckland from tide gauge and WASP model.

Selection chosen to include a large storm surge (in April 1981).

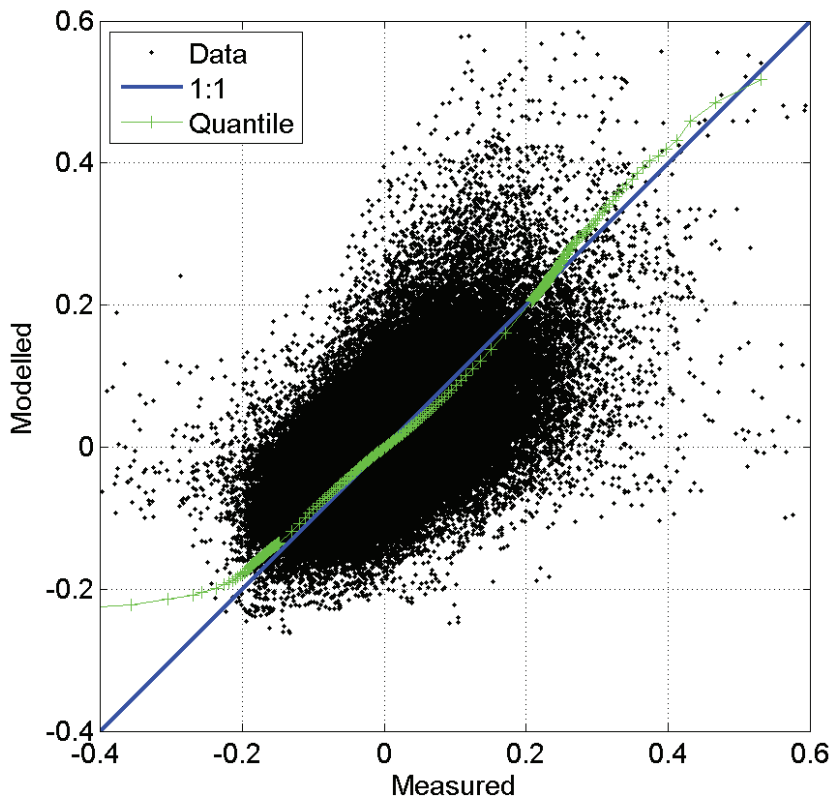


Figure 4-3: Scatter plot of measured (tide gauge) and modelled (WASP) storm surge at Port of Auckland (Waitemata), with quantile-quantile comparison.
 (Values in metres.)

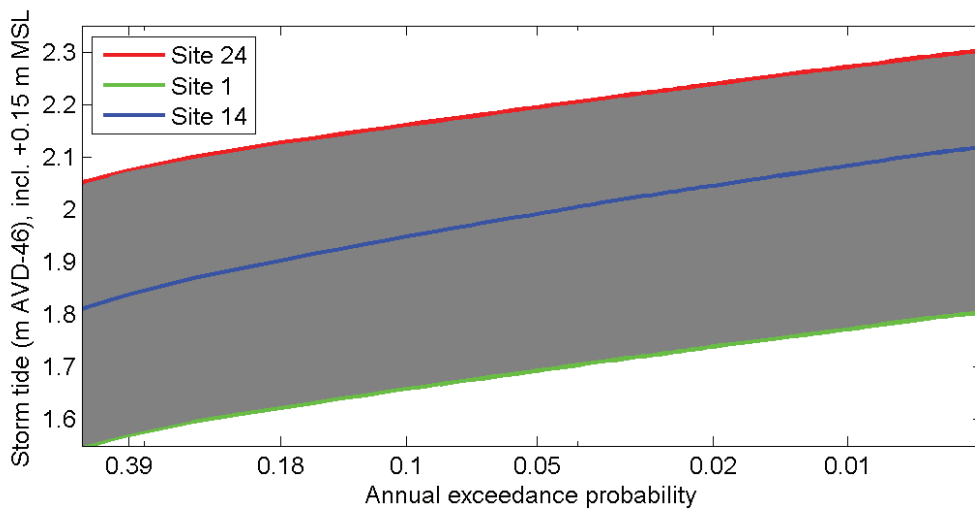


Figure 4-4: Distribution of extreme storm-tides on the open-coast of the Auckland region.
 Shaded area represents the range of elevations between the 37 sites. Examples given for individual sites 1, 14 and 24 (Figure 4-1).

Table 4-1: Storm-tide elevations on the eastern open-coast.

Elevations are relative to AVD-46 including +0.15 m offset for baseline mean sea level (present-day estimate). Sites shown in Figure 4-1.

| Site | Easting (NZTM) | Northing (NZTM) | AEP: | 0.39 | 0.18 | 0.10 | 0.05 | 0.02 | 0.01 | 0.005 |
|------|----------------|-----------------|------|------|------|-------|-------|-------|--------|--------|
| | | | ARI: | 2 yr | 5 yr | 10 yr | 20 yr | 50 yr | 100 yr | 200 yr |
| | | | | | | | | | | |
| 1 | 1746045 | 6002166 | | 1.57 | 1.62 | 1.65 | 1.68 | 1.72 | 1.76 | 1.78 |
| 2 | 1753102 | 5992291 | | 1.59 | 1.64 | 1.67 | 1.70 | 1.74 | 1.77 | 1.80 |
| 3 | 1764823 | 5983832 | | 1.62 | 1.67 | 1.70 | 1.73 | 1.76 | 1.79 | 1.81 |
| 4 | 1761674 | 5977388 | | 1.66 | 1.71 | 1.74 | 1.78 | 1.82 | 1.85 | 1.88 |
| 5 | 1768344 | 5973565 | | 1.68 | 1.72 | 1.76 | 1.78 | 1.82 | 1.84 | 1.87 |
| 6 | 1758271 | 5968983 | | 1.78 | 1.84 | 1.88 | 1.92 | 1.98 | 2.01 | 2.05 |
| 7 | 1760994 | 5965903 | | 1.77 | 1.82 | 1.86 | 1.89 | 1.94 | 1.97 | 2.00 |
| 8 | 1757358 | 5957292 | | 1.76 | 1.81 | 1.85 | 1.88 | 1.92 | 1.95 | 1.98 |
| 9 | 1755351 | 5948872 | | 1.76 | 1.82 | 1.86 | 1.89 | 1.93 | 1.97 | 2.00 |
| 10 | 1765782 | 5949110 | | 1.76 | 1.81 | 1.84 | 1.87 | 1.91 | 1.94 | 1.96 |
| 11 | 1768729 | 5945579 | | 1.77 | 1.82 | 1.85 | 1.88 | 1.91 | 1.94 | 1.96 |
| 12 | 1758449 | 5941213 | | 1.81 | 1.86 | 1.90 | 1.93 | 1.98 | 2.01 | 2.04 |
| 13 | 1757328 | 5934697 | | 1.83 | 1.89 | 1.93 | 1.96 | 2.01 | 2.04 | 2.07 |
| 14 | 1757600 | 5931984 | | 1.84 | 1.90 | 1.94 | 1.98 | 2.03 | 2.06 | 2.09 |
| 15 | 1758282 | 5929752 | | 1.85 | 1.91 | 1.95 | 1.99 | 2.04 | 2.07 | 2.10 |
| 16 | 1759748 | 5927428 | | 1.86 | 1.93 | 1.97 | 2.01 | 2.06 | 2.10 | 2.12 |
| 17 | 1762306 | 5924882 | | 1.89 | 1.96 | 2.00 | 2.04 | 2.10 | 2.13 | 2.15 |
| 18 | 1768474 | 5920856 | | 1.93 | 2.00 | 2.04 | 2.09 | 2.14 | 2.18 | 2.20 |
| 19 | 1773944 | 5917482 | | 1.94 | 2.00 | 2.05 | 2.09 | 2.14 | 2.18 | 2.20 |
| 20 | 1781649 | 5917865 | | 1.96 | 2.01 | 2.05 | 2.09 | 2.14 | 2.17 | 2.19 |
| 21 | 1789299 | 5912170 | | 2.00 | 2.06 | 2.10 | 2.14 | 2.20 | 2.23 | 2.26 |
| 22 | 1792968 | 5910034 | | 2.00 | 2.06 | 2.10 | 2.15 | 2.20 | 2.24 | 2.26 |
| 23 | 1802591 | 5907745 | | 1.99 | 2.04 | 2.07 | 2.10 | 2.14 | 2.17 | 2.19 |
| 24 | 1806261 | 5897453 | | 2.07 | 2.12 | 2.16 | 2.19 | 2.23 | 2.25 | 2.28 |
| 25 | 1798030 | 5918077 | | 1.94 | 1.98 | 2.01 | 2.04 | 2.07 | 2.10 | 2.12 |
| 26 | 1798292 | 5929361 | | 1.85 | 1.90 | 1.93 | 1.95 | 1.98 | 2.00 | 2.02 |

| Site | Easting (NZTM) | Northing (NZTM) | AEP: | 0.39 | 0.18 | 0.10 | 0.05 | 0.02 | 0.01 | 0.005 |
|------|----------------|-----------------|------|------|------|-------|-------|-------|--------|--------|
| | | | ARI: | 2 yr | 5 yr | 10 yr | 20 yr | 50 yr | 100 yr | 200 yr |
| | | | | | | | | | | |
| 27 | 1793282 | 5932939 | 1.81 | 1.85 | 1.88 | 1.91 | 1.94 | 1.96 | 1.98 | |
| 28 | 1785826 | 5930285 | 1.80 | 1.84 | 1.87 | 1.90 | 1.93 | 1.95 | 1.98 | |
| 29 | 1776063 | 5928106 | 1.84 | 1.89 | 1.93 | 1.96 | 1.99 | 2.02 | 2.05 | |
| 30 | 1782627 | 5921463 | 1.94 | 1.99 | 2.03 | 2.06 | 2.10 | 2.13 | 2.15 | |
| 31 | 1793244 | 5921007 | 1.95 | 2.00 | 2.03 | 2.06 | 2.10 | 2.12 | 2.14 | |
| 32 | 1793594 | 5926216 | 1.90 | 1.94 | 1.97 | 2.00 | 2.03 | 2.06 | 2.08 | |
| 33 | 1770683 | 5925185 | 1.90 | 1.96 | 2.00 | 2.04 | 2.09 | 2.12 | 2.14 | |
| 34 | 1766404 | 5930907 | 1.82 | 1.87 | 1.90 | 1.94 | 1.97 | 2.00 | 2.02 | |
| 35 | 1766328 | 5963017 | 1.76 | 1.81 | 1.84 | 1.87 | 1.90 | 1.93 | 1.95 | |
| 36 | 1770378 | 5967921 | 1.71 | 1.75 | 1.78 | 1.81 | 1.85 | 1.87 | 1.89 | |

4.1.2 Waves on the eastern open-coast

Time-series of wave statistics (e.g., height, period and direction) were also derived from WASP hindcasts. There are many islands offshore from Auckland’s east coast that affect the wave climate through wave refraction and sheltering, and the spatial resolution of the New Zealand-regional-scale WASP models was too coarse to resolve these features. Therefore, the WASP hindcast was used to drive a nested SWAN wave model with sufficient spatial resolution to translate the WASP wave predictions from offshore in deep water to the Auckland coastline.

4.1.3 Wave modelling methods

The SWAN model (Booij et al. 1999; Ris et al. 1999) is a spectral wave model intended for shallow water applications in coastal and estuarine environments. It computes the evolution of the wave energy spectrum in position (x, y) and time (t), explicitly taking into account the various physical processes acting on waves in shallow water. The model can incorporate boundary conditions representing waves arriving from outside the model domain.

For the present study, an outer Hauraki Gulf grid (“outer_hauraki”) was established at 750 m resolution in both X and Y, at 0 orientation. The grid origin was located at New Zealand Transverse Mercator (NZTM) coordinates (2640375E, 6437875N). The 130 × 240 cell grid extends for 96.75 km eastward, and 179.25 km northward from the origin. This places the northern limit near Whangarei, and the eastward limit at approximately 175.5E, to include the western coast of Great Barrier Island (Figure 45).

The spectral grid consisted of 33 wave frequencies between 0.0418 Hz and 0.8018 Hz (or periods of 1.2–24 s) geometrically spaced, so that successive frequencies were in the ratio $f_{n+1} / f_n = 1.125$, while 24 wave direction bins of 15 width were used. The shallow water effects of depth-limited breaking,

bed friction and triad nonlinear interactions were activated, with default parameterisations for SWAN Version 40.85 (SWAN 2011) used.

In order to simulate wave development in a given region, it is necessary to specify the winds blowing over the region. Waves entering the region through any open boundaries also need to be included, while the effects of changing water levels and currents can also be accounted for if these can be provided. In general all of these inputs vary both in space and time. The SWAN model performs interpolation of input wind, sea level and current fields to the required spatial and temporal resolution of the nearshore model.

These wave and wind forcings were derived from larger scale simulations (approximately 30 km resolution) carried out by NIWA under the Waves and Storm surge Projections (WASP) programme, described below.

The NIWA tidal model is based on an unstructured mesh that provides much finer resolution in coastal waters than the 9 km regular grid used for wave and wind inputs. Hence for the present study, tidal currents and sea levels were input on a 1 km resolution regular grid (AKLTIDE-1) covering the Auckland region, at 15 minute time intervals.

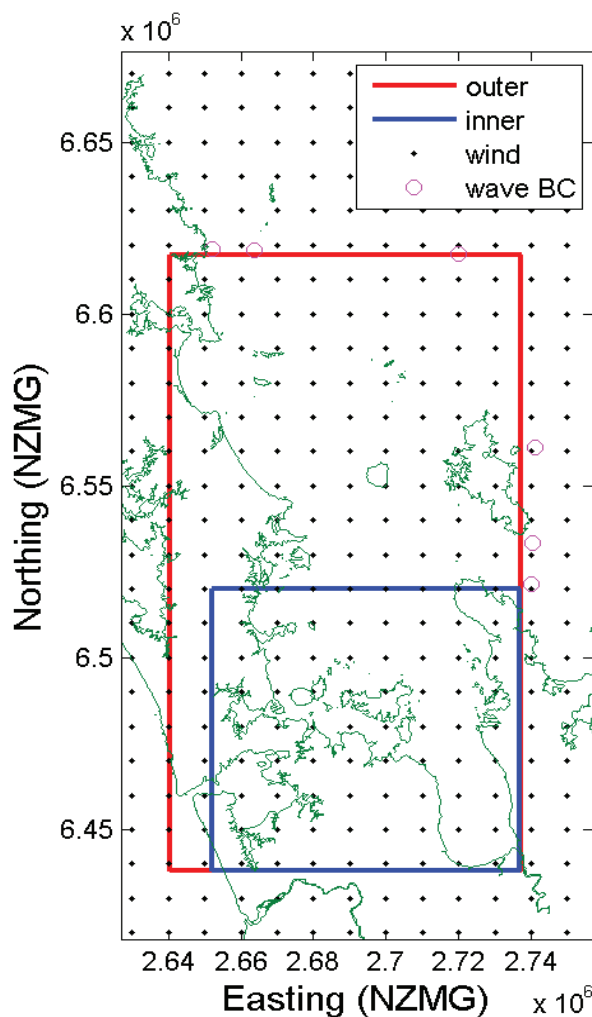


Figure 4-5: Outer and inner SWAN wave model grids of the Hauraki Gulf.

(Dots mark wind input locations on 9 km grid. Circles mark wave boundary conditions from the WASP project.)

WASP wave hindcasts

At a global level, the hindcasts in the WASP programme were based on inputs from the ERA-40 Reanalysis dataset (Uppala et al. 2005) from the European Centre for Medium Range Weather Forecasts (ECMWF), which provided wind and pressure fields over a 45-year period, from October 1957 - September 2002, on a global domain at 1.125 x 1.125 degree resolution in longitude and latitude (125 km at the equator).

To provide wave hindcasts, the Wavewatch III™ model (Tolman, H. L. 1991; Tolman, Hendrik L. 2007) was first run on a global grid ('era40gw_125') matching the input ERA40 grid (see Uppala et al. 2005) except for being reduced to the latitude range -81° to +81°. To provide more detailed outputs at a New Zealand regional scale, two different nested hindcasts were then run. The first of these ('waspnzw_10'), run on a nested subdomain covering waters around New Zealand at 0.125° x 0.09375° resolution (approximately 10 km), used the same (low resolution) wind inputs as the global wave model, so the finer resolution served only to interpolate wave conditions into nearshore locations. A second regional hindcast ('rcm_9_era') was run for the years 1970-2000, nested in the same global wave simulation. For this, ERA40 winds had been downscaled by a Regional Climate Model. These wind fields were interpolated to a regular latitude/longitude regional grid ('rcm_9') at approximately 9 km resolution for wave model simulations. No air-sea temperature difference fields were available, so no stability corrections were made to the wind input term for this simulation.

The latter ('rcm_era') hindcast was used in the present work to provide both wind and wave inputs for the Hauraki Gulf SWAN model. Wave boundary conditions were specified as directional spectra on the open boundaries of the outer Hauraki Gulf SWAN grid.

Verification

The model was tested against data from two wave buoy deployments, both in the northern part of the Gulf – no suitable records were available for the more protected inner Gulf. The first was a Waverider buoy deployed by the then Auckland Regional Council between 15 May 1998 and 10 June 2004 at (36.8833°S, 175.0833°E) near the Mokohinau Islands. The second was from a NIWA wave buoy located at (36.8833°S, 175.0833°E) near Mangawhai Beach from 1 September 1996 to 30 November 1996.

Figures 4-6 – Figure 4-11 compare data and model in the form of colour-scaled plots of the joint occurrence distribution of measured and modelled values of each wave parameter (significant height H_{m0} , peak period T_{peak} , and peak direction θ_{peak}), for all measurement times within the simulation period. Figure 4-6–Figure 4-8 cover the comparison for the Mokohinau Islands buoy site and Figure 4-9–Figure 4-11 the Mangawhai buoy site. Quantile-quantile plots of the same collocated measured and modelled values of significant wave height and peak period are overlaid (red lines). Additionally, percentile values of modelled parameters were derived for the full simulation period, along with corresponding percentile values derived from the full measurement record, seasonally-adjusted to give equal weight to each month. These are compared in the green quantile-quantile lines: this is a comparison that can be made for non-overlapping records, though it is not needed in this case.

At both locations, the model gave some over prediction of wave heights in moderate conditions but show good agreement in more energetic conditions, with quantile-quantile plots remaining close to the equivalence line. Peak wave period tends to be underestimated by the model. Peak wave directions at the Mokohinau site predominantly lie in the northeast quadrant (0–90) and the north (340–360), open to

the Pacific Ocean, with waves from the southwest quadrant (180–270) of secondary importance. Agreement between measured and modelled directions is generally good, although there is a population of events in which the model expects peak waves from the south-west while the measured waves are predominantly from the north east.

These results suggest that the model is overemphasising local generation relative to oceanic swell, possibly through input wind speeds being overestimated, at least during south-westerly conditions. A more detailed treatment of local wind fields over the Hauraki Gulf may be needed to improve this. For locations with open-ocean exposure, this will be of less importance in the most energetic conditions, which generally involve north-easterly winds acting over much longer fetches.

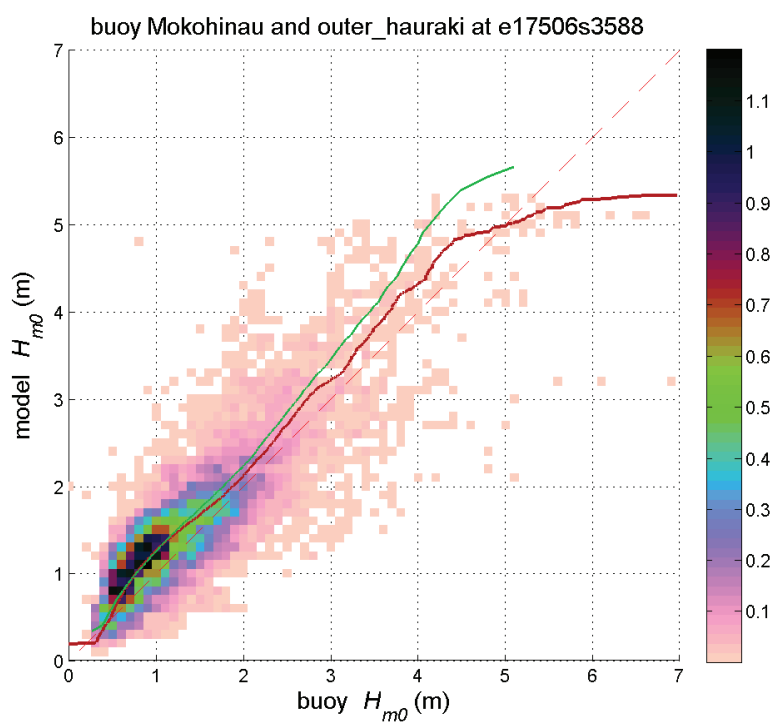


Figure 4-6: Comparison of significant wave height (H_{m0}) values predicted by the outer Hauraki Gulf SWAN model with measurements from the Mokohinau Islands Waverider buoy.

(The colour scale shows the joint occurrence distribution of measured and predicted wave heights, while the solid lines show quantile-quantile plots, either using coincident records (red line), or seasonally-adjusted statistics derived from all records (green line).

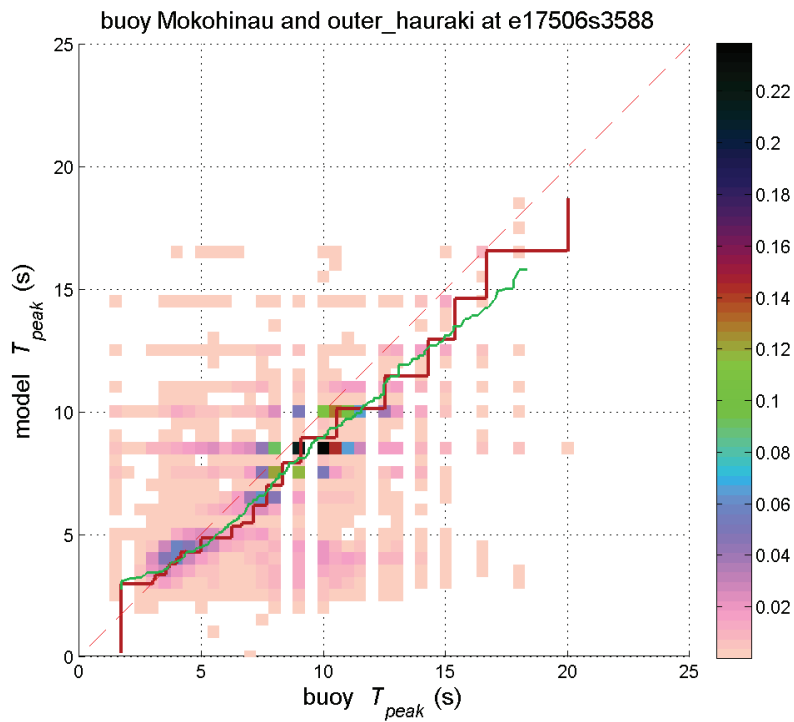


Figure 4-7: Comparison of peak wave period (T_{peak}) values predicted by the outer Hauraki Gulf SWAN model with measurements from the Mokohinau Islands Waverider buoy.

(The colour scale shows the joint occurrence distribution of measured and predicted wave heights, while the solid lines show quantile-quantile plots, either using coincident records (red line), or seasonally-adjusted statistics derived from all records (green line).

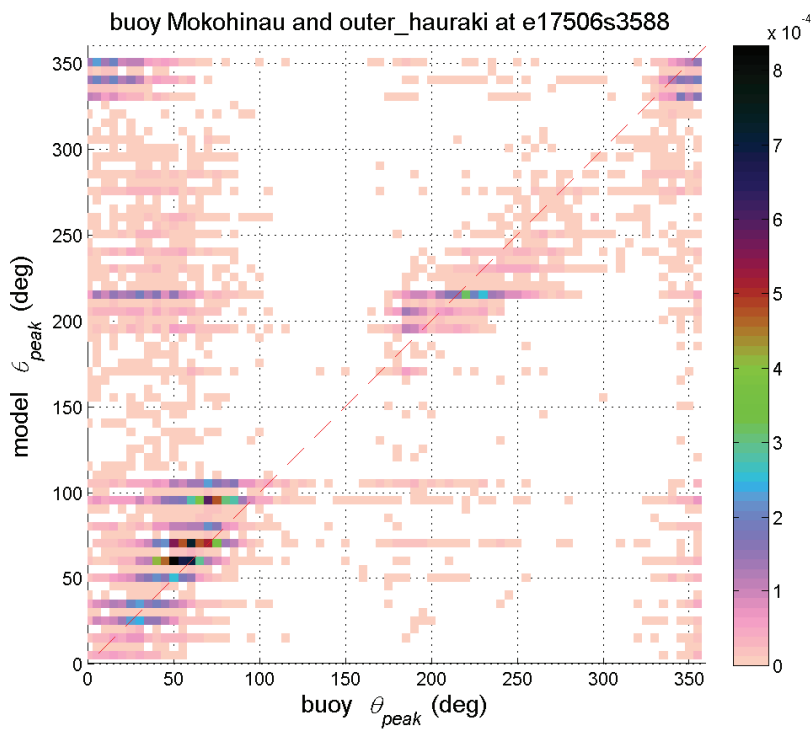


Figure 4-8: Comparison of peak wave direction (θ_{peak}) values predicted by the outer Hauraki Gulf SWAN model with measurements from the Mokohinau Islands Waverider buoy.

The colour scale shows the joint occurrence distribution of measured and predicted wave heights.

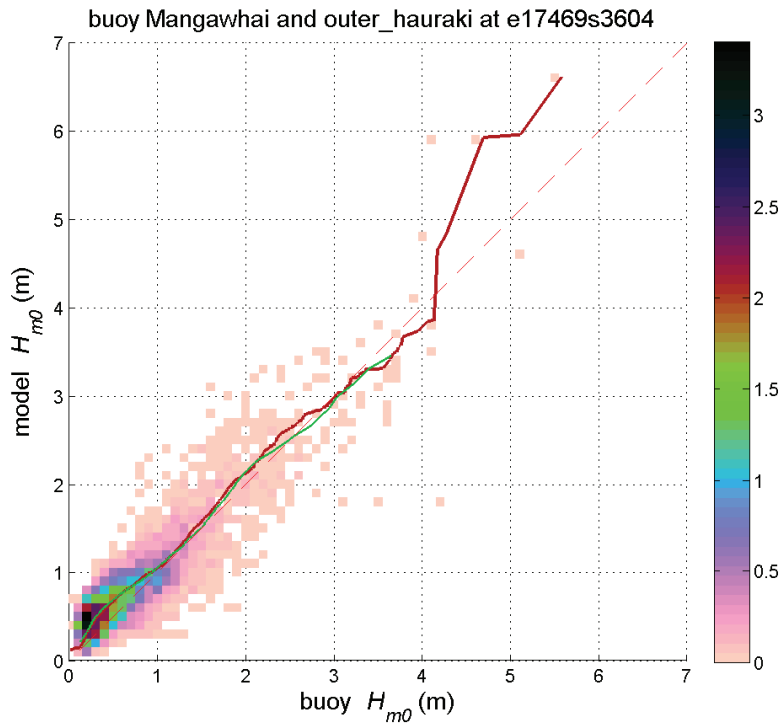


Figure 4-9: Comparison of significant wave height (H_{m0}) values predicted by the outer Hauraki Gulf SWAN model with measurements from the Mangawhai wave buoy.

(The colour scale shows the joint occurrence distribution of measured and predicted wave heights, while the solid lines show quantile-quantile plots, either using coincident records (red line), or seasonally-adjusted statistics derived from all records (green line).

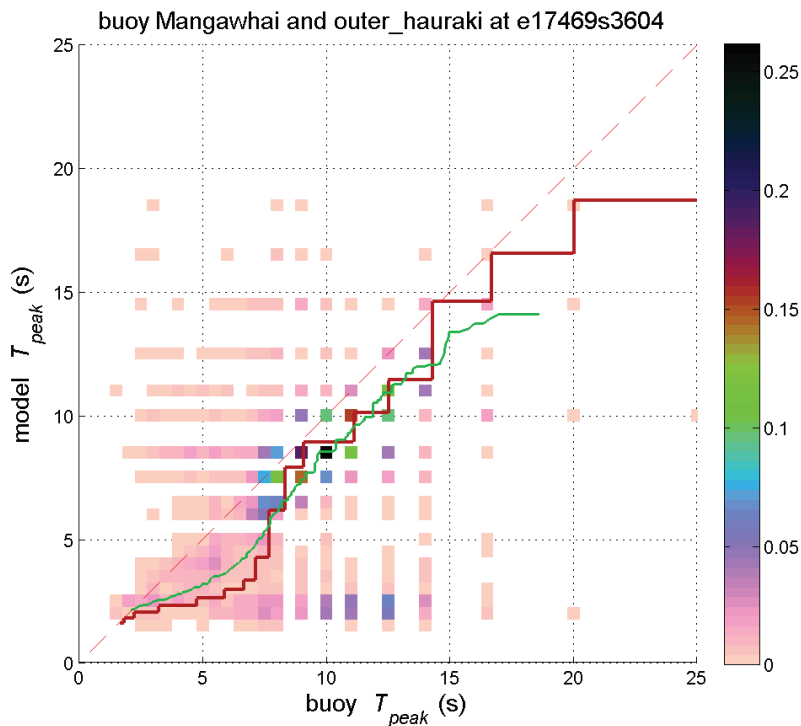


Figure 4-10: Comparison of peak wave period (T_{peak}) values predicted by the outer Hauraki Gulf SWAN model with measurements from the Mangawhai wave buoy.

(The colour scale shows the joint occurrence distribution of measured and predicted wave heights, while the solid lines show quantile-quantile plots, either using coincident records (red line), or seasonally-adjusted statistics derived from all records (green line).

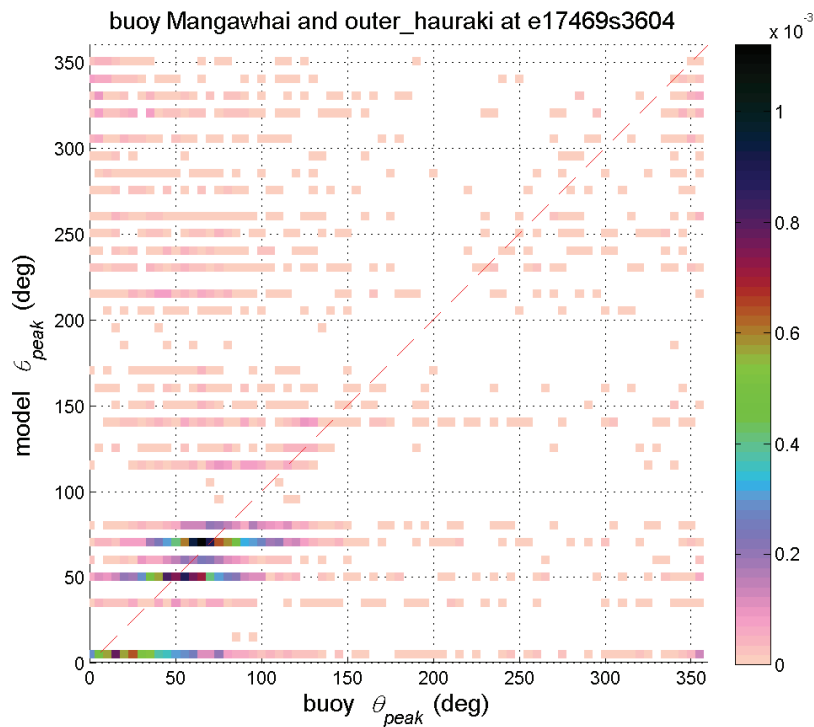


Figure 4-11: Comparison of peak wave direction (θ_{peak}) values predicted by the outer Hauraki Gulf SWAN model with measurements from the Mangawhai wave buoy.

(The colour scale shows the joint occurrence distribution of measured and predicted wave heights.)

Extreme wave analysis

The generalised Pareto distribution (GPD) was fitted to peaks-over-threshold (POT) wave data to predict the likelihood of extreme wave heights. The GPD was fitted to the largest 5% of significant wave height peaks, with peaks separated by at least three days to be classified as separate events.

As a cautionary note, regional-scale wave models such as used here are known for under-predicting the very largest waves, because they often don't have sufficient temporal and spatial resolution and accuracy of the wind-fields in the strongest storms. Although good comparisons were obtained with the available buoy records, the buoy records are short and it is likely that the wave hindcast used here is similarly affected. The buoy records themselves are too short to conduct reliable extreme-wave analyses. As a sensitivity analysis Equation 2-1 was evaluated for all 100-year ARI significant wave heights (Table 4-2), using a 1:7 beach slope and 10 s wave period. The effect of increasing the significant wave height by 50% was to increase wave setup by 0.12–0.37 m, with a medium of 0.27 m. This sensitivity has not been added to the calculated storm-tide plus wave setup elevations, but the user may wish to include an allowance for this in an additional freeboard factor.

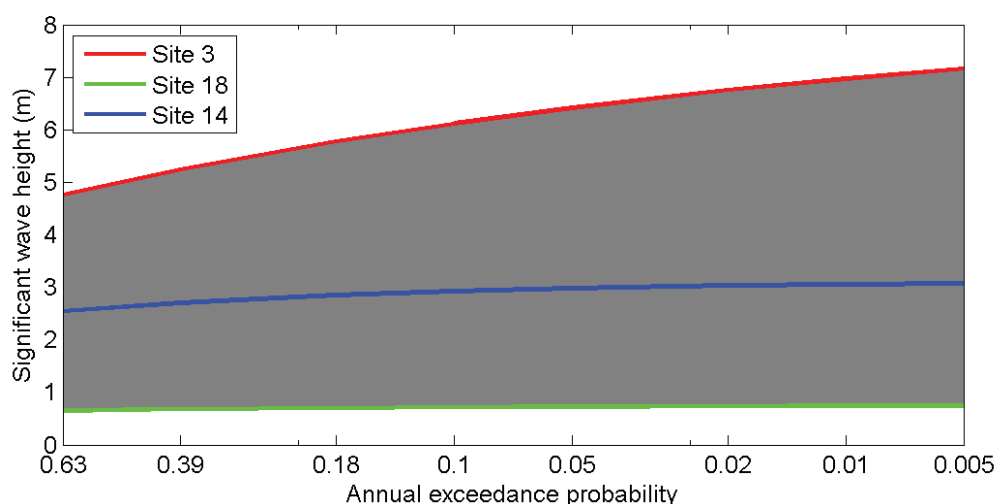


Figure 4-12: Distribution of extreme significant wave height on the eastern open-coast of the Auckland region.

Shaded area represents the range of elevations between the 37 sites. Examples given for individual sites 3, 14 and 18 (Figure 4-1).

Table 4-2: Extreme significant wave heights offshore from the eastern open coast at same sites as Table 4-1 and Figure 4-1.

Extremes calculated from 1970–2000 wave hindcast data.

| Site | Easting (NZTM) | Northing (NZTM) | AEP: | 0.39 | 0.18 | 0.10 | 0.05 | 0.02 | 0.01 | 0.005 |
|------|----------------|-----------------|------|---------|---------|-------|-------|-------|--------|--------|
| | | | ARI: | 2 yr | 5 yr | 10 yr | 20 yr | 50 yr | 100 yr | 200 yr |
| | | | 1 | 1746045 | 6002166 | 4.57 | 5.08 | 5.40 | 5.69 | 6.01 |
| 2 | 1753102 | 5992291 | 4.87 | 5.42 | 5.77 | 6.09 | 6.45 | 6.68 | 6.89 | |
| 3 | 1764823 | 5983832 | 5.24 | 5.77 | 6.12 | 6.42 | 6.76 | 6.97 | 7.16 | |
| 4 | 1761674 | 5977388 | 4.14 | 4.56 | 4.83 | 5.06 | 5.31 | 5.47 | 5.61 | |
| 5 | 1768344 | 5973565 | 4.88 | 5.34 | 5.62 | 5.87 | 6.14 | 6.31 | 6.45 | |
| 6 | 1758271 | 5968983 | 1.62 | 1.79 | 1.91 | 2.02 | 2.16 | 2.25 | 2.33 | |
| 7 | 1760994 | 5965903 | 1.64 | 1.82 | 1.95 | 2.07 | 2.22 | 2.33 | 2.44 | |
| 8 | 1757358 | 5957292 | 3.27 | 3.63 | 3.87 | 4.07 | 4.30 | 4.45 | 4.58 | |
| 9 | 1755351 | 5948872 | 3.01 | 3.27 | 3.43 | 3.56 | 3.70 | 3.78 | 3.85 | |
| 10 | 1765782 | 5949110 | 3.56 | 3.89 | 4.09 | 4.28 | 4.48 | 4.61 | 4.73 | |
| 11 | 1768729 | 5945579 | 3.29 | 3.66 | 3.90 | 4.12 | 4.37 | 4.53 | 4.68 | |
| 12 | 1758449 | 5941213 | 3.02 | 3.35 | 3.57 | 3.76 | 3.97 | 4.11 | 4.23 | |
| 13 | 1757328 | 5934697 | 2.89 | 3.14 | 3.29 | 3.42 | 3.56 | 3.65 | 3.72 | |
| 14 | 1757600 | 5931984 | 2.71 | 2.85 | 2.93 | 2.98 | 3.03 | 3.06 | 3.07 | |

| Site | Easting (NZTM) | Northing (NZTM) | AEP: | 0.39 | 0.18 | 0.10 | 0.05 | 0.02 | 0.01 | 0.005 |
|------|----------------|-----------------|------|------|------|-------|-------|-------|--------|--------|
| | | | ARI: | 2 yr | 5 yr | 10 yr | 20 yr | 50 yr | 100 yr | 200 yr |
| | | | | | | | | | | |
| 15 | 1758282 | 5929752 | | 2.76 | 2.93 | 3.02 | 3.09 | 3.15 | 3.19 | 3.22 |
| 16 | 1759748 | 5927428 | | 2.54 | 2.71 | 2.81 | 2.89 | 2.98 | 3.03 | 3.07 |
| 17 | 1762306 | 5924882 | | 2.11 | 2.26 | 2.35 | 2.44 | 2.53 | 2.58 | 2.63 |
| 18 | 1768474 | 5920856 | | 0.68 | 0.70 | 0.72 | 0.73 | 0.74 | 0.74 | 0.75 |
| 19 | 1773944 | 5917482 | | 1.71 | 1.81 | 1.87 | 1.92 | 1.98 | 2.01 | 2.04 |
| 20 | 1781649 | 5917865 | | 1.49 | 1.58 | 1.64 | 1.69 | 1.75 | 1.79 | 1.82 |
| 21 | 1789299 | 5912170 | | 1.26 | 1.31 | 1.33 | 1.35 | 1.37 | 1.38 | 1.39 |
| 22 | 1792968 | 5910034 | | 0.78 | 0.79 | 0.80 | 0.80 | 0.80 | 0.80 | 0.81 |
| 23 | 1802591 | 5907745 | | 3.09 | 3.31 | 3.45 | 3.57 | 3.70 | 3.78 | 3.85 |
| 24 | 1806261 | 5897453 | | 2.64 | 2.79 | 2.89 | 2.97 | 3.05 | 3.10 | 3.14 |
| 25 | 1798030 | 5918077 | | 3.11 | 3.33 | 3.47 | 3.58 | 3.71 | 3.79 | 3.86 |
| 26 | 1798292 | 5929361 | | 4.04 | 4.39 | 4.63 | 4.83 | 5.07 | 5.22 | 5.36 |
| 27 | 1793282 | 5932939 | | 4.25 | 4.65 | 4.91 | 5.14 | 5.41 | 5.58 | 5.74 |
| 28 | 1785826 | 5930285 | | 4.12 | 4.53 | 4.82 | 5.08 | 5.39 | 5.61 | 5.81 |
| 29 | 1776063 | 5928106 | | 2.07 | 2.15 | 2.19 | 2.22 | 2.26 | 2.28 | 2.30 |
| 30 | 1782627 | 5921463 | | 1.06 | 1.11 | 1.13 | 1.15 | 1.17 | 1.19 | 1.20 |
| 31 | 1793244 | 5921007 | | 1.13 | 1.19 | 1.23 | 1.26 | 1.30 | 1.32 | 1.34 |
| 32 | 1793594 | 5926216 | | 2.09 | 2.34 | 2.50 | 2.64 | 2.80 | 2.91 | 3.01 |
| 33 | 1770683 | 5925185 | | 0.85 | 0.88 | 0.89 | 0.90 | 0.90 | 0.91 | 0.91 |
| 34 | 1766404 | 5930907 | | 3.15 | 3.45 | 3.65 | 3.82 | 4.02 | 4.16 | 4.27 |
| 35 | 1766328 | 5963017 | | 3.87 | 4.35 | 4.67 | 4.96 | 5.30 | 5.53 | 5.74 |
| 36 | 1770378 | 5967921 | | 4.82 | 5.26 | 5.54 | 5.77 | 6.03 | 6.20 | 6.34 |

4.1.4 Combined storm-tide plus wave setup on the eastern open coast

Joint-probability analyses of both extreme storm-tides and waves were undertaken using coinciding significant wave height, wave period, and storm-tide sampled at each high tide. A joint-probability analysis of storm-tides and waves describes the combined likelihood of a high storm-tide and large wave event occurring at the same time (Figure 7-1).

At each location, the highest combined storm-tide plus wave setup elevation was determined for each annual exceedance probability, as described in Section 7.4. These values are presented in Table 4-3. A

map of the 0.01 AEP storm-tide plus wave setup elevations is shown in Figure 4-13, and the contribution of wave setup above the storm-tide alone is shown in Figure 4-14. As expected, this shows the largest contribution of wave setup (~0.8 m) to the 0.01 AEP combined storm-tide plus wave setup elevations on the more wave exposed locations, relative to wave-sheltered beaches in the inner Hauraki Gulf such as Karaka Bay (~0.1 m).

Table 4-3: Maximum storm-tide plus wave setup elevations along the eastern open-coast.

Elevations are relative to AVD-46 and include a +0.15 m mean sea-level offset (1999–2008).

| Site | Easting (NZTM) | Northing (NZTM) | Joint AEP: | 0.39 | 0.18 | 0.10 | 0.05 | 0.02 | 0.01 | 0.005 |
|------|----------------|-----------------|------------|------|------|-------|-------|-------|--------|--------|
| | | | Joint ARI: | 2 yr | 5 yr | 10 yr | 20 yr | 50 yr | 100 yr | 200 yr |
| | | | | | | | | | | |
| 1 | 1746045 | 6002166 | 2.07 | 2.23 | 2.30 | 2.39 | 2.48 | 2.54 | 2.66 | |
| 2 | 1753102 | 5992291 | 2.12 | 2.28 | 2.38 | 2.48 | 2.60 | 2.64 | 2.75 | |
| 3 | 1764823 | 5983832 | 2.15 | 2.29 | 2.40 | 2.49 | 2.60 | 2.68 | 2.76 | |
| 4 | 1761674 | 5977388 | 2.00 | 2.13 | 2.21 | 2.28 | 2.37 | 2.46 | 2.50 | |
| 5 | 1768344 | 5973565 | 2.32 | 2.47 | 2.57 | 2.67 | 2.78 | 2.84 | 2.90 | |
| 6 | 1758271 | 5968983 | 1.83 | 1.89 | 1.94 | 2.00 | 2.06 | 2.11 | 2.15 | |
| 7 | 1760994 | 5965903 | 1.86 | 1.91 | 1.95 | 2.01 | 2.08 | 2.13 | 2.19 | |
| 8 | 1757358 | 5957292 | 2.04 | 2.18 | 2.26 | 2.33 | 2.45 | 2.50 | 2.56 | |
| 9 | 1755351 | 5948872 | 2.05 | 2.17 | 2.26 | 2.35 | 2.42 | 2.50 | 2.57 | |
| 10 | 1765782 | 5949110 | 2.19 | 2.32 | 2.41 | 2.49 | 2.62 | 2.68 | 2.74 | |
| 11 | 1768729 | 5945579 | 2.08 | 2.20 | 2.28 | 2.37 | 2.45 | 2.51 | 2.60 | |
| 12 | 1758449 | 5941213 | 2.05 | 2.17 | 2.25 | 2.35 | 2.43 | 2.52 | 2.57 | |
| 13 | 1757328 | 5934697 | 2.08 | 2.20 | 2.28 | 2.35 | 2.46 | 2.52 | 2.56 | |
| 14 | 1757600 | 5931984 | 2.07 | 2.16 | 2.24 | 2.32 | 2.40 | 2.44 | 2.50 | |
| 15 | 1758282 | 5929752 | 2.07 | 2.17 | 2.25 | 2.31 | 2.41 | 2.46 | 2.55 | |
| 16 | 1759748 | 5927428 | 2.15 | 2.27 | 2.33 | 2.40 | 2.50 | 2.55 | 2.60 | |
| 17 | 1762306 | 5924882 | 2.02 | 2.14 | 2.21 | 2.29 | 2.37 | 2.40 | 2.46 | |
| 18 | 1768474 | 5920856 | 2.00 | 2.08 | 2.13 | 2.18 | 2.24 | 2.28 | 2.31 | |
| 19 | 1773944 | 5917482 | 2.07 | 2.18 | 2.25 | 2.31 | 2.39 | 2.44 | 2.48 | |
| 20 | 1781649 | 5917865 | 2.07 | 2.16 | 2.22 | 2.29 | 2.35 | 2.39 | 2.43 | |
| 21 | 1789299 | 5912170 | 2.09 | 2.18 | 2.25 | 2.31 | 2.37 | 2.42 | 2.46 | |
| 22 | 1792968 | 5910034 | 2.05 | 2.15 | 2.21 | 2.26 | 2.32 | 2.35 | 2.38 | |

| Site | Easting (NZTM) | Northing (NZTM) | Joint AEP: | 0.39 | 0.18 | 0.10 | 0.05 | 0.02 | 0.01 | 0.005 |
|------|-------------------|-----------------|------------|------|------|-------|-------|-------|--------|--------|
| | | | Joint ARI: | 2 yr | 5 yr | 10 yr | 20 yr | 50 yr | 100 yr | 200 yr |
| | | | | | | | | | | |
| 23 | 1802591 | 5907745 | | 2.38 | 2.50 | 2.58 | 2.65 | 2.75 | 2.83 | 2.87 |
| 24 | 1806261 | 5897453 | | 2.32 | 2.43 | 2.50 | 2.56 | 2.65 | 2.70 | 2.75 |
| 25 | 1798030 | 5918077 | | 2.34 | 2.46 | 2.54 | 2.63 | 2.72 | 2.78 | 2.83 |
| 26 | 1798292 | 5929361 | | 2.33 | 2.45 | 2.53 | 2.61 | 2.71 | 2.78 | 2.91 |
| 27 | 1793282 | 5932939 | | 2.28 | 2.42 | 2.50 | 2.61 | 2.73 | 2.81 | 2.90 |
| 28 | 1785826 | 5930285 | | 2.29 | 2.44 | 2.56 | 2.65 | 2.78 | 2.86 | 2.96 |
| 29 | 1776063 | 5928106 | | 2.25 | 2.35 | 2.41 | 2.48 | 2.56 | 2.61 | 2.66 |
| 30 | 1782627 | 5921463 | | 2.00 | 2.08 | 2.12 | 2.17 | 2.23 | 2.26 | 2.29 |
| 31 | 1793244 | 5921007 | | 2.00 | 2.05 | 2.09 | 2.14 | 2.20 | 2.24 | 2.28 |
| 32 | 1793594 | 5926216 | | 2.07 | 2.16 | 2.24 | 2.31 | 2.39 | 2.46 | 2.52 |
| 33 | 1770683 | 5925185 | | 2.04 | 2.13 | 2.18 | 2.23 | 2.29 | 2.31 | 2.34 |
| 34 | 1766404 | 5930907 | | 2.13 | 2.25 | 2.32 | 2.40 | 2.50 | 2.57 | 2.63 |
| 35 | 1766328 | 5963017 | | 2.15 | 2.30 | 2.42 | 2.52 | 2.65 | 2.75 | 2.77 |
| 36 | 1770378 | 5967921 | | 2.32 | 2.47 | 2.58 | 2.68 | 2.77 | 2.87 | 2.93 |

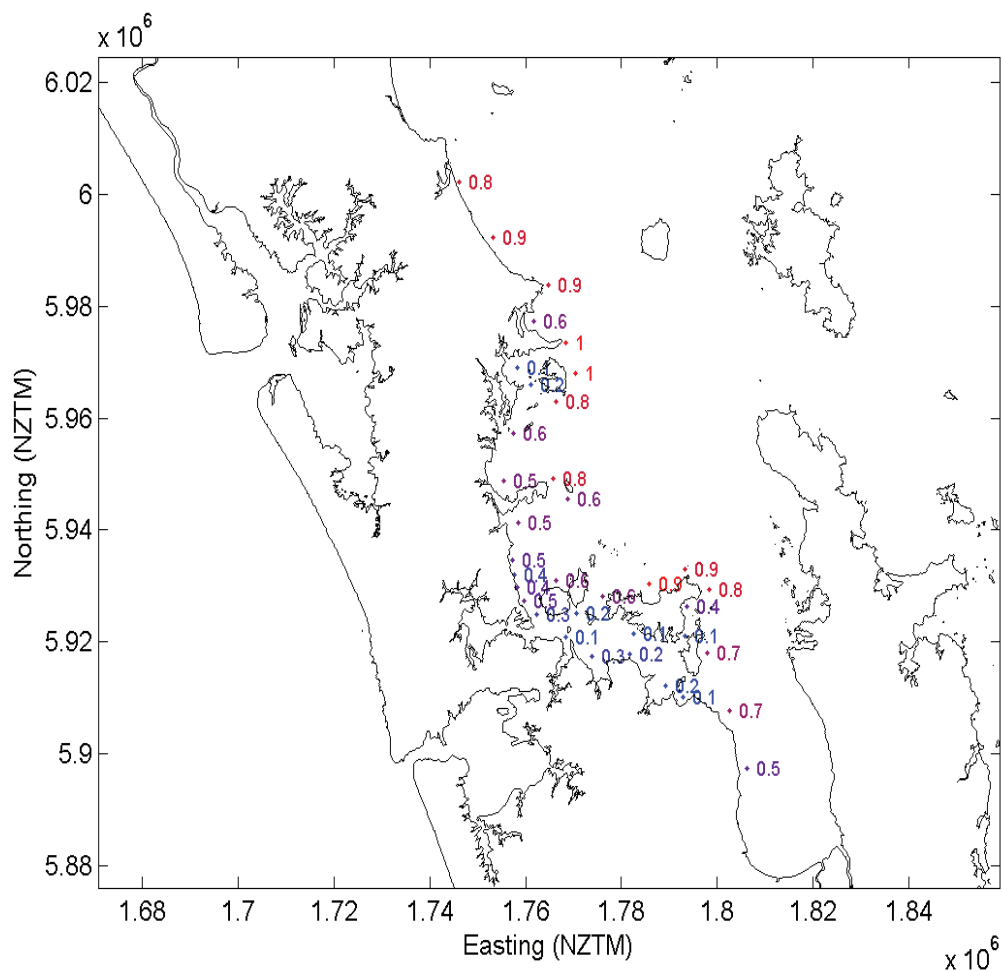


Figure 4-14: Difference between 1% annual exceedance probability storm-tide plus wave setup and storm-tide-only elevations on the eastern open-coast.
(Elevations in metres.)

4.2 East-coast estuaries

Storm-tide elevations in the numerous relatively small east-coast harbours and estuaries were calculated as follows:

- *The maximum storm-tide plus wave setup elevations calculated for the open east coast were applied to the harbour entrances³.*
- The storm-tide component is expected to amplify inside the harbours. An amplification factor that increased with distance from the harbour entrance was applied to the storm-tide component.

The calculated elevations are shown in Table 4-4.

³ *As outlined in the NIWA 2016 report (Part 2, Section 1.3), the wave set-up has been removed from the revised results*

Table 4-3: Maximum storm-tide plus wave setup elevations in small east-coast estuaries⁴.

Elevations are relative to AVD-46 and include a +0.15 m mean sea-level offset (1999–2008).

| Site | Easting (NZTM) | Northing (NZTM) | Joint AEP: | 0.39 | 0.18 | 0.10 | 0.05 | 0.02 | 0.01 | 0.005 |
|-------------------------------|-------------------|--------------------|------------|------|------|-------|-------|-------|--------|--------|
| | | | Joint ARI: | 2 yr | 5 yr | 10 yr | 20 yr | 50 yr | 100 yr | 200 yr |
| | | | | | | | | | | |
| Mangawhai Harbour | 1742349 | 6001359 | 2.11 | 2.27 | 2.35 | 2.44 | 2.52 | 2.59 | 2.70 | |
| Whangateau Harbour | 1759163 | 5974912 | 2.05 | 2.17 | 2.25 | 2.33 | 2.42 | 2.52 | 2.55 | |
| Whangateau Harbour | 1758250 | 5978697 | 2.02 | 2.15 | 2.23 | 2.31 | 2.39 | 2.49 | 2.52 | |
| Omaha R. (Whangateau Harbour) | 1756538 | 5977574 | 2.04 | 2.16 | 2.24 | 2.32 | 2.41 | 2.51 | 2.54 | |
| Matakana River estuary | 1753842 | 5971395 | 1.85 | 1.92 | 1.97 | 2.03 | 2.09 | 2.14 | 2.18 | |
| Matakana River estuary | 1754603 | 5971927 | 1.85 | 1.91 | 1.96 | 2.02 | 2.08 | 2.13 | 2.17 | |
| Matakana River estuary | 1754432 | 5974837 | 1.87 | 1.93 | 1.98 | 2.04 | 2.10 | 2.15 | 2.20 | |
| Matakana River estuary | 1755060 | 5972536 | 1.85 | 1.91 | 1.96 | 2.02 | 2.08 | 2.13 | 2.18 | |
| Matakana River estuary | 1755269 | 5974476 | 1.87 | 1.93 | 1.98 | 2.04 | 2.10 | 2.15 | 2.19 | |
| Pukapuka Inlet (Mahurangi) | 1750849 | 5961126 | 2.09 | 2.23 | 2.31 | 2.38 | 2.50 | 2.56 | 2.61 | |
| Mahurangi Harbour | 1753626 | 5960575 | 2.07 | 2.22 | 2.29 | 2.36 | 2.48 | 2.54 | 2.59 | |
| Mahurangi Harbour | 1751686 | 5968031 | 2.13 | 2.27 | 2.35 | 2.42 | 2.54 | 2.60 | 2.66 | |
| Mahurangi Harbour | 1754615 | 5960537 | 2.07 | 2.21 | 2.29 | 2.36 | 2.48 | 2.53 | 2.59 | |
| Te Kapa R. (Mahurangi) | 1756099 | 5963200 | 2.09 | 2.23 | 2.31 | 2.38 | 2.50 | 2.56 | 2.61 | |
| Mahurangi Harbour | 1753210 | 5958010 | 2.05 | 2.20 | 2.27 | 2.34 | 2.46 | 2.52 | 2.57 | |
| Puhoi River estuary | 1750338 | 5956222 | 2.07 | 2.21 | 2.29 | 2.36 | 2.48 | 2.53 | 2.59 | |
| Waiwera River estuary | 1750889 | 5954757 | 2.06 | 2.21 | 2.28 | 2.35 | 2.47 | 2.53 | 2.58 | |
| Orewa River estuary | 1749727 | 5948635 | 2.07 | 2.19 | 2.29 | 2.37 | 2.44 | 2.53 | 2.59 | |
| Weiti River | 1751800 | 5946524 | 2.10 | 2.22 | 2.30 | 2.40 | 2.48 | 2.57 | 2.62 | |
| Karepiro Bay | 1754558 | 5942016 | 2.06 | 2.19 | 2.26 | 2.36 | 2.45 | 2.53 | 2.58 | |
| Okura River | 1752751 | 5939753 | 2.08 | 2.21 | 2.28 | 2.38 | 2.47 | 2.55 | 2.61 | |
| Tamaki Estuary | 1765514 | 5913666 | 2.06 | 2.15 | 2.20 | 2.25 | 2.32 | 2.35 | 2.38 | |
| Tamaki Estuary | 1766408 | 5911555 | 2.13 | 2.23 | 2.28 | 2.33 | 2.39 | 2.42 | 2.45 | |
| Pakuranga Creek | 1769431 | 5912063 | 2.14 | 2.24 | 2.29 | 2.34 | 2.40 | 2.43 | 2.46 | |

⁴ This table has been superseded by Table 3-2 in the NIWA 2016 report (Part 2)

| Site | Easting (NZTM) | Northing (NZTM) | Joint AEP: | 0.39 | 0.18 | 0.10 | 0.05 | 0.02 | 0.01 | 0.005 |
|----------------------|-------------------|--------------------|------------|------|------|-------|-------|-------|--------|--------|
| | | | Joint ARI: | 2 yr | 5 yr | 10 yr | 20 yr | 50 yr | 100 yr | 200 yr |
| | | | | | | | | | | |
| (Tamaki) | | | | | | | | | | |
| Tamaki Estuary | 1764589 | 5907948 | 2.17 | 2.27 | 2.32 | 2.37 | 2.43 | 2.46 | 2.49 | |
| Mangamangaroa Creek | 1772868 | 5912475 | 2.08 | 2.20 | 2.26 | 2.32 | 2.40 | 2.46 | 2.49 | |
| Turanga Creek | 1775337 | 5910030 | 2.10 | 2.21 | 2.27 | 2.33 | 2.42 | 2.47 | 2.51 | |
| Waikopua Creek | 1777927 | 5912838 | 2.08 | 2.20 | 2.26 | 2.32 | 2.40 | 2.46 | 2.49 | |
| Wairoa River estuary | 1784026 | 5907369 | 2.12 | 2.21 | 2.28 | 2.34 | 2.40 | 2.46 | 2.49 | |
| Wairoa River estuary | 1784970 | 5907950 | 2.11 | 2.20 | 2.27 | 2.33 | 2.39 | 2.45 | 2.48 | |
| Wairoa River estuary | 1785600 | 5907417 | 2.12 | 2.21 | 2.28 | 2.34 | 2.41 | 2.46 | 2.50 | |

4.3 The open west coast

The 1970–2000 WASP hindcasts of storm surge and waves were also used to calculate the frequency and magnitude of combined storm-tide plus wave setup elevations on the western open-coast of the Auckland region. Figure 4-15 marks the five selected output locations along the coastline, plus the locations of model hindcast data available from the WASP modelling project (<http://wrenz.niwa.co.nz/webmodel/coastal>).

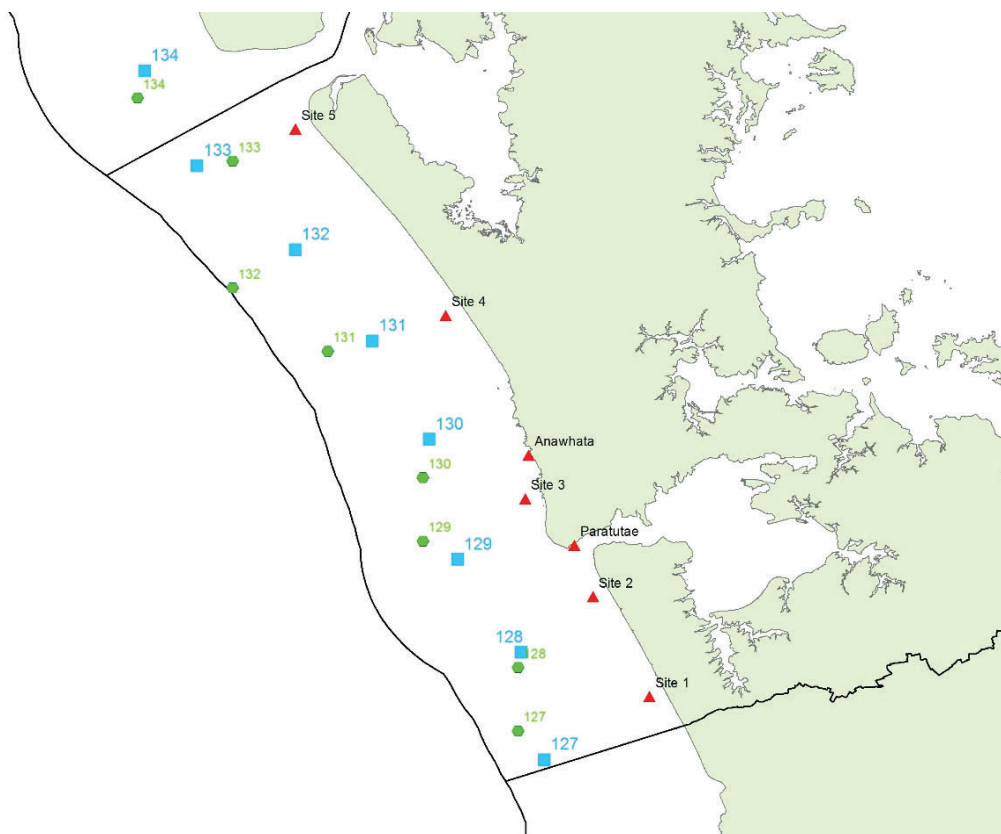


Figure 4-15: Location of combined storm-tide plus wave setup elevation calculations along the western open-coast.

(Blue squares mark the nominal WASP output locations on the 50 m isobath; green circles mark the centres of the wave model grid cells from which the wave outputs for each site were actually taken; red triangles mark output locations for coastal extreme water levels, and the location of the Anawhata tide gauge.)

4.3.1 Storm-tide on the western open-coast

Storm-tide was simulated at the five output locations (Figure 4-15) by summing:

- Predicted tide from NIWA's tide model (12 constituents) with minor bias correction for amplitude and phase for the M2, S2 and N2 main tidal constituents to align better with the Anawhata sea level gauge measurements.
- Storm surge from the WASP models extracted from the nearest location to each output location (Figure 4-15) using a wavelet filter that isolates periods of 1-16 days. The WASP storm surge was checked against measured storm surge from the Anawhata tide gauge using a quantile-quantile comparison. The quantile-quantile comparison used all available data from the gauge (1999-2011) that included two years (1999 & 2000) of data that overlapped the WASP simulation (1970–2000). The comparison revealed that the WASP model under-predicted the measured storm surge at the Anawhata gauge site (Figure 4-16), probably due to shoaling effects of the storm-surge wave and the presence of some wave setup in the coastal gauge at Anawhata. By assuming a similar under-

prediction at all five output locations the WASP storm surge was scaled using the Anawhata comparison, by adjusting each quantile

- in the modelled storm surge to match that from the Anawhata gauge (1:1 equivalence).
- Monthly mean sea-level anomaly from the WASP models extracted from the nearest location to each output location (Figure 4-15) using a low-pass wavelet filter to extract sea-level variability with periods of ≥ 32 days (1 month). This is the same way that MMSLA is extracted from the non-tidal sea-level component of the tide-gauge record. Note, however, that WASP simulated storm surge and did not explicitly simulate MMSLA. The MMSLA derived from the WASP storm-surge time-series is actually a low-pass component of simulated storm-surge. The modelled and measured MMSLA were compared using a quantile-quantile comparison. The model under-predicted the Anawhata gauge measurements, as expected (since MMSLA was not explicitly simulated). As there were large quantile-quantile deviations from the equivalence line at very high and low quantiles, and the remaining data exhibited an approximately linear trend, the modelled MMSLA was adjusted by a linear factor of 1.8 (Figure 4-17). This scaling factor was applied to simulated MMSLA for all five output locations.

The extreme storm-tide frequency–magnitude distributions calculated from measured and simulated data were compared (Figure 4-18). The simulated median extreme storm-tide distribution was under-predicting the measurement-based best-fit by ~ 8 cm at 0.01 AEP, although it lay well inside the 95% confidence intervals for the measurement-based model. For conservatism, it was decided to scale the extreme storm-tide distributions at all five locations, using relative scaling for each AEP of interest, based on the Anawhata comparisons; the resulting extreme storm-tide distributions are compared to the measurement-based distribution in Figure 4-19, and tabled in Table 4-5. The differences between the 5 sites relate mainly to tide range differences. Note that the large outlier in Figure 4-18 is the storm-tide of 17 April 1999, when a broad and deepening trough was preceded by strong north-westerly flows and followed by colder south-westerlies. A major front occurred within the trough. It brought gale force winds over the North Island, contributing to sea flooding along the west coast.

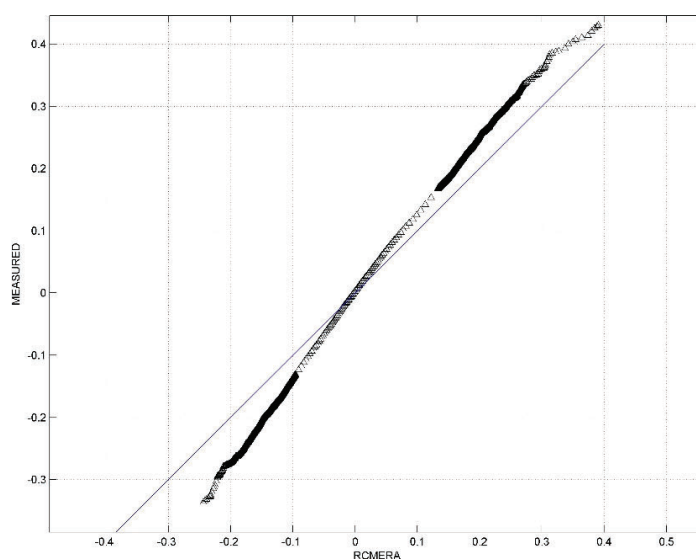


Figure 4-16: Quantile-quantile comparison of storm surge derived from the Anawhata tide gauge and the WASP model.
(RCMERA = WASP model; Measured = Anawhata tide gauge.)

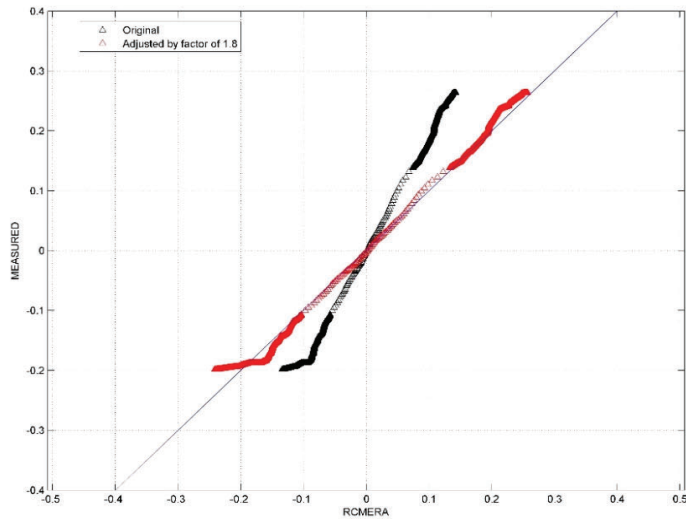


Figure 4-17: Quantile-quantile comparison of monthly mean sea-level anomaly derived from the Anawhata tide gauge and the WASP model.

(RCMERA = low-pass filtered storm-surge from WASP model; Measured = MMSLA from the Anawhata tide gauge. The adjusted distribution is plotted in red.)

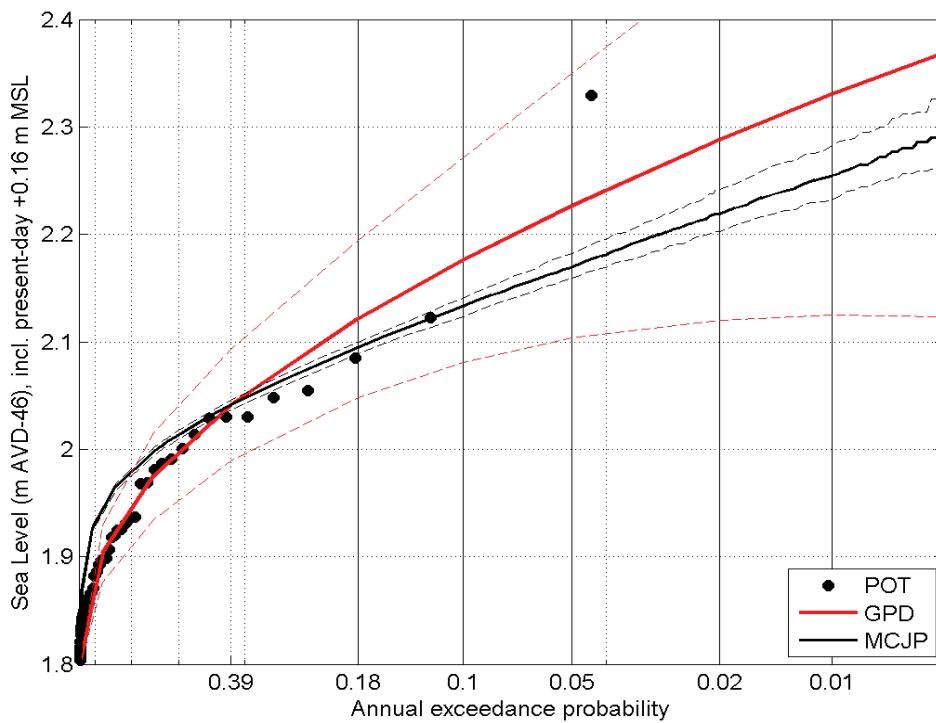


Figure 4-18: Extreme storm-tide distributions at Anawhata.

(Elevations are relative to AVD-46 including +0.16 m offset for baseline mean sea level (present-day estimate). POT = peaks-over-threshold data; GPD = generalised Pareto model fit to POT data; MCJP = Monte Carlo joint-probability model of simulated storm-tide.)

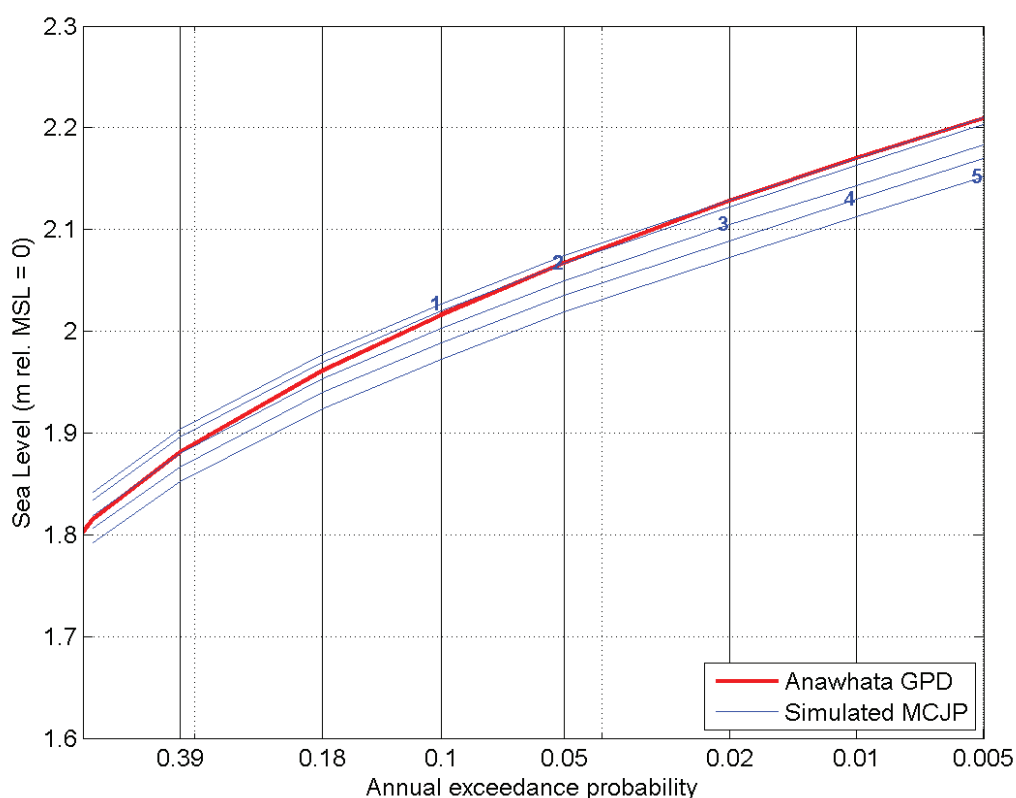


Figure 4-19: Storm-tide frequency–magnitude distributions along western open-coast.

(Number represents site locations as in Figure 4-15. The curves show relative changes; no MSL offset is applied.)

Table 4-5: Storm-tide elevations along the western open-coast.

Elevations are relative to AVD-46 and include a +0.16 m mean sea-level offset.

| Site | Easting (NZTM) | Northing (NZTM) | AEP: | 0.39 | 0.18 | 0.10 | 0.05 | 0.02 | 0.01 | 0.005 |
|------|----------------|-----------------|------|------|------|-------|-------|-------|--------|--------|
| | | | ARI: | 2 yr | 5 yr | 10 yr | 20 yr | 50 yr | 100 yr | 200 yr |
| | | | | | | | | | | |
| 1 | 1742786 | 5876179 | | 2.00 | 2.06 | 2.14 | 2.19 | 2.23 | 2.29 | 2.33 |
| 2 | 1736812 | 5890706 | | 1.99 | 2.06 | 2.13 | 2.18 | 2.23 | 2.28 | 2.32 |
| 3 | 1729036 | 5905254 | | 1.98 | 2.04 | 2.11 | 2.16 | 2.21 | 2.26 | 2.30 |
| 4 | 1719636 | 5933133 | | 1.97 | 2.03 | 2.10 | 2.15 | 2.19 | 2.25 | 2.29 |
| 5 | 1702991 | 5959977 | | 1.95 | 2.01 | 2.08 | 2.13 | 2.18 | 2.23 | 2.27 |

4.3.2 Waves on the western open-coast

The WASP wave simulations (1970-2001) were used directly for the open west coast without undergoing any rescaling. Comparisons of the WASP simulation with the nearest wave buoy data are plotted in Figure 4-20 (Taharoa wave buoy) and Figure 4-21 (Hokianga wave buoy). The dark red lines are quantile-quantile plots using the buoy-model overlap period. The green lines are quantile-quantile plots using the full records of both model and buoy, with the latter seasonally adjusted to correct for the

record not being a whole number of years, and hence having, for example, more January than June data. This can be done even with no data overlap, e.g., with the Hokianga wave buoy data (June 2006 – July 2007).

The nearest WASP wave output locations were assigned to each of the five output sites as shown in the Figure 4-15.

A GPD was fitted to the 30-year simulated wave data record from WASP from each site and used to scale the marginal extremes of the joint probability data. The extreme significant wave height data are plotted in Figure 4-22 and tabled in Table 4-6.

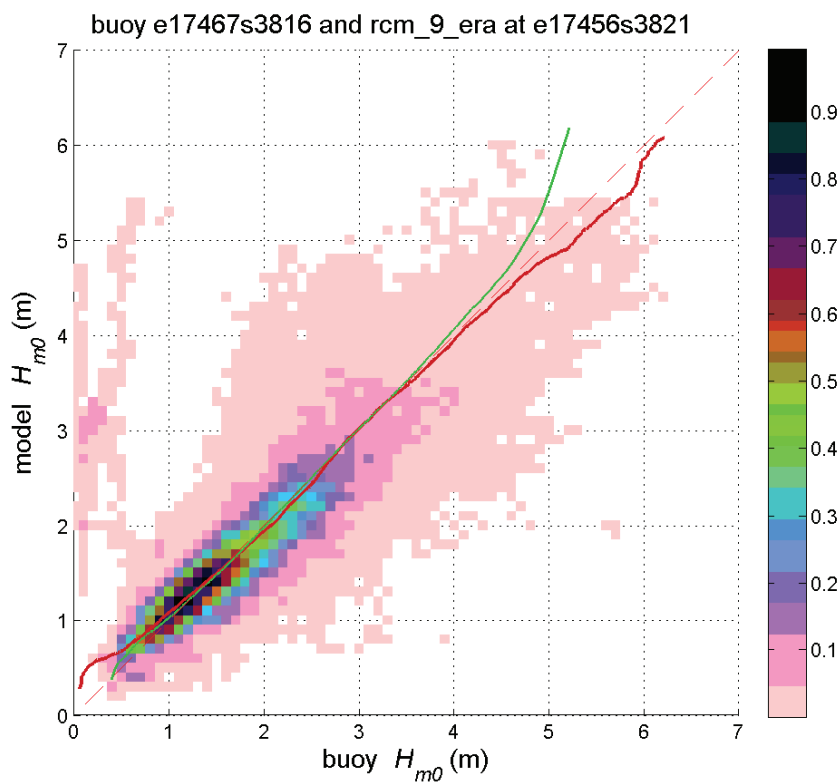


Figure 4-20: Comparison of significant wave height values predicted by the WASP rcm_9_era model with measurements from the Taharoa wave buoy.

(The colour scale shows the joint occurrence distribution of measured and predicted wave heights, while the solid lines show quantile-quantile plots, either using coincident records (red line), or seasonally-adjusted statistics derived from all records (green line).

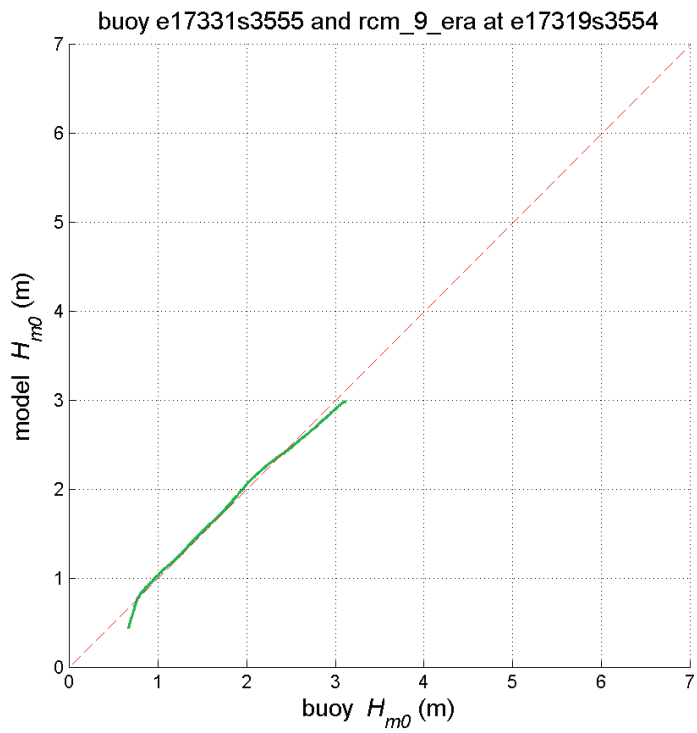


Figure 4-21: Comparison of significant wave height values predicted by the WASP rcm_9_era model with measurements off Mangonui Bluff, near Hokianga Harbour.

(The green line is a quantile-quantile plot of seasonally-adjusted statistics derived from all records.)

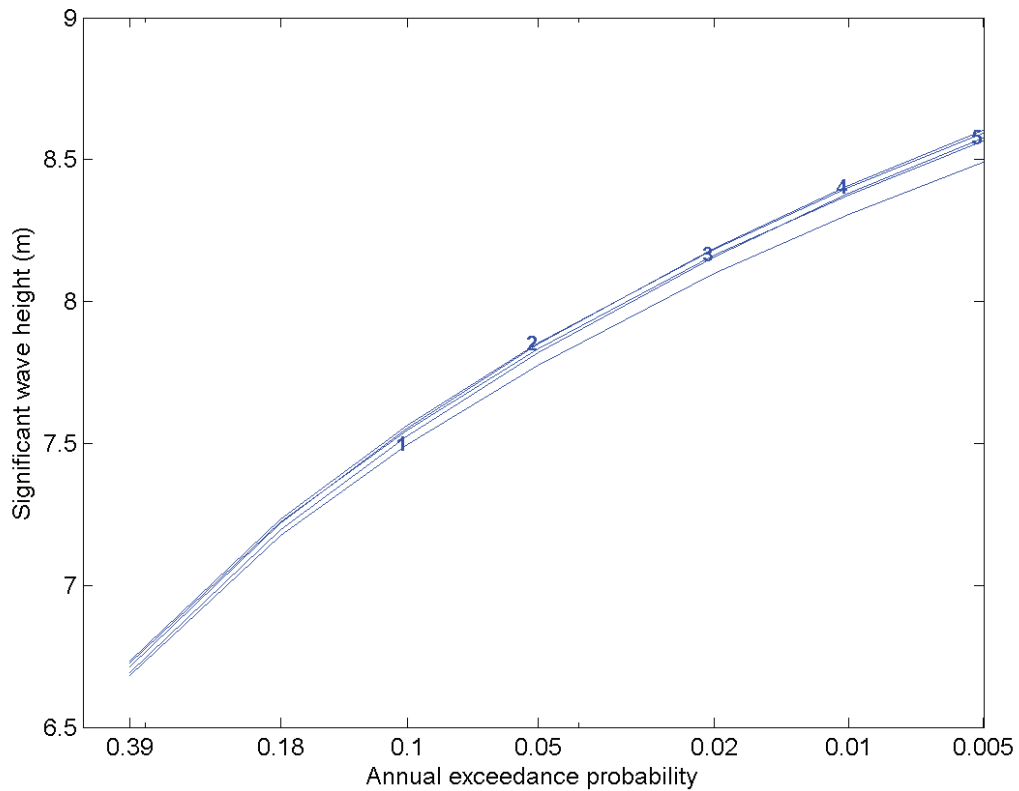


Figure 4-22: Extreme significant wave height (m) along the western open-coast at the 5 sites.

Table 4-6: Extreme significant wave height (m) along the western open-coast.

| Site | Easting (NZTM) | Northing (NZTM) | AEP: | 0.39 | 0.18 | 0.10 | 0.05 | 0.02 | 0.01 | 0.005 |
|------|----------------|-----------------|------|---------|---------|-------|-------|-------|--------|--------|
| | | | ARI: | 2 yr | 5 yr | 10 yr | 20 yr | 50 yr | 100 yr | 200 yr |
| | | | 1 | 1742786 | 5876179 | 6.68 | 7.18 | 7.50 | 7.78 | 8.10 |
| 2 | 1736812 | 5890706 | 6.71 | 7.22 | 7.55 | 7.85 | 8.19 | 8.41 | 8.60 | |
| 3 | 1729036 | 5905254 | 6.73 | 7.22 | 7.55 | 7.83 | 8.16 | 8.38 | 8.56 | |
| 4 | 1719636 | 5933133 | 6.73 | 7.24 | 7.56 | 7.85 | 8.18 | 8.40 | 8.59 | |
| 5 | 1702991 | 5959977 | 6.69 | 7.20 | 7.53 | 7.82 | 8.16 | 8.38 | 8.58 | |

4.3.3 Combined storm-tide plus wave setup on the eastern open coast

Joint-probability analyses of extreme storm-tides and waves were undertaken using coinciding significant wave height, wave period, and storm-tide sampled at each high tide. A joint-probability analysis of storm-tides and waves describes the combined likelihood of a high storm-tide and large wave event occurring at the same time (Figure 7-1).

At each location, the highest combined storm-tide plus wave setup elevation was determined for each annual exceedance probability, as described in Section 7.4. These values are presented in Table 4-7. Wave setup contributes approximately 1 m of the total inundation level over and above storm-tide alone, for a joint 1% AEP inundation event (Table 48).

Table 4-7: Maximum storm-tide plus wave setup elevations along the western open-coast.

Elevations are relative to AVD-46 and include a +0.15 m mean sea-level offset.

| Site | Easting (NZTM) | Northing (NZTM) | Joint AEP: | 0.18 | 0.05 | 0.02 | 0.01 |
|------|----------------|-----------------|------------|---------|---------|-------|--------|
| | | | Joint ARI: | 5 yr | 20 yr | 50 yr | 100 yr |
| | | | 1 | 1742786 | 5876179 | 2.90 | 3.11 |
| 2 | 1736812 | 5890706 | 2.90 | 3.13 | 3.26 | 3.36 | |
| 3 | 1729036 | 5905254 | 2.89 | 3.08 | 3.20 | 3.31 | |
| 4 | 1719636 | 5933133 | 2.87 | 3.08 | 3.19 | 3.26 | |
| 5 | 1702991 | 5959977 | 2.87 | 3.09 | 3.19 | 3.29 | |

Table 4-8: Elevation difference (m) between storm-tide + wave setup and storm-tide-only along the western open-coast.

| Site | Easting (NZTM) | Northing (NZTM) | AEP: | 0.18 | 0.05 | 0.02 | 0.01 |
|------|----------------|-----------------|------|------|-------|-------|--------|
| | | | ARI: | 5 yr | 20 yr | 50 yr | 100 yr |
| | | | | | | | |
| 1 | 1742786 | 5876179 | | 0.84 | 0.92 | 1.00 | 1.01 |
| 2 | 1736812 | 5890706 | | 0.84 | 0.95 | 1.03 | 1.08 |
| 3 | 1729036 | 5905254 | | 0.85 | 0.92 | 0.99 | 1.05 |
| 4 | 1719636 | 5933133 | | 0.84 | 0.93 | 1.00 | 1.01 |
| 5 | 1702991 | 5959977 | | 0.86 | 0.96 | 1.01 | 1.06 |

5 Glossary of abbreviations and terms

| | |
|-------------------------------------|---|
| Annual exceedance probability (AEP) | The probability of a given (usually high) sea level or wave height being equalled or exceeded in elevation, in any given calendar year. AEP can be specified as a fraction (e.g., 0.01) or a percentage (e.g., 1%). |
| AVD-46 | Auckland Vertical Datum – 1946 was established as the mean sea level at Port of Auckland from 7 years of sea level measurements collected in 1909, 1917–1919 and 1921–1923. |
| Average recurrence interval (ARI) | The average time interval (averaged over a very long time period and many “events”) that is expected to elapse between recurrences of an infrequent event of a given large magnitude (or larger). A large infrequent event would be expected to be equalled or exceeded in elevation, once, on average, every “ARI” years, but with considerable variability. |
| Bathymetry | A term for the topography that lies submerged under a water body |
| CMA | The coastal marine area is defined in s2 of the RMA as meaning: "The foreshore, seabed, and coastal water, and the air space above the water - (a) Of which the seaward boundary is the outer limits of the territorial sea. (b) Of which the landward boundary is the line of mean high water springs, except that where that line crosses a river, the landward boundary at that point shall be whichever is the lesser of - (i) One kilometre upstream from the mouth of the river; or (ii) The point upstream that is calculated by multiplying the width of the river mouth by five". |
| ENSO | El Niño Southern Oscillation. A natural global climate phenomenon involving the interaction between the tropical Pacific and the atmosphere, but has far-reaching effects on the global climate, especially for countries in the Pacific rim. ENSO is the strongest climate signal on time scales of one to several years. The quasi-periodic cycle oscillates between El Niño (unusually warm ocean waters along the tropical South American coast) and La Niña (colder-than-normal ocean waters off South America). |
| Epoch | A particular period of history that is arbitrarily selected as a point of reference – used in connection with developing a baseline sea level. |
| GIS | A geographic information system (GIS) is a system designed to capture, store, manipulate, analyse, manage, and present all types of geographical information for informing decision making. |
| Hindcast | A numerical simulation (representation) of past conditions. As opposed to a forecast or future cast that simulates the future. |
| IPO | Interdecadal Pacific Oscillation – a long timescale oscillation in the ocean–atmosphere system that shifts climate in the Pacific region every one to three decades. |
| Joint-probability | The probability of two separate processes occurring together (e.g., large waves and high storm-tide). |

| | |
|--|---|
| LiDAR | Light Detection And Ranging – an airborne laser scanning system that determines ground levels at a very high density (often as little as 1 m spacing between measurements) along a swathe of land underneath the track of the airplane. Most systems used in New Zealand collect data only on land above water levels, but systems are available that can also determine shallow water bathymetry levels in clear water. Vertical accuracy is typically better than ± 0.15 m. |
| Marginal variable | Refers to a single variable (e.g., wave height, or storm-tide) representing one axis, or “margin”, of a joint-probability plot. |
| MCJP | Monte Carlo joint-probability technique. A technique to model extreme sea-level. Suitable for short data records, and provides the flexibility to mix measured and modelled sea-level components (see Table 7-4). |
| Mean Monthly Sea Level Anomaly (MMSLA) | The sea level anomaly with periods (variations) of one month or greater due to climate variability such as seasonal effects, ENSO and IPO; obtained by detrending MMSL time-series and removing the time-series mean (to a mean of zero). |
| Mean Sea Level (MSL) | The mean non-tidal component of sea level, averaged over a defined time period, usually several years. New Zealand’s local vertical datums were obtained in this way, with AVD-46 being the MSL from sea-level measurements made between 1909 and 1923. Mean sea level changes with the averaging period used, due to climate variability and long-term sea-level rise. |
| MHWS | Mean high water springs – The high tide height associated with higher than normal high tides that result from the beat of various tidal harmonic constituents. Mean high water springs occur every 2 weeks approximately. MHWS can be defined in various ways, and the MHWS elevation varies according to definition. This has led to subjectivity when defining the CMA for RMA purposes but this report provides a pragmatic solution that builds in variability in tide range and the effect of wave setup on open coasts. |
| Monthly Mean Sea Level (MMSL) | The variation of the non-tidal sea level on time scales ranging from a monthly basis to decades, due to climate variability, relative to a specified datum. This includes ENSO and IPO patterns on sea level, winds and sea temperatures, and seasonal effects. In some older NIWA reports this might have been referred to as “mean level of the sea” or MLOS. |
| Open coast | Coastline located outside of sheltered harbours and estuaries, in locations subject to ocean waves and swell. |
| Perigean spring tide | A perigean spring tide occurs when the moon is either new or full (spring tide) and closest to Earth in its monthly orbit (i.e., the perigee). The coincidence of spring tide and perigee peaks about every 7 months. |
| Projection | A numerical simulation (representation) of future conditions. Differs from a forecast; whereas a forecast aims to predict the exact time-dependent conditions in the immediate future, such as a weather forecast a future cast aims to simulate a time-series of conditions that would be typical of the future (from which statistical properties can be calculated) but does not predict future individual events. |
| Quantile-quantile | Quantile-quantile, or Q-Q plots are a graphical method of showing how the frequencies or probabilities of two distributions compare (e.g., model versus measured). If the distributions |

| | |
|------------------------------------|---|
| | are similar, then the points will tend to lie on a straight 1:1 line. |
| Significant wave height Hm0 (m) | The average height of the highest one-third of waves in the wave record; experiments have shown that the value of this wave height is close to the value of visually estimated wave height. |
| Storm surge | The rise in sea level due to storm meteorological effects. Low-atmospheric pressure relaxes the pressure on the ocean surface causing the sea-level to rise, and wind stress on the ocean surface pushes water down-wind (onshore winds) and to the left up against any adjacent coast (alongshore winds). Storm surge has timescales of sea-level response that coincide with typical synoptic weather motions; typically 1–3 days. |
| Storm-tide | Storm-tide is defined as the sea-level peak around high tide reached during a storm event, resulting from a combination of MMSLA + tide + storm surge. |
| Tidal hysteresis | An additional rise in mean sea level in harbours relative to the open coast, caused by the differential wave speed of the tidal wave between low and high tides in shallow harbours, resulting in a setup of the half-tide level to redress the imbalance in flow capacity between the wave crest and trough. |
| WASP | The Waves And Storm surge Predictions WASP modelling project recently completed by NIWA produced 45-year (1958–2002) and 30-year (1970–2000) hindcast records of storm surge and waves around the entire New Zealand coast. An aim of the WASP project was to produce a nationally-consistent web-based hindcast of waves and storm surges, from which regional information could be extracted. Data is available on the web via NIWA's Coastal Explorer (http://wrenz.niwa.co.nz/webmodel/coastal). |
| Wave runup | The maximum vertical extent of wave “up-rush” on a beach or structure above the still water level, and thus constitutes only a short-term upper-bound fluctuation in water level relative to wave setup. |
| Wave setup | The average temporary increase in mean still-water sea level at the coast, resulting from the release of wave energy in the surf zone as waves break. |

6 References

- Amos, M.J. (2007) Quasigeoid modelling in New Zealand to unify multiple local vertical datums. PhD thesis. Curtin University of Technology, Western Australia.
- Andrews, C. (2004) North Shore City sea inundation study. Tonkin and Taylor Ltd Client Report to North Shore City Council, No. 21595.
- Auckland Harbour Board (1974) Tidal data. Drawing number S90/25 by Tubbs, C.
- Auckland Regional Council (2010) Sea level change in the Auckland region. Report prepared for the Auckland Regional Council by the University of Otago and the National Institute of Water and Atmospheric Research. ARC Technical Report, TR065 No. 36 p.
- Bell, R.G. (2010) Tidal exceedances, storm-tides and the effect of sea-level rise. Proceedings of the 17th Congress of the Asia and Pacific division of the IAHR, Auckland, New Zealand, 21-24 February 2010.
- Bell, R.G., Dumnov, S.V., Williams, B.L., Greig, M.J.N. (1998) Hydrodynamics of Manukau Harbour, New Zealand. *New Zealand Journal of Marine and Freshwater Research*, 32(1): 81–100.
- Bell, R.G., Swales, A., Hill, A.F. (1996) Field studies in Upper Tamaki Estuary for the environmental assessment of the Otahuhu power station heated cooling-water discharge. Client Report to Kingett Mitchell and Associates, Takapuna, No. KIM60203/1: 15.
- Booij, N., Ris, R.C., Holthuijsen, L.H. (1999) A third-generation wave model for coastal regions 1. Model description and validation. *Journal of Geophysical Research*, 104(C4): 7649–7666.
- Britton, R., Dahm, J., Rouse, H., Hume, T., Bell, R., Blackett, P. (2011) Coastal adaptation to climate change: pathways to change. Report prepared as part of the Coastal Adaptation to Climate Change Project, No. 106 p.
- Coles, S. (2001) An introduction to statistical modeling of extreme values. Springer, London, New York: 208.
- EurOtop (2007) Wave overtopping of sea defence and related structures: Assessment manual. Die Küste version, Archive for Research and Technology of the North Sea and Baltic Coast, No. p.
- Fairchild, J.C. (1958) Model study of wave set-up induced by hurricane waves at Narragansett Pier, Rhode Island. No. p.
- Foreman, M.G.G., Cherniawsky, J.Y., Ballantyne, V.A. (2009) Versatile Harmonic Tidal Analysis: Improvements and Applications. *Journal of Atmospheric and Oceanic Technology*, 26(4): 806–817.
- Goring, D.G. (1995) Short level variations in sea level (2-15 days) in the New Zealand region. *New Zealand Journal of Marine and Freshwater Research*, 29: 69–82.

Goring, D.G., Stephens, S.A., Bell, R.G., Pearson, C.P. (2010) Estimation of extreme sea levels in a tide-dominated environment using short data records. *Journal of Waterway, Port, Coastal and Ocean Engineering*, 137(3): 150–159.

Gringorten, I.I. (1963) A plotting rule for extreme probability paper. *Journal of Geophysical Research*, 68(3): 813–814.

Haigh, I.D., Nicholls, R., Wells, N. (2010) A comparison of the main methods for estimating probabilities of extreme still water levels. *Coastal Engineering*, 57(9): 838–849.

Hannah, J. (1990) Analysis of mean sea level data from New Zealand for the period 1899-1988. *Journal of Geophysical Research*, 95(B8): 12399–12405.

Hannah, J. (2004) An updated analysis of long-term sea level change in New Zealand. *Geophysical Research Letters*, 31(3): L03307.

Hannah, J., Bell, R.G. (2012) Regional sea level trends in New Zealand. *Journal of Geophysical Research-Oceans*, 117: 1004–1004.

Hawkes, P.J., Gouldby, B.R., Tawn, J.A., Owen, M.W. (2002) The joint probability of waves and water levels in coastal engineering design. *Journal of Hydraulic Research*, 40(3): 241–251.

HR Wallingford (web) HR Wallingford wave overtopping calculator. http://www.overtopping-manual.com/calculation_tool.html.

HR Wallingford (2000) The joint probability of waves and water levels: JOIN-SEA - Version 1.0. User Manual, No. TR 71: 12.

HR Wallingford and Lancaster University (2000) The joint probability of waves and water levels: JOIN-SEA, a rigorous but practical new approach. No. SR 537: 47.

Ministry for the Environment (2008) Coastal hazards and climate change: A guidance manual for local government in New Zealand. 2nd edition revised by Ramsay D. and Bell R. (NIWA). Prepared for the Ministry for Environment, Wellington: 127.

Mullan, B., Carey-Smith, T., Griffiths, G., Sood, A. (2011) Scenarios of storminess and regional wind extremes under climate change. NIWA Client Report to Ministry of Agriculture and Forestry, WLG2010-031: 80.

Oldman, J.W., Black, K.P. (1997) Mahurangi Estuary numerical modelling. Client Report to Auckland regional Council, No. ARC60208/1; TR 2009/041. p.

Oldman, J.W., Gorman, R.M., Lewis, M. (2007) Central Waitemata Harbour contaminant study. Harbour hydrodynamics and sediment-model calibration and implementation. . Client Report for Auckland Regional Council, No. HAM2007-102.

Pritchard, M., Stephens, S., Measures, R., Goodhue, N., Wadhwa, S. (2012) Kaipara Harbour 2-dimensional hydrodynamic modelling. Client Report to Auckland Council, No. HAM2012-128: 36.

Pugh, D.T., Vassie, J.M. (1978) "Extreme sea-levels from tide and surge probability." Presented at the Proceedings of the 16th Coastal Engineering Conference, Hamburg, 911–930.

Pugh, D.T., Vassie, J.M. (1980) Applications of the joint probability method for extreme sea-level computations. *Proceedings of the Institution of Civil Engineers Part 2*: 959–979.

Ramsay, D., Altenberger, A., Bell, R., Oldman, J., Stephens, S. (2008a) Review of rainfall intensity curves and sea levels in Manukau City. Part 2: Sea levels. Consulting Report to Manukau City Council, No. HAM2007-168: 74.

Ramsay, D., Stephens, S., Altenberger, A., Oldman, J. (2008b) The influence of climate change on extreme sea levels around Auckland City. Consulting Report to Auckland City Council, No. HAM2008-093: 74.

Reeve, G., Pritchard, M. (2010) Manukau Harbour enhancement project: hydrodynamic modelling calibration report. NIWA Client Report to Watercare Services Limited, No. HAM2010-019: 49.

Reinen-Hamill, R., Shand, T. (2005) Assessment of potential sea levels due to storms and climate change along Rodney's East Coast. Tonkin and Taylor Ltd Client Report to Rodney District Council, No. 22239.

Ris, R.C., Holthuijsen, L.H., Booij, N. (1999) A third-generation wave model for coastal regions 2. Verification. *Journal of Geophysical Research*, 104(C4): 7667–7681.

Stanton, B.R., Goring, D.G., Bell, R.G. (2001) Observed and modelled tidal currents in the New Zealand region. *New Zealand Journal of Marine and Freshwater Research*, 35: 397–415.

Stephens, S.A., Bremner, D., Budd, R., Edhouse, S., Goodhue, N., Hart, C., Reeve, G., Wadhwa, S. (2011a) Kaipara Harbour hydrodynamic data collection. Client Report to Auckland Council, No. HAM2011-131: 20.

Stephens, S.A., Coco, G., Bryan, K.R. (2011b) Numerical simulations of wave setup over barred beach profiles: implications for predictability. *Journal of Waterway Port Coastal and Ocean Engineering-ASCE*, 137(4): 175–181.

Stephens, S.A., Reeve, G., Goodhue, N. (2011c) Coastal storm-tide levels in the Auckland region. Phase 1: Rationalising and updating previous studies. Client Report to Auckland Council, No. HAM2011-102: 63.

Stephens, S.A., Wadhwa, S. (2012) Development of an updated coastal marine area boundary for the Auckland region. Client Report to Auckland Council, No. HAM2012-111: 63.

Stephenson, A., Gilleland, E. (2005) Software for the analysis of extreme events: The current state and future directions. *Extremes*, 8(3): 87–109.

Stockdon, H.F., Holman, R.A., Howd, P.A., Sallenger, A.H. (2006) Empirical parameterization of setup, swash, and runup. *Coastal Engineering*, 53(7): 573–588.

SWAN (2011) SWAN User Manual - SWAN Cycle III Version 40: 85.

Tawn, J.A., Vassie, J.M. (1989) "Extreme sea-levels: the joint probabilities method revisited and revised". Presented at the Proceedings of the Institute of Civil Engineering Part 2, 429–442: 87.

Tawn, J.A., Vassie, J.M. (1991) Recent improvements in the joint probability method for estimating extreme sea levels. In: Parker, B.B. (ed) *Tidal Hydrodynamics*: 813–828, Wiley, New York.

Tolman, H.L. (1991) A third-generation model for wind waves on slowly varying, unsteady, and inhomogeneous depths and currents. *Journal of Physical Oceanography*, 21: 782–797.

Tolman, H.L. (2007) "The 2007 release of WAVEWATCH." Presented at the 10th International Workshop on Wave Hindcasting and Forecasting and Coastal Hazard Symposium, North Shore, Oahu, Hawaii, November 11-16, 2007.

Tonkin & Taylor Ltd (1986) Manukau Harbour resources study. Consulting report on behalf of Manukau Harbour Maritime Planning Authority.

Uppala, S.M., KÅllberg, P.W., Simmons, A.J., Andrae, U., Bechtold, V.D.C., Fiorino, M., Gibson, J.K., Haseler, J., Hernandez, A., Kelly, G.A., Li, X., Onogi, K., Saarinen, S., Sokka, N., Allan, R.P., Andersson, E., Arpe, K., Balmaseda, M.A., Beljaars, A.C.M., Berg, L.V.D., Bidlot, J., Bormann, N., Caires, S., Chevallier, F., Dethof, A., Dragosavac, M., Fisher, M., Fuentes, M., Hagemann, S., Hólm, E., Hoskins, B.J., Isaksen, L., Janssen, P.A.E.M., Jenne, R., McNally, A.P., Mahfouf, J.F., Morcrette, J.J., Rayner, N.A., Saunders, R.W., Simon, P., Sterl, A., Trenberth, K.E., Untch, A., Vasiljevic, D., Viterbo, P., Woollen, J. (2005) The ERA-40 re-analysis. *Quarterly Journal of the Royal Meteorological Society*, 131(612): 2961–3012.

Van Rijn, L.C. (2010) Modelling erosion of gravel/shingle beaches and barriers: Concepts and Science for Coastal Erosion Management. Report No. D13b.

Walters, R.A., Goring, D.G., Bell, R.G. (2001) Ocean tides around New Zealand. *New Zealand Journal of Marine and Freshwater Research*, 35: 567–579.

Appendix A – How extreme sea-levels were calculated – details

The aim of an extreme sea-level analysis is to determine the height and likelihood of occurrence of unusually high (or low) sea levels. In particular, extreme sea-level analyses usually require estimation of the probability of sea levels that are more extreme than any that have already been observed (Coles 2001).

Ways to describe extreme sea level likelihood

The likelihoods associated with extreme storm-tides and/or waves, are reported in terms of their probability of occurrence. The annual exceedance probability (AEP) describes the chance of an event reaching or exceeding a certain water level in any given year. For example, if a storm-tide of 2.2 m has a 5% AEP, then there is a 5% chance of a storm-tide this high, or higher, occurring in any 1-year period. So it is unlikely in any single year, but could still happen and should be planned for. Furthermore, although the occurrence probability is only 5%, more than one storm-tide this high or higher could occur in any given year.

Alongside AEP, the likelihood of extreme events can also be described in terms of their average recurrence interval (ARI), which is the average time interval between events of a specified magnitude (or larger), when averaged over many occurrences. Table 7-1 shows the relationship between AEP and ARI; small relatively common events have a high annual exceedance probability and a low average recurrence interval, and vice versa for large, rare events.

Table 7-1: Relationship between annual exceedance probability (AEP) and average recurrence interval (ARI).

$$\text{AEP} = 1 - e^{-1/\text{ARI}}$$

| | | | | | | | | | | |
|-------------|-----|-----|-----|-----|-----|-----|----|----|-----|------|
| AEP (%) | 99% | 86% | 63% | 39% | 18% | 10% | 5% | 2% | 1% | 0.5% |
| ARI (years) | 0.2 | 0.5 | 1 | 2 | 5 | 10 | 20 | 50 | 100 | 200 |

ARI (or its often used surrogate “return period”) is an easily misinterpreted term, with the public often assuming that because one large event has just occurred, then the average recurrence interval will pass before another such event. The term AEP better conveys the message of continuous probability that large events could occur at any time.

This report provides occurrence likelihoods for extreme storm-tide and wave height magnitudes and their joint occurrences. This knowledge is only one aspect of the planning process. Another essential planning component is to consider the planning timeframe, or lifetime, of interest. For example, a typical planning lifetime for residential housing is about 100 years. Table 7-2 presents the likelihood that events with various occurrence probabilities will occur, at least once, within a specified planning lifetime. The likelihoods are shaded according to their chance of occurring in the specified timeframe:

- > 85% Almost certain
- 60%–84% Likely
- 36%–59% Possible
- 16%–35% Unlikely

- < 15% Rare

For example, a relatively common (smaller) event with a 39% AEP is almost certain to occur over a 20-year lifetime. However, a rare (larger) 2% AEP event is unlikely to occur over the same 20-year lifetime. 1% AEPs are a commonly used planning event magnitude, and 100-year planning lifetimes are common for affected infrastructure; Table 7-2 shows that a 1% AEP event is likely to occur over a 100-year planning lifetime.

In Table 7-3, the event average recurrence intervals have been converted into the expected average number of exceedances for various asset planning lifetimes. The average number of exceedances is a useful measure for estimating risk, because it tells us how often, on average, we can “expect our feet to get wet” over a given planning lifetime, for a specified event magnitude. To use the above examples, in 20 years there are likely to be 10 exceedances of a relatively common (smaller) event with a 39% AEP, but < 1 exceedances of a rare (larger) 2% AEP event over the same period. The average number of exceedances is a useful way to illustrate the effect of sea-level rise on the likely number of coastal inundation events.

Table 7-2: Likelihood of at least one exceedance event occurring within planning lifetimes

The likelihood of occurrence is described by AEP and/or ARI. $P = 1 - e^{-L / ARI}$, where L = planning lifetime and P = probability of occurrence within planning lifetime.

| AEP (%) | ARI (years) | Planning lifetime (years) | | | | | | |
|---------|-------------|---------------------------|-----|-----|------|------|------|------|
| | | 2 | 5 | 10 | 20 | 50 | 100 | 200 |
| 39% | 2 | 63% | 92% | 99% | 100% | 100% | 100% | 100% |
| 18% | 5 | 33% | 63% | 86% | 98% | 100% | 100% | 100% |
| 10% | 10 | 18% | 39% | 63% | 86% | 99% | 100% | 100% |
| 5% | 20 | 10% | 22% | 39% | 63% | 92% | 99% | 100% |
| 2% | 50 | 4% | 10% | 18% | 33% | 63% | 86% | 98% |
| 1% | 100 | 2% | 5% | 10% | 18% | 39% | 63% | 86% |
| 0.5% | 200 | 1% | 2% | 5% | 10% | 22% | 39% | 63% |

Table 7-3: Average number of exceedances occurring within planning lifetimes, for event magnitudes with a specified probability of occurrence .

(AEP / ARI). $N = L / ARI$, where L = planning lifetime and ARI = average recurrence interval.

| AEP (%) | ARI (years) | Planning lifetime (years) | | | | | | |
|---------|-------------|---------------------------|-----|-----|-----|-----|-----|-----|
| | | 2 | 5 | 10 | 20 | 50 | 100 | 200 |
| 39% | 2 | 1 | 2.5 | 5 | 10 | 25 | 50 | 100 |
| 18% | 5 | < 1 | 1 | 2 | 4 | 10 | 20 | 40 |
| 10% | 10 | < 1 | < 1 | 1 | 2 | 5 | 10 | 20 |
| 5% | 20 | < 1 | < 1 | < 1 | 1 | 2.5 | 5 | 10 |
| 2% | 50 | < 1 | < 1 | < 1 | < 1 | 1 | 2 | 4 |
| 1% | 100 | < 1 | < 1 | < 1 | < 1 | < 1 | 1 | 2 |
| 0.5% | 200 | < 1 | < 1 | < 1 | < 1 | < 1 | < 1 | 1 |

Introduction to extreme sea-level analysis

Extreme sea-level analyses are based on extrapolation from past sea-level measurements. The quality, frequency and length of the sea-level record control the accuracy and uncertainty of the extreme sea-level analysis and can govern the choice of extreme sea-level method. Each extreme sea-level method has unique data requirements; for example, the GEV fitted to annual maxima requires observed annual maximum sea levels, whereas the Monte Carlo joint probability technique (MCJP) requires a high-quality digital dataset sampled at least hourly. Extreme sea-level analyses are sensitive to outliers (erroneous large measurements). Data preparation is extremely important, and the most time-consuming component of an extreme sea-level analysis. Raw sea-level records are seldom perfect and can be affected by siltation of the recorder, timing errors (e.g., daylight saving), datum shifts and gaps in the record, for example. Sea-level measurements must be quality assured before use in an extreme sea-level analysis. No analysis technique can make up for poor data.

The results of an extreme value analysis depend on the sampling frequency and duration of the underlying data, because these factors influence the sea-level processes that are included. For example, high-frequency data (e.g., 1, 5 or 10 minute sampling) may include short-term fluctuations due to waves or seiche, whose inclusion can raise extreme sea-level estimates. Modern sea-level gauges commonly measure as frequently as every minute, which is useful for identifying short period processes such as seiche or tsunami in ports and harbours. For extreme sea-level analysis it is common to subsample the data to ½-hour or 1-hour intervals, which is sufficient to resolve the processes contributing to the storm-tide while avoiding the contribution of waves and seiche.

Direct extreme sea-level techniques

Direct methods are so called because they “directly” analyse the observed/measured sea level maxima that occur during storm-tides. The measured storm-tide maxima “directly” include all the components of higher than normal sea-level that can occasionally combine to produce unusually high sea levels, such as monthly mean sea level, spring tide, and storm surge. Direct methods use techniques based on extreme value theory, which in simple terms involves fitting an “extreme-value model” to the most

extreme sea-level maxima in the record (subject to appropriate data sampling). There are certain limitations that come with the adoption of extreme value theory:

- The results can be inaccurate when applied to short sea-level records.
- The models themselves are developed under idealised circumstances, which may not be exact (or even reasonable) for a process under study. For example, direct methods analyse the observed extremes of sea level, which in New Zealand are usually a coincidence of a moderate to high storm surge and a high spring tide. Extreme value theory is a valid approach for modelling the storm surge component of sea level because it is an approximately stochastic process. However, the tide, which makes up most of the sea-level variance, is deterministic, and so the direct application of extreme value theory is compromised.
- The models may lead to wastage of information when implemented in practice.

The above limitations imply that extreme value theory is best applied directly to sea levels when long records (sea level measured over many decades) are available, and when the stochastic storm surge component is relatively large in comparison to the tidal component. These limitations do not mean that direct methods cannot and should not be used for modelling extreme sea levels, they are widely applied, but the practitioner should be aware of the limitations and associated uncertainty when interpreting the results. (Haigh et al. 2010) showed that direct methods using extreme value theory underestimate the long (> 20 years) period return levels when the astronomical tidal variations of sea level (relative to a mean of zero) are about twice that of the non-tidal variations. In New Zealand, tidal variability is more than twice storm surge.

Direct extreme value techniques invoke the extreme value paradigm, which for sea level is: “under suitable assumptions, for a large number of sea-level observations, the approximate behaviour of the maximum sea-levels (after dividing the sea-level observations into blocks (e.g., annual maxima)), can be described by a certain family of extreme value models that can be calibrated to the observed sea-level maxima” (Coles 2001).

Examples of these classical extreme-value models are the generalised extreme value (GEV) and the generalised Pareto distribution (GPD). The GEV model is fitted to block maxima such as annual or monthly maxima, or several maxima per year (r -largest). The GPD model is fitted to maxima that exceed some high threshold. A basic assumption is that the sea-level maxima used to calibrate the extreme-value models are independent from one another. In practice, for New Zealand storm surge and wave data, this means separation using at least a 3-day time threshold, which separates the meteorological conditions that create them.

Another assumption is that the sea-level observations must exhibit stationary behaviour, i.e., there are no long-term trends such as sea-level rise or ENSO and IPO climate variability. From sea level data it may be necessary to obtain an estimate of the maximum sea level likely to occur in the next 100 or 1000 years. How can we estimate what levels may occur in the next 1000 years without knowing what climate change might occur? Although the pattern of sea-level variation may not appear to have changed in the last 50 years of measurement record, such stability may not persist in the future. The “1000-year average recurrence level” is only meaningful under the assumption of stability (or stationarity) in the prevailing process. We have predicted extreme sea levels for a maximum 200-year average recurrence level, but caution that climate change could have a pronounced influence on

extreme sea-levels over a 100-year timeframe as required by the New Zealand Coastal Policy Statement.

Indirect extreme sea-level techniques

Indirect methods involve splitting the sea level into its deterministic (predictable) tidal and stochastic (e.g., unpredictable, storm-driven) non-tidal components, and analysing the two components separately before recombining. Indirect methods are more complicated and require stringent data quality control, but make more efficient use of the available data and so give better results for short data records. The indirect methods also overcome the main theoretical limitations of extreme value theory application to sea levels, and average return sea levels can be estimated from relatively short records (<5 years) because all measured storm surge events are utilised, not just those that lead to extreme levels. The revised joint probability method (RJPM) (Pugh & Vassie 1978; Pugh & Vassie 1980; Tawn & Vassie 1989; Tawn & Vassie 1991) is a widely-applied indirect method, and the newly-developed Monte Carlo joint probability technique (MCJP) is being applied in New Zealand (Goring et al. 2010). An advantage of the MCJP relative to the RJPM is that it gives robust confidence intervals, and incorporates additional sea-level components such as MMSL. NIWA has working versions of both the RJPM and MCJP.

Generally, the methods that make use of more of the available sea-level measurements are more accurate and have the least uncertainty – they make more “efficient” use of the data and are preferred where accuracy is important. Techniques that use less data are easier to apply and are preferred where a low-effort or approximate analysis is required, and/or where long records are available.

Table 7-4: Summary of extreme value techniques used here for estimating the probabilities of extreme still water levels.

GEV = generalised extreme value model; GPD = generalised Pareto distribution.

| | Advantages | Disadvantages |
|----------------|--|---|
| Direct methods | <p>GEV fitted to annual maxima</p> <ul style="list-style-type: none"> • Simple to apply (no thresholds) with easily-obtained software. • Simple data treatment and post-processing (Annual Maxima easily obtained and quality checked). • Annual Maxima records sometimes extend beyond the modern continuous digital records. | <ul style="list-style-type: none"> • Inefficient use of data (wastage). About 40-years of Annual Maxima required for 100-year ARI estimate. • Long sea-level record required (large uncertainty for short records). In some locations this is partially compensated by Annual Maxima records that extend beyond modern digital records. • Sensitive to large outliers in the data. |
| | <p>GPD fitted to peaks-over-threshold</p> <ul style="list-style-type: none"> • Most efficient data use of the direct methods (highest confidence, lowest uncertainty). • Commonly applied with easily-obtained software. | <ul style="list-style-type: none"> • Requires subjective choice of threshold - user experience, or trial and error. • At least 10-years of data required for a 50 to 100-year ARI estimate. • Use of more data requires more stringent data quality check. |

| | Advantages | Disadvantages |
|------------------|--|---|
| Indirect methods | <p>Monte Carlo Joint Probability (MCJP)</p> <ul style="list-style-type: none"> • Most efficient use of data. • Suitable for short records (< 5-years). • Higher confidence (lower uncertainty). • Stable in the presence of large outlying events. | <ul style="list-style-type: none"> • Sensitive to data errors, requires stringent data quality assurance. • Complex and time-consuming to apply - requires high level of user experience relative to direct methods. • Less commonly applied and available software. • Assumes tide and storm surge are independent, which may not be true in estuaries |

Extreme storm-tide methods used in this project

For this project we used the indirect Monte Carlo joint probability technique (Goring et al. 2010) to calculate extreme storm-tide elevations, and cross-checked these analyses using direct techniques fitted to sea-level maxima. The MCJP technique is more accurate for the relatively short observational datasets we have available in the Manukau and Kaipara Harbours. Above all, it is more flexible in allowing us to include historical events and combine measured and modelled datasets to predict extreme storm-tide elevations. Previous studies in the Waitemata Harbour (Ramsay et al. 2008b; Stephens et al. 2011c) used a GEV model fitted to annual maxima, but this has larger uncertainty than the MCJP technique, and are also less stable when fitted to simulated sea levels, due to the strong influence that data outliers can have. Thus the extreme storm-tide elevations produced here are considered to supersede those produced in previous studies. Likewise, a hydrodynamic model with better spatial resolution has been used to re-model tidal amplification in the Manukau Harbour, leading to improved upper-harbour extreme sea-level estimates compared with Stephens et al. (2011b).

The Monte-Carlo joint-probability method (Goring et al. 2010) was used to predict the storm-tide height for a range of AEPs. The technique works by splitting the sea-level record into contributions by:

- Astronomical tide – tidal harmonic analysis is used to calculate the tidal component of the measured sea-level. The astronomical tide is subtracted from the raw sea level to obtain a non-tidal residual sea level.
- Storm surge – a wavelet filter is applied to the non-tidal residual sea level to separate periods of sea-level variability that are expected to be associated with synoptic weather systems, or “storms”. Sea-level oscillations with periods of motion from 1–16-days are separated and assigned to “storm surge”.
- Monthly mean sea level anomaly – a wavelet filter is used to separate periods of sea-level variability of 1-month or greater from the non-tidal residual, and assigned to “MMSLA”.

The components: tide, storm surge, and MMSLA are then independently recombined using a random (Monte Carlo) sampling technique that preserves the likelihood of occurrence (and coincidence) of each component. In this way, thousands of years’ worth of sea-level component combinations are simulated (assuming stationarity), which leads to tighter confidence intervals on the estimates.

Extreme sea-level frequencies and magnitudes are then calculated using the thousands of years of simulated sea levels. A count-back technique is used to calculate frequency–magnitude relationships, for example, if 1000 annual maxima are simulated, then the 10th-highest value represents the 100-year average recurrence interval.

In New Zealand and in the Auckland region, the most important sea-level component is the tide. An analysis of historical storm-tide events in New Zealand showed that extreme storm-tide levels around the open coast of New Zealand are dominated by very high tides coinciding with small to moderate storm surges (Bell 2010). Thus the tidal regime is the most important quantity to model; fortunately it is also the easiest component to model and predict.

Extreme wave heights

Wave heights cannot easily be separated into various components like storm-tides can. Therefore the direct extreme-value techniques listed above (Table 7-4) are suitable for extreme wave analysis. We used the generalised Pareto distribution (GPD) fitted to peaks-over-threshold (POT) wave data to predict the likelihood of extreme wave heights, because the POT approach makes use of more data and so has higher efficiency than the annual maxima technique. GPD was fitted to the largest 5% of significant wave heights, using code from Coles (Coles 2001), converted for use in R software (Stephenson & Gilleland 2005). The GPD was fitted to wave height peaks from independent storms separated by at least three days (POT). Given the 30-year record of modelled wave data from WASP we can reliably estimate up to a 1% AEP event (Coles 2001).

Joint probability of storm-tides and waves

A joint-probability analysis of storm-tides and waves describes the combined likelihood of a high storm-tide and large wave event occurring at the same time. In the absence of a joint-probability analysis design conditions are sometimes derived by superimposing an extreme storm-tide and an extreme wave together. However this results in over design, because the chances of this joint occurrence are very small. For example, assuming storm-tide and wave heights are independent, the coincidence of a 1% annual exceedance probability (AEP) storm-tide (100-year average recurrence interval (ARI)) with a 1% AEP wave height has a 0.01% AEP (10,000-year ARI). In New Zealand the astronomical tide is the largest source of sea-level variability and its amplitude forms the largest component of storm-tide. Therefore, most large storm-tides in New Zealand result from high perigean spring tides combining with a small to moderate storm surge. Because the astronomical tide is independent of storms, dependence between storm-tides and waves is relatively weak compared with some overseas locations. However, there is often a dependence between waves and the storm surge component of the storm-tide, because both storm surges and waves are meteorologically forced and may be heightened by the same storm, and this needs to be accounted for. The joint-probability software models the dependence between storm-tide and wave height and steepness.

Joint-probability analyses of extreme storm-tides and waves were undertaken using the JOIN-SEA software developed by HR Wallingford (Hawkes et al. 2002; HR Wallingford 2000; HR Wallingford and Lancaster University 2000). The software requires coinciding significant wave height, wave period, and storm-tide sampled at each high tide, giving 706 pairs of values per year.

The software fits a generalised Pareto distribution (GPD) to the largest 5% of waves and storm-tides to model extreme values, and samples from the empirical distribution to model more frequent event magnitudes. The software fits a bivariate normal distribution to account for any dependence between the storm-tides and waves.

The results assign AEP for each combination of storm-tide and significant wave height. Figure 7-1 illustrates these joint probability curves for Mangawhai Beach.

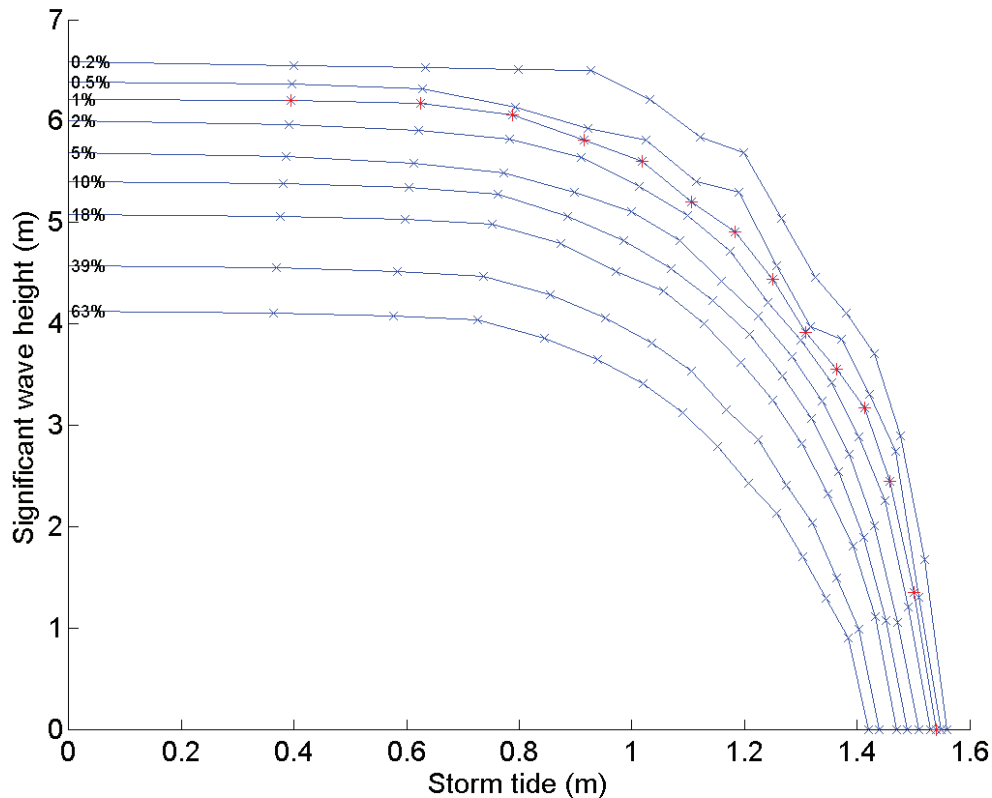


Figure 7-1: Joint-probability of storm-tide and significant wave height at Mangawhai Beach.

(Red crosses mark storm-tide and wave combinations that have an annual exceedance probability of 0.01 (100-year ARI).

Each joint AEP corresponds with a curve of wave height and storm-tide pairings. Given a beach profile for that location the total inundation level at the shoreline can be estimated for each point on the curve. By selecting the highest combined storm-tide and wave setup level from a chosen joint AEP contour the maximum joint wave and storm-tide inundation level is calculated.

Methods for calculating extreme sea levels in harbours

Extreme sea-levels in the Waitemata, Kaipara and Manukau Harbours were calculated as follows:

- Extreme sea-level analyses were undertaken using the harbour tide gauge records. These analyses return the frequency–magnitude relationship for extreme storm-tides at the gauge locations.
- Hydrodynamic models were used to simulate ~30-year sea-level time-series at multiple locations throughout the harbours, including the tide-gauge locations.
- Extreme sea-level analyses were undertaken based on the simulated sea-level records.
- At the tide-gauge locations the extreme sea-level analyses from simulated and measured data were compared as a validation check.

Extreme sea levels are, by definition, rare events. Only by observing a system for a long period of time can an understanding of the frequency and magnitude of extreme sea levels be attained. For the calculation of extreme sea levels, a sea-level record would ideally meet the following criteria:

- Sea-level gauge surveyed to datum.
- Accurate: no long-term drift or sensor subsidence, no siltation or blockage of the gauge. Known tectonic movement or local subsidence at gauge site.
- ≥ 50 -years length to incorporate up to two IPO and multiple ENSO climate variability cycles.
- Sample at least hourly to capture storm-tide peak.
- Includes all extreme sea-levels that occurred (no data gaps at crucial times).

The Port of Auckland tide gauge is a rarity where we have high-quality sea-level measurements over 107 years since 1904, and we can model the frequency and magnitude of extreme sea levels there with confidence. Shorter sea-level gauge records were available from the Kaipara Harbour at Pouto Point (2001–present) and the Manukau Harbour at Onehunga (2001–2011). Although less than ideal, these records are sufficiently long to be modelled using the Monte-Carlo joint-probability technique (Goring et al. 2010) that was specifically designed for short records, and provide a comparison for extreme-value analyses using simulated datasets.

As explained in Sections 2.1 and 7.2, extreme sea levels result from combinations of high tide, storm surge, monthly mean sea level, and wave setup that combine in different ways. All of these processes interact in different ways with the local environment such as the underwater bathymetry, topographic constriction, and wind and wave exposure. Thus the extreme sea-level frequency–magnitude relationship changes with location. For example, the tide amplifies as it shoals into the Waitemata Harbour, so the tide range is larger in the upper harbour than at Port of Auckland where the long-term sea-level record was located. It is not possible to obtain a long series of sea-level measurements everywhere. The solution is to use numerical hydrodynamic models that simulate tidal and storm long-wave propagation, calibrate them against sea-level measurements, and use them to predict extreme sea levels at many locations within the harbours.

Numerical hydrodynamic models solve the set of mathematical equations that describe the forced motion of fluids by tide, wind, storm-surge, etc. The equations are solved at a grid of discrete points within the area of interest (called the domain). The bathymetry at each point on the grid is assigned as well as a starting water level and velocity. The numerical model then calculates new water levels and velocities for each grid point as it steps forward through time. Forces such as tide level changes on the open boundary of the domain, or wind blowing across the water surface affect the fluid in the domain (numerically within a computer simulation). The accuracy of hydrodynamic models depends on several factors that include:

- Accurate bathymetry to describe the model domain.
- Accurate description of the forcing at the model boundaries, such as tidal water level elevation changes, for example.
- Accurate solutions to the numerical equations.
- Accurate representation of sub-grid scale processes (such as bottom friction).

- Sufficiently fine grid resolution to resolve the important bathymetric features that control water flow, such as sub-tidal channels and inter-tidal flats.
- Sufficiently fine computational time-step.

The finer the grid resolution and time step, the more accurate the model (assuming accurate bathymetry and boundary forcing), but the greater the computational requirements. There is always a compromise between model accuracy and computational efficiency to be made. The model is a schematisation of the real-world environment that should be sufficiently accurate to examine the main processes of interest with confidence.

Hydrodynamic models were used in two ways to represent extreme sea levels:

- The models were used to simulate an approximately 30-year time-series of sea levels at numerous locations throughout the Waitemata, Kaipara and Manukau Harbours. An extreme sea-level analysis was then able to be undertaken using these simulated sea-level time-series at each location.
- The 23 January 2011 storm-tide event was simulated in the Waitemata Harbour. This is the highest storm-tide event on record at the Port of Auckland, and has an estimated average recurrence interval of approximately 100 years. The simulated extreme sea-levels on 23 January 2011 were compared to 100-year ARI sea-level estimates made using method 1 above.

To dynamically simulate the hydrodynamics in the three harbours for 30 years would take time and computational resources beyond the scope of this project. Hence, a workaround was used that employed hydrodynamic models to simulate various sea-level components, which were then recombined, along with the sea-level gauge data, to estimate sea-level time-series throughout the harbours. The approach used was to separately model the three major components of a storm-tide: tide, storm surge and monthly mean sea-level anomaly, and recombine them to produce simulated storm-tide sequences. This approach treats the three sea-level components as independent from one another; it assumes for example that the size of the storm surge is not influenced by the state of the tide. Our tide-gauge analyses show that there is a significant dependence between storm surge and tide elevation inside the constricted harbours, and the assumption of independence is not adhered to. However, analyses of historical storm-tides in New Zealand has shown that the highest storm-tides have resulted from very high tides combining with a low to moderate storm surge (Bell 2010), because the tide is the largest source of sea-level variability. Therefore, we simulated the storm surge component at high spring-tide levels, based on the reasonable assumption that the highest storm-tides will mostly coincide with the highest spring tides, thus modelling the tide–surge dependence at these highest of tides.

A crucial part of the sea-level reconstruction was the analysis of the tide-gauge records. The tide-gauge records were used as a “base”, while the hydrodynamic models were used to spatially extrapolate from the tide-gauge locations.

The sea-level time-series were reconstructed as follows:

- Tides were simulated for a full lunar month, including two spring-neap cycles, which covered all combinations of the three main semi-diurnal tides M2, S2 and N2 that dominate tidal variability in the Auckland region. The tide models were forced at the open boundary using NIWA’s New

Zealand tide model (Stanton et al. 2001; Walters et al. 2001). Simulated tides were output at many locations throughout each harbour, including the tide-gauge locations.

- For each simulated location, the simulated tide time-series were used to derive a quantile-quantile scaling factor relative to the tide-gauge location.
- Tidal harmonic analysis (Foreman et al. 2009) was used to analyse the sea-level gauge records and predict the tides at the gauge locations. The tides were predicted at the gauge site to match the duration of the available meteorological records that were used to reconstruct the storm surge.
- The quantile-quantile scaling relationships were used to reconstruct tide records at other locations throughout the harbours, by applying them to the tides predicted from the tide-gauge. This approach ignores that fact that tidal shoaling will change the shape of the tide full wave as it propagates up and back out of the estuary. This is OK, because the subsequent extreme-value analyses sub-sample the simulated sea-level time-series only at times of peak high tide and discard the rest of the sea-level time-series. This approach of scaling the tide (peaks) was preferred to undertaking tidal harmonic analyses from simulated time-series at all locations in the harbour, because wetting and drying and the distortion of the tidal wave makes harmonic analysis problematic in some shallow upper-harbour locations.

Storm surge consists of two components:

- An inverse-barometer sea-level rise caused by a drop in atmospheric pressure and
- Wind stress pushing water up against the land boundary.

The local wind-driven component was simulated by applying a wind of constant speed and direction for the duration of a semi-diurnal tide cycle. At each output location the peak wind-driven storm surge amplitude was obtained by subtracting the maximum elevation from a simulation using only the tide (high-tide peak), from the maximum elevation from the tide + wind simulation. The base tide for the simulations was a sinusoidal tide of 12.42-hour period with perigean spring tide amplitude = $M2 + S2 + N2$. Winds were simulated from the northeast, southeast, southwest and northwest quadrants, at wind speeds of 0–25 m s⁻¹ (0–90 km/hr) in increments of 5 m s⁻¹. For each output location, a wind-driven storm surge response matrix was created. The matrix relates wind vector to wind-driven storm surge response at spring tide peak. The matrix was matched with the local meteorological wind record to interpolate a wind-driven storm surge component time-series for the duration of the meteorological record.

The inverse-barometer component of storm surge was assumed to apply ubiquitously throughout the harbours as low-pressure storm systems are mostly much larger spatially than a harbour. It was calculated from the local meteorological record using Equation 71. The inverse-barometer factor (IBfactor) was used as a calibration parameter to match the extreme sea-level frequency–magnitude relationships from measured and modelled data at the tide-gauge locations (more details below). The simulated inverse-barometer storm surge component was added to the simulated wind-driven component to obtain total storm surge.

The monthly mean sea-level anomaly was obtained from the tide-gauge record by low-pass filtering the non-tidal residual component of sea-level. MMSLA is a slowly-varying sea-level component and was assumed to apply ubiquitously throughout the harbours.

At each output location within the harbours, extreme sea-level analyses were undertaken using the simulated tide, storm surge and MMSLA time-series, applying the Monte-Carlo joint-probability technique described in Section 7.2.3.

Inverse barometer

Inverse-barometer sea level was calculated from the local meteorological record using Equation 71. The IBfactor varies between locations and also in time for a given location, depending on the local topography and the travel speed and direction of the passing pressure system. Goring (1995) found a long-term average IBfactor of 0.67 for the Waitemata Harbour. However, we are most interested in correctly predicting the IBfactor for storm events, when it is often larger.

Equation :Inverse-barometer sea-level equation.

Calculates the sea-level response to barometric pressure change. MSLP = mean sea level pressure in hecto-Pascals, and IBfactor is the inverse barometer factor that gives the local sea level response to changes in atmospheric pressure.

$$IB (m) = [MSLP - \text{mean}(MLSP)] (-10 \text{ IBfactor} \div 1000)$$

Storm-surge in harbours consists of a component that is generated locally inside the harbour (usually wind setup), but also has a component generated in the open sea outside the harbour, which propagates as a storm-surge wave through the harbour entrance. The modelling used in this project only simulated storm-surge generation inside the harbour, by local wind setup and inverse-barometer. Thus the total simulated storm-surge would be under-predicted because the simulations are missing the external storm-surge wave. This was overcome by using a larger IBfactor to compensate.

The IBfactor was used as a calibration tool to match extreme storm-tide elevations derived from modelled data with those from measured data. It was adjusted, using trial and error, to best match the extreme storm-tide distributions predicted from modelled and measured data at the tide-gauge locations (e.g., Figure 3-7, Figure 3-14 and Figure 3-24). The treatment was slightly different for each of the three major harbours, reflecting differences in harbour response to storm-surge. In the Waitemata Harbour the IBfactor was set to 1.0, and a linear ramp was applied to increase IBfactor from 1.0 to 1.4 for atmospheric pressures between the 95th and 100th percentile. In the Manukau Harbour the IBfactor was set to 0.7, and a linear ramp was applied to increase IBfactor from 0.7 to 2.3 for atmospheric pressures between the 99th and 100th percentile. In the Kaipara Harbour the IBfactor was set to 1.2, and a linear ramp was applied to increase IBfactor from 1.2 to 1.4 between the 95th and 100th percentile.

The inverse-barometer sea-level was applied uniformly to the entire harbour, because the size of the meteorological pressure systems is larger than the harbour.

Methods for calculating extreme sea levels on the open coast

For the purposes of this study the “open coast” is defined as coastline located outside of sheltered harbours and estuaries, in locations subject to ocean swell. It is important to consider the contribution of waves to the total sea level on the open coast, because wave setup can be large, up to 1 m for example (e.g., Fairchild 1958). Whereas storm-tides are the main inundation hazard inside the harbours of the Auckland region, the highest sea-levels on the open coast are likely to result from a combination of storm-tide plus wave setup. This means that measurements or models of both storm-tides and waves

are required. Furthermore, the likelihood of various combinations of storm-tide and wave magnitudes must be modelled.

Combined storm-tide and wave setup elevations on the open coastlines of the Auckland region were calculated as follows:

- Model wave and storm-tide conditions for a 30-year (1970–2000) period at locations offshore from the surf zone along the open coast. The WASP project models were used.
- Undertake a joint-probability analysis between storm-tides and waves at each output location. The joint-probability analysis calculates the likelihood of various storm-tide and wave combinations.
- Use beach profile data and an empirical wave setup formula to calculate wave setup at the shoreline for all wave conditions in the joint-probability analyses.
- Add storm-tide and wave setup to calculate the total combined storm-tide plus wave setup elevation.

The Waves And Storm surge Predictions WASP modelling project recently completed by NIWA produced 45-year (1958–2002) and 30-year (1970–2000) hindcast records of storm surge and waves around the entire New Zealand coast. An aim of the WASP project was to produce a nationally-consistent web-based hindcast from which regional information could be extracted. This will help create a more standardised approach by local government, infrastructure operators and coastal communities in their efforts to adapt to climate-change impacts. The information provides a wider basis for sustainable resource-management planning decisions for the coastal margin that adequately accounts for not only sea-level rise impact (which currently tends to be the main focus), but also potential changes to waves and storm-surge and their impact on coastal hazards. Data is available on the web via NIWA's Coastal Explorer, at the 50 m depth contour at regular intervals around the New Zealand coastline. This provides "offshore" conditions that can be used in situ, or as boundary conditions to drive more detailed coastal models. The first hindcast simulation used wind and atmospheric pressure forcing data from the global ERA40 reanalysis (Uppala et al. 2005) which covers the 45-year period 1958-2002 with a resolution of 1.225 degrees (~140 km). An additional hindcast for the thirty-year period 1970-2000 was computed using dynamically down-scaled forcing data. This "regional climate model" (RCM) which has a finer resolution of 0.27 degrees (~30 km) and the ERA40 data for boundary conditions was used for this project.

Time-series of storm-tide sea-level for 1970–2000 were estimated by adding the following three sea-level components:

- Astronomical tide – predicted using NIWA's New Zealand tide model (Stanton et al. 2001; Walters et al. 2001).
- Storm surge – hindcast by the WASP models.
- Monthly mean sea-level anomaly – derived from the nearest long-term tide gauge record as described in Section 2.1 (Port of Auckland for east coast and Anawhata for west coast).

Time-series of wave statistics (e.g., height, period and direction) were derived from WASP hindcasts. These were used directly on the west coast. There are many islands offshore from Auckland's east coast that affect the wave climate through wave refraction and sheltering, and the spatial resolution of the New Zealand-regional-scale WASP models was too coarse to resolve these features in the Hauraki Gulf. Therefore, the WASP hindcast was used to drive a nested wave model with sufficient spatial

resolution to translate the WASP wave predictions from offshore in deep water to the Auckland coastline of the inner Hauraki Gulf.

Further coast-specific detail on the prediction of open-coast combined storm-tide plus wave setup elevations is given later in Sections 4.1 and 4.2.

Beach profiles

Beach profile data were obtained from Auckland Council, for Browns Bay, Campbells Bay, Cheltenham, Kawakawa, Long Bay, Mangawhai/Pakiri, Maraetai, Milford, Muriwai, Omaha, Piha, and Takapuna Beaches (see Figure 7-2 for an example for Pakiri Beach).

Many beaches have a composite slope with flatter slopes at lower tide mark and steeper slopes at high-tide mark. At most profile locations, numerous beach profiles were available over many years, showing considerable profile variability over time (as in Figure 7-2). A representative beach slope for use in Equation 2-1 was selected as follows:

- Profiles from each location were split into a number of profile sets depending on length of record, with an approximately equal number of profiles in each set. Splitting the records was necessary to enable a clear visual examinations of the profiles; plots containing all profiles were too cluttered to analyse.
- The MHWS elevation was marked relative to the profile datum, based on known MHWS elevations in the region (Stephens & Wadhwa 2012).
- For each of the profile sets, a line was fitted by eye to the steepest slope that crossed the MHWS line, as in Figure 7-3.
- The representative beach slopes obtained from the profile sets were averaged at each location.
- Beach slopes for all locations were compared (as in Table 7-5). They were remarkably consistent around the coastline, probably as a result of tending to fit to the steepest profiles over the steepest part of the beach.
- A representative beach profile slope of 1 in 9 was adopted for Mangawhai/Pakiri, and a slope of 1 in 7 was adopted for all other beaches in the Auckland region.

These beach slopes are considered conservative in that they are relatively steep representations of the measurements over the profile near the MHWS elevation (the steepest part of the beach). Thus they will tend to return higher wave setup calculations than the use of shallower slopes in equations such as Equation 2-1.

Table 7-5: Representative beach profile slopes at MHWS elevation for Auckland east-coast beaches.

| Location | Beach slope (β s) 1:X |
|---------------|------------------------------|
| Browns Bay | 1:10 |
| Campbells Bay | 1:6 |
| Cheltenham | 1:6 |
| Long Bay | 1:9 |
| Mangawhai | 1:9 |

| Location | Beach slope (β s) 1:X |
|----------|------------------------------|
| Maraetai | 1:6 |
| Milford | 1:8 |
| Omaha | 1:9 |
| Pakiri | 1:8 |
| Takapuna | 1:8 |

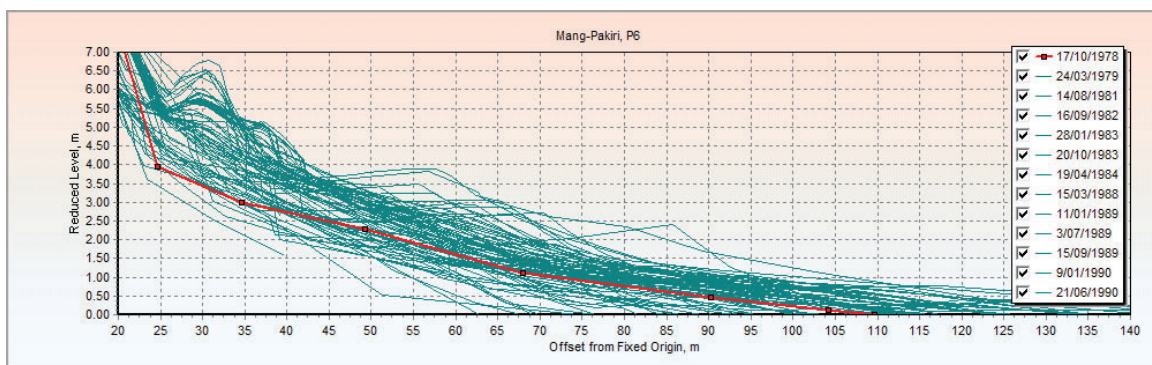


Figure 7-2: Pakiri Beach profiles, at site P6.

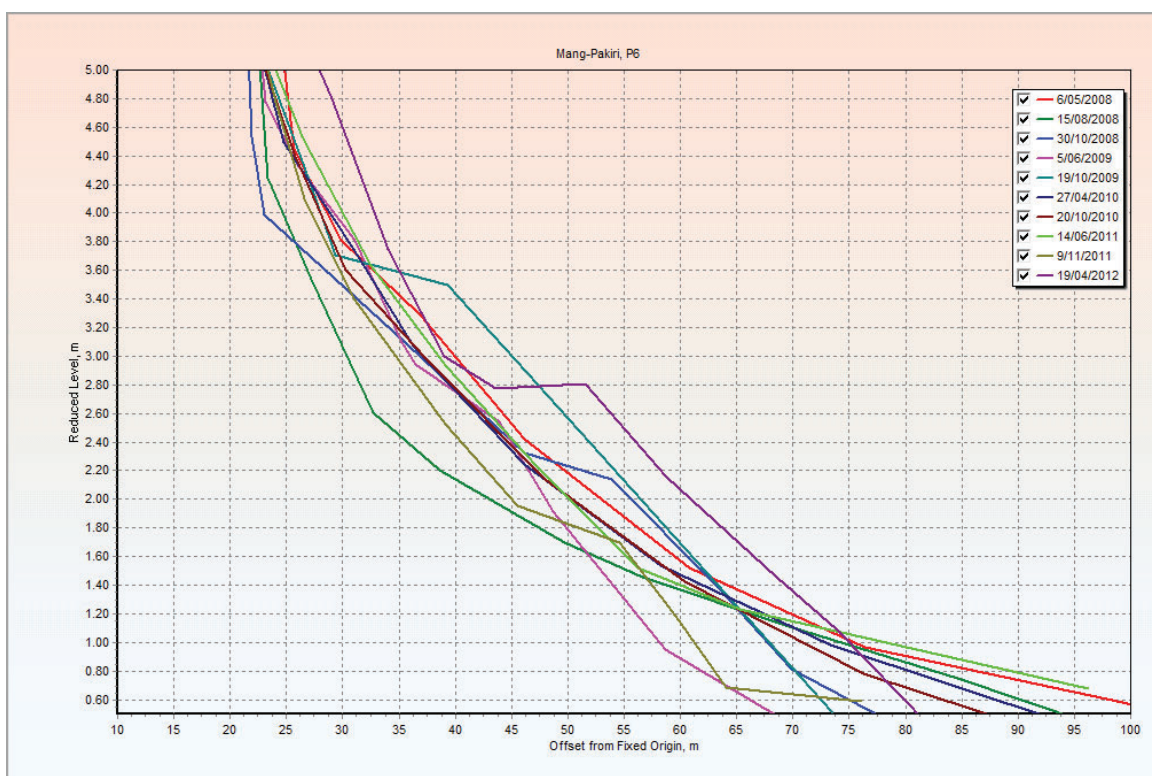


Figure 7-3: Pakiri Beach profiles near the high-tide line; profile P6.

A selection (1 of 3 for this profile location) of beach profiles (2008–2012). The orange dashed line marks the MHWS line relative to profile datum. The black dashed line marks a best fit by eye to the steepest slope of these beach profiles at the MHWS elevation.

Methods for calculating extreme sea levels in small east-coast estuaries

There are a number of estuaries on the east coast of the Auckland region for which there are no measured or modelled sea-level data. These estuaries include Tamaki Inlet, Whangateau, Matakana, Orewa and Weiti, for example. For these locations, we used a simplified approach.

The joint-probability of storm-tides and waves was calculated offshore from the estuary entrance, as described in Section 7.4 above. The storm-tide component was assumed to amplify within these small estuaries, and an amplification factor was applied that increased with distance from the entrance of each estuary. The applied amplification rate was equivalent to the tidal amplification between the Port of Auckland and Salthouse Jetty gauges in the Waitemata Harbour, being 4.2 mm of elevation per km of horizontal distance. We also calculated tidal harmonic constituents (and tidal amplification rates) using existing sea-level records at Pakuranga Bridge in Tamaki Estuary, (Bell et al. 1996) and Dawsons Landing in Mahurangi Estuary, (Oldman & Black 1997). The Tamaki estuary had a similar tidal amplification rate to the Waitemata Harbour, whereas the Mahurangi Harbour rate was approximately double. Thus there is uncertainty in the amplification rates used for the smaller estuaries that have no sea-level records. This causes an uncertainty of about 3 cm elevation, which is of minor significance to the calculation of the extreme sea-level inundation lines. The wave setup component at the entrance was assumed to translate inside the estuary, so was added to the amplified storm-tide elevations inside the estuary.

Appendix B – Mapping inundation areas

Auckland Council has LiDAR data available for the entire region. This provides the council with detailed topographic information and digital elevation models which includes the coastal margins across the region. LiDAR data utilises the AVD-46 for its elevation baseline, bearing in mind that present-day MSL is now about 0.15 m above this datum. The zero LiDAR contour therefore provides a historic MSL that is slightly lower than present-day MSL for the entire region, but is nevertheless tied into the widely-used AVD-46 vertical datum. Contouring above this line typically has a resolution of 0.125 m ground sampling distance (GSD) for urban areas and 0.5 m GSD for rural areas.

By intersecting extreme sea-level estimates with a digital elevation model constructed from LiDAR, a set of flooded coastlines can be generated that represent the inland extent of flooding from the sea. Land lying seaward of the flooded coastlines and below the extreme sea-level elevations can be mapped as flooded.

This section outlines the methods used to produce inundation area maps within GIS. To demonstrate the method, results are shown for the 0.01 annual exceedance probability (100-year ARI) event along the east coast of the Auckland region and then focussing on the Whangateau Estuary to illustrate the final mapping. The methods are the same for all regions and all annual exceedance probability scenarios. The mapped scenarios are listed in Table 1-1.

The process used to develop the inundation polygon in GIS is now described, for a single AEP scenario:

Open coast

Extreme sea-levels at model-output locations around the Auckland coastline were loaded into GIS (Figure 8-1).

Extreme sea-levels were interpolated between along connecting lines (Figure 8-2).

The sea-level elevations were transferred to the coastline using nearest-neighbour interpolation.

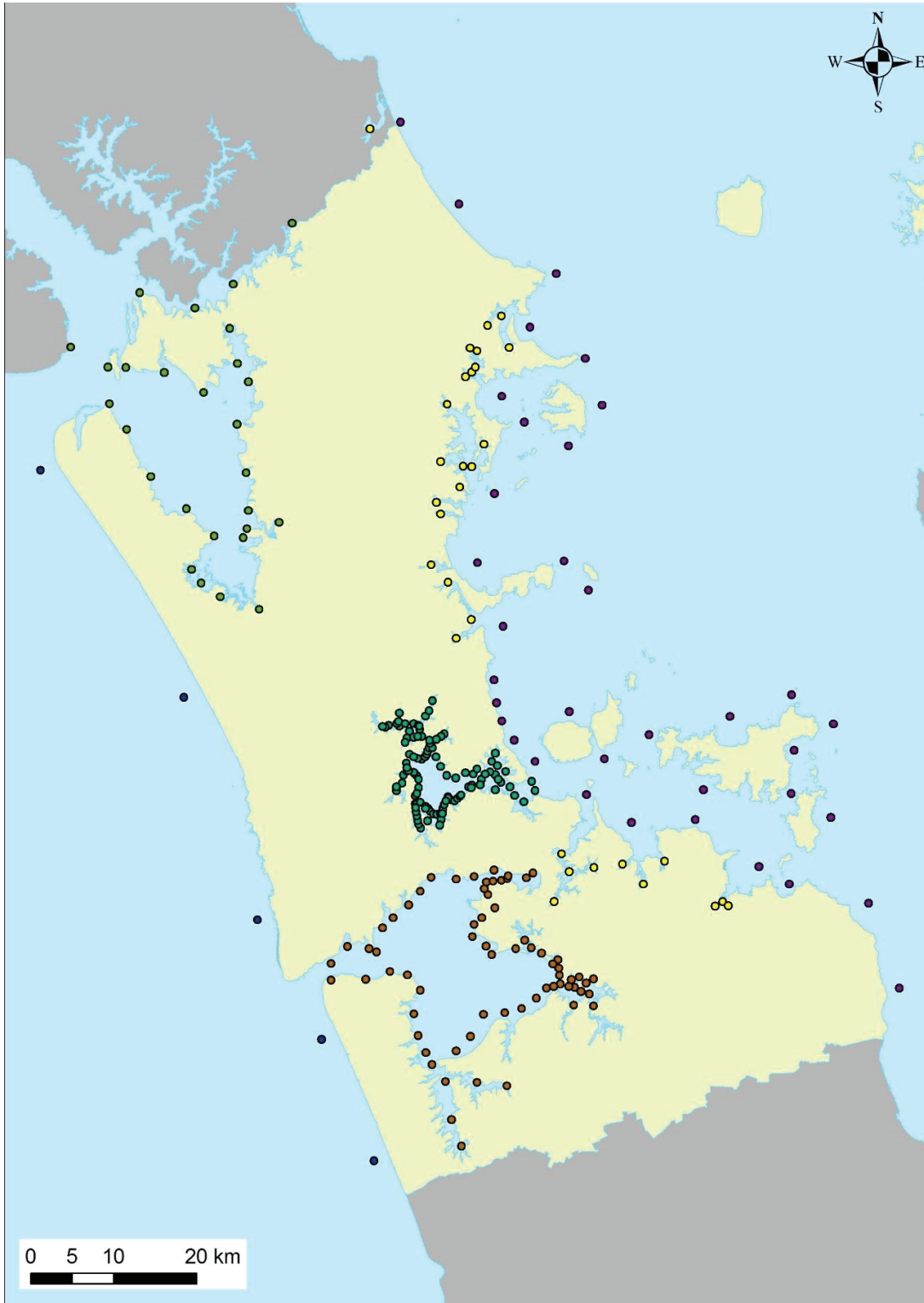


Figure 8-1: Map of the Auckland Region with 0.01 AEP storm-tide elevations marked at model-output locations.



Figure 8-2: Map of the Auckland Region with interpolated elevations on the lines connecting model output locations, and elevations transferred from offshore lines to points along the coastline.

Waitemata, Kaipara and Manukau Harbours, and small east-coast estuaries

For each extreme sea-level model-output location, the nearest point on the coast was identified and designated as a “hot point”, and the extreme sea-level elevations were transferred to it. All other coast vertices in between the hot points remain empty.

Linear interpolation was used to interpolate extreme sea-level elevations along the guiding coastline, from the hot points to all vertices between (Figure 8-3).



Figure 8-3: Map of Waitemata Harbour with interpolated elevation values on the simplified coastline.
(“Hot points” along the coastline are marked in red, modelled sea-level output locations in purple.)

Creating a regional extreme sea-level surface and generation of inundation polygons

The interpolated 0.01 AEP extreme sea-level elevations for the Auckland region are shown in Figure 8-4.

A study area polygon was created from approximately the + 20 m contour inland and to ~ 1 km offshore, to be used as the analysis area (Figure 8-5). This study area polygon can be described as a “window” within which the GIS looks for the intersection of the extreme sea-level elevation with the LiDAR DEM.

600,000 random points were picked within the study area and assigned the extreme sea level of the near coastal vertex. We used this dataset to create a 1 m raster of the spatially varying extreme sea level. This is shown in Figure 8-6 for the present-day 0.01 AEP extreme sea-level elevation line, up to 1 km from the coastline.

Sea-level rise scenarios of +1 m and +2 m were added to some of the present-day extreme sea-level scenarios (Table 1-1).

Figure 8-7 and Figure 8-8 give examples of the inundation polygons in Whangateau Harbour for 0.01 AEP extreme sea-level scenarios for present-day mean sea-level and present-day plus 2 m sea-level rise.



Figure 8-4: Map of Auckland region with interpolated elevation values on simplified coastline.



Figure 8-5: 600,000 random points in the analysis area.



Figure 8-6: Map of Auckland region with water surface for 0.01 AEP (100-year ARI) elevations.

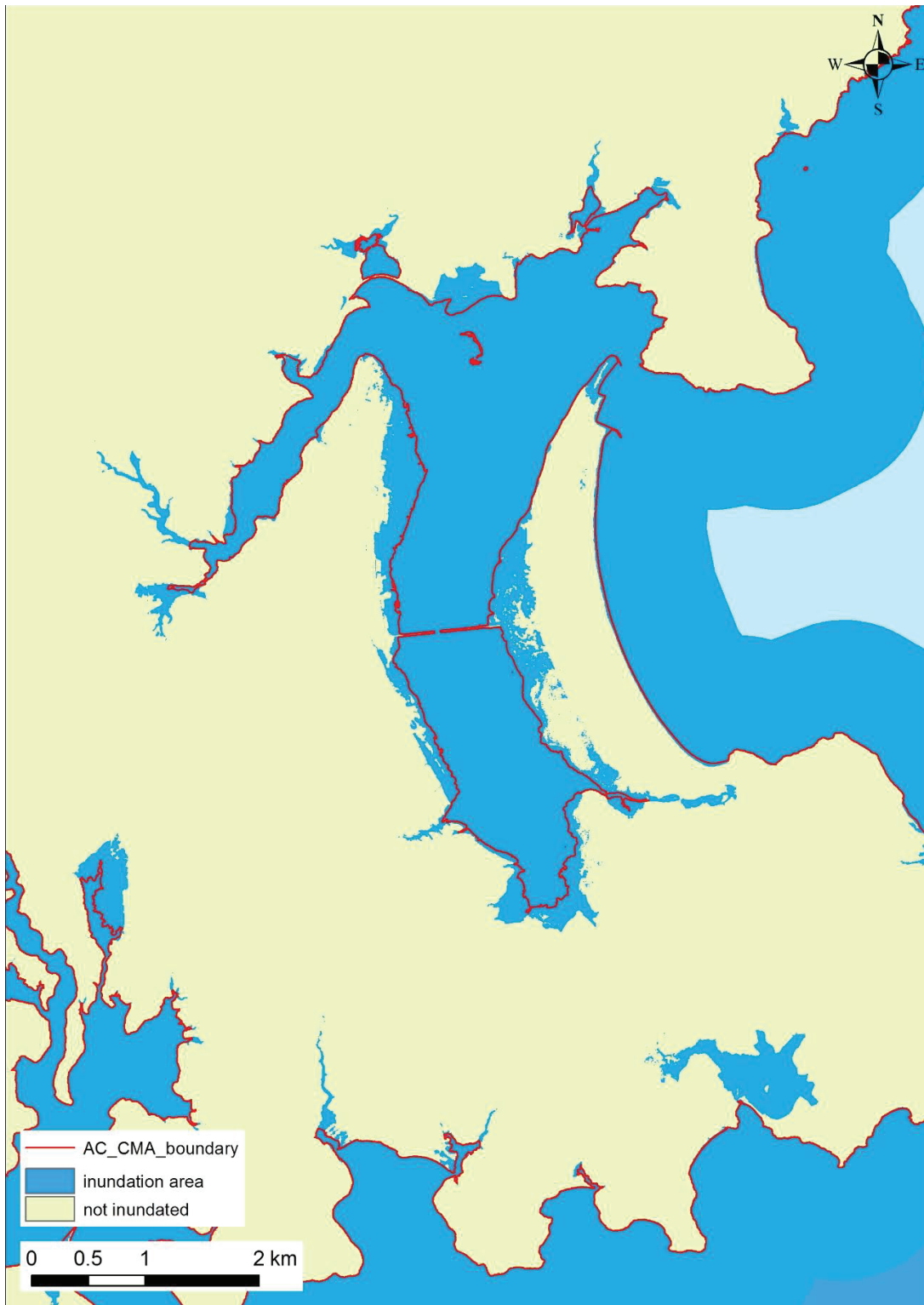


Figure 8-7: Inundation area from 0.01 AEP (100-year ARI) extreme sea-level scenario, including present-day +0.15 m mean sea-level offset to AVD-46, in Whangateau Harbour.

AC_CMA_boundary is the CMA boundary for the Auckland region (Stephens et al. 2012).

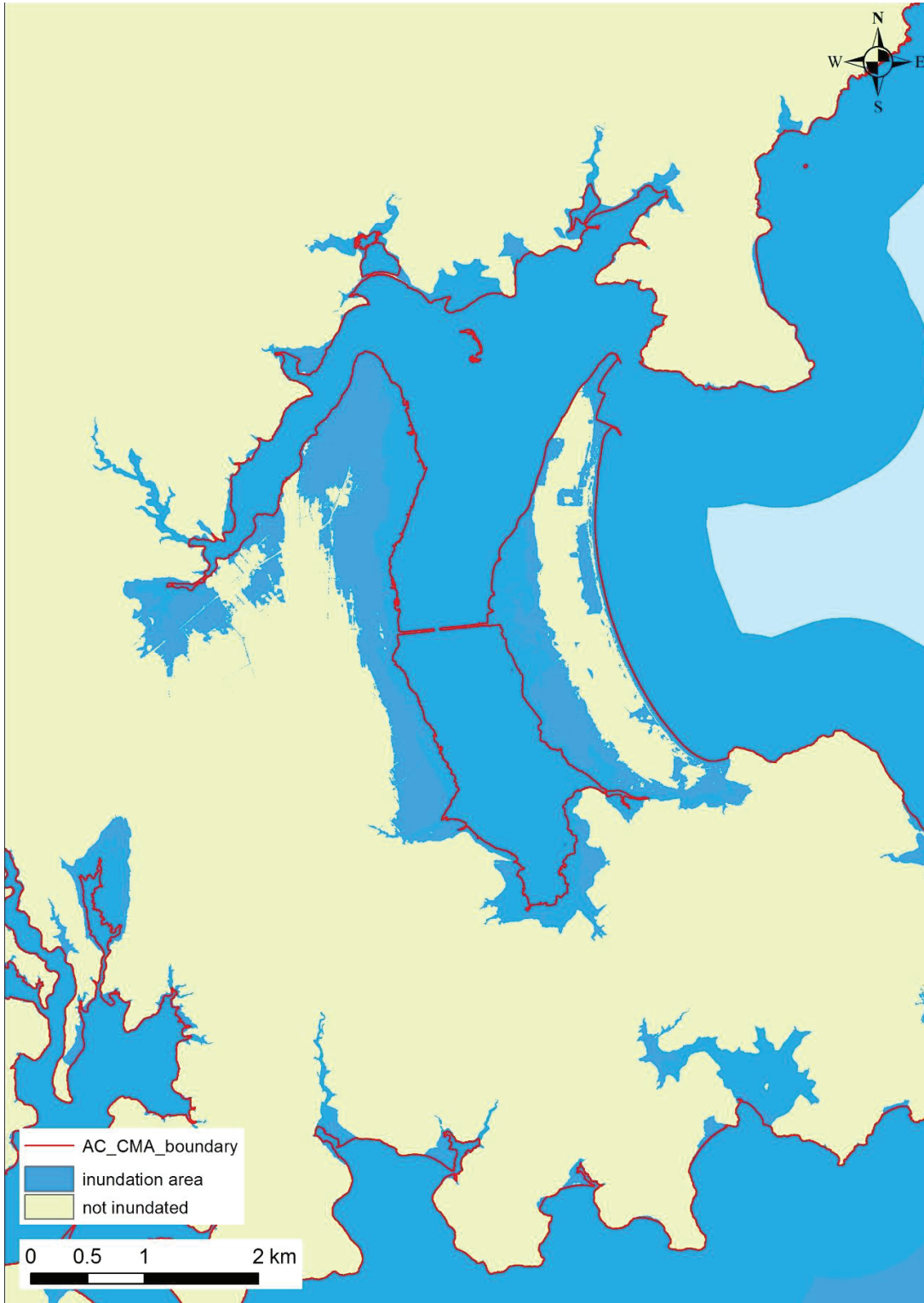


Figure 8-8: Inundation area from 0.01 AEP (100-year ARI) extreme sea-level scenario, including present-day +0.15 m mean sea-level offset to AVD-46 + 2.0 m sea-level rise, in Whangateau Harbour.

Connection by rivers and drains

The raw polygons contained numerous ponded areas that were unconnected to the sea. This occurred because they were lower than the extreme sea-level being modelled, but separated from the sea by a strip of higher land. Therefore, the final process was to overlay a GIS layer containing the drainage network. If a ponded area was connected by a river or drain, then it was included in the flood map, and if not it was deleted. In the data layers supplied to Auckland Council, these areas are flagged 'connected by drain or river'. The connections are based on the storm water and river network locations supplied by Auckland Council. Our 'bathtub' approach assumes that if an inland area is connected to the open coast via a drain/river then this area will be inundated to the equivalent level as the adjacent open coast (i.e., no lags or diminished volumes assumed in flooding through these connections).

Verification of present-day 0.01 AEP inundation polygons

The 23 January 2011 storm-tide was the highest on record at the Port of Auckland (Waitemata). The average recurrence interval for this storm-tide has been estimated at 88 years (Stephens et al. 2011c), and 126 and 205 years, depending on the method used, but the difference between a 100-year and a 200-year ARI event is only ~6 cm (Section 3.1.1). Therefore, the 100-year ARI inundation area polygon at present-day mean sea level should compare closely to the coastal flooding that occurred on 23 January 2011. The 0.01 AEP (100-year ARI) inundation polygons were validated by visually comparing it with ground photographs from the 2011 storm-tide event, for the east coast of the Auckland region. Surveys of the areal extent of inundation (from Auckland Council) were also used, and photographs during the storm-tide were also used for validation at few locations.

Verification against surveys of the 2011 storm-tide

Auckland Council surveyed locations that marked the inland edge of coastal flooding during the 23 January 2011 storm-tide. These locations are plotted alongside the landward boundary of the 0.01 AEP polygon, overlaid on aerial photographs, in Figure 8-9–Figure 8-13. The comparisons appear to verify the modelling for the 0.01 AEP scenario for present-day MSL.



Figure 8-9: Verification of present-day 0.01 AEP (100-year ARI) storm-tide line against surveyed location of maximum flood incursion during 23 Jan 2011 storm-tide, at Kohimarama.

(Pink line marks modelled 0.01 AEP storm-tide line. Blue line marks coastal marine area (CMA) boundary.)

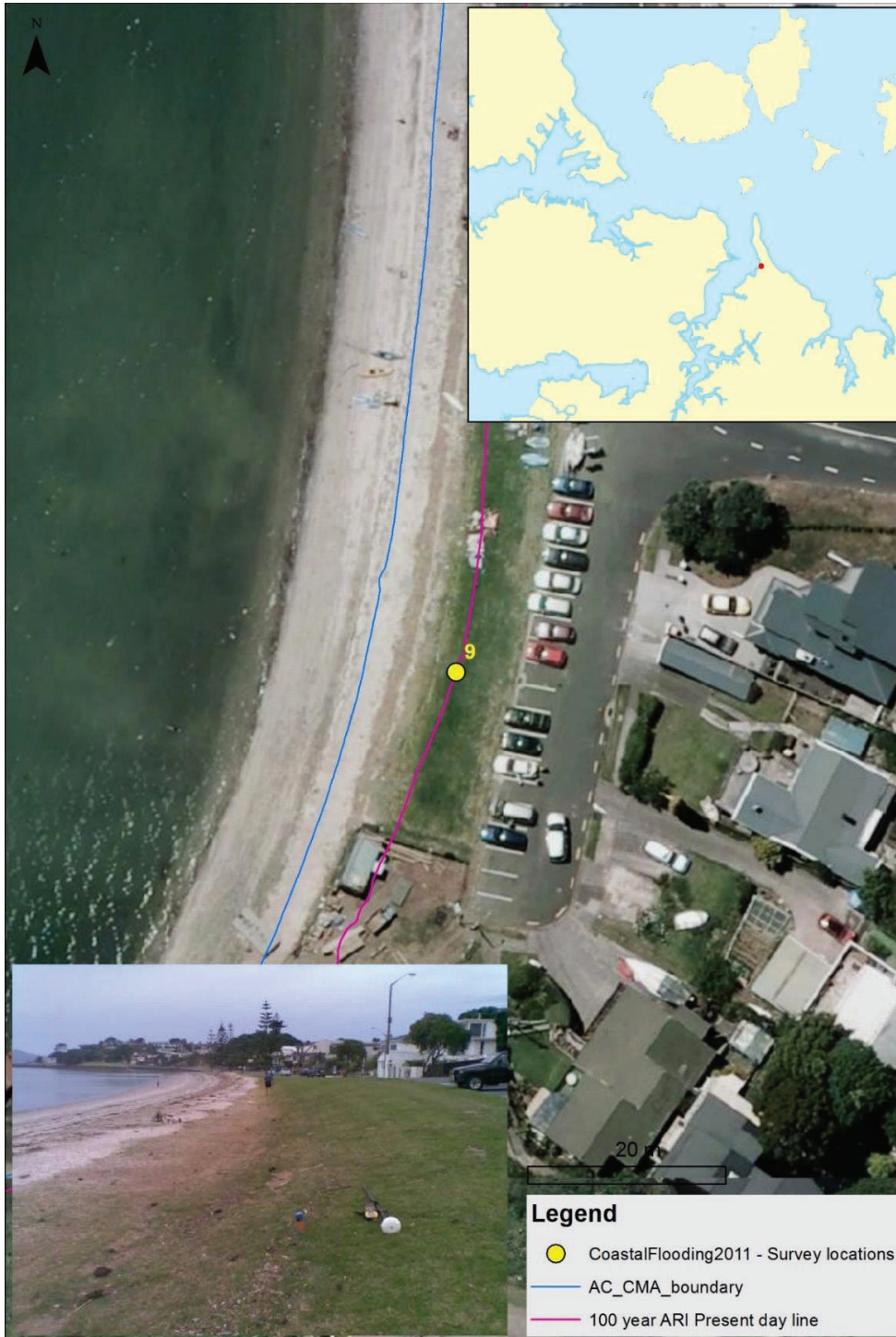


Figure 8-10: Verification of present-day 0.01 AEP (100-year ARI) storm-tide line against surveyed location of maximum flood incursion during 23 Jan 2011 storm-tide, at Half-Moon Bay.

(Pink line marks modelled 0.01 AEP storm-tide line. Blue line marks coastal marine area (CMA) boundary.)



Figure 8-11: Verification of present-day 0.01 AEP (100-year ARI) storm-tide line against surveyed location of maximum flood incursion during 23 Jan 2011 storm-tide, at St Heliers Bay.

Pink line marks modelled 0.01 AEP storm-tide line. Blue line marks coastal marine area (CMA) boundary.



Figure 8-12: Verification of present-day 0.01 AEP (100-year ARI) storm-tide line against surveyed location of maximum flood incursion during 23 Jan 2011 storm-tide, at St Heliers Bay (east).

Pink line marks modelled 0.01 AEP storm-tide line. Blue line marks coastal marine area (CMA) boundary.



Figure 8-13: Verification of present-day 0.01 AEP (100-year ARI) storm-tide line against surveyed location of maximum flood incursion during 23 Jan 2011 storm-tide, at St Marys Bay.

Pink line marks modelled 0.01 AEP storm-tide line. Blue line marks coastal marine area (CMA) boundary.

Verification against photographs of the 2011 storm-tide

The present-day 0.01 AEP GIS polygons were compared with photographs of flooding over the North-western (SH16) and Northern (SH1) motorways, with the model showing a close match (Figure 8-13, Figure 8-14). On the northern motorway the GIS polygons show inundation on the north bound lane,

which did not occur because the water was stopped by a low median barrier between the north-bound and south-bound lanes, not captured in the LiDAR data (Figure 8-14).

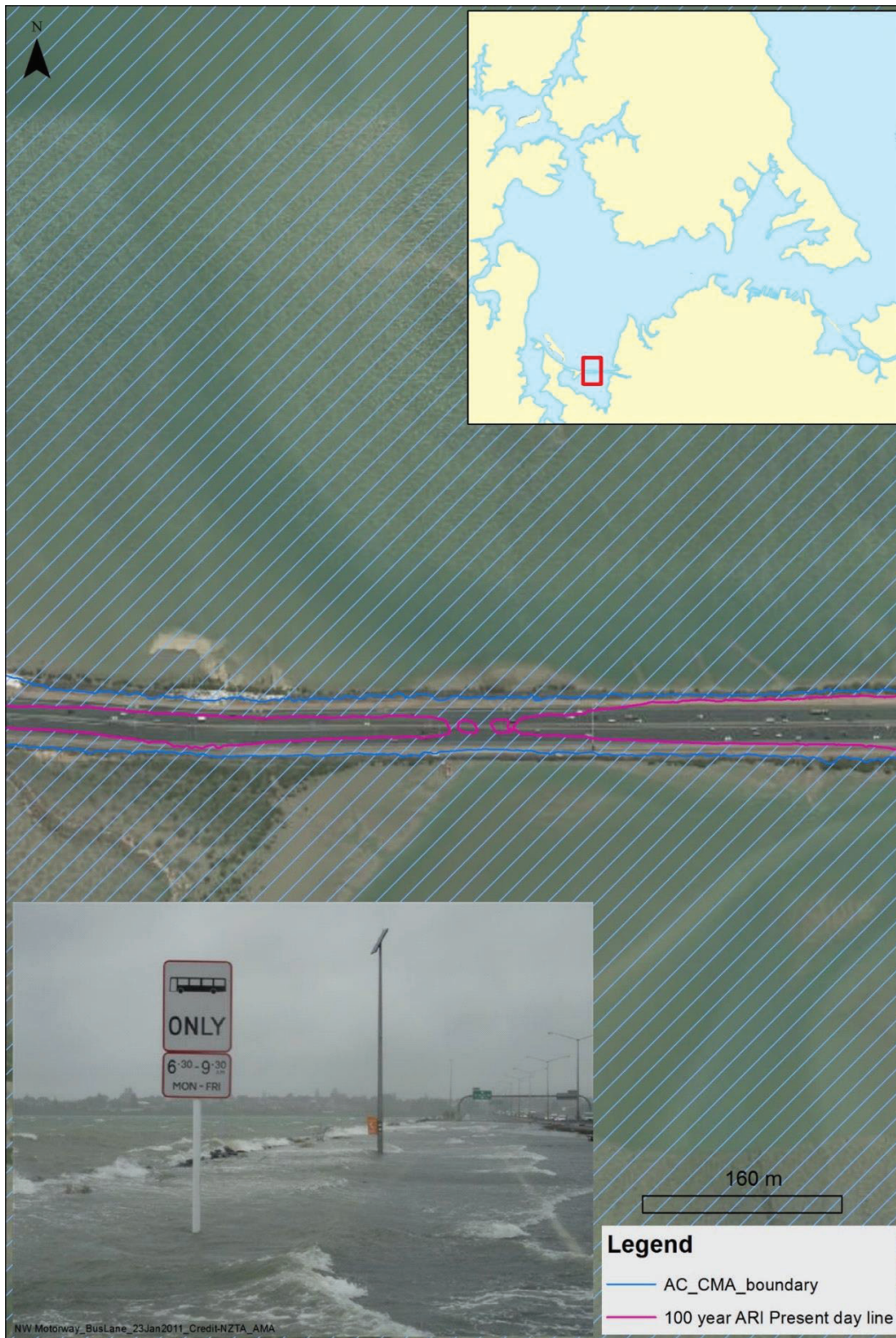


Figure 8-14: Verification of present-day 0.01 AEP (100-year ARI) storm-tide line against photograph of observed flooding on the north-western motorway during the 23 Jan 2011 storm-tide.

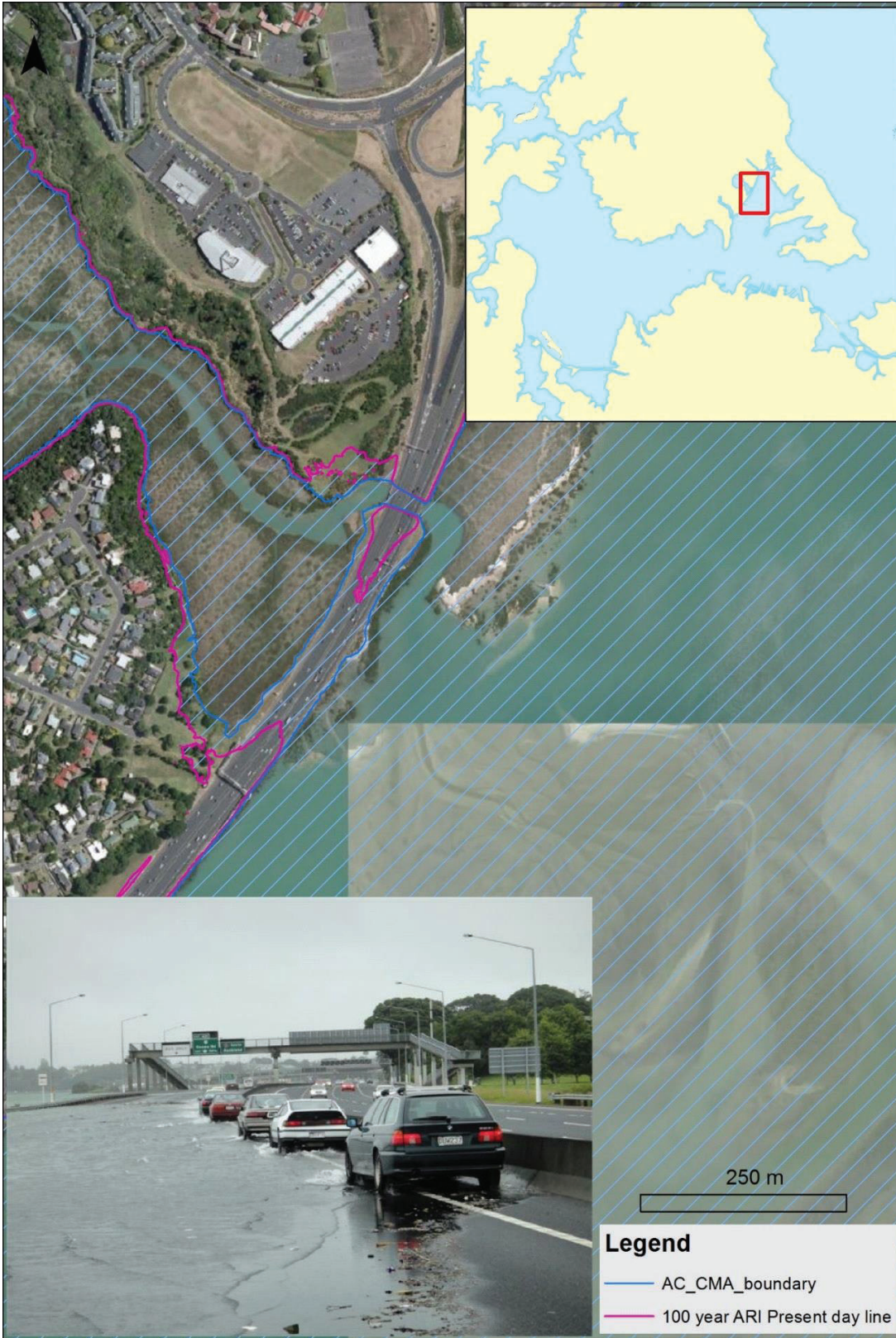


Figure 8-15: Verification of present-day 0.01 AEP (100-year ARI) storm-tide line against photograph of observed flooding on the Northern motorway during the 23 Jan 2011 storm-tide.



Part 2: Coastal-storm inundation in the
Auckland region, supplementary information:
Updated coastal-storm exposure at Parakai
and re-mapping of East Coast estuaries,
NIWA 2016





Technical report: coastal-storm inundation in the Auckland region - supplementary information

Updated coastal-storm exposure at Parakai and re-mapping of east-coast estuaries

Prepared for Auckland Council

March 2016

Prepared by:

Scott Stephens
Sanjay Wadhwa

For any information regarding this report please contact:

Scott Stephens
Coastal and Estuarine Physical Processes Scientist
Coastal and Estuarine Processes Group
+64-7-856 7026
scott.stephens@niwa.co.nz

National Institute of Water & Atmospheric Research Ltd

PO Box 11115
Hamilton 3251
Phone +64 7 856 7026

NIWA CLIENT REPORT No: HAM2016-015
Report date: March 2016
NIWA Project: ARC16204

| Quality Assurance Statement | | |
|---|--------------------------|----------------|
|  | Reviewed by: | Richard Gorman |
|  | Formatting checked by: | Alison Bartley |
|  | Approved for release by: | David Roper |

© All rights reserved. This publication may not be reproduced or copied in any form without the permission of the copyright owner(s). Such permission is only to be given in accordance with the terms of the client's contract with NIWA. This copyright extends to all forms of copying and any storage of material in any kind of information retrieval system.

Whilst NIWA has used all reasonable endeavours to ensure that the information contained in this document is accurate, NIWA does not give any express or implied warranty as to the completeness of the information contained herein, or that it will be suitable for any purpose(s) other than those specifically contemplated during the Project or agreed by NIWA and the Client.

Table of Contents

| | |
|--|-----|
| Table of Contents | iii |
| Figures | iv |
| Tables | iv |
| Technical summary..... | 1 |
| 1 Introduction | 3 |
| 1.1 Background..... | 3 |
| 1.2 Inundation modelling and mapping at Parakai/Helensville | 3 |
| 1.3 Mapping coastal-storm inundation for small east-coast estuaries..... | 3 |
| 2 Inundation modelling and mapping at Parakai/Helensville | 4 |
| 2.1 Background..... | 4 |
| 2.2 Extreme sea level at Helensville..... | 5 |
| 2.3 Coastal-storm inundation modelling in Parakai/Helensville..... | 10 |
| 2.4 Recommended approach for hydrodynamic model validation | 10 |
| 2.5 Summary of coastal-storm inundation hydrodynamic modelling | 11 |
| 2.6 Comparison between the present and the 2013 coastal-storm inundation mapping | 14 |
| 3 Coastal-storm inundation in east-coast estuaries..... | 18 |
| 3.1 Conclusions | 20 |
| 4 Acknowledgements..... | 22 |
| 5 Glossary of abbreviations and terms | 23 |
| 6 References..... | 24 |
| Appendices | 26 |
| Appendix A: Vic Freestone’s Helensville tide gauge quality analysis | 27 |
| Appendix B: Helensville tide-gauge datum..... | 31 |
| The 17 April 1999 storm-tide | 32 |

Figures

| | |
|---|----|
| Figure 2-1: High-tide exceedance curve at Helensville. | 6 |
| Figure 2-2 : Example of sea-level decomposition into tide and non-tidal residual, and skew surge definition..... | 7 |
| Figure 2-3 : Extreme skew-surge distribution at Helensville..... | 8 |
| Figure 2-4 : Extreme sea level analysis at Helensville. | 9 |
| Figure 2-5: 1% AEP coastal-storm inundation elevations at present-day MSL from this project (DHI, 2016)..... | 13 |
| Figure 2-6: 1% AEP coastal-storm inundation elevations at present-day MSL mapped by NIWA in 2013..... | 15 |
| Figure 2-7 : Difference (m) between coastal-storm inundation elevations predicted in this study from those by NIWA in 2013, during a 1% AEP storm-tide at present day MSL. | 16 |
| Figure 2-8: Depth versus area of inundation over the Parakai flood plain. | 17 |

Tables

| | |
|--|----|
| Table 2-1: Extreme sea-level in the Kaipara Harbour calculated by Stephens et al. (2013). | 4 |
| Table 2-2 : Helensville tidal constituent and mean high-water springs heights. Heights are in mm relative to mean sea level..... | 7 |
| Table 2-3 : Extreme skew surges at Helensville..... | 8 |
| Table 2-4: Extreme sea levels at Helensville..... | 10 |
| Table 2-5 : Depth versus area of inundation over the Parakai flood plain as simulated in this (2016) project..... | 12 |
| Table 2-6: Depth versus area of inundation over the Parakai flood plain, as simulated in the 2013 project..... | 17 |
| Table 2-7: Difference in the estimated area of inundation over the Parakai flood plain, between the 2013 and 2016 projects..... | 17 |
| Table 3-1: Storm-tide and maximum storm-tide plus wave setup elevations with 1% annual exceedance probability (1% AEP), and a wave setup component inferred from their difference, for locations offshore from small east-coast estuaries. | 19 |
| Table 3-2 : Maximum storm-tide plus wave setup elevations with 1% AEP at locations inside small east-coast estuaries (Table 4-4, Stephens et al. 2013), and with an inferred wave setup (from Table 3-1 above) subtracted. | 19 |

Technical summary

In 2013, NIWA calculated coastal-storm inundation elevations around the coastline of the Auckland region for Auckland Council Civil Defence and Emergency Management (Stephens et al. 2013). The Proposed Auckland Unitary Plan will also use NIWA's 2013 coastal-storm inundation elevations and maps to control development. The accuracy of NIWA's coastal-storm inundation calculations was controlled by the availability of topographic and sea-level information and the time and resources available for the study.

Coastal-storm inundation areas in the Auckland region were mapped in 2013 using a static level or "bathtub" inundation-mapping technique, in which all land lying below the coastal-storm inundation elevation is assumed to be flooded in its entirety, if there is a direct flow path to the sea or harbour waters. The coastal-storm inundation area maps do not fully capture the dynamic and time-variant processes that occur during a coastal-storm hazard event, but rather are indicative of areas in the coastal environment that are potentially affected by coastal hazards (as required by Policy 24 of the New Zealand Coastal Policy Statement).

The static inundation mapping technique is conservative in that it tends to over-predict rather than under-predict inundation by the high-water period of storm-tides that may last for 1–3 hours. The over-prediction applies more for wider coastal plains such as at Parakai, whereas for narrower coastal margins, the mapped inundation level will be much closer to the expected inundation extent. It is our opinion that the coastal inundation layers mapped by NIWA in 2013, including those with sea-level rise, provide a reasonable region-wide and consistent basis for delineating areas exposed to present-day and future coastal-storm inundation in the Auckland region. These mapped layers can be revised in future for locations where more detailed data or modelling would provide meaningfully different results.

Auckland Council requested that the Helensville water-level record (which was unknown in the 2013 study), be incorporated into a more detailed coastal-storm inundation model of the Parakai/Helensville region. This is a wide, low-lying coastal plain, intersected by the Kaipara River above its confluence with the Kaipara Harbour. This was an area identified as having relatively low confidence in the 2013 coastal-storm inundation mapping, where further gauge data and dynamic inundation modelling could substantially improve our understanding of coastal-storm inundation.

Following an extreme sea-level analysis using the Helensville sea-level record, a calibrated and validated hydrodynamic model was used to simulate coastal-storm inundation over the flood plain, for a 1% annual exceedance probability storm-tide at present-day mean sea level, plus a 1 m and a 2 m sea-level rise. This is in alignment with the extreme events and sea-level rise scenarios considered in the notified Proposed Auckland Unitary Plan. We now have high confidence in the simulated coastal-storm inundation elevations in the Parakai/Helensville region – we believe that the inundation modelling is accurate to ± 0.1 m over most of the flood plain.

The original static inundation model (2013) had assumed local stopbanks were fixed structures. The revised model assumes the stopbanks are dynamic structures and subject to change over time (see Auckland Council's executive summary). The existing stopbanks will be overtopped with increasing frequency as sea level rises in future. In the absence of stopbanks, about 19 km² of land was predicted

to be inundated by ≥ 0.01 m during a 1% annual exceedance probability storm-tide at present-day mean sea level, and about 15 km² was predicted to be inundated by at least 0.25 m.

The coastal-storm inundation elevations calculated in this study were compared with the 2013 NIWA study. Both methods gave similar elevations at the confluence of the Kaipara River and the Harbour. The static GIS-mapping technique used in 2013 did not simulate the dynamics of frictional attenuation of the storm-tide wave over the flood plain, showing a slight landward-increasing water-level surface. Conversely, the hydrodynamic model used in this study included frictional attenuation, and predicted the storm-tide elevation to drop inland. As a result, the difference between the two studies increases inland. This study predicted water levels that were up to 0.5 m lower than the 2013 study over most of the lower flood plain, and up to about 2 m lower further inland. The total area of coastal-storm inundation was predicted to be 60% less (using the dynamic modelling) than was predicted using the original static inundation model in 2013.

The coincidence of a large 2% annual exceedance probability river flood with a 1% annual exceedance probability storm-tide was modelled and the flood was found to increase water levels by about 0.2 m over the Parakai/Helensville floodplain, but with higher increases upstream. This storm-tide and flood combination is possible, but has much less than a 1% annual exceedance probability because the two will have only limited dependence. Inclusion of the river flow makes a noticeable difference to coastal-storm inundation elevations at present-day mean sea level, but its effect is small compared to future sea-level rise scenarios.

As part of the current study, Auckland Council also requested re-mapping of the small east-coast estuaries. An assumption made in the NIWA's 2013 report (when calculating coastal-storm inundation elevations in the small estuaries along the east coast of the Auckland region), was that storm-tide plus wave setup elevations at the entrance could propagate throughout the estuary. This was a conservative assumption in alignment with the precautionary principles of the Proposed Auckland Unitary Plan. In subsequent research, we have since concluded that the wave setup generated on the open coast is unlikely to propagate far inside the entrance of such estuaries and in March 2015, NIWA revised the coastal-storm inundation elevations for small east-coast estuaries in the Auckland region. As part of this project we re-mapped coastal-storm inundation zones for these areas based on the revised elevations. The revised maps were supplied to Auckland Council in GIS format and represent Auckland Council's best available data to date.

1 Introduction

1.1 Background

In 2013, NIWA calculated coastal-storm inundation elevations around the coastline of the Auckland region for Auckland Council Civil Defence and Emergency Management (Stephens et al. 2013). The Proposed Auckland Unitary Plan will also use NIWA's 2013 coastal-storm inundation elevations and maps to control development. The accuracy of NIWA's coastal-storm inundation calculations was controlled by the availability of topographic and sea-level information and the time and resources available for the study.

1.2 Inundation modelling and mapping at Parakai/Helensville

Auckland Council requested that the Helensville water-level record (which was unknown in the 2013 study), be incorporated into a more detailed coastal-storm inundation model of the Parakai/Helensville region. This is a wide, low-lying coastal plain, intersected by the Kaipara River above its confluence with the Kaipara Harbour. This was an area identified as having relatively low confidence in the 2013 coastal-storm inundation mapping, where further gauge data and dynamic inundation modelling could substantially improve our understanding of coastal-storm inundation.

In this project we re-calculated extreme sea-levels in the Helensville region using an available sea-level record, and commissioned DHI (who had the appropriate models already set up) to simulate coastal-storm inundation over the flood plain.

1.3 Mapping coastal-storm inundation for small east-coast estuaries

In 2015 NIWA revised the calculations of coastal-storm inundation resulting from storm-tide, and from storm-tide plus wave setup, as calculated by Stephens et al. (2013) for the small estuaries along the east coast of the Auckland region (Stephens 2015). When making these calculations in 2013, NIWA assumed that storm-tide plus wave setup elevations at the estuary entrances would propagate throughout the estuary. This was a conservative assumption, since the wave setup component that is generated on the open coast is unlikely to propagate far inside the entrance of an estuary (Santoso et al. 1999; Tanaka et al. 2008). NIWA revised the coastal-storm inundation elevations for small east-coast estuaries, by calculating the additional wave set up component relative to storm-tide alone, at the entrance to several of the small east-coast estuaries, and removing the inferred wave setup from the coastal-storm inundation elevations (Stephens 2015). In this project we re-mapped additional coastal-storm inundation scenarios for the small east-coast estuaries for the following scenarios:

- 1% AEP at present-day MSL (AEP = annual exceedance probability)
- 2% AEP at present-day MSL
- 2% AEP + 1 m SLR
- 2% AEP + 2 m SLR
- 5% AEP at present-day MSL
- 18% AEP at present-day MSL.

2 Inundation modelling and mapping at Parakai/Helensville

2.1 Background

Confidence in the 2013 NIWA storm-tide modelling was relatively low at Parakai, because the focus of that study was the calculation of extreme sea-levels for the entire Auckland region, compressed into a short delivery timeframe, which meant that NIWA was unable to model the dynamics of inundation at Parakai:

- The nearest location of extreme sea-level predictions is in the Kaipara Harbour which is some distance downstream from Parakai. There will be considerable shoaling of the tide and surge between the nearest output location and Parakai and so the calculated extreme sea level elevations may not accurately represent those at Parakai.
- NIWA was unaware of the Helensville sea-level data at the time of the 2013 study. That dataset has been used here to greatly increase confidence in the estimation of the frequency and magnitude of coastal-storm inundation elevations.
- The coastal plain is wide and flat, so the dynamics of inundation are likely to be important; these were not included in the static GIS-based mapping technique.
- The potential combination of high storm-tides and freshwater flooding from the catchment had not been investigated.

At the most upstream location in the Kaipara Harbour (site 16) Stephens et al. (2013) calculated a 1% AEP storm-tide elevation of 3.53 m (AVD-46), and a 39% AEP (2 year return period) storm-tide elevation of 2.95 m (Table 2-1). Although 2.95 m is higher than the highest recorded upstream storm-tide of 2.90 (47B Parakai Avenue on 17 April 1999), modelling by DHI shows rapid attenuation of the storm-tide within the Kaipara river. Tuckey (2014) showed that inclusion of the Parakai floodplain is likely to lower the sea level predicted at NIWA's site 16 location, due to dispersion of storm-tide across the floodplain. NIWA did not simulate storm-tide scenarios, but used probabilistic sampling of sea-level components that were simulated separately. It is not clear how the dynamics of the separate components would be affected by inclusion of the floodplain in the hydrodynamic model. Nevertheless, Tuckey's 2014 simulations indicate that the dynamics of inundation across the floodplain will be important for coastal-storm inundation assessment, and this was verified by the present study results (Section 2.3.3).

Table 2-1: Extreme sea-level in the Kaipara Harbour calculated by Stephens et al. (2013).

Elevations are relative to AVD-46 including +0.23 m offset for baseline mean sea level (present-day estimate). Elevations calculated from simulated data.

| AEP: | | 0.39 | 0.18 | 0.10 | 0.05 | 0.02 | 0.01 | 0.005 |
|----------------|-----------------|------|------|-------|-------|-------|--------|--------|
| ARI: | | 2 yr | 5 yr | 10 yr | 20 yr | 50 yr | 100 yr | 200 yr |
| Easting (NZTM) | Northing (NZTM) | | | | | | | |
| 1728962 | 5943240 | 2.95 | 3.10 | 3.21 | 3.32 | 3.44 | 3.53 | 3.60 |

In 2006 DHI simulated extreme sea-levels within the Kaipara Harbour using calibrated hydrodynamic models (Wo and van Kalken 2006). A two-dimensional harbour model was calibrated using tidal data, and was found to over predict spring-tide peaks by 0.11–0.30 m. The lack of land level data above the low tide level in the tidal flats around Helensville was given as the most likely cause of detrimental effects on model calibration in this area. The harbour model was coupled to a Kaipara River model that included a representation of the flood plain in the Parakai area, and the flood-plain model was used to simulate water levels at Helensville. The authors noted that the incorporation of LiDAR-derived topography would reduce current uncertainties in the results. The model was used to simulate several combinations of tide, surge, climate variability and sea-level rise, however no probabilistic analysis was undertaken to inform the likelihood of the various components combining in the scenarios modelled. Sea-level rise allowance of 0.5 m to the year 2050 was considerably lower than present-day best practice which advises “at the very least, all assessments should consider the consequences of a mean sea-level rise of at least 0.8 m relative to the 1980–1999 average” (MfE 2008). The modelling indicated that a water level of 3.16 m at the tidal gauging station was likely to occur within a hazard planning timeframe, which is of similar magnitude (0.26 m higher) to the largest historically-recorded storm-tide of 2.90 m. A 1% AEP storm-tide is likely to occur (63% chance) over a 100-year planning timeframe (Stephens and Bell 2015; Stephens et al. 2013). The modelling showed that storm-tide elevation decreased upstream, by 0.42 m over approximately 3 km between the Kaukapakapa confluence and the Mill Street bridge.

Additional LiDAR and seabed data were collected and integrated into the hydrodynamic model used for the 2009 Helensville wastewater treatment plant dilution modelling study (Senior and Tuckey 2009). Tuckey (2014) extended the model of Senior and Tuckey (2009), using available LiDAR to include the Kaipara River floodplain.

van Kalken (2009) modelled and mapped flooding from the Kaipara River catchment to the Harbour mouth, which included flooding over the Parakai floodplain. Using a downstream seaward boundary of 2.11 m, the 1% AEP (100-year ARI) flooding depth was 2.1 m at Parakai and 2.3 m at Helensville, both elevations which are commonly experienced due to the tide. Nevertheless, although the townships were not indicated to flood during 1% AEP floods, the flooding elevations were higher upstream with considerable flooding indicated over the coastal plain. This would indicate that it would be prudent to simulate the possibility of a large flood coinciding with a large storm-tide, since the flood might add around 20 cm of additional inundation.

In summary, storm-tides (from the sea) appear to produce considerably higher inundation risk than catchment (freshwater) flooding around Parakai. There was no study (before this one) that robustly calculated the magnitude and likelihood of storm-tides at Parakai/Helensville based on sea-level gauge data. There had been no dynamic modelling undertaken of the inundation extent and depth across the flood plain due to storm-tides.

2.2 Extreme sea level at Helensville

Auckland Council requested that the Helensville water-level record (which was unknown in the 2013 study), be incorporated into a more detailed coastal-storm inundation model of the Parakai/Helensville region. We used the Helensville water-level record to undertake an extreme sea-level analysis for the region.

Sea-level data from the tide gauge located at Winstone’s wharf in the Kaipara River at Helensville were supplied to NIWA by Vic Freestone. The sea-level record is 9.25-years long, beginning on 31 May 2005 and ending on 3 September 2014. The data were carefully quality-analysed by Vic, as described in his report (Appendix A). Small gaps in the record and minor timing errors of less than 1 minute were reported, which do not affect the extreme sea-level analyses undertaken here.

Data were supplied referred to Chart Datum. They were adjusted to Auckland Vertical Datum 1946 (AVD-46) as follows: $y_{AVD-46} = y_{CD} - 2934 \text{ mm}$ (Appendix B). The sampling interval varied from 1–5 minutes. For extreme sea-level analysis, data were interpolated to a common 1-minute timestep, and gaps ≤ 2 hours were linearly interpolated from data either side. The data were then decimated to 1-hour intervals for extreme sea-level analysis. For each high-water peak (data at hourly intervals) the maximum sea-level elevation measured (at 1-minute intervals) 1 hour either side of high water was used. This ensures that the peak water levels were retained for extreme sea-level analysis.

Tidal harmonic analysis was undertaken to resolve the tidal component of sea-level variability using UniTide (Foreman et al. 2009), applying a 2% signal-to-noise ratio. Harmonic analysis on an annual basis resolved a minimum 97.8% and an average 98.3% of the sea-level variance, showing a) that the tide dominates sea-level variability at Helensville and b) that the harmonic analysis is representing the tidal component of sea-level variability well. Figure 2-1 shows the distribution of high tide heights at Helensville, and Table 2-2 provides the heights of the 3 main harmonic constituents and several mean high-water springs (MHWS) measures.

The sea-level record “bottoms out” during large tides, which drop lower than the recording range of the sea-level gauge. During small to average tides the gauge measures the full tidal range. The measurements were compared with the predicted tide during smaller tides when the gauge was measuring the full tidal range, and when the difference between high and low water offsets was $\leq \pm 25$ mm. The comparison indicated that mean sea level (MSL) was approximately 280 mm AVD-46 during the measurement period.

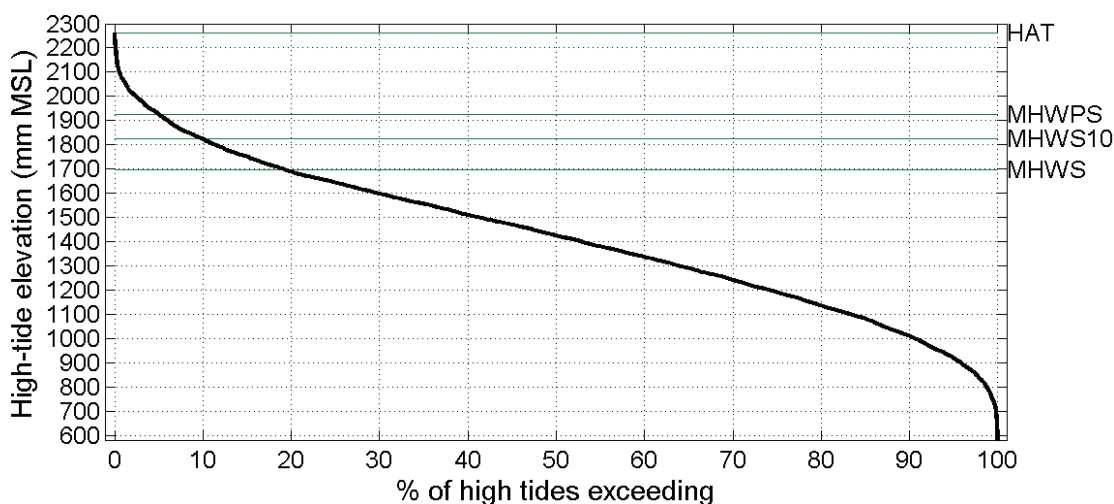


Figure 2-1: High-tide exceedance curve at Helensville.

HAT = highest astronomic tide; MHWPS = mean high-water perigean spring = $M2 + S2 + N2$; MHW S = mean high-water spring nautical = $M2 + S2$; MHW S10 = height exceeded by highest 10% of all high tides. Elevations are relative to MSL.

Table 2-2 : Helensville tidal constituent and mean high-water springs heights. Heights are in mm relative to mean sea level.

| Tide | Elevation (mm MSL) |
|--------|--------------------|
| M2 | 1371 |
| S2 | 325 |
| N2 | 231 |
| MHWPS | 1926 |
| MHWS | 1696 |
| MHWS10 | 1826 |
| HAT | 2264 |

Skew surge was calculated from each high-water measurement, as illustrated in Figure 2-2. The skew surge refers to the absolute difference between the maximum recorded sea-level during a tidal cycle and the predicted maximum astronomical tidal level for that cycle, irrespective of differences in timing between these (Batstone et al. 2013). According to Batstone et al. (2013) the skew surge parameter is a more reliable indicator of meteorological impacts on sea level than the non-tidal residual used in the revised joint-probability method (Tawn and Vassie 1989) or the Monte Carlo joint-probability method (Goring et al. 2011), which are other joint-probability extreme-sea-level methods that have been applied in New Zealand.

An extreme skew-surge analysis was conducted by fitting a generalised Pareto distribution (GPD) to peaks-over-threshold (POT) data (Coles 2001). The POT were selected as independent peaks ≥ 230 mm, separated in time by at least 3 days. The extreme skew-surge distribution is shown in Figure 2-3 and Table 2-3. The largest measured skew surge was 1058 mm above the predicted high tide, and the predicted 1% annual exceedance probability (AEP) skew surge is 1204 mm. Surges of > 1 m are considered large in New Zealand, and could generate substantial inundation if coinciding with a very high tide. For example, the highest astronomical tide (Table 2-2) + 1% AEP skew surge + 280 mm MSL is 3.75 m AVD-46.

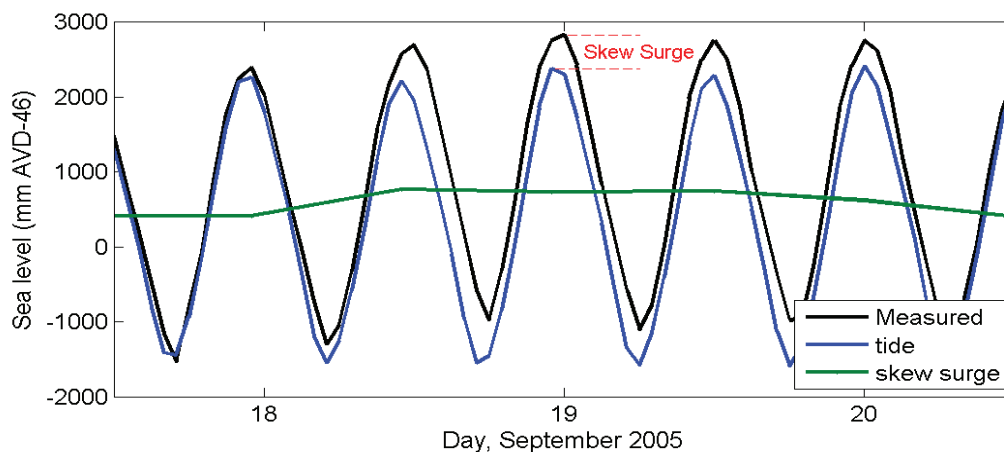


Figure 2-2 : Example of sea-level decomposition into tide and non-tidal residual, and skew surge definition.

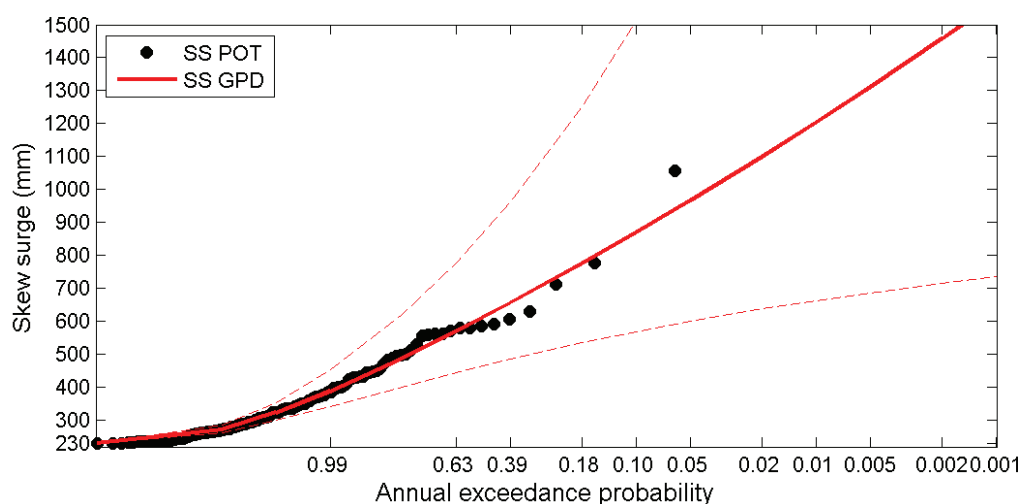


Figure 2-3 : Extreme skew-surge distribution at Helensville.

SS POT = skew-surge peaks over (230 mm) threshold, plotted in Gringorten (1963) plotting positions; SS GPD = generalised Pareto distribution fitted to SS POT (solid line =maximum likelihood, dashed lines = 95% confidence intervals).

Table 2-3 : Extreme skew surges at Helensville.

AEP = annual exceedance probability; ARI = average recurrence interval; GPD = generalised Pareto distribution fit to independent peaks over 230 mm threshold. All elevations calculated relative to MSL.

| AEP | ARI | GPD max. likelihood (mm) | GPD lower 95% confidence interval (mm) | GPD upper 95% confidence interval (mm) |
|-------|------|-----------------------------|---|---|
| 0.63 | 1 | 570 | 445 | 778 |
| 0.39 | 2 | 657 | 486 | 962 |
| 0.18 | 5 | 776 | 535 | 1252 |
| 0.10 | 10 | 870 | 569 | 1511 |
| 0.05 | 20 | 967 | 601 | 1812 |
| 0.02 | 50 | 1100 | 638 | 2281 |
| 0.01 | 100 | 1204 | 664 | 2700 |
| 0.005 | 200 | 1311 | 688 | 3184 |
| 0.002 | 500 | 1457 | 716 | 3939 |
| 0.001 | 1000 | 1571 | 735 | 4613 |

Extreme sea-level elevations were calculated using the skew-surge joint-probability method (SSJPM) and the POT/GPD method (Figure 2-4, Table 2-4). The SSJPM appears to over predict the magnitude of sea levels having expected AEPs of ≥ 0.1 , i.e., it predicts more frequent occurrence of relatively low-magnitude sea-level peaks. Both methods closely agree for large low-frequency sea-levels with $AEP < 0.1$.

The largest storm-tide elevation in the Helensville area was recorded at 2900 mm AVD-46 on 17 April 1999 (Appendix C), which preceded the sea-level gauge record (largest = 2834 mm on 19 Sep 2005).

On that day a broad and deepening trough was preceded by strong north-westerly flows and followed by colder south-westerlies. A major front occurred within the trough. It brought gale force winds over the North Island, contributing to sea flooding along the west coast. The event caused the highest storm-tide on record since 1926 at Onehunga, being estimated at 2.8–2.9 m AVD–46 (the gauge wasn't operating), and caused by far the largest sea level during the 19-year Anawhata sea-level record (Stephens et al. 2011; Stephens et al. 2013). At both Anawhata and Onehunga it plots as an anomalously large event, on the high side of the estimated extreme sea-level curve. Figure 2-4 shows that this is not the case at Helensville where it lies below the predicted extreme sea-level curves. In Figure 2-4 the return period of the 17 April 1999 event has been estimated based on the assumption that it is probably the largest sea-level in the 89 years since 1926, as at Onehunga. For lower frequency events (AEP < 0.63) the two extreme sea-level curves in Figure 2-4 agree closely and match well to the sea-level peaks from the gauge record, yet seem to over-predict the expected frequency of the 17 April 1999 storm-tide. A probable reason for this is that the 17 April 1999 event began to overtop the stopbanks, which were about 2800 mm AVD-46 in height (Appendix C) – thus the recorded height of the event was limited by the increased water storage volume in the floodplain. Conversely, the extreme sea-level analyses were conducted on measurements of smaller storm-tides that were contained entirely within the stopbanks, and so the extrapolation to high elevations at low AEP assumes that the stopbank heights are not limited, and fully contain the storm-tides.

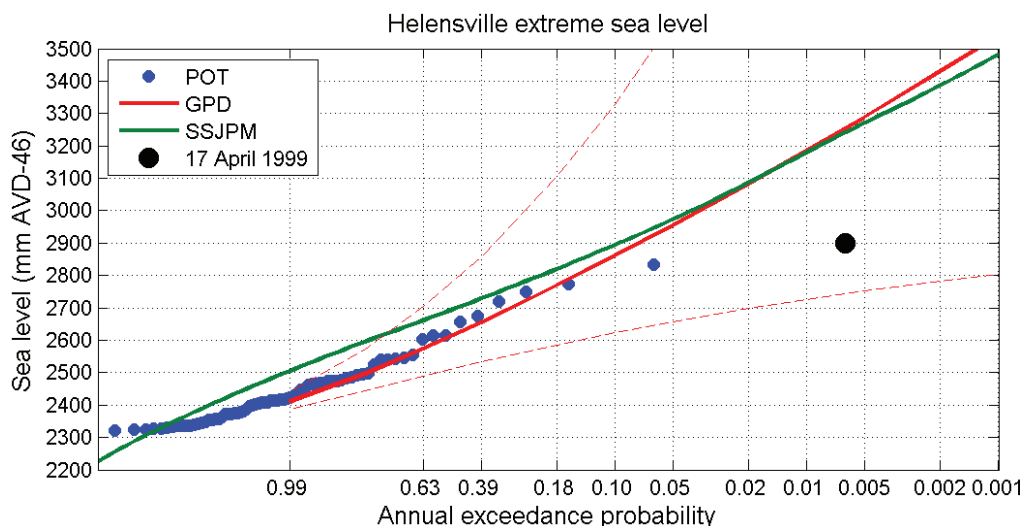


Figure 2-4 : Extreme sea level analysis at Helensville.

POT = sea-level peaks over (2040 mm) threshold, plotted in Gringorten (1963) plotting positions; GPD = generalised Pareto distribution fitted to POT (solid line =maximum likelihood, dashed lines = 95% confidence intervals); SSJPM = skew-surge joint-probability method; 17 April 2009 = measured 2900 mm storm-tide elevation plotted in Gringorten (1963) plotting position, assuming it is the largest event since 1926. Elevations are presented relative to AVD-46 and include a +0.28 m offset for present-day MSL above AVD-46.

Table 2-4: Extreme sea levels at Helensville.

AEP = annual exceedance probability; ARI = average recurrence interval; SSJPM = maximum-likelihood estimate from skew-surge joint-probability method; GPD = generalised Pareto distribution fit to independent peaks over 2040 mm threshold. Elevations are presented relative to AVD-46 and include a +0.28 m offset for present-day MSL above AVD-46.

| AEP | ARI | SSJPM (mm) | GPD max. likelihood (mm) | GPD lower 95% confidence interval (mm) | GPD upper 95% confidence interval (mm) |
|-------|------|---------------|-----------------------------|---|---|
| 0.63 | 1 | 2662 | 2574 | 2490 | 2704 |
| 0.39 | 2 | 2732 | 2656 | 2533 | 2859 |
| 0.18 | 5 | 2822 | 2770 | 2586 | 3106 |
| 0.10 | 10 | 2892 | 2861 | 2623 | 3329 |
| 0.05 | 20 | 2972 | 2955 | 2657 | 3586 |
| 0.02 | 50 | 3082 | 3083 | 2698 | 3989 |
| 0.01 | 100 | 3182 | 3184 | 2727 | 4350 |
| 0.005 | 200 | 3272 | 3288 | 2753 | 4765 |
| 0.002 | 500 | 3382 | 3430 | 2784 | 5415 |
| 0.001 | 1000 | 3482 | 3541 | 2805 | 5995 |

2.3 Coastal-storm inundation modelling in Parakai/Helensville

The next stage was to apply the extreme sea-level results to the hydrodynamic model for Parakai/Helensville.

2.4 Recommended approach for hydrodynamic model validation

The extreme sea-level analysis is only valid if it is assumed that the stopbanks are higher than at present, high enough to contain even very large storm-tides. This because almost all (with the exception of the 1999 event) of the measured sea-level maxima, on which the extreme sea-level analysis is based, were contained by the existing stopbanks. Therefore, the following approach was taken to apply this within the hydrodynamic model:

- Build the hydrodynamic model assuming the stopbanks present are at a crest height of 3750 mm AVD-46 (ensuring that the maximum expected sea level at present-day MSL would be contained to enable model calibration).
- Use the model to find boundary conditions that produce a 1% AEP (3.18 m) storm-tide using the high stopbanks.
- Using the same boundary conditions identified above, simulate inundation in a revised hydrodynamic model that does not include stopbanks (see Auckland Council executive summary).

It can be noted that presently the coastal plain is reliant on constructed stopbanks to prevent episodic inundation. However, the role of stopbanks in future is unclear in regards to their maintenance, upgrade and potential failure, particularly as sea-level rise will greatly increase the risk exposure of such failure, and will eventually cause regular overtopping. For these reasons, stopbanks were removed from the model domain (see Auckland Council executive summary).

2.5 Summary of coastal-storm inundation hydrodynamic modelling

NIWA commissioned DHI to simulate coastal-storm inundation based on the extreme sea-level elevations calculated in Section 2.2. Results from the DHI report (DHI 2016) are summarised in this Section.

DHI built a refined hydrodynamic model grid of the Kaipara Harbour and Kaipara and Kaukapakapa River, which included a representation of the flood-plain model constructed from Auckland Council's 2013 LiDAR topography data (2 m horizontal resolution). Significant obstructions to flood flow in the flood plain (e.g., Parkhurst Road) were sufficiently represented in the model bathymetry.

A varying bed roughness map (Manning number M) was generated for the floodplain based on land use characteristics for the area.

The model was calibrated to the Helensville sea-level gauge, for the significant storm-tide event of 2.83 m AVD-46 at Helensville SL gauge, which occurred in September 2005. A model validation simulation was also undertaken for a storm-tide in June 2012.

The following simulations were used to assess peak flood inundation levels due to storms tide and catchment flooding:

- A 1% AEP storm-tide elevation of 3.18 m AVD-46 at Helensville, without the flood plain included in the model.
- Same as 1 but with + 1 m sea-level rise.
- Same as 1 but with + 2 m sea-level rise.
- As for 1 above but including a large flood from the upstream catchment. This was to confirm the findings of previous work which indicates that normal river flows do not have a significant effect on sea level inundation within the southern Kaipara Harbour (DHI, 2006).

DHI created coastal-storm inundation maps from these scenarios, which are presented in their report and were delivered to Auckland Council in GIS format.

A sensitivity analysis of the hydrodynamic model to bed roughness, suggested that the inundation modelling is probably accurate to ± 0.1 m over most of the flood plain. The sea-level rise scenario results will be less sensitive to bed roughness because the water is deeper over the existing flood plain in those simulations.

Comparison of the storm-tide only simulation with the simulation including the large river flood, showed an increase in water levels for the Parakai/Helensville floodplain of up to about 0.2 m. There were higher increases in water level upstream. The joint-probability of coincident high storm-tides and freshwater flooding from the catchment was not calculated. The modelled combination of a large flood and a large storm-tide is possible, but has less than 1% AEP probability of occurrence because the two will have only limited dependence. Inclusion of the river flow makes a noticeable difference to coastal-storm inundation elevations at present-day MSL, but its effect is small compared to future SLR scenarios.

Statistics of the area of inundated land are presented in Table 2-5 and plotted in Figure 2-8. The areas included in the statistics did not include the river nor areas of active estuary presently covered by mangrove. The statistics were calculated for simulations at present-day MSL (Figure 2-5), +1 m SLR,

and +2 m SLR. In the absence of stopbanks, about 19 km² of land is predicted to be inundated by ≥ 0.01 m during a 1% AEP storm-tide at present-day MSL, with about 15 km² inundated by at least 0.25 m.

The model results indicate that SLR has the potential to make a substantial difference to the area of land that is inundated, particularly to the area of land that becomes heavily inundated. For example, the area of land inundated by ≥ 0.01 m is predicted to double with a 1 m SLR relative to present day; the area of land inundated by ≥ 1.5 m is predicted to be 11 times greater with a 1 m SLR, as most of the valley would fill with water.

Table 2-5 : Depth versus area of inundation over the Parakai flood plain as simulated in this (2016) project.

Inundation areas are given to the nearest square kilometre. Existing mangrove areas were excluded from the analysis.

| Depth of inundation | Area of inundation (km ²) at present-day MSL | Area of inundation (km ²) at present-day MSL + 1 m SLR | Area of inundation (km ²) at present-day MSL + 2 m SLR |
|---------------------|--|--|--|
| ≥ 0.01 m | 19 | 33 | 40 |
| ≥ 0.25 m | 15 | 30 | 37 |
| ≥ 0.50 m | 11 | 27 | 34 |
| ≥ 1.00 m | 4 | 21 | 31 |
| ≥ 1.50 m | 1 | 11 | 28 |

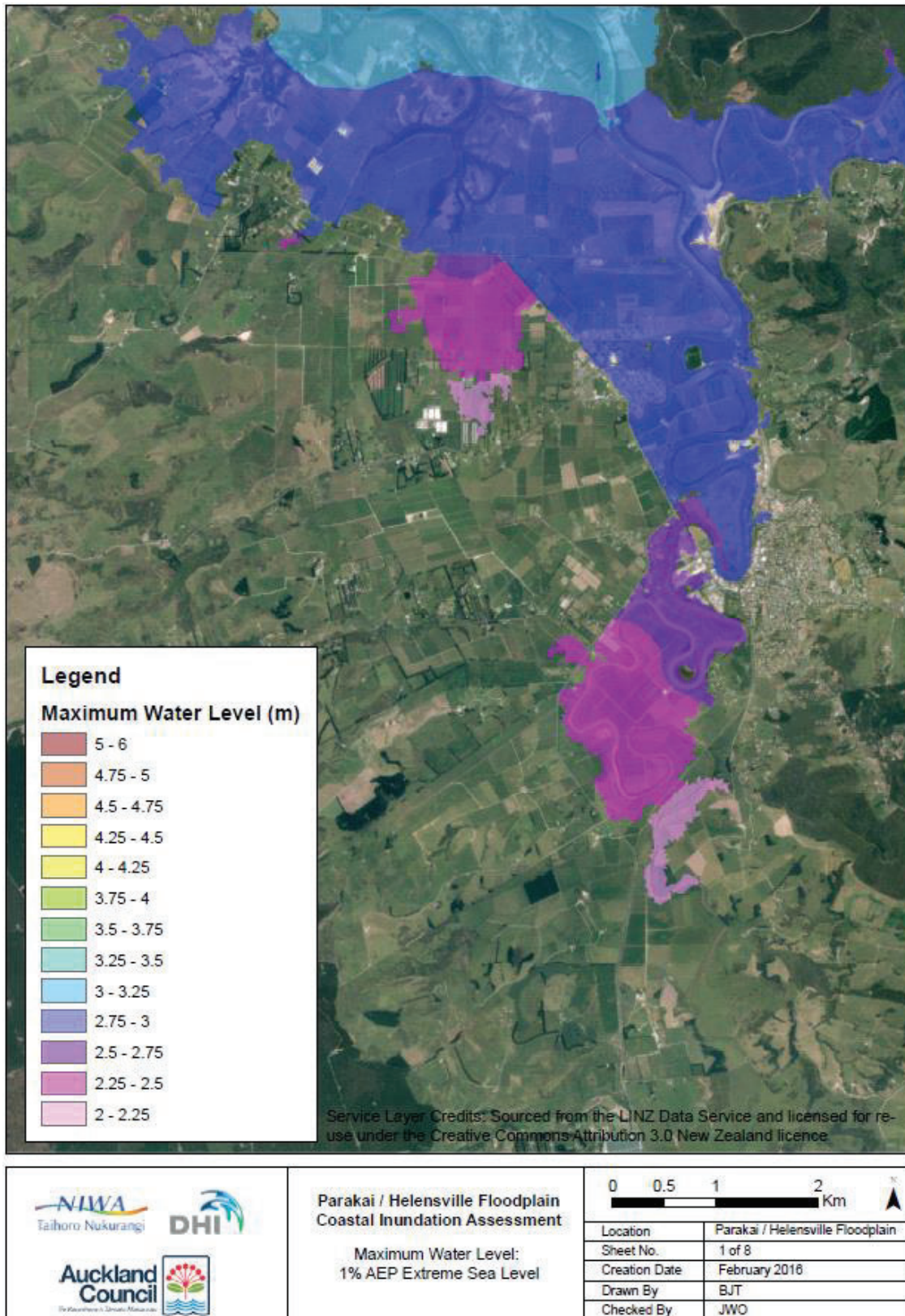


Figure 2-5: 1% AEP coastal-storm inundation elevations at present-day MSL from this project (DHI, 2016).

2.6 Comparison between the present and the 2013 coastal-storm inundation mapping

Figure 2-5 shows the 1% AEP coastal-storm inundation elevations at present-day MSL predicted in this project (reproduced from DHI, 2016).

Figure 2-6 shows the same scenario as mapped by NIWA in 2013 (Stephens et al. 2013) using the static-inundation mapping method. The same colour scale was used for both Figure 2-5 and Figure 2-6.

Figure 2-7 shows the difference in the 1% AEP coastal-storm inundation elevations mapped by NIWA in 2013 (Stephens et al. 2013) and simulated in this project. Both methods gave similar elevations at the confluence of the Kaipara River and the Harbour. The hydrodynamic model predicted considerable frictional attenuation, causing the storm-tide elevation to drop inland (Figure 2-5). Conversely, the static GIS-mapping technique used in 2013 (Figure 2-6) did not simulate the dynamics of frictional attenuation of the storm-tide wave over the flood plain. Instead, it derived an assumed water level by interpolation from nearby coastal locations. For Parakai, this interpolation resulted in a slight landward-increasing water-level surface (Figure 2-6). As a result, the difference in predicted inundation elevation between the two studies increases inland. Figure 2-7 shows the degree to which the static mapping technique gave conservatively high water levels, being mostly < 0.5 m but increases to approximately 2 m further inland.

Comparison of Figure 2-5 and Figure 2-6 shows that greater areas of inundation were predicted in 2013 using the static mapping technique, compared to this project (2016) when using the dynamic mapping technique. Coastal-storm inundation areas calculated during the 2013 study are shown in Table 2-6, for comparison with those Table 2-5. Table 2-7 shows the difference in coastal-storm inundation area between the 2013 and 2016 projects, and the information in the tables is plotted in Figure 2-8.

Comparing the total area of inundation (of ≥ 0.01 m depth), the dynamic-mapping technique used in this project predicted 12 km² (60%) less inundation than the static-mapping undertaken in 2013 (Stephens et al. 2013), at present-day MSL. The difference in total inundation area was less for the future sea-level rise scenarios, being 3 km² (9%) less after +1 m SLR, and the same after +2 m SLR. Large sea-level rise will inundate the present flood plain and fill the basin in which the Parakai/Helensville region is located. Dynamic frictional effects that hold back the flood wave at present-day MSL (when the water is shallow) will be reduced after SLR (when the water is deep – assuming no change in the flood-plain topography).

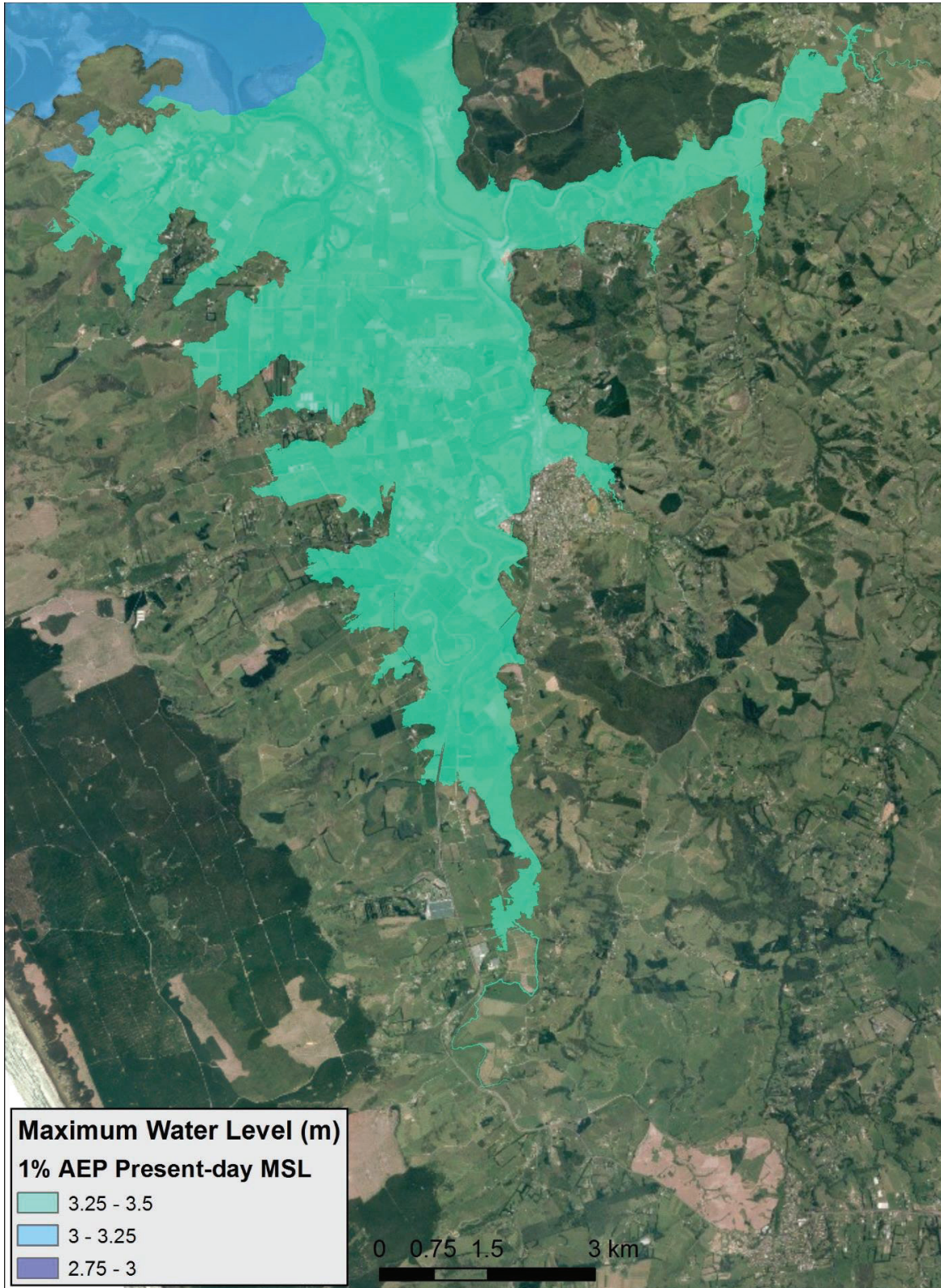


Figure 2-6: 1% AEP coastal-storm inundation elevations at present-day MSL mapped by NIWA in 2013.

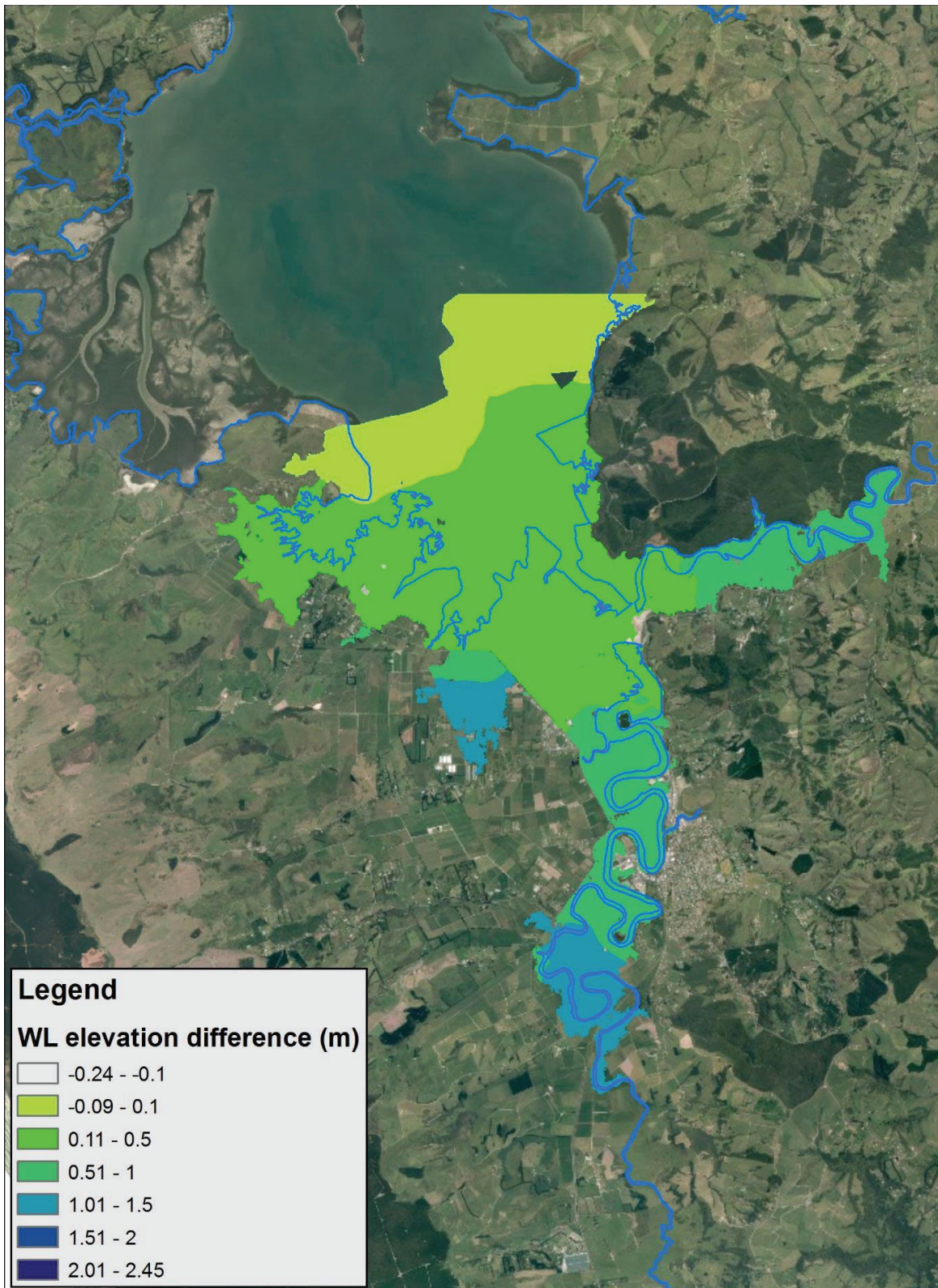


Figure 2-7 : Difference (m) between coastal-storm inundation elevations predicted in this study from those by NIWA in 2013, during a 1% AEP storm-tide at present day MSL.

Differences were calculated as NIWA (2013) minus the results of this (2016) study, and are shown only for areas of overlap between the two studies.

Table 2-6: Depth versus area of inundation over the Parakai flood plain, as simulated in the 2013 project.

Inundation areas are given to the nearest square kilometre. Existing mangrove areas were excluded from the analysis.

| Depth of inundation | Area of inundation (km ²) at present-day MSL | Area of inundation (km ²) at present-day MSL + 1 m SLR | Area of inundation (km ²) at present-day MSL + 2 m SLR |
|---------------------|--|--|--|
| ≥ 0.01 m | 31 | 36 | 40 |
| ≥ 0.25 m | 29 | 35 | 39 |
| ≥ 0.50 m | 26 | 34 | 38 |
| ≥ 1.00 m | 17 | 31 | 36 |
| ≥ 1.50 m | 5 | 26 | 34 |

Table 2-7: Difference in the estimated area of inundation over the Parakai flood plain, between the 2013 and 2016 projects.

Inundation areas are given to the nearest square kilometre.

| Depth of inundation | Difference in area of inundation (km ²) at present-day MSL | Difference in area of inundation (km ²) at present-day MSL + 1 m SLR | Difference in area of inundation (km ²) at present-day MSL + 2 m SLR |
|---------------------|--|--|--|
| ≥ 0.01 m | 12 | 3 | 0 |
| ≥ 0.25 m | 13 | 5 | 2 |
| ≥ 0.50 m | 15 | 6 | 4 |
| ≥ 1.00 m | 12 | 10 | 5 |
| ≥ 1.50 m | 3 | 15 | 6 |

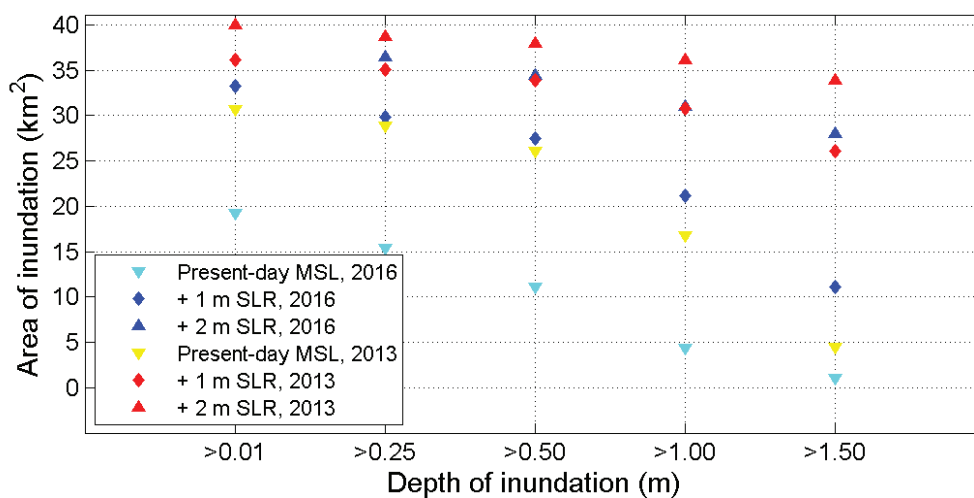


Figure 2-8: Depth versus area of inundation over the Parakai flood plain.

Existing mangrove areas were excluded from the analysis. 2016 = this project; 2013 = Stephens et al. (2013) project.

3 Coastal-storm inundation in east-coast estuaries

In March 2015, NIWA revised the coastal-storm inundation elevations for small east-coast estuaries in the Auckland region (Stephens 2015). As part of this project we re-mapped coastal-storm inundation zones for these areas based on the revised elevations. The revised maps have been supplied to Auckland Council in GIS format. This section reproduces relevant content of NIWA's letter of revision dated 6 March 2015 (Stephens 2015).

The letter addressed coastal-storm inundation resulting from storm-tide, and from storm-tide plus wave setup, as calculated by Stephens et al. (2013) for the small estuaries along the east coast of the Auckland region. When making these calculations, we assumed that storm-tide plus wave setup elevations at the estuary entrances would propagate throughout the estuary. This is a conservative assumption, since the wave setup component that is generated on the open coast is unlikely to propagate far inside the entrance of an estuary (Santoso et al. 1999; Tanaka et al. 2008).

NIWA has now revised the coastal-storm inundation elevations for small east-coast estuaries. This was done by first identifying the additional wave set up component relative to storm-tide alone computed by Stephens et al. (2013) at the entrance to several of the small east-coast estuaries (Table 3-1). This inferred wave setup, which had been included in coastal-storm inundation elevations within each estuary (Stephens et al. 2013), was removed as shown in Table 3-2.

The calculations in the tables represent coastal-storm inundation events with a one percent annual exceedance probability (1% AEP), or equivalently, a one-hundred-year average recurrence interval (100-year ARI). The tabulated elevations include +0.15 m present-day mean sea level relative to AVD-46.

NIWA recommended that the revised elevations, described in Table 3-2 as *1% AEP maximum storm-tide plus wave setup elevations, with inferred wave setup component subtracted*, be adopted within the Proposed Auckland Unitary Plan (Stephens 2015).

As part of this project we re-mapped additional coastal-storm inundation scenarios for the small east-coast estuaries and supplied Auckland Council with GIS polygons for the following scenarios:

- 1% AEP at present-day MSL
- 2% AEP at present-day MSL
- 2% AEP + 1 m SLR
- 2% AEP + 2 m SLR
- 5% AEP at present-day MSL
- 18% AEP at present-day MSL.

Table 3-1: Storm-tide and maximum storm-tide plus wave setup elevations with 1% annual exceedance probability (1% AEP), and a wave setup component inferred from their difference, for locations offshore from small east-coast estuaries.

Elevations include +0.15 m present-day mean sea level relative to AVD-4.

| Estuary | 1% AEP storm-tide (Table 4-1, Stephens et al. 2013) | 1% AEP maximum storm-tide plus wave setup elevations (Table 4-3, Stephens et al. 2013) | Maximum storm-tide plus wave setup minus storm-tide (inferred wave setup) |
|---------------------------|---|--|---|
| Mangawhai | 1.76 | 2.54 | 0.78 |
| Whangateau | 1.85 | 2.46 | 0.61 |
| Matakana | 2.01 | 2.11 | 0.1 |
| Mahurangi, Puhoi, Waiwera | 1.95 | 2.5 | 0.55 |
| Orewa | 1.97 | 2.5 | 0.53 |
| Weiti, Okura | 2.01 | 2.52 | 0.51 |
| Tamaki | 2.18 | 2.28 | 0.1 |
| Whitford, Waikopua | 2.18 | 2.44 | 0.26 |
| Wairoa R. | 2.23 | 2.42 | 0.19 |

Table 3-2 : Maximum storm-tide plus wave setup elevations with 1% AEP at locations inside small east-coast estuaries (Table 4-4, Stephens et al. 2013), and with an inferred wave setup (from Table 3-1 above) subtracted.

Elevations include +0.15 m present-day mean sea level relative to AVD-46.

| Estuary | Easting (NZTM) | Northing (NZTM) | 1% AEP maximum storm-tide plus wave setup elevations (Table 4-4, Stephens et al. 2013) | 1% AEP maximum storm-tide plus wave setup elevations, with inferred wave setup component subtracted |
|---------------------------|----------------|-----------------|--|---|
| Mangawhai Harbour | 1742349 | 6001359 | 2.59 | 1.81 |
| Whangateau Harbour | 1759163 | 5974912 | 2.52 | 1.91 |
| Whangateau Harbour | 1758250 | 5978697 | 2.49 | 1.88 |
| Omaha R. (Whangateau Hbr) | 1756538 | 5977574 | 2.51 | 1.9 |
| Matakana River estuary | 1753842 | 5971395 | 2.14 | 2.04 |
| Matakana River estuary | 1754603 | 5971927 | 2.13 | 2.03 |
| Matakana River estuary | 1754432 | 5974837 | 2.15 | 2.05 |
| Matakana River estuary | 1755060 | 5972536 | 2.13 | 2.03 |
| Matakana River estuary | 1755269 | 5974476 | 2.15 | 2.05 |

| Estuary | Easting (NZTM) | Northing (NZTM) | 1% AEP maximum storm-tide plus wave setup elevations (Table 4-4, Stephens et al. 2013) | 1% AEP maximum storm-tide plus wave setup elevations, with inferred wave setup component subtracted |
|----------------------------|----------------|-----------------|--|---|
| Pukapuka Inlet (Mahurangi) | 1750849 | 5961126 | 2.56 | 2.01 |
| Mahurangi Harbour | 1753626 | 5960575 | 2.54 | 1.99 |
| Mahurangi Harbour | 1751686 | 5968031 | 2.6 | 2.05 |
| Mahurangi Harbour | 1754615 | 5960537 | 2.53 | 1.98 |
| Te Kapa R. (Mahurangi) | 1756099 | 5963200 | 2.56 | 2.01 |
| Mahurangi Harbour | 1753210 | 5958010 | 2.52 | 1.97 |
| Puhoi River estuary | 1750338 | 5956222 | 2.53 | 1.98 |
| Waiwera River estuary | 1750889 | 5954757 | 2.53 | 1.98 |
| Orewa River estuary | 1749727 | 5948635 | 2.53 | 2 |
| Weiti River | 1751800 | 5946524 | 2.57 | 2.06 |
| Karepiro Bay | 1754558 | 5942016 | 2.53 | 2.02 |
| Okura River | 1752751 | 5939753 | 2.55 | 2.04 |
| Tamaki Estuary | 1765514 | 5913666 | 2.35 | 2.25 |
| Tamaki Estuary | 1766408 | 5911555 | 2.42 | 2.32 |
| Pakuranga Creek (Tamaki) | 1769431 | 5912063 | 2.43 | 2.33 |
| Tamaki Estuary | 1764589 | 5907948 | 2.46 | 2.36 |
| Mangamangaroa Creek | 1772868 | 5912475 | 2.46 | 2.2 |
| Turanga Creek | 1775337 | 5910030 | 2.47 | 2.21 |
| Waikopua Creek | 1777927 | 5912838 | 2.46 | 2.2 |
| Wairoa River estuary | 1784026 | 5907369 | 2.46 | 2.27 |
| Wairoa River estuary | 1784970 | 5907950 | 2.45 | 2.26 |
| Wairoa River estuary | 1785600 | 5907417 | 2.46 | 2.27 |

3.1 Conclusions

An extreme sea-level analysis using the Helensville sea-level record showed that if the stopbanks were sufficiently high to contain even the highest expected storm-tides, then there is a 1% chance per year (0.01 AEP) that sea-level would reach 3.18 m AVD-46 inside the stopbanks. In reality the stopbanks

are only approximately 2.8 m high. The extreme sea-level analysis suggests we can expect 2.8 m to be reached every 5–10 years (on average, 10–18% AEP) at present-day mean sea level. This frequency will increase as the sea level continues to rise, which will reduce the effectiveness of the existing stopbanks for flood protection.

A calibrated and validated hydrodynamic model was used to simulate coastal-storm inundation over the flood plain, for a 1% AEP storm-tide at present-day MSL, plus a 1 m and a 2 m SLR. We now have high confidence in the simulated coastal-storm inundation elevations in the Parakai/Helensville region – we believe that the inundation modelling is accurate to ± 0.1 m over most of the flood plain.

In the simulations, approximately 19 km² of land was predicted to be inundated by ≥ 0.01 m during a 1% AEP storm-tide at present-day MSL, and about 15 km² was predicted to be inundated by at least 0.25 m. With SLR, the area of land that becomes heavily inundated was found to increase.

The area of inundation predicted in this project was 60% less than that predicted in the 2013 project (Stephens et al. 2013) for the present-day MSL scenario. This difference is due to the difference between the dynamic-mapping method used here and the static-mapping method used in 2013. However, for the future SLR scenarios, the results were less sensitive to the mapping method used, being 9% less for the +1 m SLR scenario, and the same for the +2 m SLR scenario. Large sea-level rises will inundate the flood plain and fill the basin in which the Parakai/Helensville region is located. Dynamic frictional effects that hold back the flood wave at present-day MSL when the water is relatively shallow, will be reduced after SLR when the water is relatively deep (assuming no change in the flood-plain topography).

The coastal-storm inundation elevations calculated in this study were compared with the 2013 NIWA study. Both methods gave similar elevations at the confluence of the Kaipara River and the Harbour. The static GIS-mapping technique used in 2013 did not simulate the dynamics of frictional attenuation of the storm-tide wave over the flood plain, showing a slight landward-increasing water-level surface. Conversely, the hydrodynamic model used in this study included frictional attenuation, and predicted the storm-tide elevation to drop inland. As a result, the difference in predicted inundation elevations between the two studies increases inland. This study predicted water levels that were up to 0.5 m lower than the 2013 study over most of the lower flood plain, and up to about 2 m lower further inland.

The coincidence of a large (2% AEP) river flood with a 1% AEP storm-tide would increase water levels by about 0.2 m over the Parakai/Helensville floodplain, but with higher increases upstream. The joint-probability of coincident high storm-tides and freshwater flooding from the catchment was not calculated. The modelled combination of a large flood and a large storm-tide is possible, but has less than 1% AEP probability of occurrence because the two will have only limited dependence. Inclusion of the river flow makes a noticeable difference to coastal-storm inundation elevations at present-day MSL, but its effect is small compared to future SLR scenarios.

In March 2015, NIWA revised the coastal-storm inundation elevations for small east-coast estuaries in the Auckland region. As part of this project we re-mapped coastal-storm inundation zones for these areas based on the revised elevations. The revised maps were supplied to Auckland Council in GIS format. Although we re-mapped the small east-coast estuaries to remove a wave setup allowance, confidence in these areas remains relatively low for the reasons described below.

4 Acknowledgements

Thanks to Vic Freestone whose careful quality analysis made of the Helensville tide gauge record enabled a robust extreme sea-level analysis.

5 Glossary of abbreviations and terms

| | |
|---------------------------------------|---|
| Annual exceedance probability (AEP) | The probability of a given (usually high) sea level being equalled or exceeded in elevation, in any calendar year. AEP can be specified as a fraction of 1 (e.g., 0.01) or a percentage (e.g., 1%). |
| AVD-46 | Auckland Vertical Datum-1946 is the region-wide vertical datum used by Auckland Council. |
| Average recurrence interval (ARI) | The average time interval (averaged over a long time period and many “events”) that is expected to elapse between recurrences of an infrequent event of a given large magnitude (or larger). A large infrequent event would be expected to be equalled or exceeded in elevation, once, on average, every “ARI” years. |
| generalised Pareto distribution (GPD) | Extreme-value model suitable for use with peaks-over-threshold data. |
| MHWS | Mean high-water springs. The high tide height associated with higher than normal high tides that result from the beat of various tidal harmonic constituents. Mean high water springs occur every 2 weeks approximately. MHWS can be defined in various ways, and the MHWS elevation varies according to definition. |
| MSL | Mean sea level – the mean level of the sea relative to a vertical datum over a defined epoch, usually of several years. |
| peaks-over-threshold (POT) | Independent (separated in time by at least 3 days) sea level peaks above a defined height threshold. |
| Skew surge | Skew surge refers to the absolute difference between the maximum recorded sea-level during a tidal cycle and the predicted maximum astronomical tidal level for that cycle, irrespective of differences in timing between these. |
| Storm surge | The temporary rise in sea level due to storm meteorological effects. Low-atmospheric pressure causes the sea-level to rise, and wind stress on the ocean surface pushes water down-wind and to the left up against any adjacent coast. |
| Storm-tide | Storm-tide is defined as the sea-level peak during a storm event, resulting from a combination of MSL + SLA + tide + storm surge. In New Zealand this is generally reached around high tide. |

6 References

- Batstone, C., Lawless, M., Tawn, J., Horsburgh, K., Blackman, D., McMillan, A., Worth, D., Laeger, S., Hunt, T. (2013) A UK best-practice approach for extreme sea-level analysis along complex topographic coastlines. *Ocean Engineering*, 71: 28-39.
- Coles, S. (2001) *An introduction to statistical modeling of extreme values*. Springer. London; New York.
- DHI (2016) Parakai/Helensville Coastal Flood Inundation. Numerical Modelling. Client Report to NIWA 44800852.
- Foreman, M.G.G., Cherniawsky, J.Y., Ballantyne, V.A. (2009) *Versatile Harmonic Tidal Analysis: Improvements and Applications*. *Journal of Atmospheric and Oceanic Technology*, 26: 806-817.
- Goring, D.G., Stephens, S.A., Bell, R.G., Pearson, C.P. (2011) *Estimation of Extreme Sea Levels in a Tide-Dominated Environment Using Short Data Records*. *Journal of Waterway Port Coastal and Ocean Engineering-Asce*, 137: 150-159.
- Gringorten, I.I. (1963) *A plotting rule for extreme probability paper*. *Journal of Geophysical Research*, 68: 813-814.
- MfE (2008) *Coastal Hazards and Climate Change: A Guidance Manual for Local Government in New Zealand*. 2nd edition. Revised by Ramsay, D. and Bell, R. (NIWA). Ministry for the Environment. Wellington.
- Santoso, E., Hanslow, D., Nielsen, P., Hibbert, K. (1999) *Wave setup and other tidal anomalies in coastal rivers*.
- Senior, A., Tuckey, B. (2009) *Helensville wastewater treatment plant dilution modelling*. DHI Water and Environment Ltd report to Rodney District Council, April 2009.
- Stephens, S.A. (2015) *Revision of coastal-storm inundation elevations for small east-coast estuaries in the Auckland region*. Letter to Auckland Council 6 March 2015. Letter ARC15201.
- Stephens, S.A., Bell, R.G. (2015) *Planning for coastal-storm inundation and sea-level rise*. Peer-reviewed paper and presented at the Australasian Coasts & Ports Conference 2015, Auckland, New Zealand, 15 - 18 September 2015.
- Stephens, S.A., Reeve, G., Goodhue, N. (2011) *Coastal storm-tide levels in the Auckland Region. Phase 1: Rationalising and updating previous studies*. NIWA. Client Report to Auckland Council HAM2011-102.
- Stephens, S.A., Wadhwa, S., Gorman, R., Goodhue, N., Pritchard, M., Ovenden, R., Reeve, G. (2013) *Coastal inundation by storm-tides and waves in the Auckland Region*. NIWA Client Report to Auckland Council HAM2013-059: 138.

Tanaka, H., Nguyen, X.-T., Nagabayashi, H. (2008) *Wave setup at different river entrance morphologies*. Proceedings of 31st International Conference on Coastal Engineering, ASCE: 975-985.

Tawn, J.A., Vassie, J.M. (1989) *Extreme sea-levels: the joint probabilities method revisited and revised*. Proceedings of the Institute of Civil Engineering, Part 2: 429-442

Tuckey, B. (2014) *Rough order assessment of inclusion of floodplain storage volumes on predicting extreme water levels at Parakai*. DHI Water and Environment Ltd letter report to Ken Tomkins, Auckland Council, 10 December 2014.

van Kalken, T. (2009) *Kaipara - Kumeu attachment management plan. Hydraulic modelling. Part 1 - Model build, calibration and flood mapping*. DHI Report to Rodney District Council, December 2009.

Wo, Y.G.K., van Kalken, T. (2006) *Determination of water levels in Kaipara Harbour. Kaipara Harbour hydrodynamic modelling*. DHI Water and Environment Ltd report to Rodney District Council, August 2006.

Appendices

Appendix A: Vic Freestone's Helensville tide gauge quality analysis

This Appendix contains Vic Freestone's report: "Auckland Council Helensville Tide Gauge – Kaipara River (formerly RDC site) Records May 2005 to September 2014" report, supplied to NIWA on 28 September 2015.

Introduction

A tidal recording system was established on 31 May 2005 at Winstone's Wharf located on the north side of Helensville Township. The main objective at that time was to obtain a continuous record of water levels with particular interest in the peak levels and upper part of the tidal cycle. From the beginning it was accepted that a record of the full tidal cycle would only be obtained for modest tidal events and that the lower range would not be recorded for those tidal cycles with a greater range.

The main purpose of reporting at this time is to present an updated summary of tidal 'peaks and troughs' in terms of both chart and LINZ datums, together with the differences in water level and time between these maximum and minimum levels. My involvement with recording at this site ended on 3 September 2014 with the removal of the recording equipment as requested by Watercare.

Installation and Equipment

The recording system was comprised of a float/counterweight sensor, connected directly to the drive pulley of a shaft encoder, which also incorporates the electronic datalogger. This unit is a NIWA 'Hydrologger' and was installed directly above the stilling well.

A sheet metal housing is attached to the stilling well and both of these were hot dipped galvanised. The internal diameter of the stilling well is 560 mm and the overall height of the well itself is 6 metres. The 'intake' to the well is by way of series of 15 mm diameter holes drilled at 200 mm centres, on both sides, up to 1 metre above the bottom of the well. A staff gauge was attached directly to the steel well and is made of a tanalised timber backing with a series of 1 metre long graduated (1cm), plastic plates attached. As a result of marine growth on the staff gauge external water level readings were subsequently taken from the top of the staff gauge down to water level using a tape with weight attached.

In view of water levels falling below the 'bottom' of the stilling well it was decided that the invert of the well would represent the 1 metre mark in terms of the staff gauge and EPB, and in turn the datum to which the datalogger has been set.

Recording - Time Interval and Frequency of Site Visits

The recording of water levels at this site has been at fixed time intervals. Initially recording was set at 5 minute intervals before changing to 1 minute. There was a short period in 2009 when recording was set at 2 minute intervals, before being set back to 1 minute. The recording interval was again changed to 2 minutes in August 2011 to permit servicing once every six weeks approximately. The recording interval and the period to which it relates are presented below:

- 5 minute intervals 31/5/2005 – 1/8/2005
- 1 minute intervals 1/8/2005 – 26/8/2009

- 2 minute intervals 26/8/2009 – 19/10/2009
- 1 minute intervals 19/10/2009 – 31/8/2011
- 2 minute intervals 31/8/2011 – 3/9/2014.

From commencement of recording on 31 May 2005 up to March 2006 servicing and downloading of data was carried out at approximately fortnightly intervals. From March 2006 to August 2011 servicing was predominately at monthly intervals, after which the frequency of servicing was changed to be approximately every 6 weeks.

Recording - Time Accuracy

The accuracy to which 'time' is recorded for all logged water level readings has been checked by taking comparative readings of actual and logger time. These checks are made in the 'scheme test mode' at the beginning and end of each 'record period'. The checks are not made at the first and last logged values, but a few minutes after logging has commenced and a few minutes before logging ends for each record period.

The comparison of actual and logger times has been tabled in Excel format for all record periods to date, and is attached to the covering email, together with this report. The 'time keeping' by the datalogger to date has been very accurate. At the start of each record period the difference between actual and logger time is minimal, and this is mostly within 5 seconds, and only on 3 occasions is this greater than 10 seconds, with the maximum difference being 25 seconds. On occasions where the difference is more than a few seconds it probably relates to site inspections when the 'laptop' time was not reset.

The time difference between actual and datalogger time at the end of each record period is more relevant. The difference in time at the end of the record period is mostly less than 30 seconds, and only on 10 occasions is it more than this. The greatest time discrepancy is 53 seconds. The site inspections where the time difference at the end of the record is more than 20 – 30 seconds are probably a reflection of time errors associated with the laptop and or 'watch' accuracy.

The actual and logged times at the beginning and end of each record period have been tabled on a standard form during routine processing of records. Although this has not been reproduced at this time the start and end 'dates' are included in the Excel summaries attached to the covering email, along with this report. The 'time checks' discussed above are taken just a short time after starting and before ending respectively.

Quality of Records

Since records began in May 2005 the continuity of records has been good with a short period of missing data from the 4th to 5th December 2007. There are 3 other very short periods of missing record in 2012, when the water level sensing equipment was removed during stilling well desilting operations. These 'gaps' in the record are summarised below:

- 4/12/2007 (0721) to 5/12/2007 (1051), 1.15 days
- 3/4/2012 (1242) to 3/4/2012 (1604), 3.37 hours
- 31/5/2012 (0938) to 31/5/2012 (1510), 5.53 hours
- 11/7/2012 (1014) to 11/7/2012 (1214), 2 hours.

The Excel file which lists the maximum and minimum water levels for each tidal cycle does not identify the above periods of missing record in the record itself. Maximum and minimum water levels immediately before and after periods of missing record will be erroneous where such extremes occur during the gap in the record.

The accuracy and reliability of recorded water levels is generally good but there are a number of occasions when there is a significant difference between these and manual check readings.

Not long after the site was established there were two 'record periods' between 10 June to 4 July 2005 when the datalogger malfunctioned and erroneous values were recorded. However, in both instances it was possible to edit and correct the record to an acceptable level. The problem related to the Hydrologger which was replaced.

A more significant problem has been the disengagement of the float cable on the encoder pulley, where the beaded cable has come out of the recessed holes. This is reflected in a discrepancy between recorded water levels and EPB check readings at the time of downloading data. There are four record periods when this difference is greater than 100 mm (115 to 136), but most of the time when this occurs the difference is less than 40 mm. This only relates to differences observed when downloading data, and it is not known if this was greater or less throughout the record period, and when in fact the cable was dislodged.

No corrections have been made at this stage in relation to the problem described above, but data over these periods should be used with caution. With intensive editing it may be possible to identify the time when the discrepancy occurred and make appropriate corrections.

There have also been a number of site visits when the river level was very low and below the level of silt surrounding the stilling well and/or below the level of silt inside the stilling well. At such times, one or a number of SG, EPB, and Encoder readings, together with recorded values, may be invalid. Although, at such times there may be significant differences between readings, as the actual water level is lower this has no real relevance, other than being at the lower end of meaningful recordings. As no adjustments were made under such conditions, reliable recording would have continued when the tide came in and water levels increased. The minimum recorded values will only be the true or absolute minimums for modest tidal cycles where the minimum water level is above the silt level within the well.

A summary, in Excel format, of the 'record periods' between downloading, is attached to the covering email, along with this report. This shows the differences between recorded water levels and staff gauge, EPB and Encoder readings. Periods where anomalies have occurred have been highlighted in different colours to identify the various nature of the problem as described above, and show the time and frequency when these took place.

Extraction of Tidal Peaks and Troughs

The maximum and minimum water levels for each tidal cycle have not been extracted from the records since 2010. The main purpose of the current work has been to update this information so that it represents the period from the time records commenced in May 2005 up to September 2014, when Watercare took over water level observations at this site. The results have been expressed in terms of both Chart and LINZ datums. In addition, the differences in both 'water level and time' between these peaks and troughs have also been obtained. The listing and presentation of this information for the

period 31 May 2005 to 3 September 2014 has been compiled in Excel and is also attached to the covering email along with this report.

Care should be taken when evaluating and using this information, taking particular note of the comments made in Section 5 above, and the identification of 'time and water level' discrepancies as shown in the Excel summaries.

Conclusion and Recommendations

The Tidal records at Helensville, as discussed above, represent over 9 years of data, with excellent continuity of record to date, and where the quality of data is very good most of the time.

However, there are several periods when there is a moderate to significant difference between the recorded data and manual check readings, when compared at the end of each record period. As discussed in Section 5 above the reason for most of these differences relate to the beaded float cable not being correctly positioned in the recesses on the Encoder pulley.

There are a number of possible explanations why the float cable comes out of position, but the most plausible causes are: the sand barge hitting the wharf too hard when tying up, the float sticking in the silt inside the stilling well at low tides, and the float cable sticking on the guide pulley. Although a heavier counterweight was fitted, and this may have helped, it did not solve the problem. Also, at a later date a dual guide pulley system was mounted on the underside of the recorder house floor in order to steepen the angle at which the beaded cable 'leaves' the encoder pulley, but again this did not solve the problem.

From the records it can be seen that where the tides are 'average' the entire tidal cycle will be recorded. Where the tidal range is more extreme the upper part of the 'cycle' will be reliable, but where the 'troughs' go below the invert level of the stilling well or below the silt level in the well, both the record itself and any extracted minimum water levels will be unreliable.

Appendix B: Helensville tide-gauge datum

This information was supplied to Vic Freestone from Ken Tomkins in July 2005.

The levels of the wharf pins at Winstone's Wharf are as follows:

- Pin 1 (nearest to recorder) LINZ RL 3.098m
- Pin 2 (nearest to shore) LINZ RL 3.102m

LINZ levels are the old Lands and survey levels and are approx. MSL at Auckland in 1946.

The Chart Datum Levels from Port Taranaki and Onehunga may be converted to LINZ Datum as follows:

- Chart Datum Levels Port Taranaki = LINZ level + 1.715m.
- Chart Datum Levels Onehunga = LINZ level + 2.201m.

Examples

Reading of LINZ level of +2.100m at Helensville tide-gauge is equates to a Chart Level of 4.301m at Onehunga.

Reading of LINZ level of +2.100m at Helensville tide-gauge is equates to a Chart Level of 3.815m at Port Taranaki.

Ken arranged for the levels to be placed on the BM pins that Vic had previously installed on Winstone's Wharf. From Vic's levelling in relation to these BM pins and setting of the EPB/Datalogger he was able to derive the conversion from Chart to LINZ datum. Vic noted that "it would seem the datum used was AVD 1946".

The 17 April 1999 storm-tide



On 17th April 1999 the owner of 47B Parakai Avenue reported that the high water level was 2.9 metres (established by RDC survey) and flooded his property, several others and parts of the road. In response to this event, an internal RDC memo commented:

The events of 17 April 1999 indicate that a combination of low atmospheric pressure and strong on-shore winds can lead to an increase in tide level 700mm above the predicted level. In this case the high tide level was assessed to be 2.80m above LINZ Datum, which gives no freeboard whatsoever for the design crest level of 2.80m. Unfortunately no reliable records are available to establish the frequency of such events.

Prior to the stopbank upgrading in 1996, stopbank levels adjacent to Parakai Avenue were only in the order of RL 2.30m over a length of several hundred metres. The relatively minor flooding experienced on 17 April 1999 shows that the upgraded stopbanks at of Parakai Avenue provided a considerable degree of protection. However it must be stated that the entire length of stopbank was on the verge of overtopping when the tide finally turned.

In August 2004, RDC forward planning staff recommended a minimum floor level for new development of 3.4 metres.

The latest results of harbour and river modeling work by DHI Water Environments Ltd in 2006 have lead RDC to propose an H2 hazard minimum floor level of 3.9 metres, which includes a 500m freeboard.

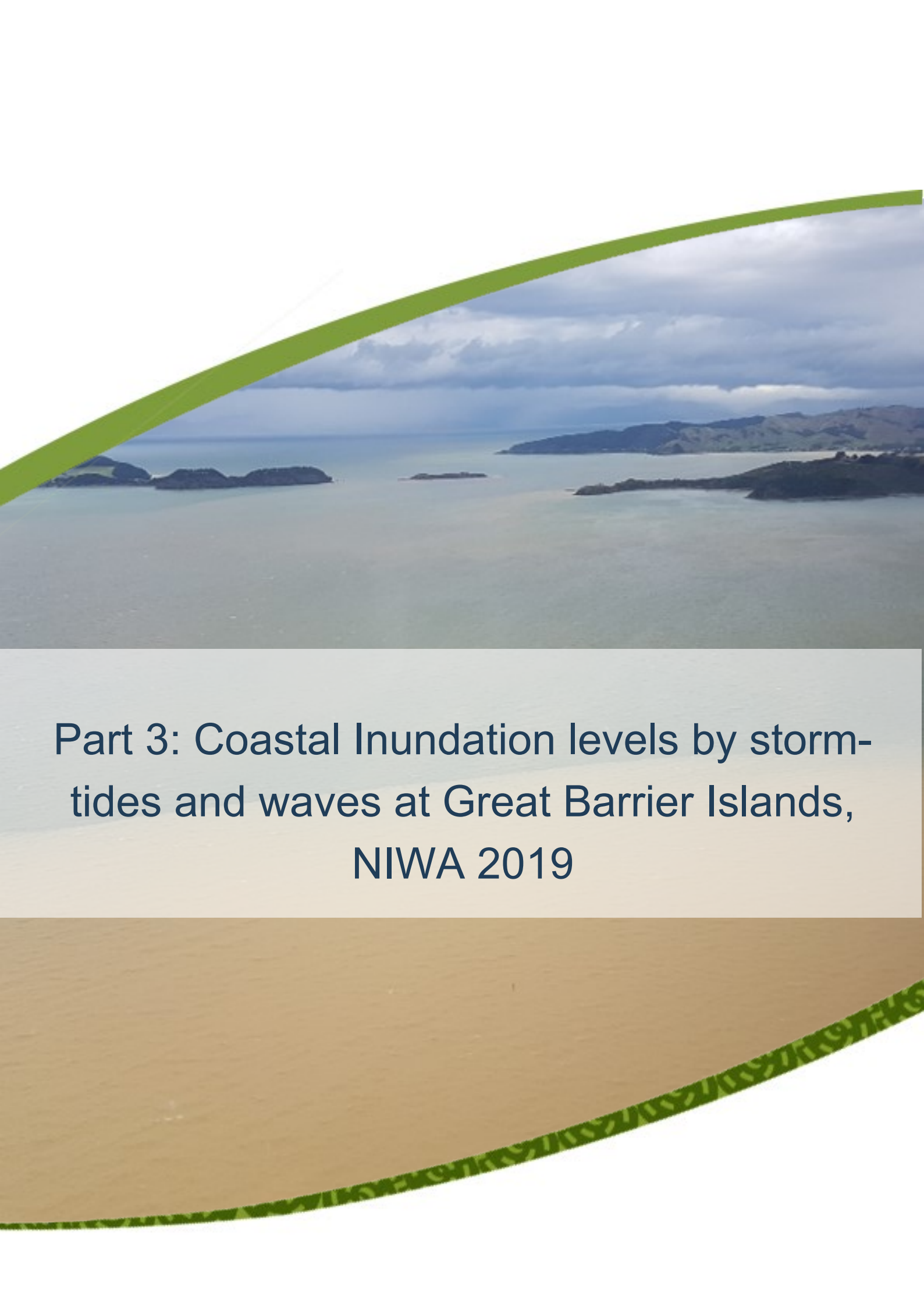
Summary

Recent history shows that Parakai and the surrounding area is susceptible to flooding from both its own catchment to the west and from tidal and/or flood events in the Kaipara River and Harbour. While flooding from the greater Parakai catchment tends to be of a nuisance nature, it is this second situation - tidal inundation - that poses the most threat of widespread flooding to the town, should the existing stopbanks be overtopped significantly.

This has occurred on a number of occasions since the early 1990s and since 2000, both when the stopbank crest level was 2.6m and later 2.8m. Earlier history indicates more widespread flooding used to occur in the area.

The 2006 studies for RDC by DHI Water Environments Ltd conclude that an H4 hazard water level, to be applied to major infrastructure including stopbank crest levels, should be 4.1 metres above datum – adding 200mm freeboard, this is 1.5 metres above the existing stopbanks.

Appendix 4 contains maps showing the questionnaire responses recorded in 1996.



Part 3: Coastal Inundation levels by storm-tides and waves at Great Barrier Islands, NIWA 2019

Coastal Inundation levels by storm-tides and waves at Great Barrier Islands

Prepared for Auckland Council

November 2019

Prepared by:
Michael Allis
Richard Gorman
Scott Stephens
Ron Ovenden
Chris Eager

For any information regarding this report please contact:

Michael Allis
Coastal Engineer
Coastal and Estuarine Processes Group
+64-7-856 1714
michael.allis@niwa.co.nz

National Institute of Water & Atmospheric Research Ltd
PO Box 11115
Hamilton 3251

Phone +64 7 856 7026

NIWA CLIENT REPORT No: 2019336HN
Report date: November 2019
NIWA Project: ARC20201

| Quality Assurance Statement | | |
|---|--------------------------|----------------|
|  | Reviewed by: | Rob Bell |
|  | Formatting checked by: | Alison Bartley |
|  | Approved for release by: | Michael Bruce |

© All rights reserved. This publication may not be reproduced or copied in any form without the permission of the copyright owner(s). Such permission is only to be given in accordance with the terms of the client's contract with NIWA. This copyright extends to all forms of copying and any storage of material in any kind of information retrieval system.

Whilst NIWA has used all reasonable endeavours to ensure that the information contained in this document is accurate, NIWA does not give any express or implied warranty as to the completeness of the information contained herein, or that it will be suitable for any purpose(s) other than those specifically contemplated during the Project or agreed by NIWA and the Client.

Contents

| | |
|--|-----------|
| Executive summary | 8 |
| 1 Introduction | 9 |
| 1.1 Background | 9 |
| 1.2 Scope..... | 10 |
| 2 Methodology | 14 |
| 2.1 Summary of methods used to calculate coastal-storm inundation elevations | 14 |
| 2.2 Site visit..... | 15 |
| 2.3 Sea-level gauges..... | 24 |
| 2.4 Wave buoy (Mokohinau) | 28 |
| 2.5 Wave and storm surge hindcasts..... | 29 |
| 2.6 Joint probability extreme value analysis | 36 |
| 2.7 Wave setup and runup estimates..... | 39 |
| 2.8 Calibration with site survey data | 39 |
| 2.9 Validation checks on wave runup estimates | 41 |
| 2.10 Exceptions..... | 46 |
| 3 Results for extreme total water level and contributing components | 49 |
| 3.1 Discussion | 53 |
| 3.2 Mapping limitations..... | 53 |
| 4 Acknowledgements | 57 |
| 5 Glossary of abbreviations and terms | 58 |
| 6 References | 60 |
| Appendix A Coordinates of output locations | 63 |
| Appendix B Wave hindcast corrections | 64 |
| Appendix C Validation plotting of surveyed debris features and predicted storm-tide plus wave runup (including setup) elevations | 67 |

Tables

| | | |
|------------|---|----|
| Table 2-1: | Beach slope values from Figure 2-10. | 23 |
| Table 2-2: | Tidal constituents, maximum high tide and MHWS elevations for all sites and tsunami gauge data. | 25 |
| Table 2-3: | Extreme significant wave height around Great Barrier Island. | 33 |
| Table 2-4: | Extreme peak wave period around Great Barrier Island. | 34 |
| Table 2-5: | Extreme skew-surge magnitude around Great Barrier Island. | 36 |
| Table 3-1: | Extreme sea-level (storm-tide + wave setup) around Great Barrier Island. | 50 |
| Table 3-2: | Extreme storm-tide elevations around Great Barrier Island. | 51 |
| Table 3-3: | Extreme wave setup magnitude (m) around Great Barrier Island. | 52 |
| Table A-1: | Location coordinates for predictions of hindcast wave, tide and storm surge statistics. | 63 |
| Table C-1: | Extreme sea-levels from storm-tide + wave runup (including setup) around Great Barrier Island. | 67 |

Figures

| | | |
|--------------|---|----|
| Figure 1-1: | Schematic of coastal storm inundation processes. | 9 |
| Figure 1-2: | Requested location of extreme sea level elevations. | 11 |
| Figure 1-3: | Study site locations around Great Barrier Island. | 13 |
| Figure 2-1: | Study site locations and surveyed features from Great Barrier Island site visit 15–19 September 2019. | 15 |
| Figure 2-2: | Example survey point distribution at Kaitoke Beach showing cross-shore beach profiles and elevation of survey points. | 16 |
| Figure 2-3: | Debris lines at Whangaparapara (Left, 16/7/2019 1:34 pm) and Tryphena (right, 15/7/2019 2:36 pm). | 18 |
| Figure 2-4: | Example debris behind vegetation edge at Kaitoke Beach (left, 18/7/2019 1:31 pm) and Awana Bay (right, log circled, 18/7/2019 9:51 am). | 18 |
| Figure 2-5: | Bay by bay overview of surveyed debris features. | 19 |
| Figure 2-6: | Intra-bay variation in beach feature elevation at Oruawharo Bay; Debris lines (left) and edge of vegetation or EV (right). | 20 |
| Figure 2-7: | Example distribution and elevation of survey point elevation at Okupu Bay. | 20 |
| Figure 2-8: | Example beach profiles at Kaitoke Beach (A) and Okupu Bay (B). | 21 |
| Figure 2-9: | Example beach profiles at Mulberry Grove (A) and Shoal Bay (B). | 21 |
| Figure 2-10: | Bay by bay overview of measured beach slopes around Great Barrier Island: (top) upper beach/backshore in 2–3 m elevation range, (bottom) beach face in 1-2 m elevation range. | 23 |
| Figure 2-11: | Sea level data from Great Barrier Island tsunami monitoring gauge (green), with modelled tide (red) and non-tidal residual (blue). [Raw Data: GeoNet (Station ID: GBIT), tide data: NIWA EEZ tide model] | 24 |
| Figure 2-12: | Spatial distribution of MHWS10 elevations around Great Barrier Island. Colour represents elevation relative to MSL - to make them relative to AVD-46 requires the addition of MSL datum offset (+0.15 m). | 27 |

| | | |
|--------------|--|----|
| Figure 2-13: | Non-tidal residual sea level (blue) and estimated MSLA (red). | 28 |
| Figure 2-14: | MSLA magnitude probability distribution. | 28 |
| Figure 2-15: | Map showing locations from which WASP hindcast outputs were extracted for each nearshore location. | 30 |
| Figure 2-16: | Occurrence distributions of significant wave height from four WASP hindcast locations around Great Barrier Island. | 31 |
| Figure 2-17: | Wave roses (joint distributions of significant wave height and mean wave direction) from four WASP hindcast locations around Great Barrier Island. | 32 |
| Figure 2-18: | Quantile-quantile plot of skew surge values measured by the Great Barrier Island tsunami gauge, and from the WASP hindcast extracted for the same location. | 35 |
| Figure 2-19: | Illustration of the definition of skew surge. | 37 |
| Figure 2-20: | Return values of the vertical level of storm tide plus wave runup (including setup), with beach slope tuned to match the 63% AEP value against the 50th percentile value of debris line elevation. | 40 |
| Figure 2-21: | Return values of the vertical level of storm tide plus wave runup and setup, with beach slope tuned to match the 63% AEP value against the 75th percentile value of debris line elevation. | 41 |
| Figure 2-22: | Values of the beach slope β resulting from calibration of storm tide plus wave runup and setup against debris line records, compared with beach slopes derived from survey records within the elevation range 1-2 m above AVD-46. | 42 |
| Figure 2-23: | Values of the beach slope β resulting from calibration of storm tide plus wave runup and setup against debris line records, compared with beach slopes derived from survey records within the elevation range 2-3 m above AVD-46. | 43 |
| Figure 2-24: | Cross-shore transects (coloured lines) measured at Oruawharo Bay with predicted 1% AEP and 63% AEP (annotations, dashed lines) extreme storm-tide + wave runup (including setup) elevations, and identified "slope break" zone (black oval). | 44 |
| Figure 2-25: | Cross-shore transects (coloured lines) measured at Awana Bay with predicted 1% AEP and 63% AEP (annotations, dashed lines) extreme storm-tide + wave runup (including setup) elevations, and identified "slope break" zone (black oval). | 45 |
| Figure 2-26: | Example of runup overprediction up a coastal stream mouth for Motairehe. | 46 |
| Figure 2-27: | Port Fitzroy and Rarohara Bay aerial Photograph. | 47 |
| Figure 2-28: | Te Tikoti Point is one of the two low-lying beaches on Little Barrier Island. | 47 |
| Figure 2-29: | Gravel/Cobble beach formation on eastern flank of Te Tikoti Point. | 48 |
| Figure 3-1: | Example storm-tide plus wave setup (no runup) modelling at Whangapoua using static "bathtub" approach. | 55 |
| Figure 3-2: | Example storm-tide plus wave setup modelling at Oruawharo Bay using static "bathtub" approach. | 56 |
| Figure B-1: | Illustration of the sheltering correction method. | 64 |

| | | |
|--------------|--|----|
| Figure B-2: | Scatter plot of significant wave height at the Mokohinau buoy location derived from the WASP hindcast (with sheltering correction) against values measured by the buoy. | 66 |
| Figure C-1: | Validation mapping of surveyed debris line (red circles) and estimated inundation extents from storm-tide plus wave runup (including setup) elevation at 1-year ARI (yellow) for Motairehe. | 68 |
| Figure C-2: | Survey photo at Motairehe showing small debris (sticks, dried seaweed) within grasses (lower left) below steep bank leading up to driveway at right. | 68 |
| Figure C-3: | Validation mapping of surveyed debris line (red circles) and estimated inundation extents from storm-tide plus wave runup (including setup) elevation at 1-year ARI (yellow) for Kawa. | 69 |
| Figure C-4: | Survey photo at Kawa showing debris (sticks, logs) below grassed bank (lower left). | 69 |
| Figure C-5: | Validation mapping of surveyed debris line (red circles) and estimated inundation extents from storm-tide plus wave runup (including setup) elevation at 1-year ARI (yellow) for Port Fitzroy. | 70 |
| Figure C-6: | Survey photo at Port Fitzroy showing debris (sticks, logs) within grassed bank (centre, centre left) and embedded in sandy-mud beach (lower left). | 70 |
| Figure C-7: | Validation mapping of surveyed debris line (red circles) and estimated inundation extents from storm-tide plus wave runup (including setup) elevation at 1-year ARI (yellow) for Whangaparapara. | 71 |
| Figure C-8: | Survey photo at Whangaparapara showing debris (sticks, logs) above rocky beach. | 71 |
| Figure C-9: | Validation mapping of surveyed debris line (red circles) and estimated inundation extents from storm-tide plus wave runup (including setup) elevation at 1-year ARI (yellow) for Blind Bay. | 72 |
| Figure C-10: | Survey photo at Blind Bay showing stranded seaweed (on sand) and small debris (sticks, dried seaweed) within grasses (centre right). | 72 |
| Figure C-11: | Validation mapping of surveyed debris line (red circles) and estimated inundation extents from storm-tide plus wave runup (including setup) elevation at 1-year ARI (yellow) for Okupu Bay. | 73 |
| Figure C-12: | Survey photo at Okupu Beach showing stranded seaweed (on sand) and small debris (sticks, dried seaweed) within grasses (centre right). | 73 |
| Figure C-13: | Validation mapping of surveyed debris line (red circles) and estimated inundation extents from storm-tide plus wave runup (including setup) elevation at 1-year ARI (yellow) for Puriri Bay. | 74 |
| Figure C-14: | Validation mapping of surveyed debris line (red circles) and estimated inundation extents from storm-tide plus wave runup (including setup) elevation at 1-year ARI (yellow) for Tryphena. | 75 |
| Figure C-15: | Survey photo at Tryphena showing stranded seaweed and small debris (sticks, dried seaweed) at base of cliff (centre right). | 75 |
| Figure C-16: | Validation mapping of surveyed debris line (red circles) and estimated inundation extents from storm-tide plus wave runup (including setup) elevation at 1-year ARI (yellow) for Mulberry Grove. | 76 |
| Figure C-17: | Survey photo at Mulberry Grove showing stranded seaweed and small debris (sticks, dried seaweed) within grasses (centre left). | 76 |

| | | |
|--------------|--|----|
| Figure C-18: | Validation mapping of surveyed debris line (red and blue circles) and estimated inundation extents from storm-tide plus wave runup (including setup) elevation at 1-year ARI (yellow) for Shoal Bay. | 77 |
| Figure C-19: | Survey photo at Shoal Bay showing stranded seaweed and small debris (sticks, dried seaweed) at base of grass causeway (centre left). | 77 |
| Figure C-20: | Validation mapping of surveyed debris line (red circles) and estimated inundation extents from storm-tide plus wave runup (including setup) elevation at 1-year ARI (yellow) for Oruawharo Bay. | 78 |
| Figure C-21: | Survey photo at Oruawharo Bay showing stranded seaweed and small debris (sticks, dried seaweed) within vegetation and at base foredune (lower left). | 79 |
| Figure C-22: | Validation mapping of surveyed debris line (red and blue circles) and estimated inundation extents from storm-tide plus wave runup (including setup) elevation at 1-year ARI (yellow) for Kaitoke Beach. | 80 |
| Figure C-23: | Survey photo at Kaitoke Beach showing stranded seaweed and small debris (sticks, dried seaweed) within vegetation and at base foredune. | 81 |
| Figure C-24: | Validation mapping of surveyed debris line (red circles) and estimated inundation extents from storm-tide plus wave runup (including setup) elevation at 1-year ARI (yellow) for Awana Bay. | 82 |
| Figure C-25: | Awana beach showing seaweeds scattered along beach face and some debris below vegetation line below toe of vegetated but steep foredune. | 82 |
| Figure C-26: | Validation mapping of surveyed debris line (red circles) and estimated inundation extents from storm-tide plus wave runup (including setup) elevation at 1-year ARI (yellow) for Whangapoua. | 83 |
| Figure C-27: | Whangapoua beach showing seaweeds scattered along beach face and some debris. | 84 |

Executive summary

NIWA was commissioned to provide estimates of extreme sea-level elevations at coastal locations around Great Barrier Island and Little Barrier Island. The methods used are compatible with the previous analysis described in the report Stephens et al. (2016) "Coastal Inundation by Storm-tides and Waves in the Auckland Region, June 2016, Auckland Council, Technical Report 2016/17". Site surveys provided debris-line locations, beach features and measured beach slope data which were used to calibrate and validate the extreme sea-level modelling.

The extreme sea levels were calculated using wave and storm-tide conditions simulated for the 1970–2000 period, at 16 inshore locations around the Islands with a further 10 offshore points. A joint-probability analysis was undertaken to calculate the likelihood of various offshore coincident storm-tide and wave combinations. Within the joint-probability analysis, the contribution of waves to the extreme sea levels at the shore was then calculated using a linear-equivalent beach slope calibrated from wave-deposited debris-line surveys and wave runup (including storm-tide and setup) predictions. The frequency and magnitude of extreme sea-level elevations was calculated from the summed combinations of wave setup and storm-tide elevations after accounting for their joint-probability.

The extreme sea-level elevations were estimated for seven likelihoods: 1, 2, 5, 10, 20, 50 and 100-year average recurrence interval (ARI), corresponding to 63%, 39%, 18%, 10%, 5%, 2% and 2% Annual Exceedance Probability (AEP). These extreme storm-generated sea levels are likely to persist for only short periods of 1–2 hours either side of the nearest high tide. The extreme sea-level elevations are provided relative to Auckland Vertical Datum 1946. The results are consistent with the 2016 study, but extreme sea levels are lower than on the mainland due to the smaller tidal range at Great Barrier and, to a lesser extent, the smaller skew-surge. For example, the 1% AEP storm-tide plus wave setup is 2.68 m at Cape Rodney compared to 2.46 m at Little Barrier.

Note that the calculated storm-tide heights and calculated wave-setup heights will not sum to equal the total storm-tide + wave setup elevations. This is because storm-tide and wave-setup are not 100% dependent, i.e., very high storm-tides do *not* always occur at the same time as very high wave setup and to simply add them together is overly conservative.

This study does not include the effects of tsunami on inundation, any ongoing effects of coastal erosion or beach profile changes on the wave setup and runup estimates. The mean sea level anomaly is calculated for comparison with other studies, although it is not included as a separate component to extreme sea levels because it is already included in the extreme skew-surge. The mapping of wave runup elevation contours is appended to the report to validate the method using surveyed debris features. The wave runup maps should not be used to indicate potential coastal inundation extents.

Future studies of this type could benefit from longer sea-level records, regular beach-profile surveys and post-storm surveys (photographs, GPS) to calibrate and validate extreme sea-level and inundation models.

1 Introduction

1.1 Background

Coastal hazards are a significant issue within the Auckland region and Auckland Council are tasked with identifying and managing such hazards under the RMA and associated NZ Coastal Policy Statement (e.g., Objective 5, Policies 24–27). Coastal hazards around the Auckland region generally include coastal erosion (beaches, estuarine shores or cliffs) and coastal inundation flooding (low-lying land) which arise during tsunami, large wave events and extremely-high sea levels.

Extreme sea-levels arise from a number of meteorological and astronomical processes (such as normal astronomical tides, monthly mean sea level anomalies and storm-surge) which can combine to inundate low-lying coastal margins and/or cause coastal erosion (Figure 1-1). Waves also further raise the effective sea level at the coastline where wave setup increases in the sea level within the surf zone from the release of wave energy, and waves also runup and overtop the coastal fringe and can exacerbate coastal flooding hazards (Figure 1-1). Other contributors to coastal hazards such as combined rainfall/runoff flooding (from rivers, streams and stormwater), tsunami inundation, and coastal erosion were not considered in this phase of the project.

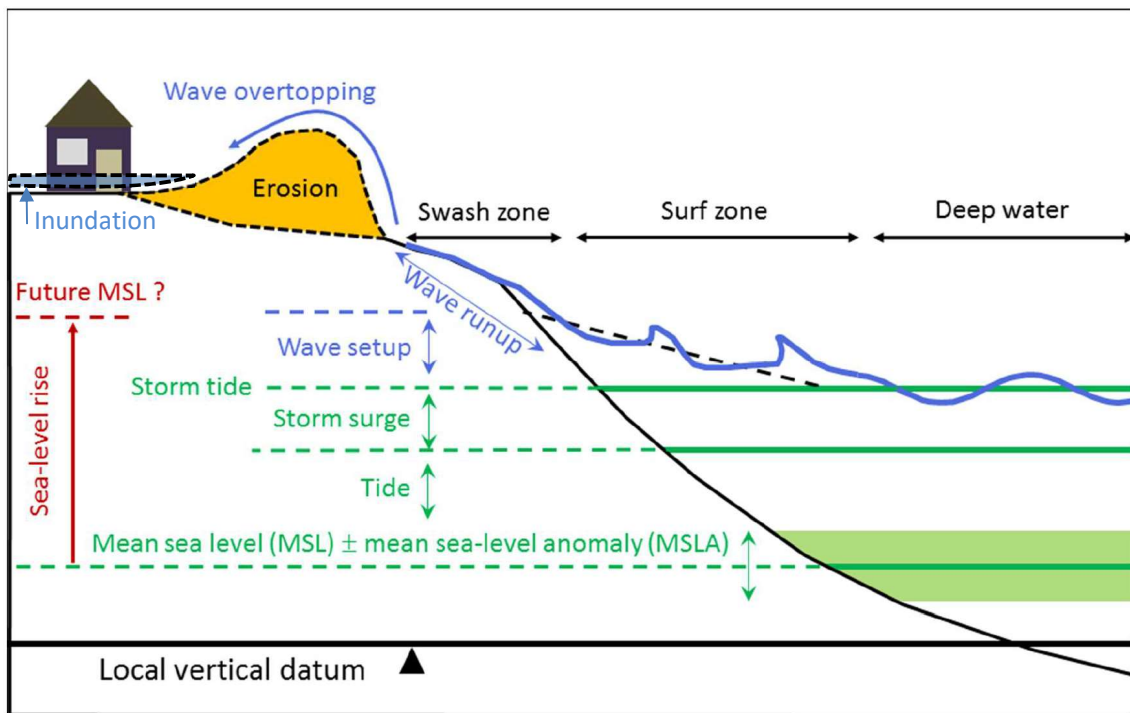


Figure 1-1: Schematic of coastal storm inundation processes. [Credit: S. Stephens (NIWA)].

Added to these coastal processes are the increasing effects of climate change and especially, the prospect of a projected rise in sea level of 0.5–1.3 m (or greater) by 2120 (MfE 2017) within the 100 years planning timeframe for coastal hazards (NZCPS, Policy 27). Secondary to sea-level rise are expected climate change effects on weather-related coastal hazard drivers such as storm surges, waves, winds, and frequency and intensity of storms. No climate change effects are considered in this phase of the project.

For this study Auckland Council requires estimates of present-day extreme sea level elevations and their likelihood around the whole coastline of the Auckland region that are well-founded on robust and defensible science. In 2013, NIWA calculated the height of high storm-tides and large waves around the mainland coastline of the Auckland region (Stephens et al. 2013). This work was updated for the Parakai/Helensville region in 2016 (Stephens 2016). However, the 2013 and 2016 studies did not include Great Barrier Island or Little Barrier Islands which are the focus of this investigation.

Great Barrier and Little Barrier Islands are geographically close to Auckland and are expected to have similar extreme sea-level characteristics to those established on mainland in the earlier assessments. This is due to the Islands being exposed to similar size and magnitude of the regional coastal hazard drivers such as large waves, storm-surge and mean sea level anomaly. However, underpinning all sea levels is the astronomical tide, which is smaller on the Islands compared to the mainland due to the deeper continental shelf and lack of topographic restriction of the tidal waveform. For example, at Port of Auckland the springs tide range is 2.9 m which compares to 2.2 m at Tryphena with the half-tide difference being 0.35 m¹. Hence, the high-tide component of extreme storm-tides is expected to be smaller on Great Barrier Island compared to Auckland, leading to (all other factors being equal) lower extreme sea-level elevations.

This report is intended to be read alongside the earlier reports (e.g., Stephens et al. 2013, 2016) which provide more background, explanation and context to the overall physical processes underpinning the coastal hazards in the Auckland region. Refer to these earlier reports and the glossary section (p. 58) for further clarification of terms used throughout this report.

Note that no inundation mapping was requested for this study and NIWA understands Auckland Council will manage the mapping through an external provider.

1.2 Scope

Auckland Council have requested that extreme sea-level elevations be provided for the locations shown in Figure 1-2 around Great Barrier Island and Little Barrier Island. The methods employed to determine sea levels are to be compatible with the previous storm-tide + wave setup analysis described in the report Stephens et al. (2016) "Coastal Inundation by Storm-tides and Waves in the Auckland Region, June 2016, Auckland Council, Technical Report 2016/17".

¹ LINZ tidal almanac for secondary ports 2019-2020 at Auckland compared with Korotiti Bay and Tryphena. (<https://www.linz.govt.nz/sites/default/files/docs/hydro/tidal-info/tide-tables/secondary-ports-2019-20.csv>)

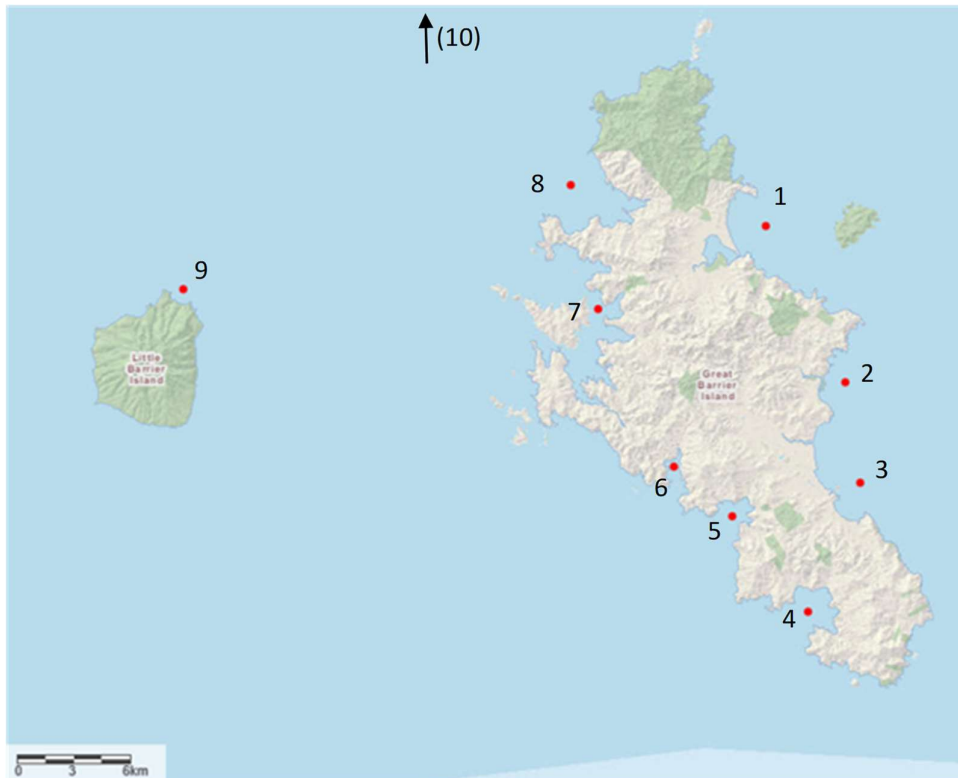


Figure 1-2: Requested location of extreme sea level elevations. Supplied by Auckland Council. Location names and coordinates in Table A-1

Extreme sea-level results were requested at average recurrence interval (ARI) scenarios of: 1, 2, 5, 10, 20, 50 and 100-year ARI. Extreme sea-level elevations were to be provided relative to Auckland Vertical Datum 1946 (AVD-46).

The proposed scope of the work was to undertake the following:

1. Complete a Great Barrier Island site visit to collect beach profiles and morphological evidence of extreme sea levels—this is required to ground-truth the modelling because there are no local sea-level, wave or beach profile datasets.
2. Extract 30-year hindcasts of tide, storm-surge and waves from our Tide and our Waves and Storm-surge Projections (WASP) models, at the study sites (Figure 1-2), and at Mokohinau Island. Apply wave-sheltering algorithms to account for the sheltering effect of the islands on the waves.
3. Analyse the Mokohinau Island sea-level and wave records to determine extreme storm-tide and wave distributions.
4. Use the Mokohinau Island data to scale the WASP model data to produce reliable extreme-value distributions.
5. Undertake joint-probability analysis for storm-tide and waves.
6. Merge the joint-probability analyses with the beach surveys to calculate extreme-value distributions for the total water level from storm-tide + wave setup at the study sites.

However, during the course of the investigation some changes to this proposed method were required, specifically:

- Expanding the number of study sites from 9 to 16 to better reflect the bay-by-bay variation in beach conditions, wave exposure and predicted extreme sea level elevation. The expanded site list is illustrated in Figure 1-3 below with location coordinates in Table A-1.
- Inclusion of the Great Barrier Island tsunami monitoring gauge as a local record of sea levels (location shown in Figure 1-3).
- Exclusion of the Mokohinau sea level record (not waves) as the data did not reach the required quality for this study (the bubbler gauge appears to read low during vigorous wave activity, compromising the measurement of storm surge).
- Mapping contours of the predicted extreme sea level elevations *including* wave runup at the 1-yr and 5-yr ARI for comparison to the debris line features observed during the site visit. This is to validate the method used and ensure results are consistent and realistic when plotted by Auckland Council's external mapping provider.

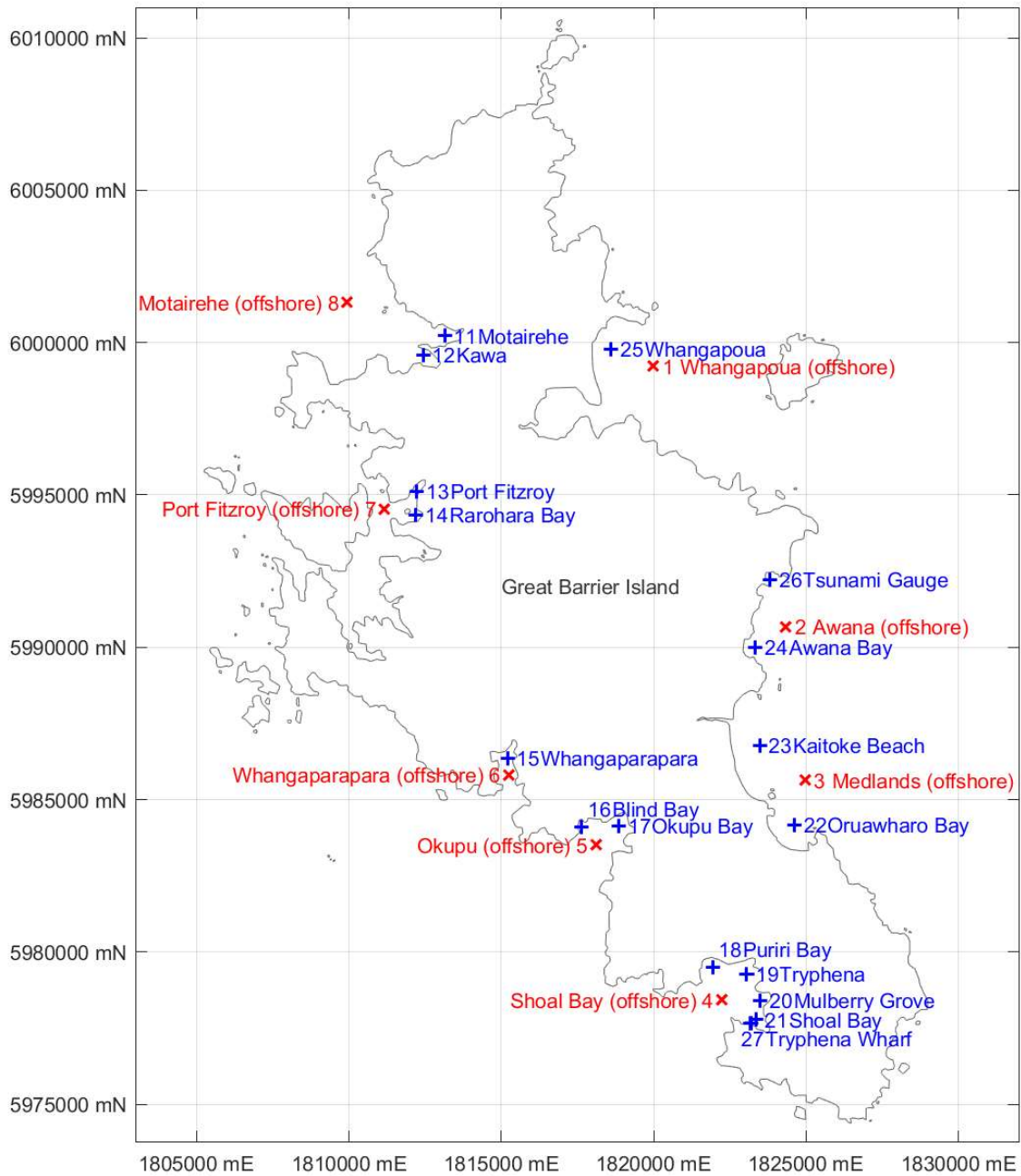


Figure 1-3: Study site locations around Great Barrier Island. Names as of inshore (blue) and offshore (red) sites as referred to throughout text. Not shown: Little Barrier Island (#9), Mokohinau Island (#10) sites and Mokohinau wave buoy (offshore) (#28). See Table A-1 for coordinates [Coordinate system: NZTM 2000].

2 Methodology

2.1 Summary of methods used to calculate coastal-storm inundation elevations

We undertook the following tasks to calculate extreme sea-level elevations for the Great Barrier and Little Barrier Island coastlines:

- Obtained and quality checked sea-level data from the Geonet/GNS Science Tsunami Gauge at Korotiti Bay.
- Decomposed tidal constituents from Korotiti Bay gauge record, compared to NIWA tide model prediction around the Island.
- Adopted MSL of 0.15 m Auckland Vertical Datum 1946 (AVD-46), for consistency with the 2016 study (Stephens et al. 2016).
- Extracted a 30-year hindcast of wave, tide and storm surge conditions for the 1970–2000 period, applying sheltering and calibration corrections to the hindcast outputs, to produce outputs applicable at a set of nearshore sites.
- Extracted High Water values of storm tide (i.e., tidal water level plus skew surge), and coincident wave statistics, at each location.
- Applied the joint-probability methods of Heffernan and Tawn (2004) to characterise the statistical distribution and interdependence of extreme values of the variables contributing to storm-tide inundation on beaches, i.e., tidal water level, skew surge, significant wave height and peak wave period.
- Applied the resulting statistical model to derive a synthetic 5,000-year record of extreme values of the same variables.
- Applied empirical methods to estimate the resulting wave setup and wave runup that would be associated with the derived 5,000-year synthetic record of storm-tide and wave conditions, dependent on assigned beach slope parameters for each location.
- Used the 5,000-year synthetic record to derive frequency–magnitude relationships for all relevant quantities (i.e., skew surge, wave height and period, wave runup, wave setup, and the resultant combined storm-tide levels). These predict the *size* and *likelihood of occurrence* of each quantity, in the form of return values with specified Annual Exceedance Probabilities.
- Compared the surveyed elevation and location of debris line features to the predicted frequency-magnitude relationship for storm tide level including wave setup and runup to calibrate the model for a dependant beach slope parameter at each of the 16 shoreline sites (since beach gradient influences the wave setup and runup height). This establishes the beach slopes used to predict the wave setup component of extreme sea-levels.

2.2 Site visit

Great Barrier Island coastal features were manually surveyed over 15–19 September 2019 by NIWA Coastal Engineer Dr Michael Allis and NIWA Coastal Technician Ron Ovenden. The survey traversed most of the targeted sites (Figure 2-1) accessible by public road. Little Barrier Island and Rarohara Bay (south of Port Fitzroy) were not accessed.

The RTK-GPS² survey equipment used Trimble R10 base stations, which were set up at a prominent location near each beach access point, with a minimum base-station occupation time of 3 hours. The base stations connected to Trimble TSC3 receivers which travelled the sites with the surveyors. Check shots were made at nearby LINZ benchmarks with excellent agreement. The average vertical precision of survey points was ± 0.0204 m with average horizontal precision of ± 0.0114 m. This precision is well within the natural change to beach elevation which can occur over a tidal cycle or storm. Survey elevations were collected in New Zealand Ellipsoidal height and converted to AVD-46. Horizontal coordinates were collected in New Zealand Transverse Mercator 2000 (NZTM2000).

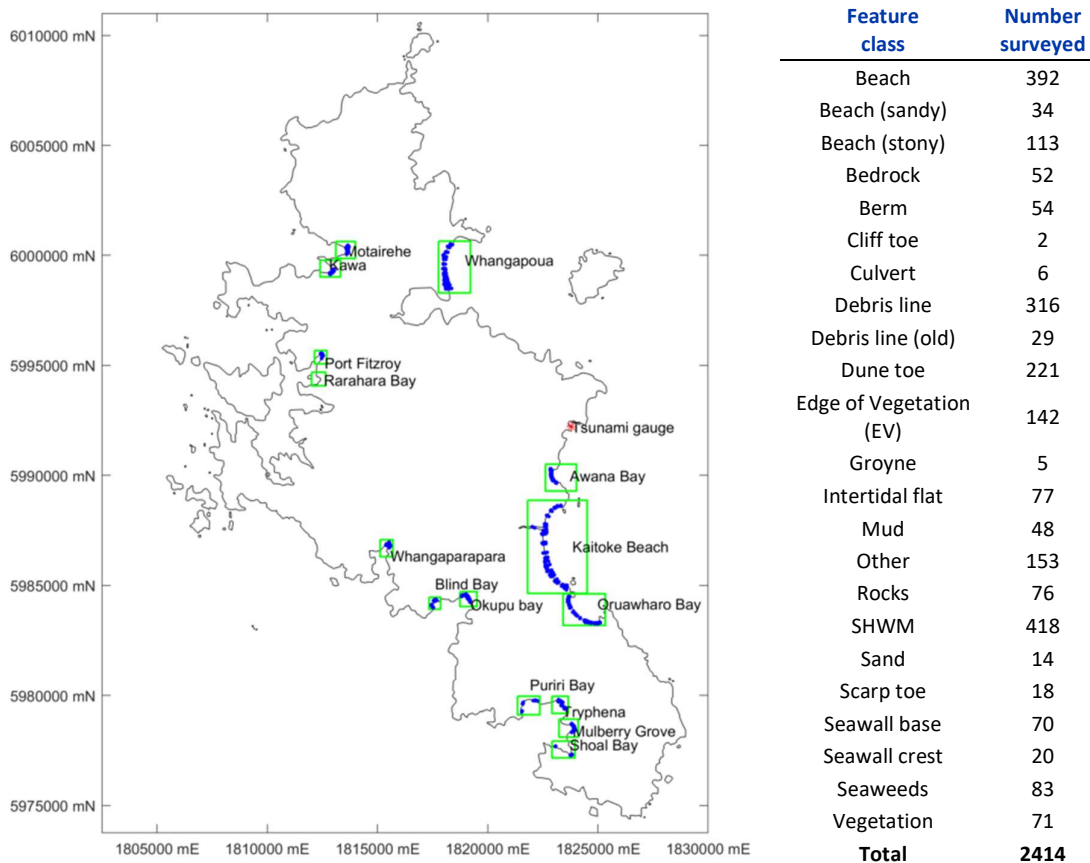


Figure 2-1: Study site locations and surveyed features from Great Barrier Island site visit 15–19 September 2019. Names as referred to throughout text, green boxes indicate approximate extent of each site, also shown is tsunami gauge location. Not shown: Little Barrier Island. [Coordinate system: NZ Transverse Mercator 2000].

² Real Time Kinematic – Global Positioning System

The site survey collected approximately 2400 individual points over the 4 survey days with points grouped into beach feature types (Figure 2-1). The points were generally arranged as cross-shore transects (Figure 2-2) with typical alongshore spacing of 150–400 m depending on the alongshore variability in beach form (i.e., fewer survey points in featureless areas, but greater sampling around built up and variable shorelines). Photographs were regularly collected throughout the survey and used to quality check the data.

The purpose of the survey was to collect beach profiles and morphological evidence of extreme sea levels required to ground-truth the numerical modelling.

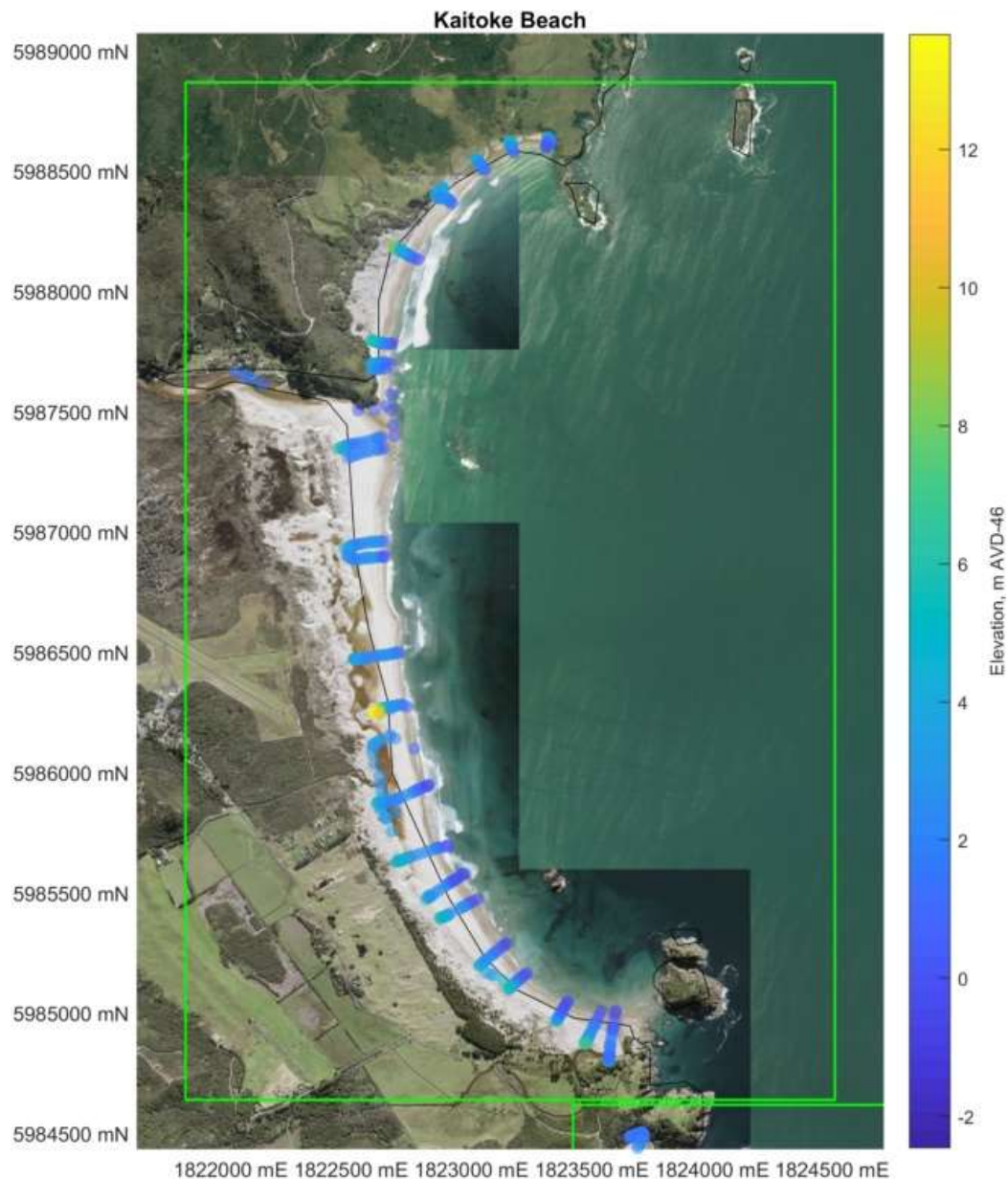


Figure 2-2: Example survey point distribution at Kaitoke Beach showing cross-shore beach profiles and elevation of survey points. Figure includes all survey points and does not delineate between beach features. [Aerial photograph: Auckland Council GIS, Coordinate system: NZ Transverse Mercator 2000].

2.2.1 Field survey of beach features

The features surveyed include a range of geomorphic identifiers useful for establishing and validating numerical model predictions of extreme sea levels. The features identified include those within the categories of:

- Active beach features which were identified as the elevation of the beach (sandy, stony, muddy), stream beds or stream banks which are clearly tide/wave dominated features and are expected to be below the wave up-rush limit on a regular basis. These were surveyed as far offshore as permitted by the water level at the time.
- Beach interface features which identify the *transition* from the tide/wave dominated active beach processes to the quasi-static backshore features. This includes the beach elevation at the base of a seawall (rock, wooden or other), the beach elevation at the toe of the dunes, or the elevation of the crest of a berm (where the beach sediments are gravel-dominant, as near to the Otaki River Mouth).
- Backshore features which were identified as features not regulated by direct wave attack but depend on subsequent processes (e.g., slumping of dune face following wave undercutting at the toe of the dune). This includes the vegetation line(s), scarp(s) the berm elevation, and dune features which represent elevations within the dune field which are considered stable behind and above any wave-controlled shoreline features.
- Debris such as driftwood, wave deposited seaweed (wrack) and general wave-transported debris (i.e., fishing floats, seeds etc.,) or a high water mark from a recent storm (SHWM) are deposited in a reasonably obvious debris line or bulk accumulation within and above the backshore features.
- Structural features such as man-made structural features such as the top of wall(s), top of rocks, paved carparks or fence lines.
- Other points not associated with specific features but used to infill the cross-shore beach profile between specific beach features. Cross-shore transects usually extended from the water level at the time of survey inland to the backshore.

The features most relevant to this investigation were the debris lines (Section 2.2.2) and the beach profiles (Section 2.2.3) which were used for calibrating/validating the numerical model predictions (Section 2.8).

2.2.2 Debris features

Debris lines represent floating material which is deposited by the runup of the highest individual wave during a particular tide. Debris lines show the bay-wide distribution of the ‘total water level’ including all wave, tide and surge processes during a particular storm.

The largest debris (logs and stumps) were surveyed on Kaitoke beach which could indicate deposition from a large historic storm as logs can survive for 20–30 years before rotting away. However, debris interpreted to be deposited by older storms (i.e., usually larger, more weathered and further inland) was sparse (29 points surveyed only) and inconsistent with recent debris lines. This indicates the debris may have been deposited by other means (e.g., tsunami, terrestrial flooding, humans) or indicating the beach has changed (i.e., progradation, dune advance) since the debris was deposited.

For these reason, the older debris points were not considered to be of high enough quality for this work and were not used further.

Most surveyed debris on the more-sheltered west coast of Great Barrier Island were composed of small branches, sticks and floating seaweeds which appeared recent due to degree of decomposition (Figure 2-3, left). This was confirmed during conversations with Island residents who suggested that a storm had recently affected the west coast, resulting in nuisance flooding (splash/overwash of seawalls) and depositing the debris lines on the grass verge above seawalls. We infer this type of debris to be deposited from a <1-year ARI event.



Figure 2-3: Debris lines at Whangaparapara (Left, 16/7/2019 1:34 pm) and Tryphena (right, 15/7/2019 2:36 pm). [Credit: M Allis (NIWA)].



Figure 2-4: Example debris behind vegetation edge at Kaitoke Beach (left, 18/7/2019 1:31 pm) and Awana Bay (right, log circled, 18/7/2019 9:51 am). [Credit: M Allis (NIWA)].

On the exposed east coast, debris was less-recent than the west, but also with several debris line features identified. Some were very recent with others inferred to be up to 1–2 years old (Figure 2-4). The older features contained branches and wood material, with recent composed of dried and brittle seaweeds.

Distribution of debris line elevations for each bay are shown in Figure 2-5.

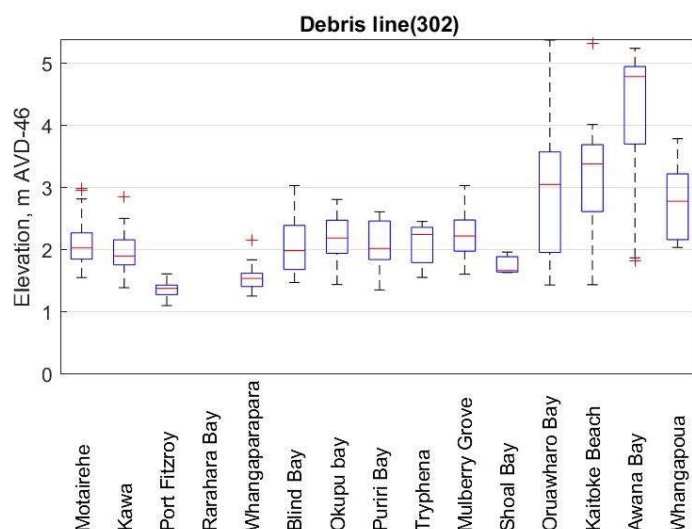


Figure 2-5: Bay by bay overview of surveyed debris features. Refer to Figure 1-3 for site location – with the last 4 sites being those on the exposed east coast. On each box, the central mark is the median, the edges of the box are the 25th and 75th percentiles, the whiskers extend $\pm 2.7\sigma$ or 99.3 percent data coverage.

The island-wide distribution of debris is a consequence of the various sheltering of beaches from large waves according to islands, headlands, inlets and valleys, and other bathymetric features. The beaches on the east coast are higher energy wave-dominated sites with higher wave runup and debris deposition, conversely, embayments on the western side of the island have lower overall debris line elevations due to their sheltered nature. On average, the lowest median debris line elevations were measured at Port Fitzroy (1.4 m) and Whangaparapara (1.5 m), with median debris line elevations for other west coast sites being typically 1.9–2.4 m. Debris lines on the east coast are in the 2–5 m elevation range, with Awana Bay showing the highest median debris line elevation (4.9 m), but the other eastern sites 2.8–3.5 m range. The validity of >1 m higher debris lines at Awana Bay compared to other east coast beaches is confirmed by the anecdotal observations³ that Awana Bay is a “swell magnet” and the results of this study which show that Awana Bay has the largest waves (Table 2-3).

The interquartile range of debris line elevations at each site was typically smaller for western site (0.6 m) than eastern (1.2 m). This interquartile range represents the variation in surveyed debris line elevations *within* a single bay (i.e., intra-bay) which is a function of wave exposure/sheltering around each embayment. Generally, we observed higher elevations in the centre of a bay and diminishing to the edges where more protected from waves by headlands. This is most apparent for the eastern wave-exposed beaches (Oruawharo, Kaitoke, Awana and Whangapoua) as shown for Oruawharo in Figure 2-6.

³ Conversation with unnamed surfer at Awana Bay during site visit.

The location of all debris line features for all sites are mapped in Appendix C as a validation exercise for the estimated extreme sea level calculated in the following sections.

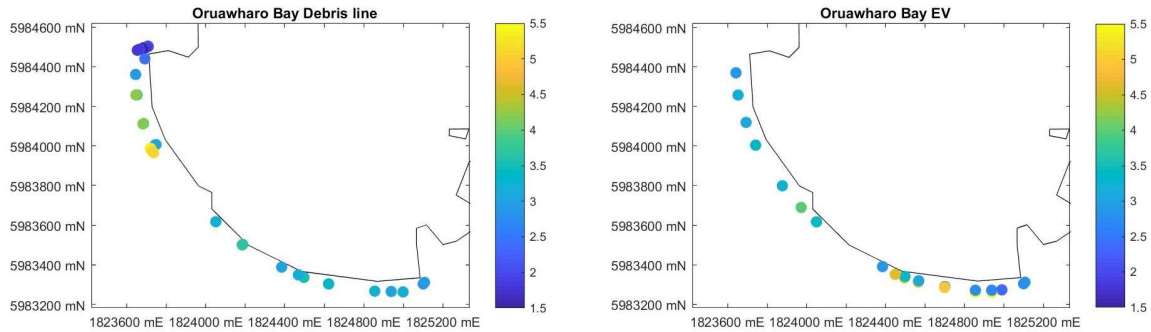


Figure 2-6: Intra-bay variation in beach feature elevation at Oruawhoro Bay; Debris lines (left) and edge of vegetation or EV (right). NZ coast outline (black). Coloured points show surveyed elevation in m AVD-46. [Coordinate system: NZ Transverse Mercator 2000].

2.2.3 Field survey of beach slopes

The beach slopes measured in the field were used as to check the predicted wave runup and setup components which were calibrated to the surveyed debris line features (see Section 2.8 for analysis). The beach slopes at each bay were taken directly from the survey points that were aligned in cross-shore transects (e.g., Figure 2-2 and Figure 2-7).

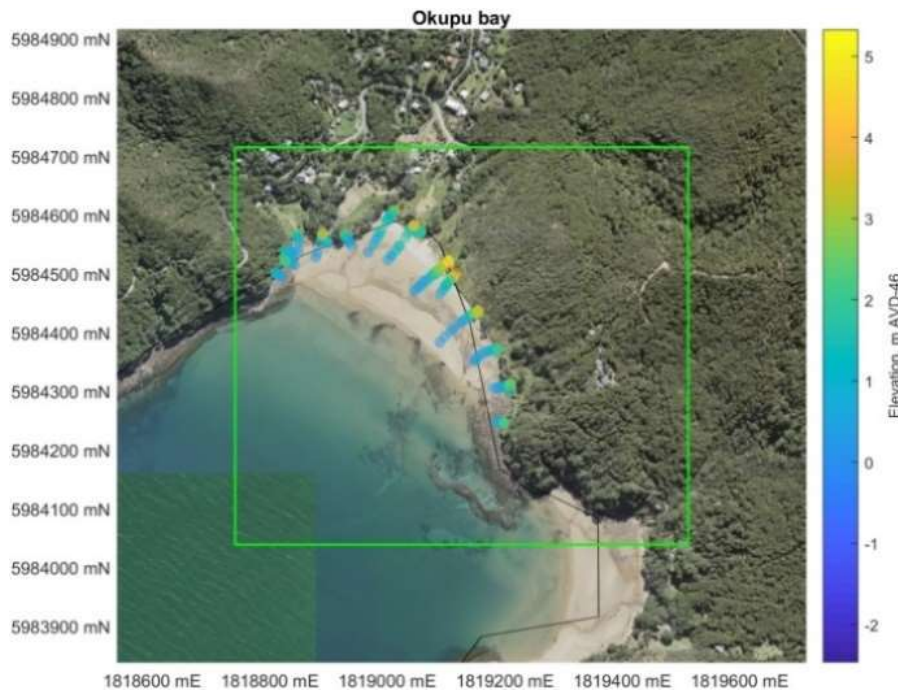


Figure 2-7: Example distribution and elevation of survey point elevation at Okupu Bay. Figure includes all survey points at each bay and does not delineate between beach feature types. [Aerial photograph: Auckland Council GIS, Coordinate system: NZ Transverse Mercator 2000, Vertical Datum: m AVD-46].

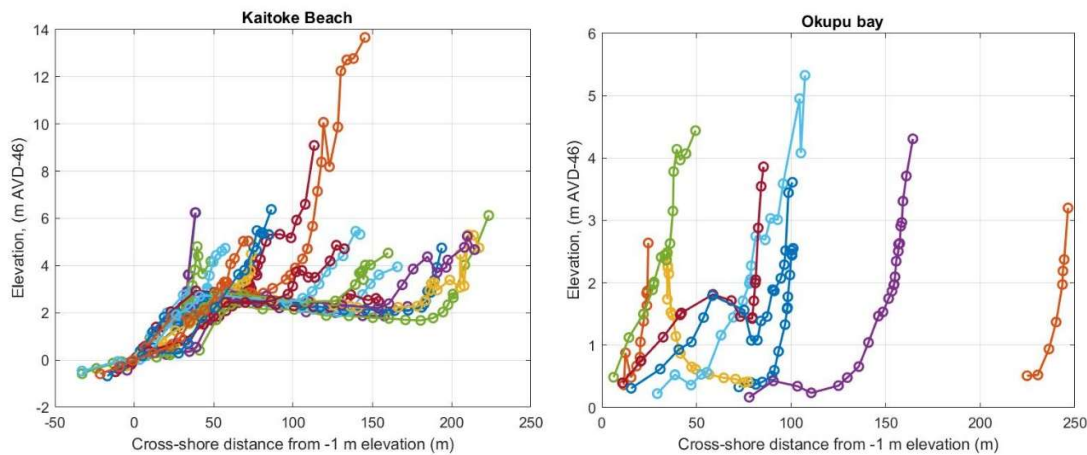


Figure 2-8: Example beach profiles at Kaitoke Beach (A) and Okupu Bay (B). See maps of survey points in Figure 2-2 (Kaitoke Beach) and Figure 2-7 (Okupu Bay). Horizontal axis is the linear cross-shore distance from the profile interpolated to the -1 m elevation. Elevations in m AVD-46.

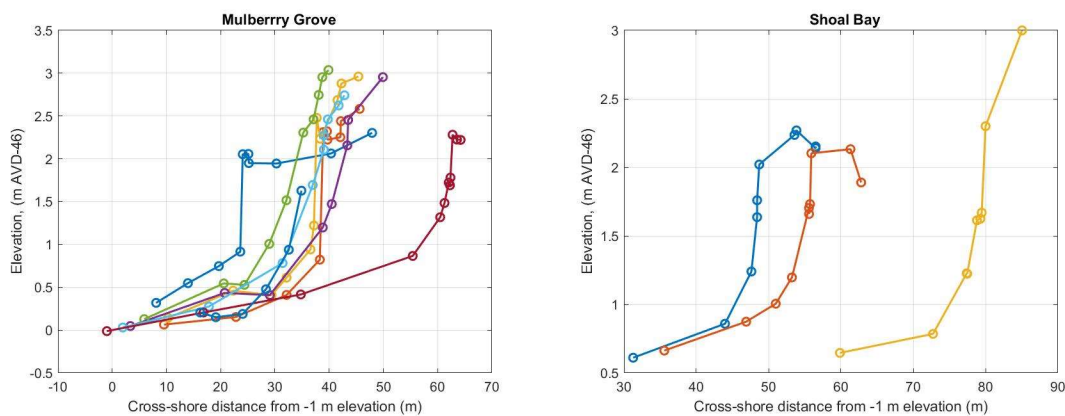


Figure 2-9: Example beach profiles at Mulberry Grove (A) and Shoal Bay (B). Horizontal axis is the linear cross-shore distance from the profile interpolated to the -1 m elevation. Elevations in m AVD-46.

The beach gradient (or slope) is one of the key parameters which affects wave setup, wave runup and wave overtopping on a beach. The gradient of a beach is not fixed, it is a consequence of interaction between the beach material and offshore wave conditions where the beach shape naturally adjusts to best dissipate the incoming wave energy. A steep beach scarp forms on most beaches during storm-wave conditions, however beaches generally behave differently according to their sediment composition:

- On sandy beaches, the sand moves offshore as large waves erode into the upper beach face and dunes, creating a flatter surf-zone bathymetric gradient but a steeper beach face gradient and erosion scarp. In the absence of storm-waves the sand slowly returns from the surf zone and accretes on the beach face with the assistance of wind. Sandy beaches of the east coast sites exemplify this during storm conditions (e.g., Figure 2-8A).

- For gravel-dominant beaches, the gravel moves on-shore and up the beach face to increase the beach gradient and beach crest height. This higher crest may also be breached and flattened by large overtopping flows, which redistributes the gravel sediment on the backshore.
- On rocky shorelines, the storm-waves mobilise the smaller sands and gravels more than the relatively immobile rocks and boulders. Generally, the beach face steepens, with sediment movement trends as above, although localised scour also occurs around the immobile rocks/boulders and obstructions.
- There are other semi-independent factors which influence the beach gradient, such as sediment sorting, beach sheltering, wave steepness, wave direction, level of water table and tidal range, bedrock outcrops, seawalls; however the most important variable which affects beach gradient is the sediment size (Komar 1998).

The beach gradient should be measured over the upper beach-face close to the high-tide mark because this is the general shore zone where the active wave swash or potential overtopping occurs. We calculated the beach slope over a vertical range of 1 m for each site which is a simplified version of the beach slope range defined used for wave setup/runup estimation equations (Stockdon et al. 2006). We calculated the beach slopes over two sets of a 1 m vertical elevation range; from 1–2 m and from 2–3 m. Figure 2-10 below illustrates the bay by bay variation in the measured beach slope values.

The wave exposed sites on the east of Great Barrier Island have the lowest and most consistent beach slopes as a consequence of being wave-dominated sites with predominantly sandy substrates except for headlands at either end of a beach. The sites on the Hauraki Gulf side are more variable reflecting the changing underpinning substrate and features between each bay (e.g., cobbles, rocky cliffs, seawalls, mud flats, rock reef outcrops, mangroves and some sandy pocket beaches) and the more tidally dominated beaches (reflecting the smaller wave climate).

As will be seen in Section 2.8, the measured beach slopes are used to compare to the beach slope back-calculated from the wave runup / debris-line evaluation. This method was required because measured beach slopes:

- Only represent a snapshot of the beach slopes on a *single* day. Repeat surveys as part of a monitoring programme would build a picture of the long-term equilibrium beach profile for use as a better predictor of wave setup/runup at each site.
- The slope of a beach changes during storm conditions and the energetic waves erode the sand and transport it offshore, often leading to a steep or scarped profile.
- The slope on a beach is also controlled by geologic setting. For example, southern Whangapoua beach has an old peat layer outcropping in the upper intertidal zone – acting as another control on bay shape and wave processes. And most west coast sites have subtidal rock platforms extending from the bounding headlands which act as a further control on wave processes.
- The profiles are composite profiles where slope changes with elevation. i.e., flatter beach at the low tide mark and steeper slopes at high-tide mark. Many west coast beaches also have vertical seawall supporting the road immediately behind the beach.

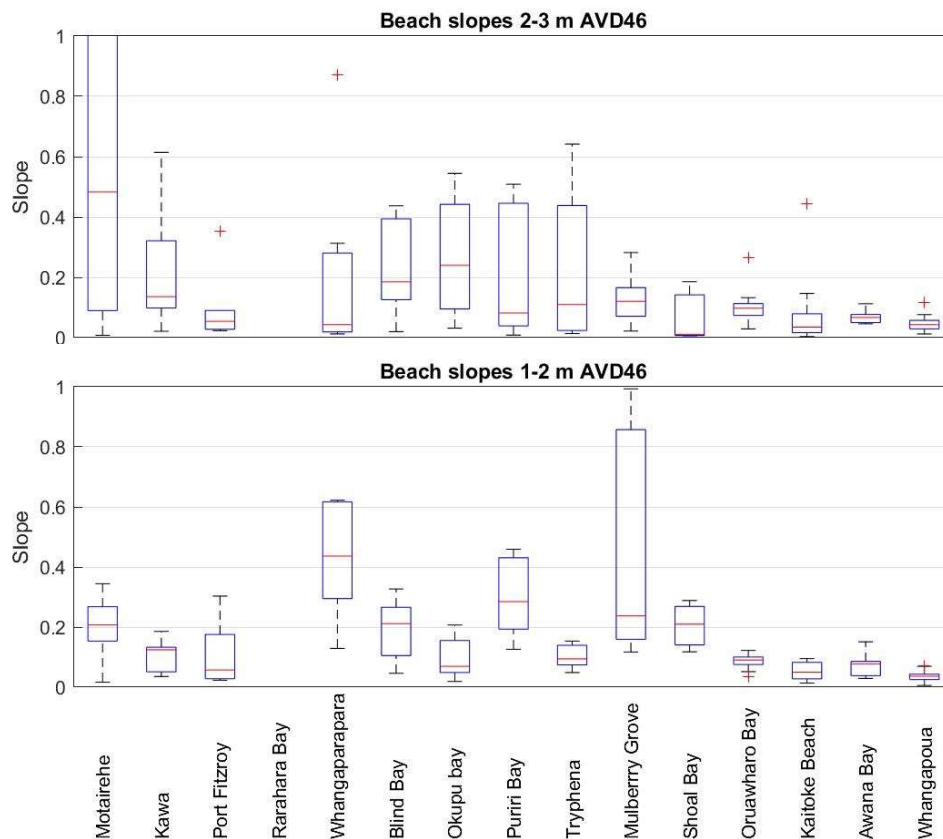


Figure 2-10: Bay by bay overview of measured beach slopes around Great Barrier Island: (top) upper beach/backshore in 2–3 m elevation range, (bottom) beach face in 1-2 m elevation range. Refer to Figure 1-3 for bay location. On each box, the central mark is the median, the edges of the box are the 25th and 75th percentiles, the whiskers extend $\pm 2.7\sigma$ or 99.3 percent data coverage. The crosses are deemed to be outliers. Values are tabulated in Table 2-1.

Table 2-1: Beach slope values from Figure 2-10. Refer to Figure 1-3 for site location.

| Value/Site | Motairehe | Kawa | Port Fitzroy | Rarahara Bay | Whangaparapara | Blind Bay | Okupu bay | Puriri Bay | Tryphena | Mulberry Grove | Shoal Bay | Oruawhoro Bay | Kaitoke Beach | Awana Bay | Whangapoua |
|---|-----------|-------|--------------|--------------|----------------|-----------|-----------|------------|----------|----------------|-----------|---------------|---------------|-----------|------------|
| 1-2 m AVD-46 elevation band (beach face) | | | | | | | | | | | | | | | |
| 25th centile | 0.154 | 0.051 | 0.028 | - | 0.295 | 0.105 | 0.049 | 0.193 | 0.074 | 0.160 | 0.141 | 0.075 | 0.028 | 0.038 | 0.025 |
| median | 0.207 | 0.124 | 0.057 | - | 0.436 | 0.211 | 0.069 | 0.285 | 0.094 | 0.237 | 0.210 | 0.090 | 0.050 | 0.077 | 0.036 |
| 75th centile | 0.268 | 0.133 | 0.175 | - | 0.617 | 0.266 | 0.155 | 0.431 | 0.139 | 0.857 | 0.269 | 0.100 | 0.083 | 0.086 | 0.043 |
| 2-3 m AVD-46 elevation band (upper beach/backshore) | | | | | | | | | | | | | | | |
| 25th centile | 0.090 | 0.098 | 0.028 | - | 0.019 | 0.126 | 0.095 | 0.039 | 0.024 | 0.071 | 0.007 | 0.074 | 0.017 | 0.050 | 0.029 |
| median | 0.483 | 0.136 | 0.054 | - | 0.043 | 0.185 | 0.240 | 0.082 | 0.110 | 0.120 | 0.011 | 0.098 | 0.035 | 0.067 | 0.043 |
| 75th centile | 2.467 | 0.321 | 0.090 | - | 0.281 | 0.394 | 0.442 | 0.445 | 0.438 | 0.166 | 0.142 | 0.113 | 0.079 | 0.077 | 0.057 |

2.3 Sea-level gauges

GeoNet operates a tsunami monitoring gauge (Station ID: GBIT⁴) at Korotiti Bay (2.5 km north of Awana Bay, see Figure 1-3). The gauge has been operating continuously since 26/7/2010, however only a short record of this was usable. The data before 11/2013 was not available from the archive and the whole of the 2017 year was unreliable and discarded due to data drift. The resulting time-series was approximately 6 years in duration (Figure 2-11). This record was used to verify the tidal model and calibrate the extreme sea level elevations – see Section 2.5.2.

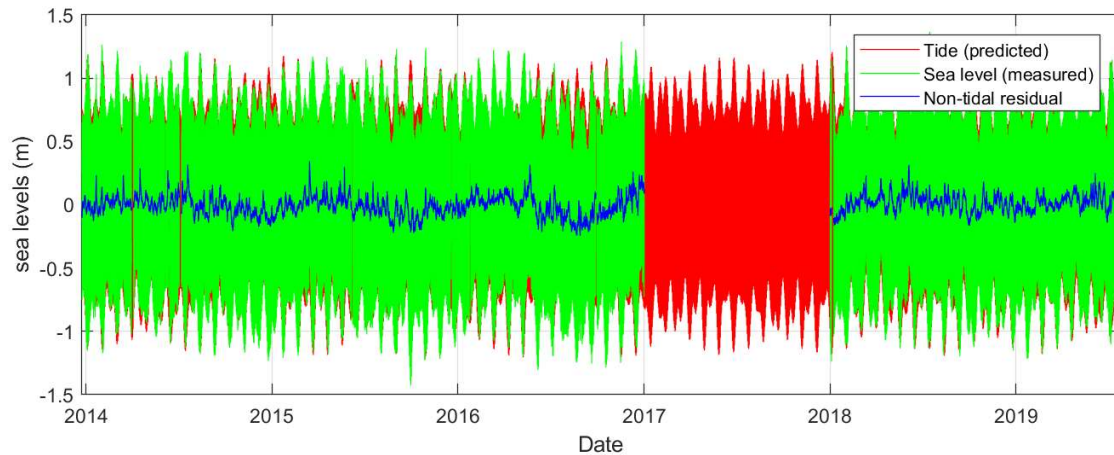


Figure 2-11: Sea level data from Great Barrier Island tsunami monitoring gauge (green), with modelled tide (red) and non-tidal residual (blue). [Raw Data: GeoNet (Station ID: GBIT), tide data: NIWA EEZ tide model]

Three tsunami records were removed from the sea level record to not corrupt the resulting skew surge estimates (8-Mar-2019, 5-Dec-2018 and 17-Sep-2015). The tsunami gauge record is not long enough to establish if GBI has any sea level rise trends different to that measured at the Port of Auckland, and this estimation is unlikely to be possible in the future because the type of gauge (pressure transducer) is prone to drifting making long-term records unreliable.

The sea level gauge at Korotiti Bay was decomposed into the constituents of tide, non-tidal residual using the NIWA tide model predictions for the same coordinates.

A pressure transducer was installed a depth of ~3 m at Tryphena Wharf during the 2019 field survey. This record was used to verify the M_2 tidal model prediction (longer records are required for other tides). The M_2 tide constituents determined from measured data had an amplitude of 0.8530 ± 0.0034 m with a phase of 211.6 ± 2.5 degrees (data and analysis not shown). The predicted M_2 tide amplitude was 0.8526 m with a phase of 207.4 degrees. These two are in good agreement especially considering the short 4 day deployment window, giving confidence that the tide model (discussed below) reproduces the tide characteristics on the Hauraki Gulf side of Great Barrier Island.

2.3.1 Tidal elevations

Tidal elevations were modelled at each site around Great Barrier Island using NIWA's Exclusive Economic Zone (EEZ) tide model which simulates 13 of the most important tides around New Zealand

⁴ <https://www.geonet.org.nz/data/network/sensor/GBIT>

(Stanton et al. 2001; Walters et al. 2001)⁵. The model has been calibrated with measurements from NIWA’s sea-level network and is the basis of the NIWA tide forecasting service⁶. The model was run for each study site (Figure 1-3) to predict 100-years of high-tides, from which the maximum high water (max HW) and tidal exceedance elevations. The Tsunami gauge at Korotiti Bay was also analysed for to interpret the tide model constituents for validation with the tide model at the same coordinates. The tide elevations predicted here are included within the extreme storm-tide calculations.

Table 2-2 contains the three largest tidal constituents at each site, the maximum tide elevation and includes common and recommended definitions of the mean high-water springs (MHWS) elevation which defines the landward jurisdictional boundary of the coastal marine area (CMA). Although there are several definitions of MHWS, Bell (2010) showed that high-tide exceedance curves, based on the cumulative distribution function (CDF) of long-term tide predictions, allow MHWS to be consistently defined based on a common exceedance threshold that is independent of tide regime. This leads to the definition of MHWS-10, for example, as the elevation equalled or exceeded only by the largest 10% of all high tides.

Alternatively, NIWA’s red-alert⁷ tide calendar uses the mean high-water perigean springs (MHWPS) definition. MHWPS is the sum of the three largest tidal harmonics: M₂ (principal lunar semi-diurnal) + S₂ (principal solar semi-diurnal) + N₂ (larger lunar elliptic semi-diurnal). MHWPS is the elevation used within for “king tides” where even a minor storm surge or river flood could cause coastal flooding in low-lying areas because the tides are extreme for those dates.

Table 2-2: Tidal constituents, maximum high tide and MHWS elevations for all sites and tsunami gauge data. Elevations are relative to MSL - to make them relative to AVD-46 requires the addition of MSL datum offset (+0.15 m).

| Name | Site number | M ₂ | S ₂ | N ₂ | Max HW | MHWPS | MHWS10 |
|---------------------------|-------------|----------------|----------------|----------------|--------|-------|--------|
| Awana (offshore) | 2 | 0.7829 | 0.1014 | 0.1607 | 1.225 | 1.045 | 1.013 |
| Medlands (offshore) | 3 | 0.7837 | 0.1012 | 0.1609 | 1.224 | 1.045 | 1.014 |
| Shoal Bay (offshore) | 4 | 0.8543 | 0.1145 | 0.1739 | 1.327 | 1.142 | 1.105 |
| Okupu (offshore) | 5 | 0.8858 | 0.1217 | 0.1795 | 1.376 | 1.187 | 1.146 |
| Whangaparapara (offshore) | 6 | 0.8901 | 0.1228 | 0.1803 | 1.383 | 1.193 | 1.152 |
| Port Fitzroy (offshore) | 7 | 0.8622 | 0.1207 | 0.1745 | 1.343 | 1.157 | 1.117 |
| Motairehe (offshore) | 8 | 0.8378 | 0.1169 | 0.1699 | 1.307 | 1.124 | 1.086 |
| Little Barrier | 9 | 0.8658 | 0.1207 | 0.1752 | 1.349 | 1.161 | 1.121 |
| Mokohinau Islands | 10 | 0.8157 | 0.1153 | 0.1651 | 1.275 | 1.096 | 1.058 |
| Motairehe | 11 | 0.8397 | 0.1173 | 0.1703 | 1.31 | 1.127 | 1.089 |
| Kawa | 12 | 0.8394 | 0.1173 | 0.1702 | 1.31 | 1.126 | 1.088 |
| Port Fitzroy | 13 | 0.8624 | 0.1208 | 0.1746 | 1.344 | 1.157 | 1.118 |
| Rarahara Bay | 14 | 0.8625 | 0.1208 | 0.1746 | 1.344 | 1.157 | 1.118 |
| Whangaparapara | 15 | 0.8901 | 0.1228 | 0.1803 | 1.383 | 1.193 | 1.152 |

⁵ <https://niwa.co.nz/our-science/coasts/research-projects/all/physical-hazards-affecting-coastal-margins-and-the-continental-shelf/news/coastal#tidal>

⁶ <https://niwa.co.nz/services/online-services/tide-forecaster>

⁷ <https://niwa.co.nz/natural-hazards/physical-hazards-affecting-coastal-margins-and-the-continental-shelf/Storm-tide-red-alert-days-2019>

| Name | Site number | M ₂ | S ₂ | N ₂ | Max HW | MHWPS | MHWS10 |
|--------------------------------|-------------|----------------|----------------|----------------|--------------|--------------|--------------|
| Blind Bay | 16 | 0.8854 | 0.1217 | 0.1794 | 1.375 | 1.186 | 1.145 |
| Okupu Bay | 17 | 0.8854 | 0.1217 | 0.1794 | 1.375 | 1.186 | 1.145 |
| Puriri Bay | 18 | 0.8551 | 0.1147 | 0.174 | 1.329 | 1.143 | 1.106 |
| Tryphena | 19 | 0.8541 | 0.1145 | 0.1738 | 1.327 | 1.142 | 1.104 |
| Mulberry Grove | 20 | 0.8533 | 0.1143 | 0.1737 | 1.326 | 1.141 | 1.103 |
| Shoal Bay | 21 | 0.8529 | 0.1143 | 0.1736 | 1.325 | 1.14 | 1.103 |
| Oruawharo Bay | 22 | 0.7844 | 0.1012 | 0.161 | 1.225 | 1.046 | 1.014 |
| Kaitoke Beach | 23 | 0.7836 | 0.1012 | 0.1609 | 1.225 | 1.045 | 1.014 |
| Awana Bay | 24 | 0.7832 | 0.1013 | 0.1608 | 1.226 | 1.045 | 1.014 |
| Whangapoua | 25 | 0.7885 | 0.1043 | 0.1614 | 1.237 | 1.054 | 1.022 |
| Tsunami Gauge (model) | 26 | 0.7833 | 0.1014 | 0.1608 | 1.226 | 1.045 | 1.014 |
| <i>Tsunami Gauge (data)</i> | | <i>0.7818</i> | <i>0.1121</i> | <i>0.1675</i> | <i>1.254</i> | <i>1.061</i> | <i>1.021</i> |
| Tryphena Wharf | 27 | 0.8526 | 0.1142 | 0.1736 | 1.325 | 1.14 | 1.103 |
| Mokohinau wave buoy (offshore) | | 0.814 | 0.1156 | 0.1646 | 1.273 | 1.094 | 1.056 |

The modelled tidal constituents and tide constituents from the Tsunami gauge are included in Table 2-2. This shows that there are only small differences (<0.02 m) between the model and gauge elevations for all tidal constituents, Max HW and MHWPS elevations.

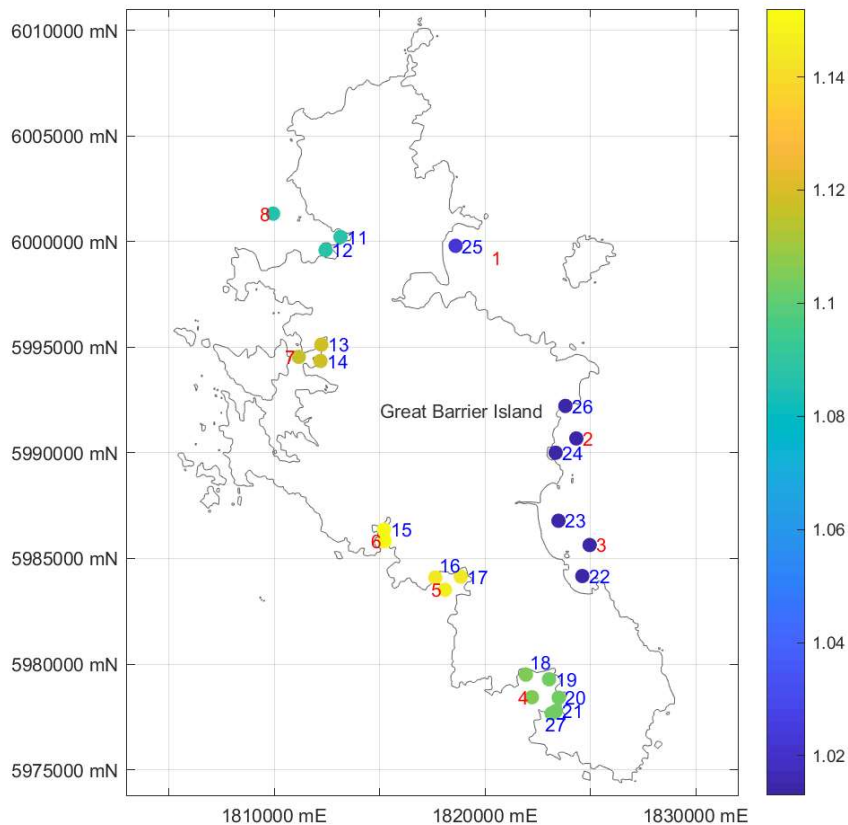


Figure 2-12: Spatial distribution of MHWS10 elevations around Great Barrier Island. Colour represents elevation relative to MSL - to make them relative to AVD-46 requires the addition of MSL datum offset (+0.15 m). Refer to Table A-1 for site coordinates and site name/number reference. [Coordinate system: NZTM].

In Figure 2-12 illustrates that the MHWS-10 tidal elevations around the Island vary within a range of 0.15 with the highest MHWS-10 elevation at Whangaparapara (1.152 m) and the lowest at Awana (offshore)(1.013 m). The MHWS-10 tide elevation is nearly uniform at all east coast sites as it varies by only 0.01 m between (minimum = 1.013 m Awana (offshore), maximum 1.022 m (Whangapoua)). MHWS-10 tide elevations are more variable on the west coast being highest in the middle (1.152 m Whangaparapara) and up to 0.066 m lower to the north (Motairehe) and 0.049 m lower to the south (Tryphena). The differences between the sites mostly due to the M_2 tide being slightly larger at Whangaparapara than the other west coast sites (Table 2-2).

2.3.2 Mean Sea Level Anomaly

Mean Sea Level Anomaly (MSLA) defines the monthly (and greater) sea level anomaly due to climate variability such as seasonal effects, or interannual/interdecadal climate patterns such as ENSO and IPO. MSLA was calculated as the 30-day running average over the full data set after tide has been removed (Figure 2-13). Data is then compiled into a cumulative probability distribution (Figure 2-14) and follows the expected gaussian distribution. The Measured MSLA at Korotiti Bay is ± 0.15 m for 95% of the time, has exceeded ± 0.2 m at times, but was not recorded outside ± 0.25 m (Figure 2-14). This MSLA range aligns with the ± 0.2 m measured on the mainland (Stephens et al. 2016).

MSLA is calculated only here for completeness because the numerical hindcast (Section 2.5) simulated storm surge does not explicitly simulate MSLA, hence separate MSLA calculations were not required for WASP validation. However, the measure of sea level fluctuations that MSLA represents is included within the skew surge distribution and corresponding WASP validation (Section 2.5.2).

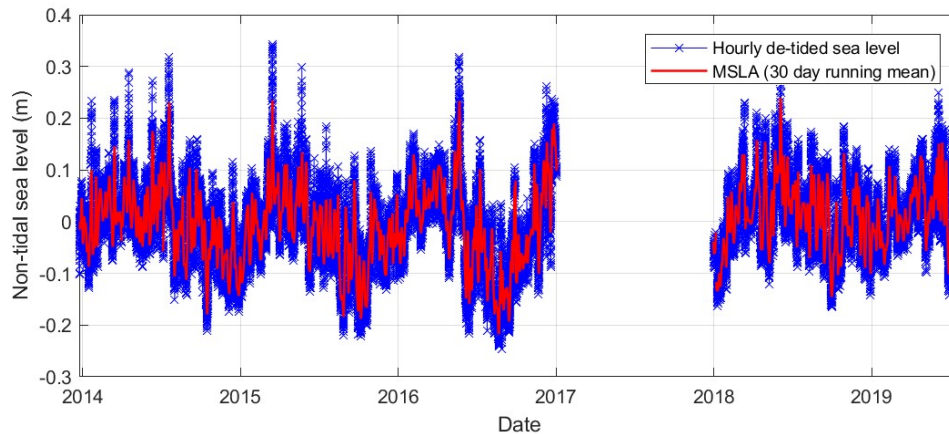


Figure 2-13: Non-tidal residual sea level (blue) and estimated MSLA (red). [Raw Data: GeoNet (Station ID: GBIT), tide data: NIWA EEZ tide model].

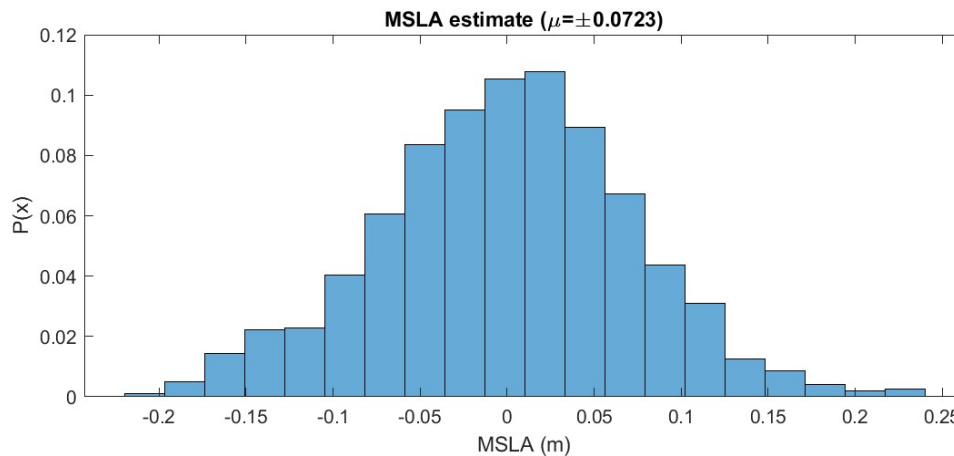


Figure 2-14: MSLA magnitude probability distribution. Vertical axis is probability $P(x)$ of MSLA being observed within each MSLA (m) bin range.

2.4 Wave buoy (Mokohinau)

In February 1998, the Auckland Regional Council deployed a Directional Waverider buoy at (35.91°S, 175.13°E), approximately 2 km north of the Mokohinau Islands group in the approaches to the Hauraki Gulf. The buoy became fully operational in May 1998, recording wave statistics and spectra until June 2004. Complete details on this deployment and the data recorded were outlined in a series of reports to ARC (Gorman, 1999; Gorman and Stephens 2003a,b,c,d). This record was used to verify and calibrate wave records derived from the WASP hindcasts as described below.

2.5 Wave and storm surge hindcasts

NIWA's WASP ("Wave and Storm surge Projections") modelling project derived a set of hindcast records of storm-surge and waves around the entire New Zealand coast. The hindcasts used wind and atmospheric pressure forcing data from the global ERA40 reanalysis (Uppala, Kållberg et al. 2005) which covers the period 1958–2002 with a resolution of 1.225 degrees (~140 km). For the thirty-year period 1970–2000, a "regional climate model" (RCM) has been used (Ackerley, Dean et al. 2012) to dynamically down-scaled ERA40 outputs to a finer resolution of 0.27 degrees (~30 km).

In the WASP project, inputs from these sources were used to provide forcing for both wave and storm surge simulations, covering either the full period 1958–2002 using only ERA40 forcing, or for the 1970–2000 period using both ERA40 and RCM-downscaled forcing. The latter simulations were used in the present application.

Storm surge was modelled using RiCOM (River and Coastal Ocean Model) which is an unstructured grid, finite element model (Walters, Lane et al. 2007) which is used to predict storm surge on an operational basis (Lane, Walters et al. 2009) and has been verified against a comprehensive New Zealand sea level gauge network (Lane and Walters 2009). NIWA also operates a tidal model on the same unstructured mesh.

For wave simulations, the Wavewatch III™ wave model (Tolman 1999, 2009) was used. This is a spectral model that describes the evolution of the wave energy spectrum using an action balance equation that accounts for the transfer of wave energy subject to the processes of generation by wind stress, propagation, four-wave weakly non-linear interactions, and dissipation by white-capping. This was applied on two nested domains (1) a global grid at the same resolution as the ERA40 reanalysis by which it was forced, and (2) a regional grid at 0.125°(longitude) × 0.0833°(latitude) resolution (approximately 9 km), forced by RCM wind fields.

Hourly outputs from both storm surge and wave hindcasts were produced. For the purposes of the present study, for each of the output locations shown in Figure 1-2 and Table A-1 we used archived wave outputs from the nearest grid cell of the regional (9 km) wave model grid, while storm surge and tide outputs were extracted from the nearest of a set of archived output locations on the 50 m depth contour at regular intervals around the New Zealand coastline (Figure 2-15).

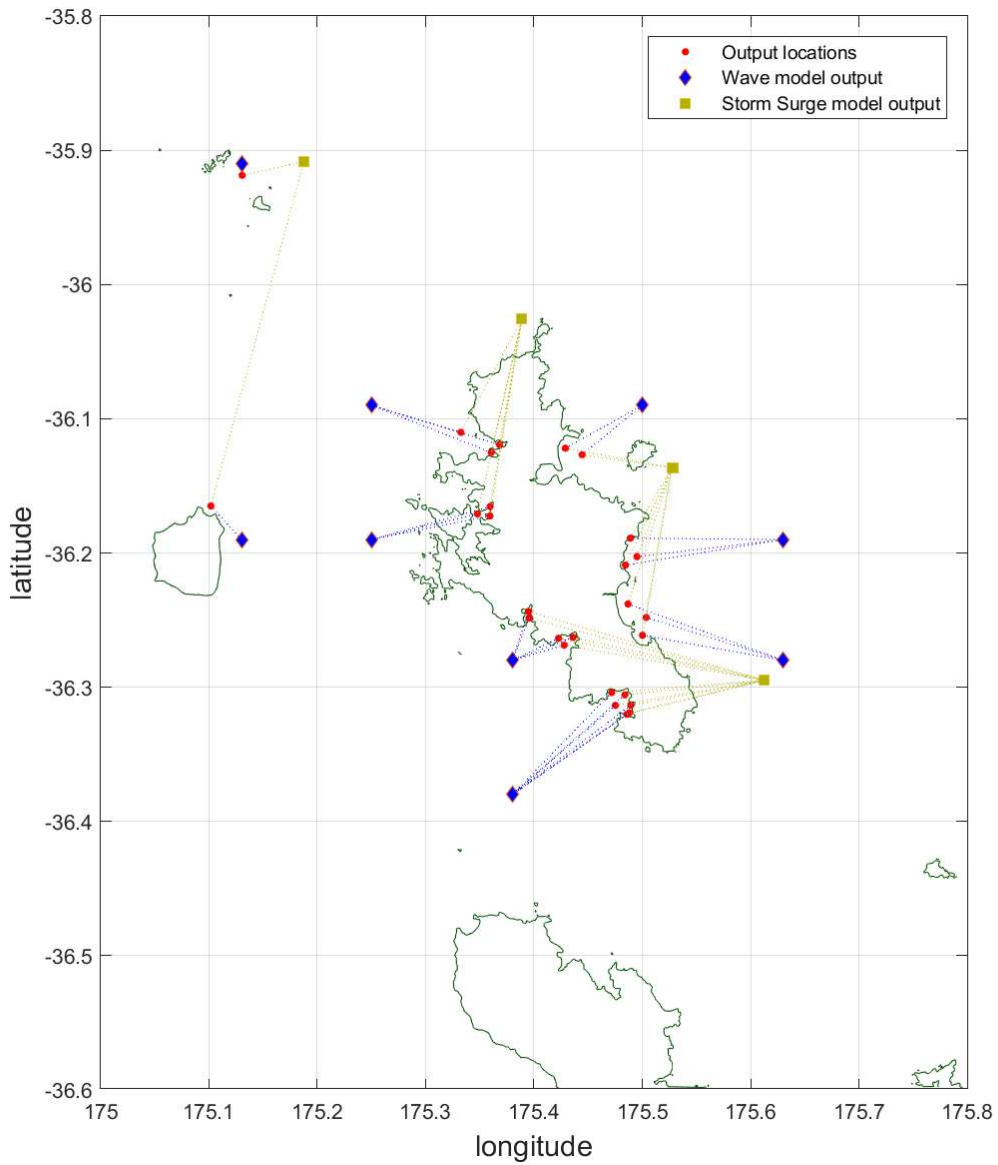


Figure 2-15: Map showing locations from which WASP hindcast outputs were extracted for each nearshore location. Sheltering and scaling corrections were applied to wave model outputs (from locations marked by triangles), while scaling corrections were applied to storm surge outputs (from locations marked by squares) to derive nearshore conditions (locations marked by red dots). Dotted lines connect nearshore locations with the relevant offshore model output locations.

The general wave climate in four quadrants surrounding Great Barrier Island is illustrated by Figure 2-16, which shows occurrence distributions for significant wave height, and Figure 2-17, which shows wave roses, for four WASP output locations located in these quadrants. From Figure 2-16 we observe that the three more exposed sites, NW, NE and SE of Great Barrier Island, all most commonly have significant wave heights in the 0-2 m range, with summer producing the narrowest range of conditions, i.e., with reduced occurrence of both the highest and lowest energy conditions compared to other seasons. On the other hand, winter produces the highest occurrence of the highest energy conditions, but calm conditions are also common. This inter-seasonal variation is most marked to the NW. At the more sheltered southern site (in Colville Channel) the occurrence distribution is notably shifted to lower wave heights compared to the other locations.

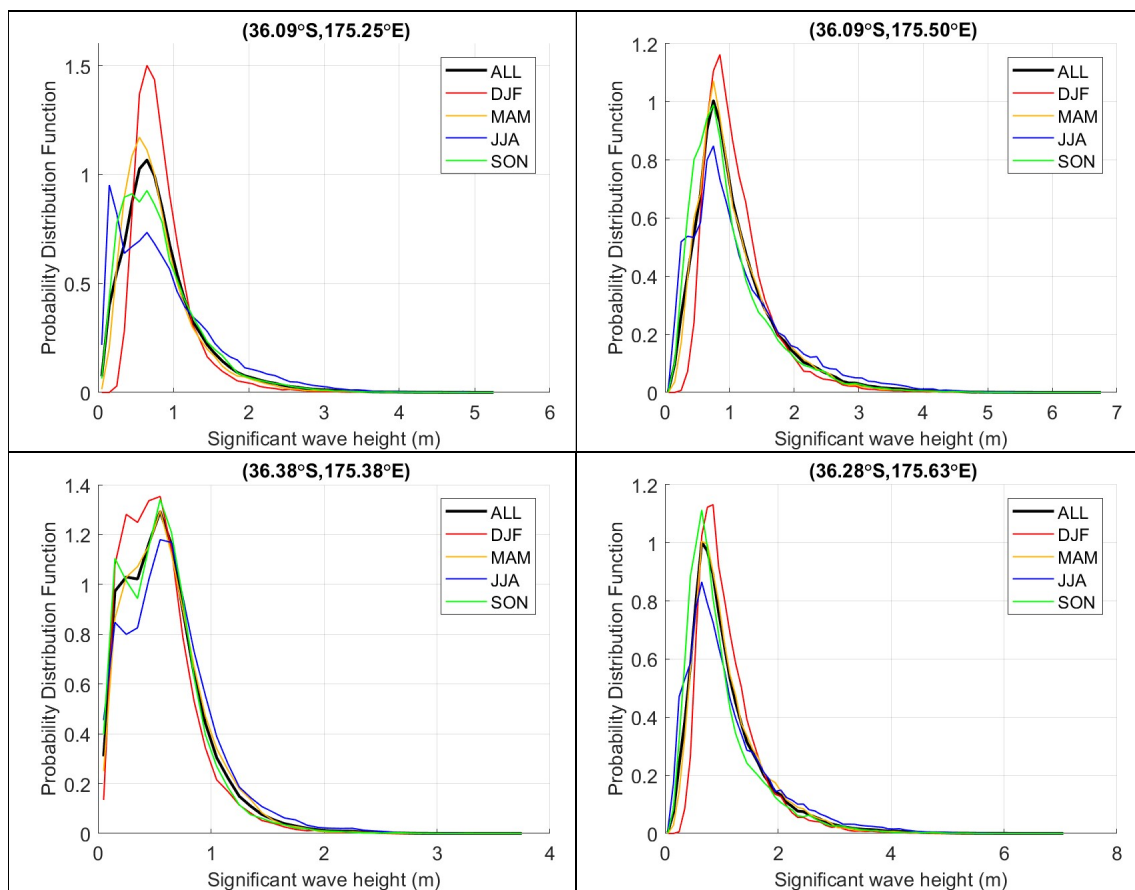


Figure 2-16: Occurrence distributions of significant wave height from four WASP hindcast locations around Great Barrier Island. Output sites are NW (top left panel), NE (top right), S (bottom left) and SE (bottom right) of Great Barrier Island. Coloured lines show seasonal occurrence distributions (red = DJF = summer, yellow = MAM = autumn, blue = JJA = winter, green = SON = spring), while the thicker black line shows the overall (year-round) distribution. Note that different horizontal and vertical scales are used in the four plots.

The wave roses (Figure 2-17) show a predominance of waves from the NE quadrant on the ocean side of the Island (right hand panels). The NW site (top left) is sheltered from the more easterly of these directions, while wave climate in Colville Channel is dominated by easterly swell entering the Hauraki Gulf through the channel, with local generation within the Gulf by south-westerly winds produces a secondary peak in the directional distribution.

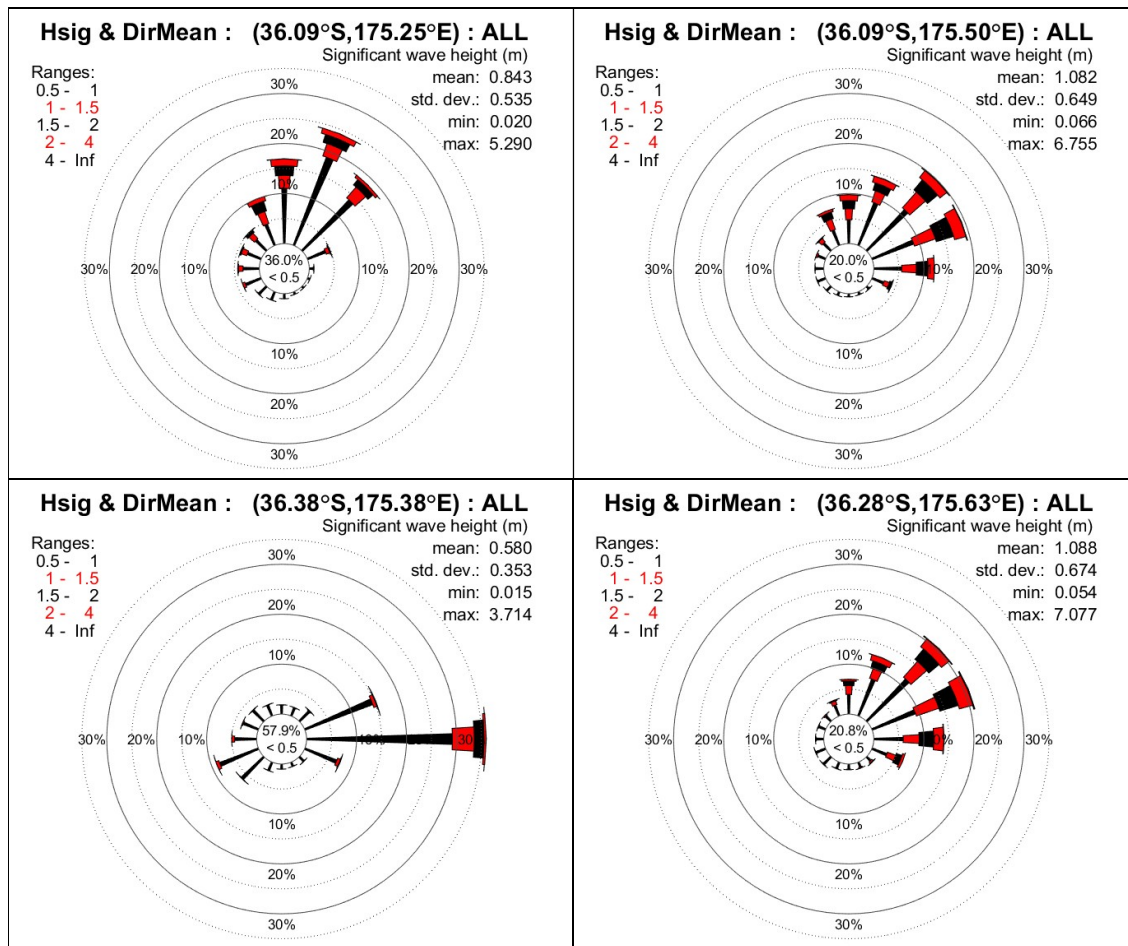


Figure 2-17: Wave roses (joint distributions of significant wave height and mean wave direction) from four WASP hindcast locations around Great Barrier Island. Output sites are NW (top left panel), NE (top right), S (bottom left) and SE (bottom right) of Great Barrier Island. Bars are oriented in the directions FROM which waves are incident.

2.5.1 Wave hindcast corrections

As will be seen in the results (Table 2-5), the extreme skew surge elevations around the island are effectively the same (0.03 m range over all sites at 1% AEP). Extreme sea levels (including wave processes) at each site are therefore differentiated from one another based on the wave climate at each site. Therefore, it is crucial the overall wave climate and inter-site variation is accurate and well verified, as described below.

The regional wave model used in the WASP hindcasts gives a satisfactory representation of typical wave conditions in deep water but has some limitations. Firstly, the model does not adequately resolve wave conditions near the coast, where they are affected by interactions with the coastline and nearshore bathymetry at smaller spatial scales than are represented in the model. For example, a site within a bay will be partially sheltered by nearby headlands from waves arriving from certain directions. Secondly, even in the open ocean the hindcast, tuned to accurately represent wave conditions in the mean, can often underestimate the severity of the most severe storms, especially when these are associated with rapidly-varying weather conditions that are not fully resolved either temporally or spatially. For both these reasons, some adjustment is needed to derive nearshore wave statistics that best represent the extreme events of mostly interest in this study.

The method for estimating wave height adjustments, bring waves onshore, local sheltering and local wind seas, is described in Appendix B. Hindcast storm surge is verified and calibrated against gauge data in Section 2.5.2.

The resulting extreme wave heights results are shown in Table 2-3 and extreme peak wave periods in Table 2-4.

Table 2-3: Extreme significant wave height around Great Barrier Island. Extremes calculated from wave hindcast data and includes wave-sheltering algorithm for embayments. See Figure 1-3 for location map and Table A-1 for coordinates.

| ID | Name | AEP (%) | 63 | 39 | 18 | 10 | 5 | 2 | 1 |
|----|---------------------------|-------------|------|------|------|------|------|------|------|
| | | ARI (years) | 1 | 2 | 5 | 10 | 20 | 50 | 100 |
| 1 | Whangapoua (offshore) | | 3.94 | 4.40 | 4.94 | 5.31 | 5.64 | 6.06 | 6.38 |
| 2 | Awana (offshore) | | 4.64 | 5.21 | 5.91 | 6.42 | 6.88 | 7.59 | 8.11 |
| 3 | Medlands (offshore) | | 4.65 | 5.19 | 5.85 | 6.30 | 6.73 | 7.30 | 7.73 |
| 4 | Shoal Bay (offshore) | | 1.22 | 1.31 | 1.42 | 1.49 | 1.55 | 1.61 | 1.66 |
| 5 | Okupu (offshore) | | 1.27 | 1.36 | 1.46 | 1.53 | 1.59 | 1.65 | 1.70 |
| 6 | Whangaparapara (offshore) | | 0.61 | 0.68 | 0.78 | 0.86 | 0.95 | 1.07 | 1.18 |
| 7 | Port Fitzroy (offshore) | | 0.30 | 0.32 | 0.34 | 0.36 | 0.38 | 0.40 | 0.41 |
| 8 | Motairehe (offshore) | | 3.20 | 3.51 | 3.91 | 4.17 | 4.37 | 4.60 | 4.79 |
| 9 | Little Barrier | | 2.87 | 3.18 | 3.54 | 3.78 | 4.00 | 4.26 | 4.47 |
| 10 | Mokohinau Islands | | 4.70 | 5.20 | 5.80 | 6.19 | 6.59 | 7.08 | 7.48 |
| 11 | Motairehe | | 1.08 | 1.16 | 1.24 | 1.30 | 1.33 | 1.38 | 1.40 |
| 12 | Kawa | | 1.57 | 1.69 | 1.86 | 1.96 | 2.06 | 2.16 | 2.25 |
| 13 | Port Fitzroy | | 0.20 | 0.21 | 0.22 | 0.23 | 0.24 | 0.25 | 0.26 |
| 14 | Rarohara Bay | | 0.20 | 0.21 | 0.22 | 0.23 | 0.24 | 0.25 | 0.26 |
| 15 | Whangaparapara | | 0.41 | 0.47 | 0.53 | 0.59 | 0.64 | 0.72 | 0.78 |
| 16 | Blind Bay | | 0.65 | 0.73 | 0.83 | 0.90 | 0.98 | 1.08 | 1.15 |
| 17 | Okupu bay | | 1.11 | 1.19 | 1.28 | 1.34 | 1.39 | 1.46 | 1.50 |
| 18 | Puriri Bay | | 0.53 | 0.58 | 0.64 | 0.68 | 0.72 | 0.78 | 0.82 |
| 19 | Tryphena | | 1.05 | 1.13 | 1.22 | 1.28 | 1.32 | 1.38 | 1.41 |
| 20 | Mulberry Grove | | 1.00 | 1.07 | 1.16 | 1.21 | 1.25 | 1.29 | 1.32 |
| 21 | Shoal Bay | | 0.60 | 0.64 | 0.69 | 0.72 | 0.75 | 0.77 | 0.79 |

| ID | Name | AEP (%) | 63 | 39 | 18 | 10 | 5 | 2 | 1 |
|----|---------------|-------------|------|------|------|------|------|------|------|
| | | ARI (years) | 1 | 2 | 5 | 10 | 20 | 50 | 100 |
| 22 | Oruawharo Bay | | 4.35 | 4.85 | 5.44 | 5.88 | 6.26 | 6.77 | 7.16 |
| 23 | Kaitoke Beach | | 4.43 | 4.98 | 5.65 | 6.13 | 6.58 | 7.23 | 7.66 |
| 24 | Awana Bay | | 4.46 | 5.02 | 5.67 | 6.17 | 6.65 | 7.31 | 7.79 |
| 25 | Whangapoua | | 2.85 | 3.21 | 3.62 | 3.94 | 4.24 | 4.63 | 4.89 |

Table 2-4: Extreme peak wave period around Great Barrier Island. Extremes calculated from wave hindcast data and includes wave-sheltering algorithm for embayments. See Figure 1-3 for location map and Table A-1 for coordinates.

| ID | Name | AEP (%) | 63 | 39 | 18 | 10 | 5 | 2 | 1 |
|----|---------------------------|-------------|------|------|------|------|------|------|------|
| | | ARI (years) | 1 | 2 | 5 | 10 | 20 | 50 | 100 |
| 1 | Whangapoua (offshore) | | 14.1 | 14.8 | 15.6 | 16.1 | 16.5 | 17.0 | 17.4 |
| 2 | Awana (offshore) | | 14.1 | 14.8 | 15.8 | 16.5 | 17.2 | 18.0 | 18.9 |
| 3 | Medlands (offshore) | | 14.7 | 15.5 | 16.6 | 17.3 | 18.1 | 19.2 | 20.0 |
| 4 | Shoal Bay (offshore) | | 7.6 | 8.0 | 8.5 | 8.9 | 9.2 | 9.5 | 9.7 |
| 5 | Okupu (offshore) | | 9.5 | 10.2 | 11.0 | 11.5 | 12.1 | 12.7 | 13.2 |
| 6 | Whangaparapara (offshore) | | 4.4 | 4.7 | 4.9 | 5.1 | 5.3 | 5.4 | 5.6 |
| 7 | Port Fitzroy (offshore) | | 2.0 | 2.1 | 2.2 | 2.2 | 2.3 | 2.3 | 2.4 |
| 8 | Motairhe (offshore) | | 13.9 | 14.6 | 15.5 | 16.2 | 16.9 | 17.6 | 18.2 |
| 9 | Little Barrier | | 16.5 | 17.3 | 18.3 | 19.0 | 19.6 | 20.4 | 21.0 |
| 10 | Mokohinau Islands | | 16.1 | 16.9 | 17.8 | 18.3 | 18.8 | 19.5 | 20.0 |
| 11 | Motairhe | | 7.0 | 7.4 | 7.8 | 8.1 | 8.4 | 8.7 | 8.9 |
| 12 | Kawa | | 8.9 | 9.4 | 10.0 | 10.5 | 10.9 | 11.3 | 11.7 |
| 13 | Port Fitzroy | | 1.7 | 1.7 | 1.8 | 1.8 | 1.8 | 1.8 | 1.9 |
| 14 | Rarohara Bay | | 1.7 | 1.7 | 1.8 | 1.8 | 1.8 | 1.8 | 1.9 |
| 15 | Whangaparapara | | 3.9 | 4.1 | 4.3 | 4.5 | 4.6 | 4.8 | 4.9 |
| 16 | Blind Bay | | 5.0 | 5.2 | 5.5 | 5.7 | 5.9 | 6.1 | 6.2 |
| 17 | Okupu bay | | 8.0 | 8.6 | 9.3 | 9.8 | 10.2 | 10.7 | 11.1 |
| 18 | Puriri Bay | | 2.8 | 2.9 | 3.1 | 3.2 | 3.3 | 3.4 | 3.5 |
| 19 | Tryphena | | 6.5 | 6.8 | 7.2 | 7.5 | 7.7 | 8.0 | 8.2 |
| 20 | Mulberry Grove | | 5.8 | 6.2 | 6.5 | 6.8 | 7.0 | 7.2 | 7.4 |
| 21 | Shoal Bay | | 3.4 | 3.6 | 3.8 | 4.0 | 4.1 | 4.2 | 4.3 |
| 22 | Oruawharo Bay | | 14.1 | 14.9 | 15.9 | 16.5 | 17.1 | 17.8 | 18.4 |
| 23 | Kaitoke Beach | | 13.8 | 14.5 | 15.6 | 16.4 | 17.3 | 18.5 | 19.7 |
| 24 | Awana Bay | | 13.4 | 14.1 | 15.0 | 15.7 | 16.4 | 17.3 | 18.1 |
| 25 | Whangapoua | | 9.9 | 10.3 | 10.9 | 11.2 | 11.6 | 12.1 | 12.4 |

2.5.2 Storm surge hindcast validation against tsunami gauge data

The record from the Great Barrier Island tsunami gauge commenced after the end of the WASP hindcast, so the two cannot be directly compared. Instead, we can compare the statistical occurrence of skew surge (defined as illustrated in Figure 2-19) derived from the two sources. A quantile-quantile plot (Figure 2-18) shows that the hindcast somewhat underestimates the observed skew surge. Therefore, a linear rescaling of the form

$$\text{corrected skew surge} = 0.018712 + 1.105109 \times \text{hindcast skew surge}$$

is appropriate to bring the hindcast estimates into line with the gauge data.

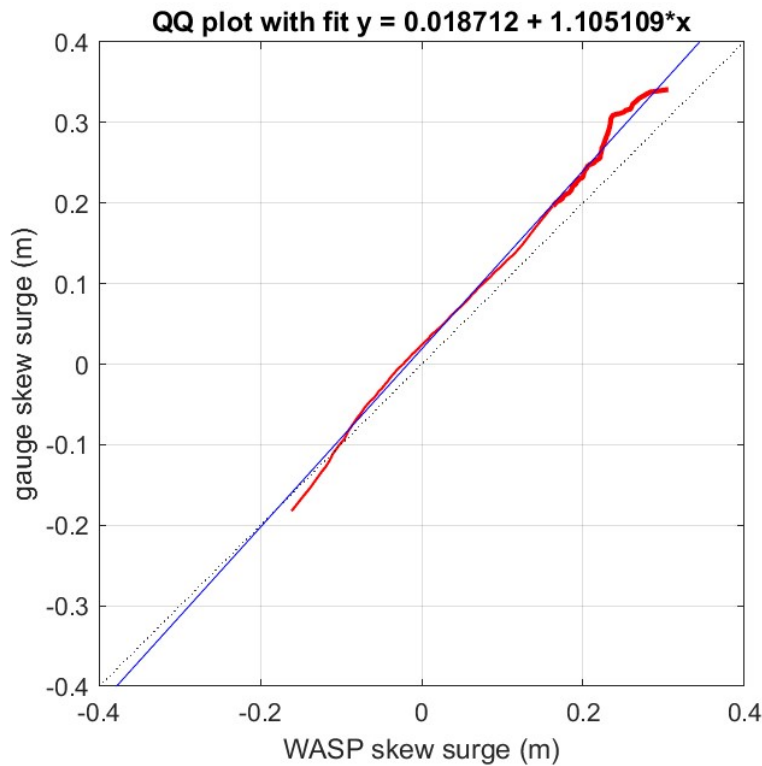


Figure 2-18: Quantile-quantile plot of skew surge values measured by the Great Barrier Island tsunami gauge, and from the WASP hindcast extracted for the same location. The red line compares corresponding quantiles from the two records, while the blue line is a linear fit to the quantile data. An equivalence line (dotted) is also shown.

The resulting extreme skew surge results are shown in Table 2-5.

Table 2-5: Extreme skew-surge magnitude around Great Barrier Island. Extremes calculated from hindcast data. See Figure 1-3 for location map and Table A-1 for coordinates.

| ID | Name | AEP (%) | 63 | 39 | 18 | 10 | 5 | 2 | 1 |
|----|---------------------------|-------------|------|------|------|------|------|------|-----|
| | | ARI (years) | 1 | 2 | 5 | 10 | 20 | 50 | 100 |
| 1 | Whangapoua (offshore) | 0.25 | 0.27 | 0.30 | 0.33 | 0.35 | 0.37 | 0.39 | |
| 2 | Awana (offshore) | 0.25 | 0.27 | 0.30 | 0.33 | 0.35 | 0.37 | 0.40 | |
| 3 | Medlands (offshore) | 0.25 | 0.27 | 0.30 | 0.33 | 0.35 | 0.37 | 0.39 | |
| 4 | Shoal Bay (offshore) | 0.24 | 0.27 | 0.30 | 0.33 | 0.35 | 0.38 | 0.39 | |
| 5 | Okupu (offshore) | 0.24 | 0.27 | 0.31 | 0.33 | 0.35 | 0.38 | 0.40 | |
| 6 | Whangaparapara (offshore) | 0.25 | 0.27 | 0.31 | 0.33 | 0.35 | 0.38 | 0.40 | |
| 7 | Port Fitzroy (offshore) | 0.24 | 0.27 | 0.30 | 0.33 | 0.35 | 0.38 | 0.40 | |
| 8 | Motairehe (offshore) | 0.24 | 0.27 | 0.30 | 0.32 | 0.35 | 0.37 | 0.39 | |
| 9 | Little Barrier | 0.24 | 0.27 | 0.30 | 0.33 | 0.35 | 0.37 | 0.39 | |
| 10 | Mokohinau Islands | 0.24 | 0.27 | 0.30 | 0.33 | 0.35 | 0.38 | 0.40 | |
| 11 | Motairehe | 0.24 | 0.27 | 0.30 | 0.33 | 0.35 | 0.38 | 0.40 | |
| 12 | Kawa | 0.24 | 0.27 | 0.30 | 0.32 | 0.35 | 0.37 | 0.39 | |
| 13 | Port Fitzroy | 0.24 | 0.27 | 0.30 | 0.33 | 0.35 | 0.38 | 0.40 | |
| 14 | Rarohara Bay | 0.24 | 0.27 | 0.30 | 0.33 | 0.35 | 0.38 | 0.40 | |
| 15 | Whangaparapara | 0.25 | 0.27 | 0.31 | 0.33 | 0.35 | 0.38 | 0.40 | |
| 16 | Blind Bay | 0.25 | 0.27 | 0.31 | 0.33 | 0.35 | 0.38 | 0.40 | |
| 17 | Okupu bay | 0.24 | 0.27 | 0.30 | 0.33 | 0.35 | 0.38 | 0.40 | |
| 18 | Puriri Bay | 0.24 | 0.27 | 0.31 | 0.34 | 0.36 | 0.39 | 0.42 | |
| 19 | Tryphena | 0.24 | 0.27 | 0.30 | 0.33 | 0.35 | 0.38 | 0.40 | |
| 20 | Mulberry Grove | 0.24 | 0.27 | 0.30 | 0.33 | 0.35 | 0.38 | 0.40 | |
| 21 | Shoal Bay | 0.24 | 0.27 | 0.30 | 0.32 | 0.35 | 0.37 | 0.39 | |
| 22 | Oruawharo Bay | 0.25 | 0.27 | 0.30 | 0.33 | 0.35 | 0.37 | 0.39 | |
| 23 | Kaitoke Beach | 0.25 | 0.27 | 0.30 | 0.33 | 0.35 | 0.37 | 0.39 | |
| 24 | Awana Bay | 0.25 | 0.27 | 0.30 | 0.33 | 0.35 | 0.38 | 0.40 | |
| 25 | Whangapoua | 0.25 | 0.27 | 0.30 | 0.33 | 0.35 | 0.38 | 0.40 | |

2.6 Joint probability extreme value analysis

The above procedures provide a 30-year (1970–2000) hindcast of significant wave height, peak wave period, and tidal and storm surge components that contribute to total water level at each site.

Note that both components of the model-derived water level are referred to a nominal present-day Mean Sea Level (MSL) datum of zero, not including any datum offsets or longer-term variation in sea level, e.g., from large scale climatic variations in ocean circulation. A vertical offset of 0.15 m was added to these levels to produce water levels referred to AVD-46. The offset of 0.15 m represents the mean sea level observed at the port of Auckland in the 2006–2011 period (Stephens et al. 2016) and also 1999–2008 (Hannah and Bell, 2012). For consistency with the 2016 study we have assumed the mean sea level is similar between Great Barrier Island and Auckland—the Great Barrier gauge is

not reliable for MSL calculation due to drifts in the pressure sensor (but is capable of resolving shorter-term sea-level fluctuations like tides and storm surge).

From the sea-level gauge record, times and tidal elevation at each high water were identified. Similarly, each peak in the total water level was identified, allowing the skew surge to be computed, as the difference (total – tide) between each high tide level and the nearest peak high-water level (Figure 2-19).

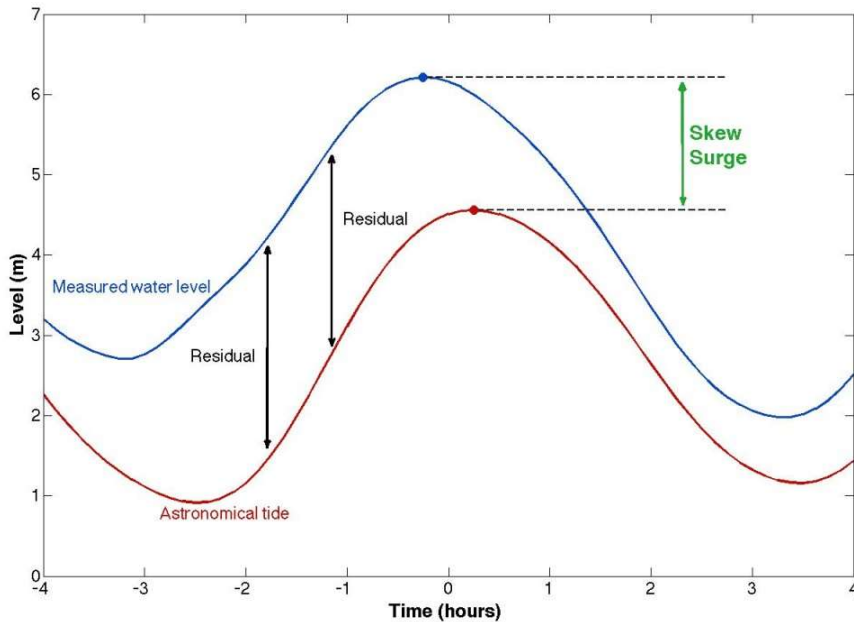


Figure 2-19: Illustration of the definition of skew surge. Skew surge is the difference between the maximum observed water level and the maximum predicted tidal level, which may occur at different times. [Source: <https://www.surgewatch.org/definition/skew-surge/>].

Extreme value analyses of the combined effects of waves and water levels were carried out using a multivariate joint-probability approach as described by Heffernan and Tawn (2004). This method is similar to the JOIN-SEA software developed by HR Wallingford (Hawkes et al. 2002), which was used in the 2016 project—both methods calculate the joint probability of simultaneous large waves and storm tides. Like JOIN-SEA, the Heffernan, Tawn (2004) method recognises that the various contributors to extreme conditions, e.g., tides, storm surge and waves, rarely achieve their individual extreme values simultaneously. For example, the storm surge, tidal level, and wave height values that individually have a 1% AEP would be expected to occur simultaneously with a much lower AEP (much smaller than 1%), unless they were perfectly correlated and coincide in time. On the other hand, they have *some* correlation, as, for example, large storm surge and high waves will both tend to occur sometime during the passage of intense storms, while higher water levels also allow larger waves to reach a given nearshore location. Hence, they cannot be treated as completely independent (in which case the joint AEP would be $1\% \times 1\% \times 1\% = 0.0001\%$, which is too low in reality). Therefore, in the results tables in Section 3, the singular water level components for a specific AEP from the different Tables cannot simply be added to obtain the total water level for the same AEP.

Instead, the Heffernan and Tawn (2004) approach quantifies the actual interdependence between extreme values of several variables, based on available records. This then allows a statistical model to be developed to simulate extreme values of these “dependent” variables over a longer time period. Secondary variables can also be simulated, where they either have a known dependency on the original “base” variables, or to be completely independent.

In our case, we selected skew surge, significant wave height, and peak wave period as the base variables.

In the first step the original data, consisting of values of all variables at high water, were decluttered, to select independent peak events with at least one of the base variables above its 50th percentile value, separated by at least two days (and therefore assumed to be distinct events).

Extreme value distributions for each of the base variables, considered separately (i.e., “marginal” distributions), were then computed. This involved fitting a Generalised Pareto Distribution to the extreme values individually, defined as the peaks above the 95th percentile. This allowed return values (with 95% confidence intervals) for each of the dependent variables to be estimated. Inter-dependencies were then derived, again based on peak values above the 95th percentile.

We then generated 5,000-year simulations of the base variables, sampling for each time from the computed marginal (individual component) distributions and inter-component dependencies. High water tide levels for each of the simulation times were then derived by random selection from the distribution of high tide levels obtained from the original record, i.e., tides were treated as independent of the skew surge and wave variables, because a storm event can occur at any high tide (the tide is solely generated by astronomical forcing).

Given the 5,000-year length of the resulting simulated record, it is now possible to compute return values for intermediate return periods by a direct ‘countback’ method, rather than by extrapolating a fitted extreme value distribution fitted to a shorter record. For example, the 100th highest event of a 5,000-year record represents the 2% AEP (50-year return period) value. This approach was applied to estimate return values for each of the simulated variables listed below, for Annual Exceedance Probability (AEP) ranging as low as 1%, i.e., Annual Recurrence Interval (ARI) up to 100 years

- Skew surge
- Storm-tide
- Significant wave height
- Peak wave period
- Wave setup
- Wave runup
- Storm-tide with wave setup
- Storm-tide with wave runup (including setup)

where the simulated values of wave setup and runup were derived using a linear-equivalent beach slope (see Section 2.7 following) and the predicted water levels, significant wave heights and peak wave periods in the 5,000 year simulated record.

2.7 Wave setup and runup estimates

Wave runup and wave setup are coincident processes caused solely by the interaction of waves with the sloping coast (e.g., Figure 1-1).

Individual waves reaching the coast produce a surge of water up the slope followed by a return flow down the slope, often after the wave has broken. The vertical level reached by this flow is called the “runup” level (and the vertical level by the return flow is the run-down “level”). The runup level will vary from wave to wave, so it is necessary to characterise it by a representative upper value, appropriate to estimate extreme conditions. The standard measure in coastal engineering studies is $Ru_{2\%}$, the vertical level or runup (above the still water level) exceeded by only 2% of individual waves.

Wave setup is a sustained increase in the mean water level at the shore compared to the level further offshore beyond the surf zone that is induced by the transfer of momentum from waves as they break over a sloping foreshore. Setup is localised to the surf zone but is a meaningful addition to the extreme storm-tide levels.

The magnitude of wave setup can be estimated (Stockdon, Holman et al. 2006) as

$$z_{setup} = 0.35\beta\sqrt{H_{m0}L_{m-1,0}}$$

where β is the mean beach slope. H_{m0} and $L_{m-1,0}$ are the significant wave height and mean wavelength in deep water. The mean wavelength is related to the mean wave period $T_{m-1,0}$ (derived from spectral moments) by

$$L_{m-1,0} = \frac{g}{2\pi}T_{m-1,0}^2$$

Where, as in our case, the peak wave period T_p is more directly available than the mean period, an empirical relationship

$$T_p = 1.1T_{m-1,0}$$

can be used. In these definitions, the “deep water” parameters H_{m0} , $L_{m-1,0}$, T_p refer to conditions outside the surf zone before shoaling and breaking effects begin to take effect: in our case we took these values from the sheltering-corrected values derived from the hindcast as described in Section 2.5.1.

The total wave runup, including setup, can be estimated (Stockdon, Holman et al. 2006) as

$$Ru_{2\%} = 1.1(0.35\beta\sqrt{H_{m0}L_{m-1,0}} + 0.5H_{m0}L_{m-1,0}(0.563\beta^2 + 0.004))$$

2.8 Calibration with site survey data

Wave setup and runup are strongly dependent on the assumed beach slope, as described above. The beach surveys described in Section 2.1 provide a means of estimating values of beach slope to use in deriving estimates of runup and setup, which can then be compared with the evidence of debris lines observed in the same surveys. However, because of the high spatial and temporal variability in surveyed beach slopes discussed in Section 2.1, we took the approach of treating β as an adjustable local parameter at each of the 16 inshore sites, and used it to calibrate the predicted storm-tide + wave runup (including setup) elevations against the distributions of surveyed debris lines. This procedure effectively calculates a linear-equivalent beach slope by tuning the predicted runup

elevation to debris features to obtain a site-specific β . This process allows for a consistent approach to each site for estimating the wave setup contribution to the extreme sea levels.

In particular, β values were adjusted so that the 63% AEP (1-year ARI) value of storm-tide + combined wave runoff (including setup) matched either to the 50th or the 75th percentile value of debris line elevation. These elevations are plotted in Figure 2-20 and Figure 2-21, respectively, with box plots of surveyed debris line elevations overlaid for comparison. Calibrating to these elevations effectively assumes that the 50th or 75th percentile highest debris lines on the island were deposited by a 1-year ARI event. This assumption is reasonable based on the observations of debris composition around the Island as discussed in Section 2.2.2.

Results of the extreme storm-tide + wave runoff (including setup) are included in Table C-1 (Appendix C).

Note that an extensive internet search yielded no reliable photographs of extreme sea-level inundation or flooding, and none associated with specific events which could be assigned a return interval to provide an independent validation event. If these become available, then the results may be further checked.

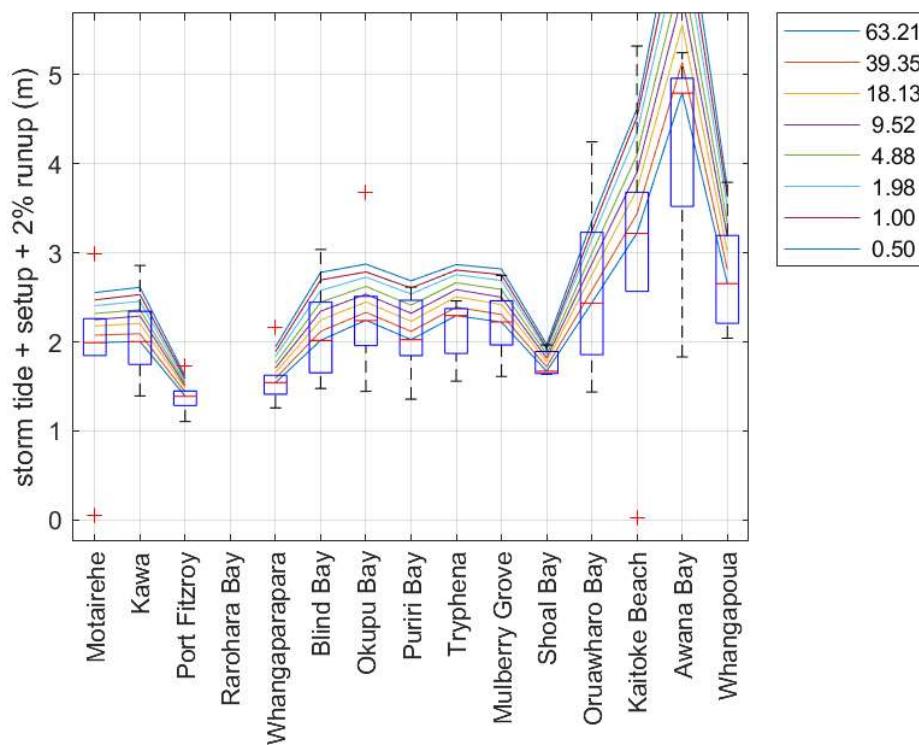


Figure 2-20: Return values of the vertical level of storm tide plus wave runoff (including setup), with beach slope tuned to match the 63% AEP value against the 50th percentile value of debris line elevation. Corresponding AEP values for total water level are shown in the legend. Box plots show the minimum, maximum, 25th, 50th and 75th percentile values of debris line elevation.

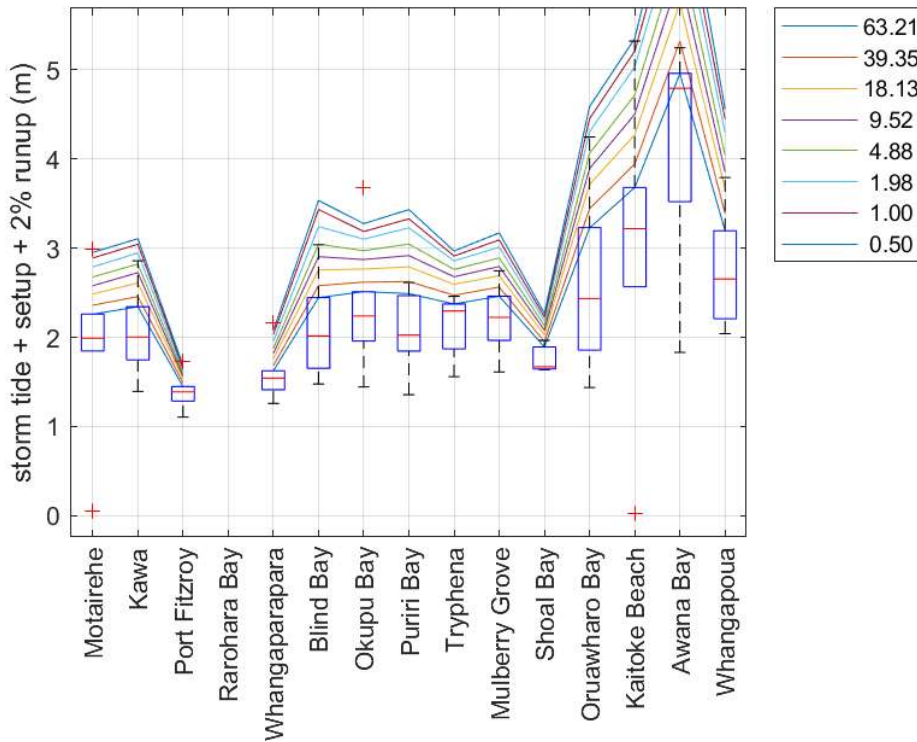


Figure 2-21: Return values of the vertical level of storm tide plus wave runoff and setup, with beach slope tuned to match the 63% AEP value against the 75th percentile value of debris line elevation. Corresponding AEP values for total water level are shown in the legend. Box plots show the minimum, maximum, 25th, 50th and 75th percentile values of debris line elevation.

The average difference between the estimated storm-tide + wave runoff (including setup) elevations as calibrated to the 50th and 75th percentile debris line elevations is 0.34 m (range = 0.1–0.8 m) at 63% AEP, where the 75th centile value is always greater. We adopted the higher beach slopes (and hence higher elevations) to be conservative in the estimation of extreme sea-levels at the coast which include wave runoff and setup. This conservatism is commensurate with the uncertainty associated with using short data records (e.g., tide gauge, single day of beach observations) to adjust the 63% AEP predictions and then extrapolating to more extreme events.

Validation checks were performed to confirm this calibration produced reasonable results at each site and across the range of AEP events.

2.9 Validation checks on wave runoff estimates

Validation checks include 1) comparison with beach features, 2) bay-wide mapping comparison with debris lines and 3) comparison with measures beach slopes.

2.9.1 Comparison with surveyed beach slopes

The beach slopes obtained from this twin calibration/validation procedure are compared with data obtained from survey records within 1–2 m above AVD-46 in Figure 2-22, and from survey records within 2–3 m above AVD-46 in Figure 2-23.

Using the beach slope as an adjustable parameter allowed tuning of the wave runup elevation to each site based on site-specific data. The main reason for this is because the measured beach profiles are non-linear or composite profiles (i.e., β varies throughout elevation - refer to Section 2.2.3) whereas the Stockdon et al. (2006) equations use a constant linear slope.

The calculated linear equivalent beach slopes are generally steeper than the median measured beach slopes (Figure 2-22 and Figure 2-23), and can be steeper than the 75th percentile measured slope. This indicates that if the beach were linear then a storm-steepened beach slope would be required to reproduce the wave runup elevations. However, many Great Barrier beaches have composite profiles, can include near-vertical seawalls, storm-berms and offshore rock platforms which affect the wave runup and resulting beach profile.

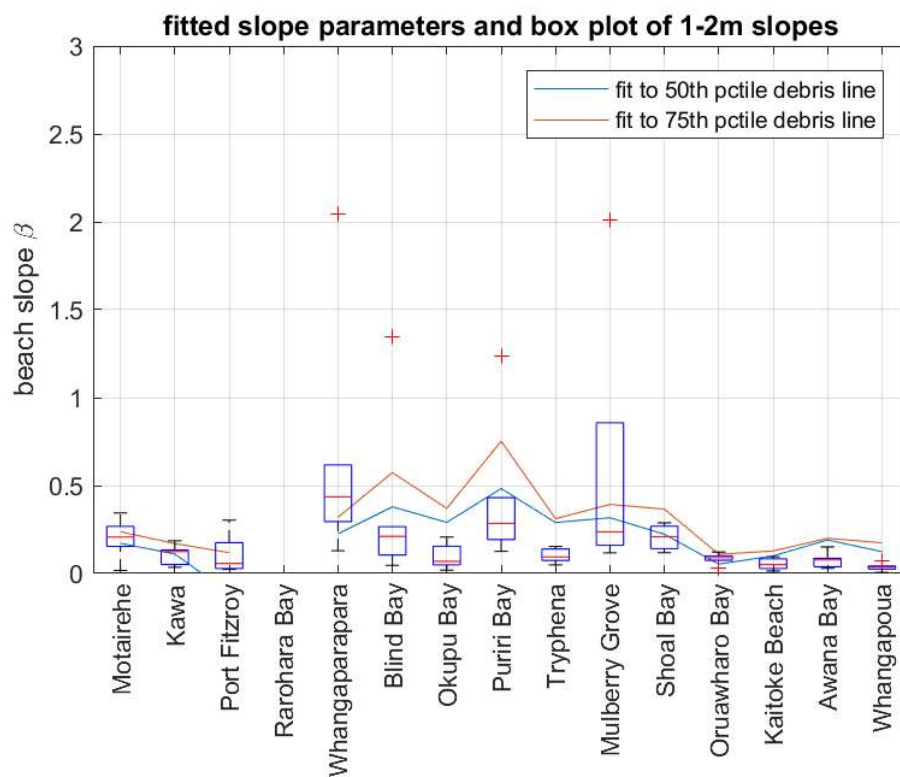


Figure 2-22: Values of the beach slope β resulting from calibration of storm tide plus wave runup and setup against debris line records, compared with beach slopes derived from survey records within the elevation range 1-2 m above AVD-46. Coloured lines show results of fitting the 63% AEP value of storm tide + setup + runup against either the 50th or 75th percentile value of debris line elevation. Box plots show the minimum, maximum, 25th, 50th and 75th percentile values of beach slopes. The crosses are deemed to be outliers.

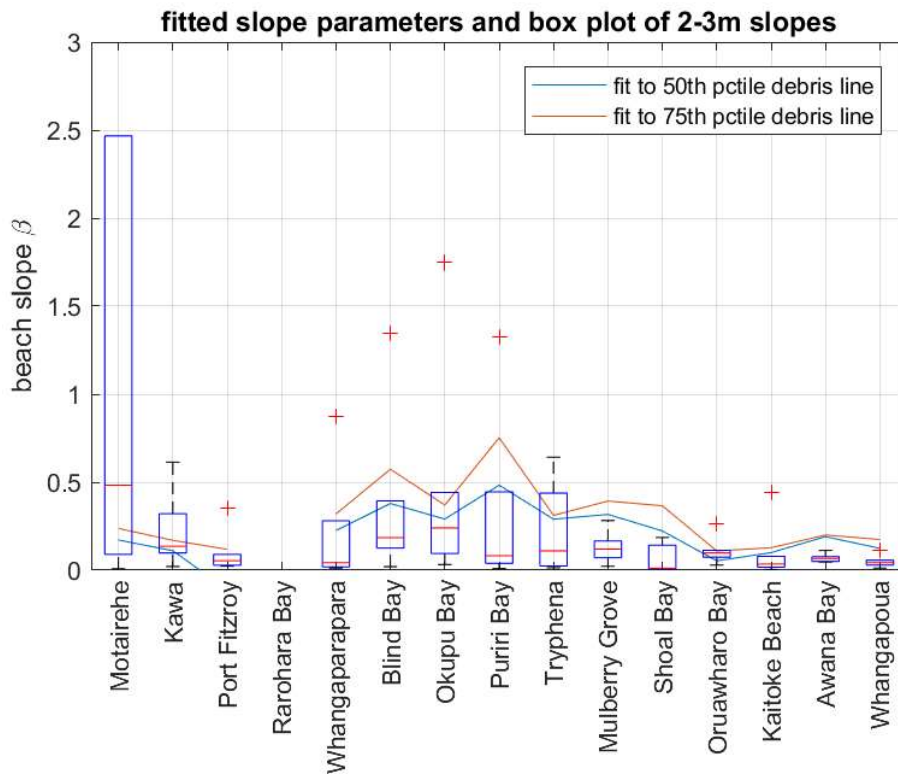


Figure 2-23: Values of the beach slope β resulting from calibration of storm tide plus wave runup and setup against debris line records, compared with beach slopes derived from survey records within the elevation range 2-3 m above AVD-46. Coloured lines show results of fitting the 63% AEP value of storm tide + setup + runup against either the 50th or 75th percentile value of debris line elevation. Box plots show the minimum, maximum, 25th, 50th and 75th percentile values of beach slopes. The crosses are deemed to be outliers.

If there were long-term beach profile monitoring data available, then we would have examined the beach slope variability and chosen a relatively steep beach slope to be conservative (steep beach = larger runup and setup). This method has been applied where a long-term beach profile monitoring records is available (e.g., Bay of Plenty and Canterbury see Stephens et al. (2015a, 2018a)) with good correlation between predicted wave runup and historic survey debris/runup records when using the “storm” beach slope is established as the 97th percentile beach slope from a long survey record. Hence, we expect that the fit of the linear equivalent beach slope would align with this “storm” beach slope if a long-term monitoring record were available for Great Barrier. Therefore, that the calculated beach slopes align or exceed the 75th percentile beach slope (Figure 2-22 and Figure 2-23) is not unexpected from a single day of surveying and therefore validates the approach used here.

2.9.2 Beach feature check

A change in slope (“break in slope” or “slope break”) occurs some distance inland from the high-tide line where the wave/tide dominant processes have less effect on beach slope than secondary processes such as vegetation growth and wind transport of sand. On a simple beach (i.e., no berms, seawalls or nearshore reefs such as Oruawharo or Awana) this slope break is also a geomorphic identifier which indicates the wave runup limit during a storm when sand dunes would be undercut and eroded.

The slope-break was observed at an elevation of about 4 m at Oruawharo Beach (Figure 2-24) and 5.5 m at Awana Bay (Figure 2-25). On a bay-wide basis this geomorphic identifier is within the range of predicted storm-tide + wave runup (including setup) elevations for all predicted exceedance probabilities. This validates that the use of a single beach slope value (which had been calibrated to only the 63% AEP event at 75th percentile debris line elevations) results in a realistic series of extreme runup elevations when applied to the less frequent events.

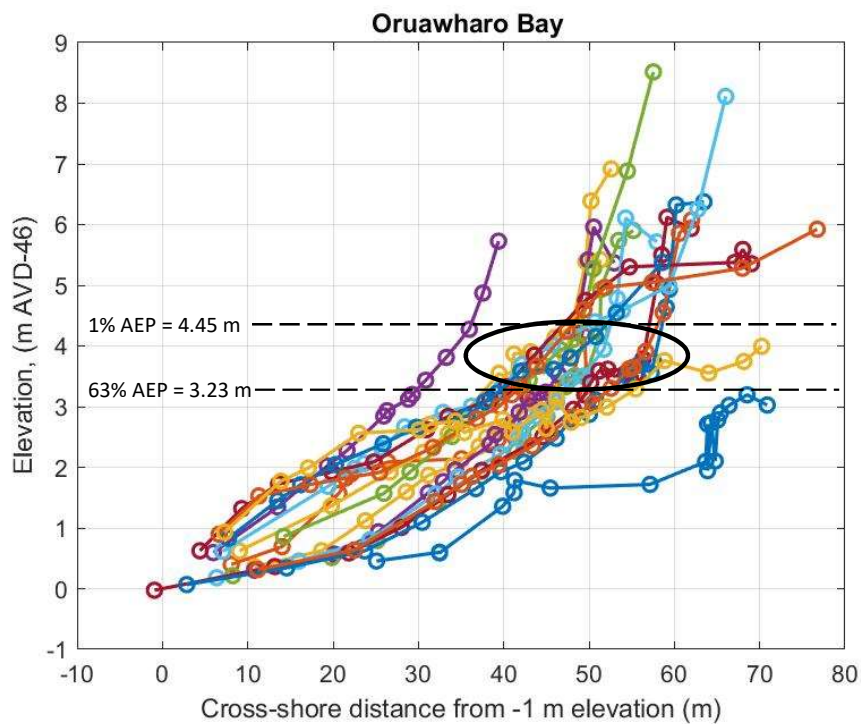


Figure 2-24: Cross-shore transects (coloured lines) measured at Oruawharo Bay with predicted 1% AEP and 63% AEP (annotations, dashed lines) extreme storm-tide + wave runup (including setup) elevations, and identified “slope break” zone (black oval). Horizontal axis is the linear cross-shore distance from the profile interpolated to the -1 m elevation. Elevations in m AVD-46.

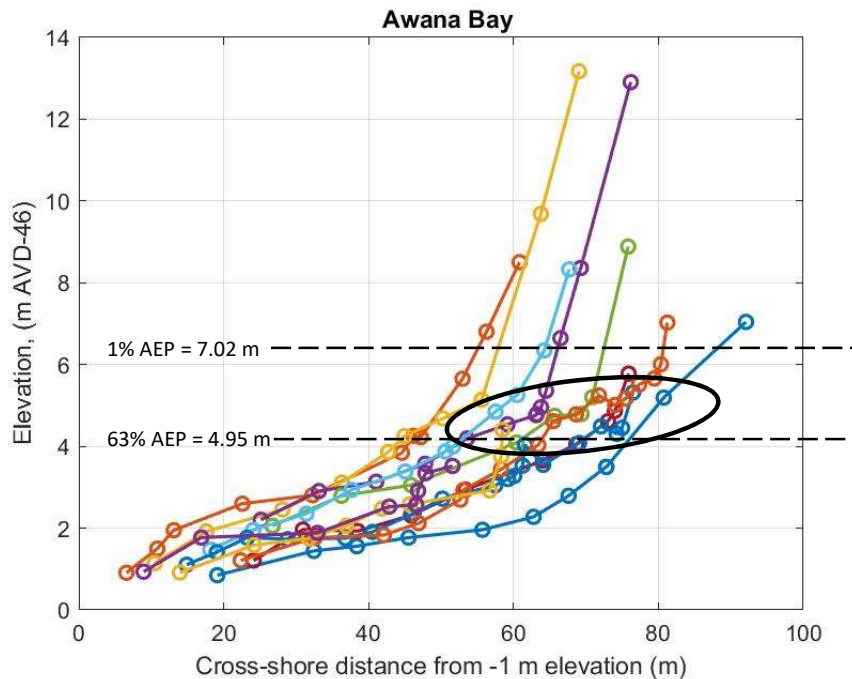


Figure 2-25: Cross-shore transects (coloured lines) measured at Awana Bay with predicted 1% AEP and 63% AEP (annotations, dashed lines) extreme storm-tide + wave runup (including setup) elevations, and identified “slope break” zone (black oval). Horizontal axis is the linear cross-shore distance from the profile interpolated to the -1 m elevation. Elevations in m AV/D-46.

2.9.3 Bay-wide mapping comparison

To confirm this procedure produced reasonable results at each of the 16 inshore sites, we plotted an aerial photograph, the measured debris features and the elevation contour (from LiDAR) of the 1-year ARI storm-tide + wave runup (including setup). Full results shown in Appendix C.

The simulated wave runup contours are only expected to be in general agreement around each bay with the debris features because:

- Each bay only has a single extreme sea-level elevation (based on 75th centile beach debris line elevation) and hence the simple does not reproduce the intra-bay variability in debris features which can be 2 metres or more within a single bay (e.g., Figure 2-6) depending on the local effects of wave sheltering by headlands and other features (see discussion in Section 2.2.2).
- The runup equations assumes the linear equivalent beach slope is planar and continues upwards and inland from the coast. However, local beach features will also affect the wave runup elevation (i.e., features such as sand bars, local shoreline berms, rock outcrops, seawalls, stream mouths, composite beach slopes and vegetation/mangroves) but the model cannot account for these local reductions to wave runup and hence the output contours may be further inland than the surveyed debris lines. This is evident at Motairehe (Figure 2-26) where the inland runup on the beach/shore matches the observations, however the runup contour extends far inland up the stream mouth and appears to ‘overpredict’.

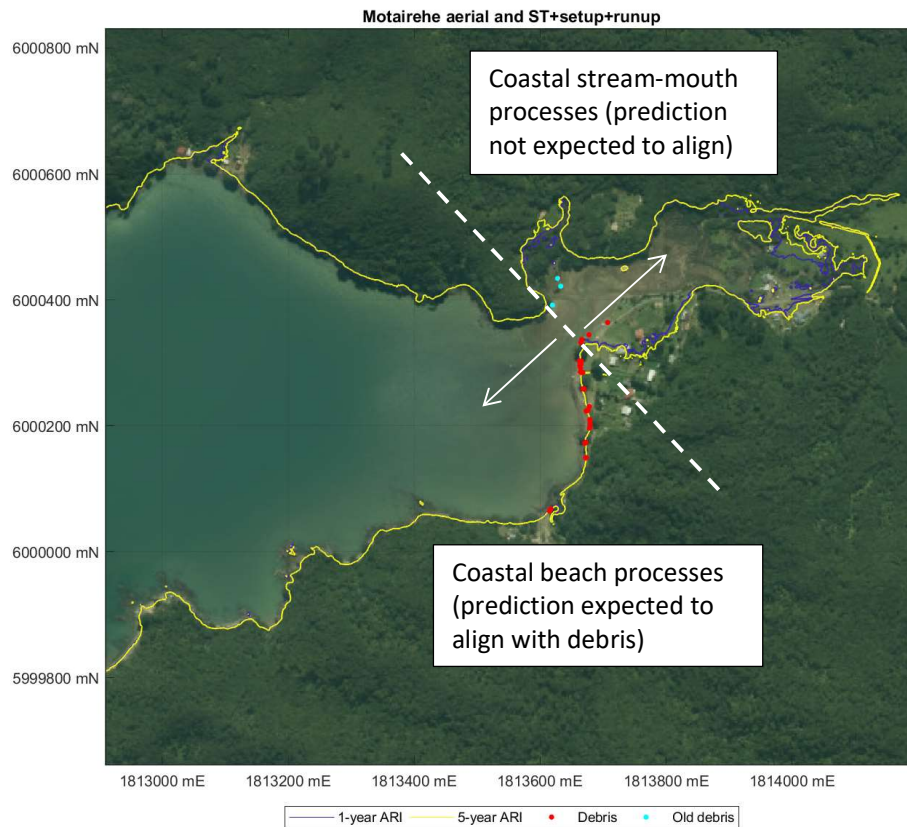


Figure 2-26: Example of runup overprediction up a coastal stream mouth for Motairehe. The runup elevation contours (1-year ARI and 5-year ARI) intersect the land far inland from the beach, and surveyed debris features are present throughout (red and blue circles) because the modelling excludes other processes which may locally affect sea levels and debris features such as river flows and wave overtopping flows around the stream mouth. [Aerial photograph: Auckland Council GIS, Coordinate system: NZ Transverse Mercator 2000].

2.10 Exceptions

This approach could not be used at the Little Barrier Island or Rarohara Bay sites, where no surveys were done. For these locations, exceptions to the method were made by:

Rarohara Bay was not accessed during the survey and was assigned the same values as the adjacent Port Fitzroy on the assumption that Rarohara Bay is exposed to similar extreme coastal conditions as Port Fitzroy. Both are sheltered from the larger waves of Hauraki Gulf by Kaikoura Island, and are only exposed to locally-generated wind waves over a 1–2 km fetch (Figure 2-27). These locally-generated waves have the potential to generate significant wave heights only up to 0.26 m at 1% AEP, with wave setup <0.1 m, based on the WASP wind records. Consequently, tide and storm-tide are the dominant factors contributing to extreme water levels in these bays, and the tide and storm-tide will not vary materially over the 1 km which separates Rarohara Bay from Port Fitzroy (Figure 2-27). The calculated extreme sea level elevations are shown in Table 3-1.



Figure 2-27: Port Fitzroy and Rarohara Bay aerial Photograph. [Photograph date: 10-2-2013, Source: Google Earth].

Little Barrier Island. The model-extraction location for tide, wave and storm surge data at Little Barrier is off the north coast of the island (Figure 1-2), but the wave climate will differ considerably around the near-circular island. To fully simulate the wave exposure on each quadrant of the Island would require, say, 4 additional model outputs. However, water depths are 40+ m surrounding the predominantly cliff-backed shoreline and there are only two “beach” shorelines on the island. These beaches are to the south at Te Titoki Point (a cusped foreland where DOC facilities are located, Figure 2-28) and north east at Puhutakawa Flat (debris fan from a 19 Mm³ rock-slide; Lindsay and Moore, 1995) and are predominantly composed of cobbles and boulders e.g., (Figure 2-29).



Figure 2-28: Te Tikoti Point is one of the two low-lying beaches on Little Barrier Island. [Credit: Te Tikoti Point and Te Marareroa flat as viewed from the Parihakoakoa pa (T. Greene 1989), courtesy Dodd (2004)].



Figure 2-29: Gravel/Cobble beach formation on eastern flank of Te Tikoti Point. [Left Credit: Don Merton 1995, Source: DoC (2007); Right: Cliff Taylor, NZHerald⁸].

It could be argued that wave setup at Little Barrier Island is minimal because the surrounding deep water, steep submarine cliffs and island shape dampens wave setup from being generated (i.e., the wave energy released at breaking would be able to ‘escape’ around the sides of the island unlike a typical embayment which ‘traps’ the wave energy released at breaking). However, without any surveyed debris-line markers or beach slopes to validate the numerical model runup/setup predictions with, we resorted to a conservative approach which simply translated the largest simulated wave setup values from the Hauraki Gulf sites on Great Barrier Island to Little Barrier Island. The site selected was at Blind Bay (northern Tryphena Harbour) and has a wave-setup magnitude between 0.61 m at 1-year ARI and 0.98 m at 100-year ARI (Table 3-3). This wave setup was added to the extreme storm-tide elevation as shown in Table 3-1. This assumption can be revisited with collection of debris line and beach slope data on Little Barrier Island.

⁸ https://www.nzherald.co.nz/travel/news/article.cfm?c_id=7&objectid=10807523

3 Results for extreme total water level and contributing components

The predicted extreme sea level estimates around Great Barrier Island and Little Barrier Island elevations are shown in Table 3-1 for each of the 16 shoreline sites for the present-day situation. This describes storm tide elevation including wave setup (but not runup), which is akin to conditions that potentially could generate near-continuous coastal flooding if it exceeds the local shoreline berm or structure (in contrast to the inclusion of wave runup that leads to more intermittent flooding).

Average recurrence interval (ARI) estimates for the separate contributions of storm tide (i.e., tide plus skew surge) and wave setup are given in Table 3-2 and Table 3-3 respectively. The ARI estimates for the driver processes i.e., significant wave height, skew surge and peak wave period are given in Table 2-3, Table 2-5 and Table 2-4 respectively.

Notes on Tables:

- 1) The storm-tide heights in Table 3-2 and wave-setup heights in Table 3-3 will not sum to equal the storm-tide + wave setup elevations in Table 3-1. This is because storm-tide and wave-setup are not 100% dependent, i.e., very high storm-tides do not always occur at the same time as very high wave setup. For example, the tidal component of storm-tide is driven by the gravitational pull of the moon and sun, whereas wave setup is driven by breaking waves—these two processes are essentially independent. But there will be *some* correlation between the components due to storm surge and wave-induced setup and runup, which are ultimately driven by weather conditions. Table 3-1 takes into account the observed degree of dependence between the wave setup and the skew-surge component of storm-tide, which was quantified using the joint-probability method.
- 2) the extreme water levels don't include sea-level rise and vertical land movement – which will need to be added for forward planning and design.

To briefly recap the methodology to this point, both wave and storm-tide conditions were simulated for the 1970–2000 period, at locations around the Islands (Figure 1-3). A joint-probability analysis was undertaken to calculate the likelihood of various coincident storm-tide and wave combinations. Wave setup was then calculated based on validation comparisons between debris line surveys and calculated wave setup + runup elevations. Wave setup was then added to storm-tide elevations to calculate the total combined storm-tide plus wave setup elevation.

Table 3-1: Extreme sea-level (storm-tide + wave setup) around Great Barrier Island. Elevations are relative to AVD-46 including +0.15 m offset for baseline mean sea level (present-day estimate). Elevations calculated from simulated data. See Figure 1-3 for location map and Table A-1 for coordinates.

| ID | Name | AEP (%) | 63 | 39 | 18 | 10 | 5 | 2 | 1 |
|----|---------------------------|-------------|------|------|------|------|------|------|-----|
| | | ARI (years) | 1 | 2 | 5 | 10 | 20 | 50 | 100 |
| 1 | Whangapoua (offshore) | - | - | - | - | - | - | - | - |
| 2 | Awana (offshore) | - | - | - | - | - | - | - | - |
| 3 | Medlands (offshore) | - | - | - | - | - | - | - | - |
| 4 | Shoal Bay (offshore) | - | - | - | - | - | - | - | - |
| 5 | Okupu (offshore) | - | - | - | - | - | - | - | - |
| 6 | Whangaparapara (offshore) | - | - | - | - | - | - | - | - |
| 7 | Port Fitzroy (offshore) | - | - | - | - | - | - | - | - |
| 8 | Motairehe (offshore) | - | - | - | - | - | - | - | - |
| 9 | Little Barrier | 1.86 | 1.96 | 2.07 | 2.15 | 2.24 | 2.36 | 2.46 | |
| 10 | Mokohinau Islands | - | - | - | - | - | - | - | |
| 11 | Motairehe | 1.69 | 1.74 | 1.81 | 1.86 | 1.90 | 1.95 | 2.00 | |
| 12 | Kawa | 1.72 | 1.77 | 1.85 | 1.90 | 1.95 | 2.01 | 2.06 | |
| 13 | Port Fitzroy | 1.42 | 1.47 | 1.51 | 1.54 | 1.57 | 1.61 | 1.63 | |
| 14 | Rarohara Bay | 1.42 | 1.47 | 1.51 | 1.54 | 1.57 | 1.61 | 1.63 | |
| 15 | Whangaparapara | 1.47 | 1.51 | 1.56 | 1.60 | 1.63 | 1.68 | 1.72 | |
| 16 | Blind Bay | 1.74 | 1.81 | 1.90 | 1.97 | 2.04 | 2.14 | 2.21 | |
| 17 | Okupu bay | 1.79 | 1.85 | 1.92 | 1.98 | 2.03 | 2.09 | 2.12 | |
| 18 | Puriri Bay | 1.77 | 1.84 | 1.93 | 2.00 | 2.06 | 2.15 | 2.21 | |
| 19 | Tryphena | 1.74 | 1.79 | 1.86 | 1.90 | 1.94 | 1.99 | 2.03 | |
| 20 | Mulberry Grove | 1.77 | 1.83 | 1.90 | 1.94 | 1.99 | 2.05 | 2.09 | |
| 21 | Shoal Bay | 1.57 | 1.61 | 1.66 | 1.70 | 1.73 | 1.77 | 1.79 | |
| 22 | Oruawharo Bay | 1.96 | 2.05 | 2.16 | 2.25 | 2.33 | 2.44 | 2.51 | |
| 23 | Kaitoke Beach | 2.14 | 2.25 | 2.39 | 2.50 | 2.62 | 2.73 | 2.83 | |
| 24 | Awana Bay | 2.70 | 2.87 | 3.06 | 3.21 | 3.34 | 3.50 | 3.60 | |
| 25 | Whangapoua | 1.98 | 2.08 | 2.20 | 2.29 | 2.39 | 2.51 | 2.58 | |

Table 3-2: Extreme storm-tide elevations around Great Barrier Island. Elevations are relative to AVD-46 including +0.15 m offset for baseline mean sea level (present-day estimate). Elevations calculated from simulated data. See Figure 1-3 for location map and Table A-1 for coordinates.

| ID | Name | AEP (%) | 63 | 39 | 18 | 10 | 5 | 2 | 1 |
|----|---------------------------|-------------|------|------|------|------|------|------|------|
| | | ARI (years) | 1 | 2 | 5 | 10 | 20 | 50 | 100 |
| 1 | Whangapoua (offshore) | | 1.24 | 1.28 | 1.32 | 1.35 | 1.38 | 1.41 | 1.43 |
| 2 | Awana (offshore) | | 1.23 | 1.28 | 1.33 | 1.36 | 1.39 | 1.42 | 1.45 |
| 3 | Medlands (offshore) | | 1.24 | 1.28 | 1.33 | 1.36 | 1.38 | 1.41 | 1.44 |
| 4 | Shoal Bay (offshore) | | 1.23 | 1.28 | 1.32 | 1.35 | 1.38 | 1.42 | 1.44 |
| 5 | Okupu (offshore) | | 1.23 | 1.27 | 1.32 | 1.35 | 1.38 | 1.42 | 1.44 |
| 6 | Whangaparapara (offshore) | | 1.24 | 1.28 | 1.32 | 1.36 | 1.39 | 1.42 | 1.44 |
| 7 | Port Fitzroy (offshore) | | 1.26 | 1.30 | 1.35 | 1.38 | 1.41 | 1.44 | 1.47 |
| 8 | Motairehe (offshore) | | 1.26 | 1.31 | 1.35 | 1.38 | 1.40 | 1.45 | 1.48 |
| 9 | Little Barrier | | 1.26 | 1.31 | 1.35 | 1.38 | 1.41 | 1.45 | 1.48 |
| 10 | Mokohinau Islands | | 1.27 | 1.31 | 1.36 | 1.39 | 1.41 | 1.45 | 1.47 |
| 11 | Motairehe | | 1.25 | 1.30 | 1.34 | 1.37 | 1.40 | 1.44 | 1.47 |
| 12 | Kawa | | 1.26 | 1.30 | 1.34 | 1.38 | 1.40 | 1.44 | 1.46 |
| 13 | Port Fitzroy | | 1.26 | 1.30 | 1.35 | 1.38 | 1.41 | 1.45 | 1.47 |
| 14 | Rarohara Bay | | 1.26 | 1.30 | 1.35 | 1.38 | 1.41 | 1.45 | 1.47 |
| 15 | Whangaparapara | | 1.23 | 1.28 | 1.32 | 1.35 | 1.38 | 1.42 | 1.45 |
| 16 | Blind Bay | | 1.24 | 1.28 | 1.32 | 1.35 | 1.38 | 1.41 | 1.44 |
| 17 | Okupu bay | | 1.24 | 1.28 | 1.32 | 1.35 | 1.38 | 1.42 | 1.44 |
| 18 | Puriri Bay | | 1.24 | 1.28 | 1.33 | 1.36 | 1.39 | 1.42 | 1.45 |
| 19 | Tryphena | | 1.23 | 1.28 | 1.32 | 1.35 | 1.39 | 1.43 | 1.45 |
| 20 | Mulberry Grove | | 1.24 | 1.28 | 1.32 | 1.35 | 1.38 | 1.41 | 1.45 |
| 21 | Shoal Bay | | 1.23 | 1.27 | 1.31 | 1.34 | 1.37 | 1.40 | 1.44 |
| 22 | Oruawharo Bay | | 1.23 | 1.28 | 1.32 | 1.35 | 1.38 | 1.42 | 1.45 |
| 23 | Kaitoke Beach | | 1.23 | 1.28 | 1.32 | 1.35 | 1.38 | 1.43 | 1.45 |
| 24 | Awana Bay | | 1.23 | 1.28 | 1.33 | 1.36 | 1.39 | 1.42 | 1.44 |
| 25 | Whangapoua | | 1.24 | 1.28 | 1.32 | 1.35 | 1.38 | 1.42 | 1.44 |

Table 3-3: Extreme wave setup magnitude (m) around Great Barrier Island. Wave setup calculated from wave hindcast data and predicted using back-calculated planar beach slope for each inshore site. See Figure 1-3 for location map and Table A-1 for coordinates.

| ID | Name | AEP (%) | 63 | 39 | 18 | 10 | 5 | 2 | 1 |
|----|---------------------------|-------------|------|------|------|------|------|------|-----|
| | | ARI (years) | 1 | 2 | 5 | 10 | 20 | 50 | 100 |
| 1 | Whangapoua (offshore) | - | - | - | - | - | - | - | - |
| 2 | Awana (offshore) | - | - | - | - | - | - | - | - |
| 3 | Medlands (offshore) | - | - | - | - | - | - | - | - |
| 4 | Shoal Bay (offshore) | - | - | - | - | - | - | - | - |
| 5 | Okupu (offshore) | - | - | - | - | - | - | - | - |
| 6 | Whangaparapara (offshore) | - | - | - | - | - | - | - | - |
| 7 | Port Fitzroy (offshore) | - | - | - | - | - | - | - | - |
| 8 | Motairehe (offshore) | - | - | - | - | - | - | - | - |
| 9 | Little Barrier | 0.60 | 0.65 | 0.72 | 0.77 | 0.83 | 0.91 | 0.98 | |
| 10 | Mokohinau Islands | - | - | - | - | - | - | - | - |
| 11 | Motairehe | 0.49 | 0.53 | 0.58 | 0.62 | 0.65 | 0.69 | 0.73 | |
| 12 | Kawa | 0.51 | 0.55 | 0.61 | 0.65 | 0.69 | 0.73 | 0.77 | |
| 13 | Port Fitzroy | 0.03 | 0.04 | 0.04 | 0.04 | 0.04 | 0.04 | 0.05 | |
| 14 | Rarohara Bay | 0.03 | 0.04 | 0.04 | 0.04 | 0.04 | 0.04 | 0.05 | |
| 15 | Whangaparapara | 0.20 | 0.21 | 0.24 | 0.26 | 0.27 | 0.30 | 0.32 | |
| 16 | Blind Bay | 0.60 | 0.65 | 0.72 | 0.77 | 0.83 | 0.91 | 0.98 | |
| 17 | Okupu bay | 0.61 | 0.65 | 0.71 | 0.75 | 0.80 | 0.85 | 0.89 | |
| 18 | Puriri Bay | 0.61 | 0.67 | 0.73 | 0.79 | 0.84 | 0.90 | 0.95 | |
| 19 | Tryphena | 0.55 | 0.59 | 0.64 | 0.67 | 0.70 | 0.74 | 0.77 | |
| 20 | Mulberry Grove | 0.59 | 0.63 | 0.69 | 0.72 | 0.76 | 0.80 | 0.83 | |
| 21 | Shoal Bay | 0.30 | 0.32 | 0.35 | 0.36 | 0.38 | 0.40 | 0.42 | |
| 22 | Oruawharo Bay | 0.85 | 0.92 | 1.02 | 1.08 | 1.15 | 1.23 | 1.28 | |
| 23 | Kaitoke Beach | 1.06 | 1.16 | 1.28 | 1.36 | 1.45 | 1.55 | 1.63 | |
| 24 | Awana Bay | 1.66 | 1.80 | 1.98 | 2.12 | 2.23 | 2.39 | 2.51 | |
| 25 | Whangapoua | 0.90 | 0.97 | 1.08 | 1.17 | 1.25 | 1.34 | 1.38 | |

3.1 Discussion

A brief comparison of the nearest values from the previous extreme sea-level modelling for the Eastern Open Coast bays (Stephens et al. 2016) shows that the two approaches are consistent. The nearest site to the present study is at Cape Rodney (Eastern open-coast, Site 3) where the 1% AEP storm-tide is 1.79 m at Cape Rodney (Table 4-1 in Stephens et al. 2016) compared to 1.41 m at Little Barrier (a -0.38 m difference), and the 1% AEP storm-tide + wave setup is 2.68 m at Cape Rodney compared (Table 4-3 in Stephens et al. 2016) to 2.46 m at Little Barrier (a -0.22 m difference). The difference between these two elevations can be explained primarily by the smaller tidal range at Great and Little Barrier Islands than on the mainland (see Section 1.1, and below) and, to a lesser extent, differences in the storm-surge component and wave exposure.

LINZ⁹ calculates that the half-tide difference between the MHWS¹⁰ tide range Port of Auckland and at Tryphena is 0.35 m. This means that all high-tides are lower, and hence the high-tide component of extreme storm-tides is smaller on Great Barrier Island compared to Auckland, leading to (all other factors being equal) lower extreme sea-level elevations. Thus, of the 0.4 m difference between Cape Rodney and Little Barrier, approximately 0.30 m can be attributed to the smaller tidal range. Further, the half-tide range is approximately 0.1 smaller again on the exposed east coast (e.g., Figure 2-12) and hence extreme storm-tide elevations will be smaller here, although this is offset by larger wave setup in the extreme storm-tide plus wave setup results. This a key factor for explaining the small differences between the previous work and this new work. This reduced tidal range is due to the deeper continental shelf and lack of topographic restriction of the tidal waveform on Great Barrier Island.

Similarly, storm-tide elevations are expected to be smaller at Great Barrier compared to Auckland due to the lack of topographic constriction (i.e., the storm-surge wave does not pile-up and amplify at Great Barrier because the surge can 'escape' around the island via Colville Channel or Craddock Channel). The 1% AEP storm-surge height at Port of Auckland is approximately 0.6 m (Stephens et al. 2016) compared to the 0.4 m height at Great Barrier (Table 2-5). A better comparison of this would require a longer-time series of tide gauge data at Great Barrier to further compare with the Auckland gauges.

3.2 Mapping limitations

The extreme sea-level modelling used a joint-probability method to determine the offshore "drivers" (tide, storm-surge and waves) of extreme sea level, coupled with empirical wave setup and runup formulae. This is consistent with approaches taken elsewhere in NZ (Stephens et al. 2011 (minor edits 2012); Stephens et al. 2014; Stephens et al. 2015a; Stephens et al. 2015b; Stephens et al. 2016; Stephens et al. 2018a; Stephens et al. 2018b), The method makes no allowance for the dynamic effects of the following processes which can influence the level of the sea as it propagates inland from open water:

- The storm-tide component is expected to amplify inside the harbours.
- Vegetation (such as mangroves) attenuates extreme sea levels inside estuaries by dampening wave process.

⁹ LINZ tidal almanac for secondary ports 2019-2020 at Auckland compared with Korotiti Bay and Tryphena. (<https://www.linz.govt.nz/sites/default/files/docs/hydro/tidal-info/tide-tables/secondary-ports-2019-20.csv>)

¹⁰ Note LINZ calculates the nautical definition of MHWS which is the sum of the M2 and S2 tides.

- Attenuation by restrictions at a narrow harbour entrances, or at river/stream mouths.
- Attenuation by bottom roughness within a shallow estuary.
- Additions from the effect of short-period waves (aka “chop”) generated *within* estuaries which are not included in our model.
- Mean sea-level anomaly of +/- 0.25 m which could increase or decrease the extreme sea level elevation.

For these reasons static (“bathtub”) mapping of these extreme sea-levels can produce conservatively large estimates of inundation extent and depth at distances far inland from the sea, but where treated with caution this can still represent residual risk and has been commonly applied in other studies (e.g., Stephens et al. 2016). Recent studies have used dynamic inundation models (Bosserele and Lane 2019; Stephens et al. 2019).

An example of where bathtub mapping could be conservative is at Whangapoua (Figure 3-1) where the large and shallow Whangapoua Estuary is sheltered behind Whangapoua Beach barrier and will not be subject to the full-height of the extreme sea level. Wave setup is expected to reduce within the estuary as the waves break over the river mouth, and diffract and reduce in elevation as they spread into the estuary. Waves are further attenuated through bottom roughness and vegetation within the estuary. However, the storm-tide component could amplify (or reduce) inside the harbour or could be held up (setup) by onshore winds. Runup should not be modelled with bathtub mapping as it only represents the short-term elevation of intermittent wave runup processes on the beach face. Runup can be hazardous to people and property but does not meaningfully contribute to inundation unlike the wave setup.

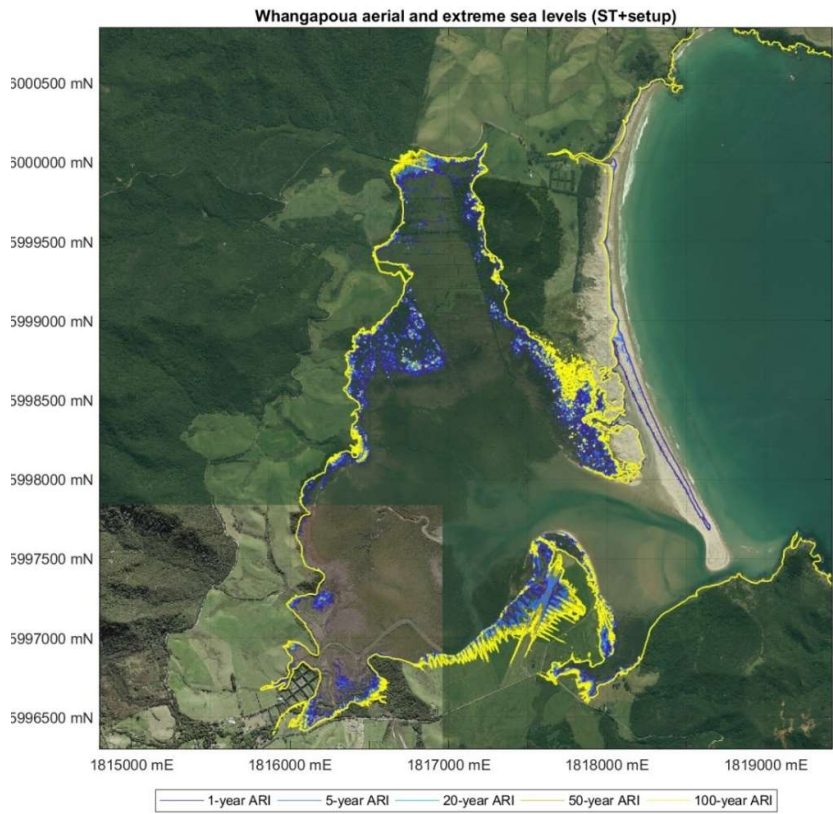


Figure 3-1: Example storm-tide plus wave setup (no runup) modelling at Whangapoua using static "bathtub" approach. Elevations from Table 3-1. [Aerial photograph: Auckland Council GIS, Coordinate system: NZ Transverse Mercator 2000].

The extreme sea level elevations may also increase locally inside stream mouths from added effect of stream/river flows which cannot drain to the sea when sea levels are high, or if a large rainfall event precedes/coincides with the extreme sea levels. Such 'backing up' of river flows may cause streams to breach their stream beds and flood the adjacent land. This potential contribution to coastal inundation has not been addressed. On Great Barrier Island, the sites most likely to experience this are those with relatively large catchments draining across the beach, for example, Oruawhoro (unnamed Creeks draining the hinterland – Figure 3-2) and Whangapoua (Whangapoua Creek and swamp – Figure 3-1).



Figure 3-2: Example storm-tide plus wave setup modelling at Oruawharo Bay using static "bathtub" approach. Elevations from Table 3-1. Note that the inland areas shown to be below the model elevation are away from the coast and are subject to the limitations above streams [Aerial photograph: Auckland Council GIS, Coordinate system: NZ Transverse Mercator 2000].

4 Acknowledgements

This study used the Geonet/GNS Science Tsunami Gauge at Korotiti Bay. Jade Arnold (NIWA) extracted the sea-level data.

Auckland Council provided LiDAR and aerial photographs.

5 Glossary of abbreviations and terms

| | |
|-------------------|---|
| AEP | Annual Exceedance Probability. The probability of a given (usually high) sea level or wave height being equalled or exceeded in elevation in any given calendar year. AEP can be specified as a fraction (e.g., 0.01) or a percentage (e.g., 1%). |
| ARI | Average Recurrence Interval. The average time interval (averaged over a very long time period and many “events”) that is expected to elapse between recurrences of an infrequent event of a given large magnitude (or larger). A large infrequent event would be expected to be equalled or exceeded in elevation, once, on average, every “ARI” years, but with considerable variability. |
| AVD-46 | Auckland Vertical Datum - 1946 was established as the mean sea level at Port of Auckland from 7 years of measurements collected in 1909, 1917-1919 and 1921-1923. |
| ENSO | El Niño Southern Oscillation. A natural global climate phenomenon involving the interaction between the tropical Pacific and the atmosphere, but has far-reaching effects on the global climate, especially for countries in the Pacific rim. ENSO is the strongest climate signal on time scales of one to several years. The quasi-periodic cycle oscillates between El Niño (unusually warm ocean waters along the tropical South American coast) and La Niña (colder-than-normal ocean waters off South America). |
| Hindcast | A numerical simulation (representation) of past conditions. As opposed to a forecast or future cast that simulates the future. |
| IPO | Interdecadal Pacific Oscillation – a long timescale oscillation in the ocean–atmosphere system that shifts climate in the Pacific region every one to three decades. |
| Joint-Probability | The probability of two separate processes occurring together (e.g., large waves and high storm-tide). |
| LiDAR | Light Detection And Ranging – an airborne laser scanning system that determines ground levels at a very high density (often as little as 1 m spacing between measurements) along a swathe of land underneath the track of the airplane. Most systems used in New Zealand collect data only on land above water levels, but systems are available that can also determine shallow water bathymetry levels in clear water. Vertical accuracy is typically better than ± 0.15 m. |
| MHWS | Mean high water springs – The high tide height associated with higher than normal high tides that result from the superposition of various tidal harmonic constituents. Mean high water springs occur every 2 weeks approximately. MHWS can be defined in various ways, and the MHWS elevation varies according to definition. |

| | |
|-------------------------|--|
| MSL | Mean Sea Level. The mean non-tidal component of sea level, averaged over a defined time period, usually several years. New Zealand’s local vertical datums were obtained in this way, with AVD-46 being the MSL from sea-level measurements made between 1909 and 1923. Mean sea level changes with the averaging period used, due to climate variability and long-term sea-level rise. |
| MSLA | Mean sea-level anomaly – the variation of the non-tidal sea level about the longer term MSL on time scales ranging from a monthly basis to decades, due to climate variability. This includes ENSO and IPO patterns on sea level, winds and sea temperatures, and seasonal effects. |
| Significant wave height | The average height of the highest one-third of waves in the wave record; experiments have shown that the value of this wave height is close to the value of visually estimated wave height. |
| Storm surge | The rise in sea level due to storm meteorological effects. Low-atmospheric pressure relaxes the pressure on the ocean surface causing the sea-level to rise, and wind stress on the ocean surface pushes water down-wind (onshore winds) and to the left up against any adjacent coast (alongshore winds). Storm surge has timescales of sea-level response that coincide with typical synoptic weather motions; typically 1–3 days. |
| Storm-tide | Storm-tide is defined as the sea-level peak around high tide reached during a storm event, resulting from a combination of sea-level + tide + storm surge. |
| WASP | The Waves And Storm surge Predictions WASP modelling project recently completed by NIWA produced 45-year (1958–2002) and 30-year (1970–2000) hindcast records of storm surge and waves around the entire New Zealand coast. An aim of the WASP project was to produce a nationally-consistent web-based hindcast of waves and storm surges, from which regional information could be extracted. |
| Wave runup | The maximum vertical extent of wave “up-rush” on a beach or structure above the still water level, and thus constitutes only a short-term upper-bound fluctuation in water level relative to wave setup. |
| Wave setup | A sustained increase in the mean water level at the shore compared to the level further offshore beyond the surf zone that is induced by the transfer of momentum from waves as they break over a sloping foreshore. Setup is localised to the surf zone but is a meaningful addition to the extreme storm-tide levels at the coast. |

6 References

- Ackerley, D., Dean, S., Sood, A., Mullan, A.B. (2012) Regional climate modelling in New Zealand: Comparison to gridded and satellite observations. *Weather and Climate*, 32(1): 3-22.
- Bell, R.G. (2010) Tidal exceedances, storm tides and the effect of sea-level rise. *Proceedings of the 17th Congress of the Asia and Pacific division of the IAHR*, Auckland, New Zealand, 21-24 February 2010.
- Bosserelle, C., Lane, M. (2019) Coastal storm-surge maps for the Kapiti coast. *NIWA Client Report 2019113CH* to Greater Wellington Regional Council, May 2019: 65.
- DoC (2007) Te Maraeroa Flat, Little Barrier Island: Heritage Assessment Andy Dodd, Department of Conservation, Auckland Conservancy. ISBN 978-0-478-14299-0 (web PDF). <https://www.doc.govt.nz/globalassets/documents/conservation/historic/by-region/auckland/te-maraeroa-flat/little-barrier-island-heritage-assessment-full.pdf>
- DoC (2010) New Zealand Coastal Policy Statement (NZCPS) 2010. *Department of Conservation*. <https://www.doc.govt.nz/Documents/conservation/marine-and-coastal/coastal-management/nz-coastal-policy-statement-2010.pdf>
- Gorman, R., Stephens, S. (2003a) Wave buoy deployment at the Mokohinau Islands: Data Report May 1998-April 1999.
- Gorman, R., Stephens, S. (2003b) Wave buoy deployment at the Mokohinau Islands: Data Report May 1999-April 2000.
- Gorman, R., Stephens, S. (2003c) Wave buoy deployment at the Mokohinau Islands: Data Report May 2000-April 2001.
- Gorman, R., Stephens, S. (2003d) Wave buoy deployment at the Mokohinau Islands: Data Report May 2001-April 2002.
- Gorman, R.M. (1999) Wave buoy deployment at the Mokohinau Islands: Data Report May 1998-December 1998.
- Hannah, J., Bell, R.G. (2012) Regional sea level trends in New Zealand. *Journal of Geophysical Research-Oceans*, 117: C01004.
- Hawkes, P.J., Gouldby, B.R., Tawn, J.A., Owen, M.W. (2002) The joint probability of waves and water levels in coastal engineering design. *Journal of Hydraulic Research*, 40(3): 241–251.
- Heffernan, J.E., Tawn, J.A. (2004) A conditional approach for multivariate extreme values (with discussion). *Journal of the Royal Statistical Society: Series B (Statistical Methodology)*, 66(3): 497-546. 10.1111/j.1467-9868.2004.02050.x
- Komar, P.D. (1998) *Beach processes and sedimentation*. Prentice-Hall, New Jersey: 544.
- Lane, E.M., Walters, R.A. (2009) Verification of RiCOM for Storm Surge Forecasting. *Marine Geodesy*, 32(2): 118-132. 10.1080/01490410902869227

- Lane, E.M., Walters, R.A., Gillibrand, P.A., Uddstrom, M. (2009) Operational forecasting of sea level height using an unstructured grid ocean model. *Ocean Modelling*, 28(1-3): 88-96. 10.1016/j.ocemod.2008.11.004
- Lindsay, J., Moore, P. (1995) Geological Features of Little Barrier Island, Hauraki Gulf. *Tane*, 35: 25-38.
- Ministry for the Environment (2017) Coastal hazards and climate change: Guidance for local government. Bell, R.G., Lawrence, J., Allan, S., Blackett, P., Stephens, S., (Eds). *Ministry for the Environment Publication*, ME 1341: 279 + Appendices.
- Stanton, B.R., Goring, D.G., Bell, R.G. (2001) Observed and modelled tidal currents in the New Zealand region. *New Zealand Journal of Marine and Freshwater Research*, 35: 397–415.
- Stephens, S.A., Gorman, R.M., Lane, E. (2011) (minor edits 2012) Joint-probability of storm tide and waves on the open coast of Wellington. *NIWA*: 44.
- Stephens, S.A., Robinson, B., Gorman, R.M. (2014) Extreme sea-level elevations from storm-tides and waves along the Gisborne District coastline: 106.
- Stephens, S.A., Allis, M., Robinson, B., Gorman, R.M. (2015a) Storm-tides and wave runup in the Canterbury Region: 133.
- Stephens, S.A., Reeve, G., Wadhwa, S., Bell, R.G. (2015b) Areas in the Gisborne region potentially affected by coastal-storm inundation: 30.
- Stephens, S.A., Wadhwa, S., Tuckey, B. (2016) Coastal inundation by storm-tides and waves in the Auckland Region. Prepared by the National Institute of Water and Atmospheric Research and DHI Ltd for Auckland Council. *Auckland Council Technical Report*, TR2016/017: 206. <https://www.aucklandcouncil.govt.nz/environment/what-we-do-to-help-environment/Documents/coastal-inundation-in-auckland.pdf>
- Stephens, S.A., Allis, M., Gorman, R., Robinson, B., Goodhue, N. (2018a) Storm-tide and wave hazards in the Bay of Plenty: Revised and updated September 2018. *NIWA Client Report* 2018136HN, to Bay of Plenty Regional Council, September 2018: 125.
- Stephens, S.A., Robinson, B., Allis, M. (2018b) Storm-tide and wave hazards in Tasman and Golden Bays. *NIWA Client Report to Tasman District Council and Nelson City Council*, June 2018, 2018208HN: 61.
- Stephens, S.A., Bosserelle, C., Wadhwa, S. (2019) Mapping coastal inundation in Tauranga: Waihi Beach to Te Tumu and Tauranga Harbour. *NIWA Client Report* 2018269HN to Bay of Plenty Regional Council, September 2019: 37.
- Stockdon, H.F., Holman, R.A., Howd, P.A., Sallenger, J.A.H. (2006) Empirical parameterization of setup, swash, and runup. *Coastal Engineering*, 53(7): 573-588. <http://www.sciencedirect.com/science/article/B6VCX-4J9X2XY-1/2/a8a8998ee7c46522825f72edc3a188ab>

- Tolman, H.L. (1991) A third-generation model for wind waves on slowly varying, unsteady, and inhomogeneous depths and currents. *Journal of Physical Oceanography*, 21: 782-797.
- Tolman, H.L. (2009) User manual and system documentation of WAVEWATCH-III version 3.14: 194. <http://polar.wwb.noaa.gov/waves/wavewatch/wavewatch.html>
- Uppala, S.M., Kållberg, P.W., Simmons, A.J., Andrae, U., Bechtold, V.D.C., Fiorino, M., Gibson, J.K., Haseler, J., Hernandez, A., Kelly, G.A., Li, X., Onogi, K., Saarinen, S., Sokka, N., Allan, R.P., Andersson, E., Arpe, K., Balmaseda, M.A., Beljaars, A.C.M., Berg, L.V.D., Bidlot, J., Bormann, N., Caires, S., Chevallier, F., Dethof, A., Dragosavac, M., Fisher, M., Fuentes, M., Hagemann, S., Hólm, E., Hoskins, B.J., Isaksen, L., Janssen, P.A.E.M., Jenne, R., McNally, A.P., Mahfouf, J.F., Morcrette, J.J., Rayner, N.A., Saunders, R.W., Simon, P., Sterl, A., Trenberth, K.E., Untch, A., Vasiljevic, D., Viterbo, P., Woollen, J. (2005) The ERA-40 re-analysis. *Quarterly Journal of the Royal Meteorological Society*, 131(612): 2961-3012. <http://dx.doi.org/10.1256/qj.04.176>
- Walters, R.A., Lane, E.M., Henry, R.F. (2007) Semi-Lagrangian methods for a finite element coastal ocean model. *Ocean Modelling*, 19(3-4): 112-124. <Go to ISI>://CCC:000250541800002
- Young, I.R., Verhagen, L.A. (1996) The growth of fetch limited waves in water of finite depth. Part 1. Total energy and peak frequency. *Coastal Engineering*, 29: 47-78.

Appendix A Coordinates of output locations

Table A-1: Location coordinates for predictions of hindcast wave, tide and storm surge statistics.

Coordinates in NZ Transverse Mercator (NZTM). Site numbers used in output plots and tables are given in the fourth column (refer to Figure 1-3 for map of site locations, the originally proposed first 10 sites are shown in Figure 1-1).

| Name | Easting | Northing | Site number |
|--------------------------------|-------------|-------------|-------------|
| Whangapoua (offshore) | 1819976.494 | 5999220.275 | 1 |
| Awana (offshore) | 1824323.158 | 5990679.076 | 2 |
| Medlands (offshore) | 1824953.906 | 5985636.128 | 3 |
| Shoal Bay (offshore) | 1822217.795 | 5978434.231 | 4 |
| Okupu (offshore) | 1818097.583 | 5983517.698 | 5 |
| Whangaparapara (offshore) | 1815240.965 | 5985818.208 | 6 |
| Port Fitzroy (offshore) | 1811163.814 | 5994541.654 | 7 |
| Motairehe (offshore) | 1809946.123 | 6001317.684 | 8 |
| Little Barrier | 1789043.041 | 5995700.168 | 9 |
| Mokohinau Islands | 1792237.700 | 6022979.638 | 10 |
| Motairehe | 1813140.878 | 6000217.099 | 11 |
| Kawa | 1812434.1 | 5999595.457 | 12 |
| Port Fitzroy | 1812232.645 | 5995120.224 | 13 |
| Rarahara Bay | 1812194.779 | 5994346.271 | 14 |
| Whangaparapara | 1815201.917 | 5986360.409 | 15 |
| Blind Bay | 1817638.379 | 5984096.707 | 16 |
| Okupu Bay | 1818843.284 | 5984139.746 | 17 |
| Puriri Bay | 1821933.478 | 5979500.736 | 18 |
| Tryphena | 1823028.848 | 5979282.689 | 19 |
| Mulberry Grove | 1823485.49 | 5978412.47 | 20 |
| Shoal Bay | 1823348.305 | 5977778.926 | 21 |
| Orouaharo Bay | 1824606.376 | 5984166.872 | 22 |
| Kaitoke Beach | 1823475.88 | 5986784.129 | 23 |
| Awana Bay | 1823342.125 | 5990003.216 | 24 |
| Whangapoua | 1818600.245 | 5999794.276 | 25 |
| Tsunami Gauge (Korotiti Bay) | 1823803.665 | 5992217.147 | 26 |
| Tryphena Wharf | 1823151.310 | 5977666.537 | 27 |
| Mokohinau wave buoy (offshore) | 1788052.200 | 6026990.740 | |

$$s = \frac{2}{\theta_{spr}^2} - 1$$

and N is a normalisation constant. This was used to compute a “blocking factor” B as the weighted sum of the distribution over the “open fetch” window centred on the mean direction:

$$B = \int_0^{2\pi} D(\theta)K(\theta)d\theta$$

and a “mean fetch” as the weighted sum of fetches over the “short fetch” directions

$$F_{mean} = \int_0^{2\pi} D(\theta)(1 - K(\theta))F(\theta)d\theta$$

where $K(\theta)$ is the “window” function

$$K(\theta) = \begin{cases} 1, & F(\theta) > F_{thres} \\ 0, & F(\theta) \leq F_{thres} \end{cases}$$

The final estimate of wave statistics at A is then

$$H_{m0}(A) = B * H_{m0,hindcast}(G) + (1 - B) * \tilde{H}_{m0}(F_{mean}, U_{10})$$

$$T_p(A) = B * T_{p,hindcast}(G) + (1 - B) * \tilde{T}_p(F_{mean}, U_{10})$$

Calibration against Mokohinau buoy data

Significant wave height derived from the hindcast for the location of the Mokohinau buoy site, as described in Section 2.5, was compared with the buoy record (Figure B-2). Note that minimal sheltering correction was required (i.e., $B \approx 1$) for this location, i.e., well away from interference by land. We note that the hindcast somewhat underestimates measured wave heights at the higher-energy conditions of most relevance to an extreme value study. We therefore chose to apply a scaling factor of 1.130, derived from the ratio of the upper 1 percentile of measured and modelled significant wave heights at the Mokohinau buoy, to all nearshore significant wave height estimates in this study.

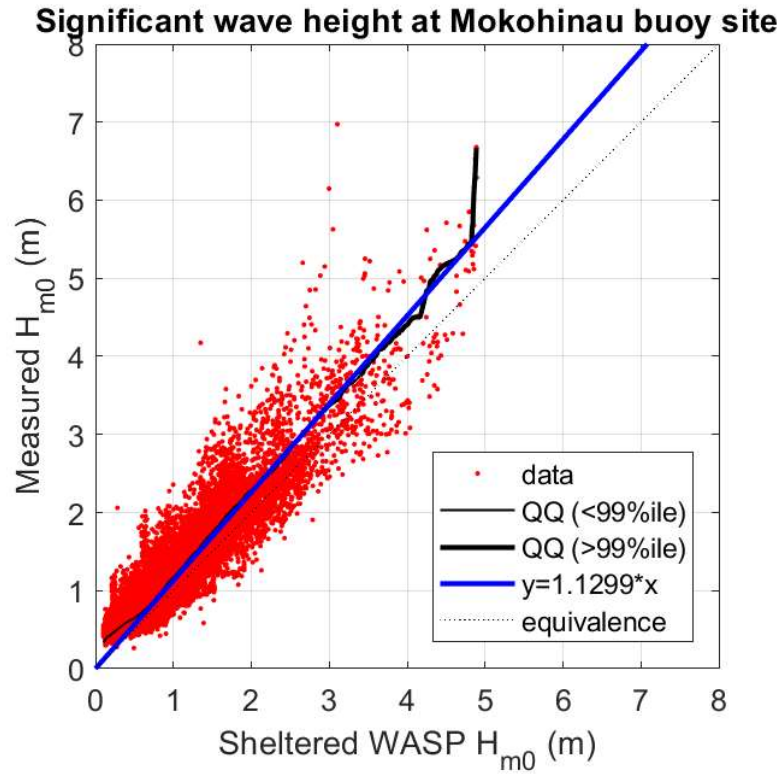


Figure B-2: Scatter plot of significant wave height at the Mokohinau buoy location derived from the WASP hindcast (with sheltering correction) against values measured by the buoy. A quantile-quantile plot is overlaid (black line), as well as a linear fit through the origin and the mean of the upper 1 percentile of the data.

Appendix C Validation plotting of surveyed debris features and predicted storm-tide plus wave runup (including setup) elevations

Table C-1: Extreme sea-levels from storm-tide + wave runup (including setup) around Great Barrier Island. Elevations are relative to AVD-46 including +0.15 m offset for baseline mean sea level (present-day estimate). Elevations calculated from simulated data. See Figure 1-3 for location map and Table A-1 for coordinates. Results only calculated for 16 inshore sites.

| ID | Name | AEP (%) | 63 | 39 | 18 | 10 | 5 | 2 | 1 |
|----|---------------------------|-------------|------|------|------|------|------|------|-----|
| | | ARI (years) | 1 | 2 | 5 | 10 | 20 | 50 | 100 |
| 1 | Whangapoua (offshore) | - | - | - | - | - | - | - | - |
| 2 | Awana (offshore) | - | - | - | - | - | - | - | - |
| 3 | Medlands (offshore) | - | - | - | - | - | - | - | - |
| 4 | Shoal Bay (offshore) | - | - | - | - | - | - | - | - |
| 5 | Okupu (offshore) | - | - | - | - | - | - | - | - |
| 6 | Whangaparapara (offshore) | - | - | - | - | - | - | - | - |
| 7 | Port Fitzroy (offshore) | - | - | - | - | - | - | - | - |
| 8 | Motairehe (offshore) | - | - | - | - | - | - | - | - |
| 9 | Little Barrier | - | - | - | - | - | - | - | - |
| 10 | Mokohinau Islands | - | - | - | - | - | - | - | - |
| 11 | Motairehe | 2.26 | 2.36 | 2.49 | 2.58 | 2.68 | 2.79 | 2.89 | |
| 12 | Kawa | 2.34 | 2.46 | 2.61 | 2.72 | 2.82 | 2.95 | 3.04 | |
| 13 | Port Fitzroy | 1.45 | 1.49 | 1.54 | 1.56 | 1.60 | 1.63 | 1.65 | |
| 14 | Rarohara Bay | 1.45 | 1.49 | 1.54 | 1.56 | 1.60 | 1.63 | 1.65 | |
| 15 | Whangaparapara | 1.63 | 1.68 | 1.76 | 1.82 | 1.88 | 1.96 | 2.03 | |
| 16 | Blind Bay | 2.44 | 2.58 | 2.76 | 2.90 | 3.04 | 3.24 | 3.43 | |
| 17 | Okupu bay | 2.51 | 2.62 | 2.76 | 2.87 | 2.97 | 3.10 | 3.18 | |
| 18 | Puriri Bay | 2.49 | 2.62 | 2.79 | 2.92 | 3.04 | 3.23 | 3.33 | |
| 19 | Tryphena | 2.37 | 2.47 | 2.59 | 2.68 | 2.76 | 2.86 | 2.91 | |
| 20 | Mulberry Grove | 2.46 | 2.56 | 2.69 | 2.79 | 2.89 | 3.01 | 3.09 | |
| 21 | Shoal Bay | 1.89 | 1.95 | 2.03 | 2.08 | 2.13 | 2.19 | 2.23 | |
| 22 | Oruawharo Bay | 3.23 | 3.44 | 3.71 | 3.89 | 4.06 | 4.30 | 4.45 | |
| 23 | Kaitoke Beach | 3.68 | 3.94 | 4.27 | 4.50 | 4.72 | 5.03 | 5.21 | |
| 24 | Awana Bay | 4.95 | 5.32 | 5.75 | 6.06 | 6.37 | 6.75 | 7.02 | |
| 25 | Whangapoua | 3.19 | 3.39 | 3.66 | 3.85 | 4.04 | 4.29 | 4.44 | |

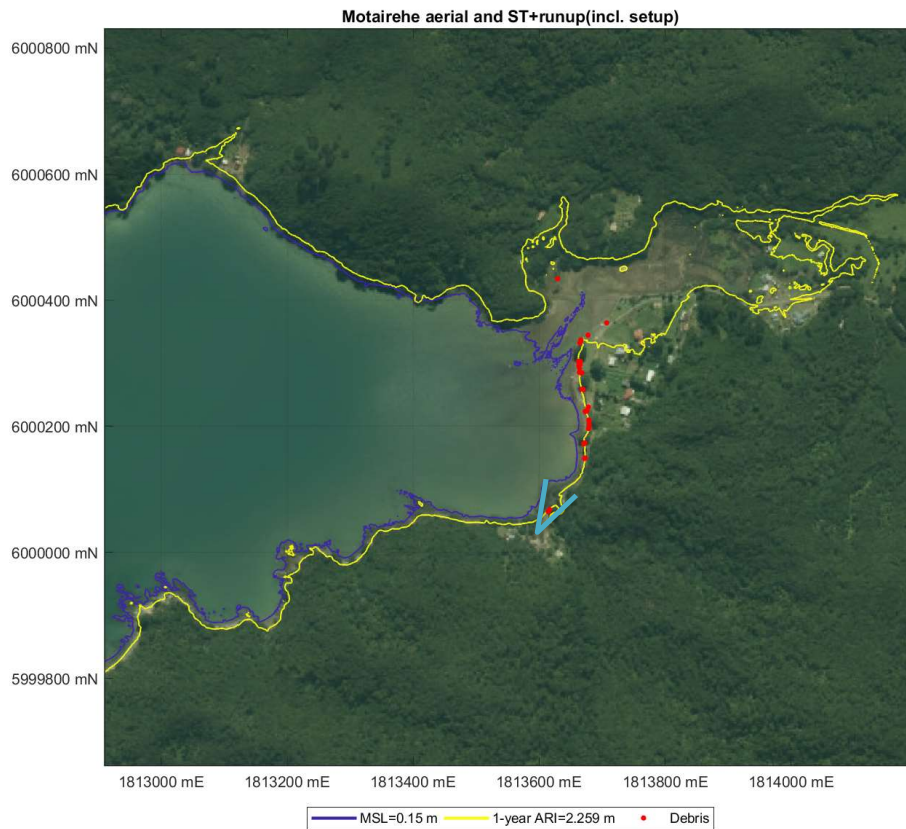


Figure C-1: Validation mapping of surveyed debris line (red circles) and estimated inundation extents from storm-tide plus wave runup (including setup) elevation at 1-year ARI (yellow) for Motairehe. MSL elevation also shown (Purple) and location of photo below (blue). Note inundation extents are for sea flooding only. Modelling excludes other processes which may locally affect sea levels such as river flows and wave overtopping flows around the stream mouth. [Aerial photograph: Auckland Council GIS, Coordinate system: NZ Transverse Mercator 2000].



Figure C-2: Survey photo at Motairehe showing small debris (sticks, dried seaweed) within grasses (lower left) below steep bank leading up to driveway at right. [Date: 17/7/2019 10:50 am, Credit: M. Allis (NIWA)].

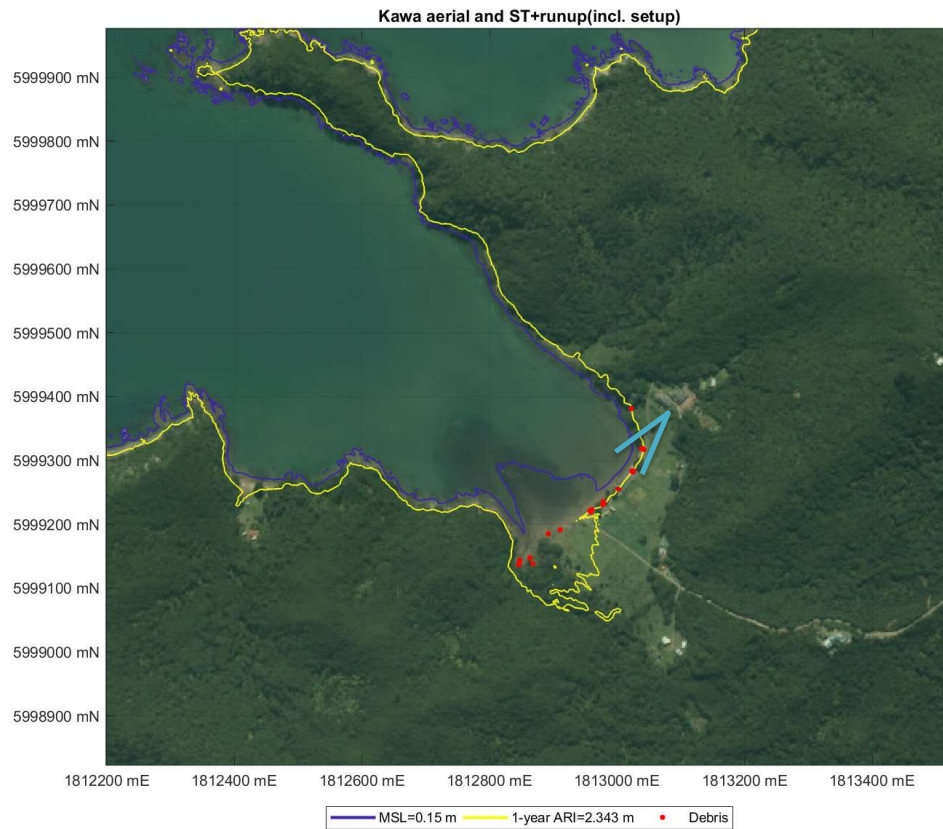


Figure C-3: Validation mapping of surveyed debris line (red circles) and estimated inundation extents from storm-tide plus wave runup (including setup) elevation at 1-year ARI (yellow) for Kawa. MSL elevation also shown (purple) and location of photo below (blue). Note inundation extents are for sea flooding only. Modelling excludes other processes which may locally affect sea levels and debris features such as stream flows and wave overtopping flows. [Aerial photograph: Auckland Council GIS, Coordinate system: NZ Transverse Mercator 2000].



Figure C-4: Survey photo at Kawa showing debris (sticks, logs) below grassed bank (lower left). [Date: 17/7/2019 11:51 am, Credit: M. Allis (NIWA)].

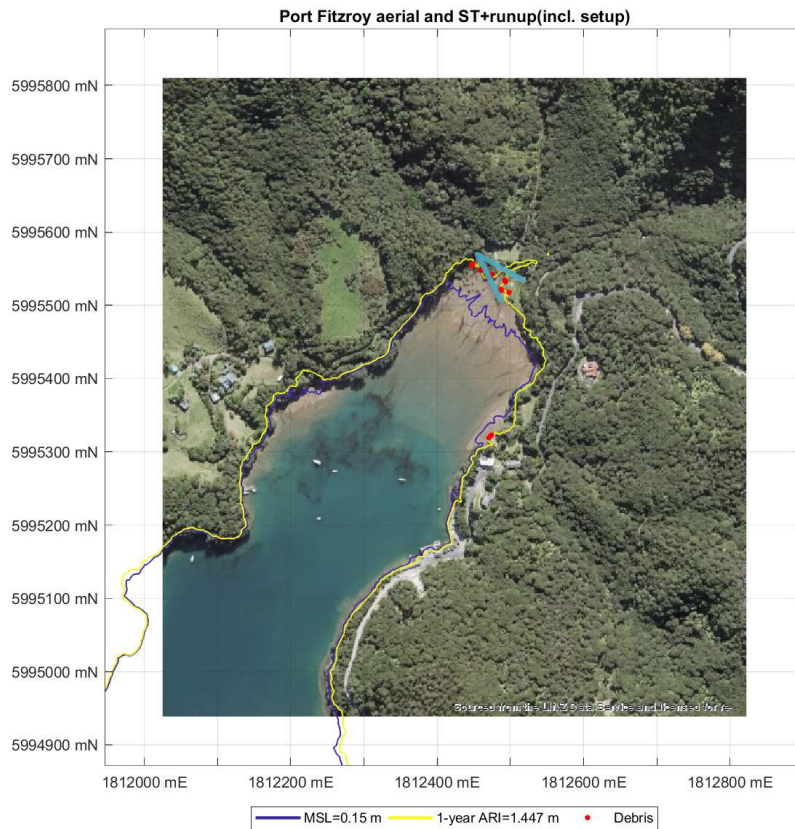


Figure C-5: Validation mapping of surveyed debris line (red circles) and estimated inundation extents from storm-tide plus wave runup (including setup) elevation at 1-year ARI (yellow) for Port Fitzroy. MSL elevation also shown (Purple) and location of photo below (blue). Note inundation extents are for sea flooding only. Modelling excludes other processes which may locally affect sea levels such as river flows and wave overtopping flows. [Aerial photograph: Auckland Council GIS, Coordinate system: NZ Transverse Mercator 2000].



Figure C-6: Survey photo at Port Fitzroy showing debris (sticks, logs) within grassed bank (centre, centre left) and embedded in sandy-mud beach (lower left). [Date: 17/7/2019 3:48 pm, Credit: M. Allis (NIWA)].

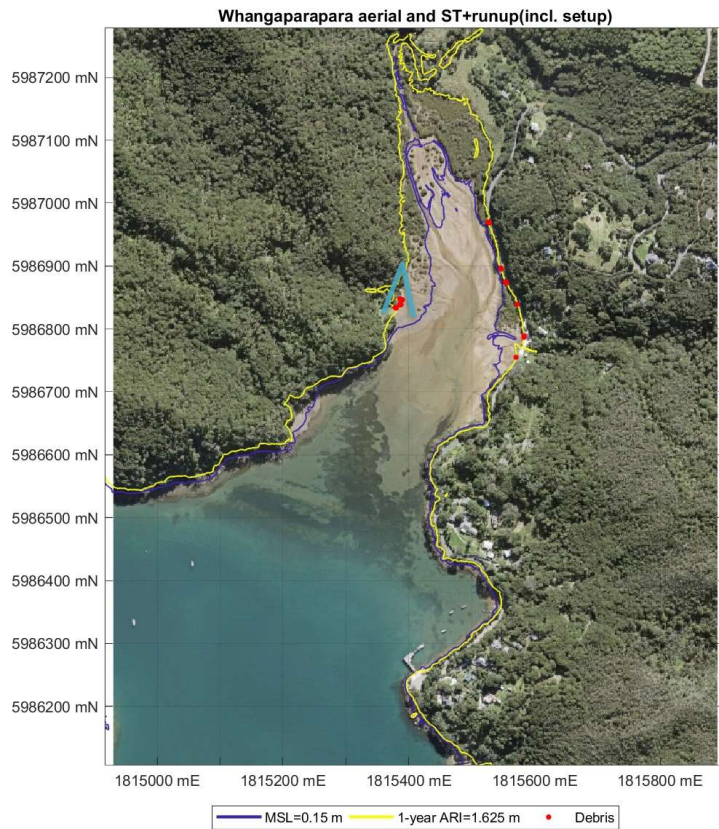


Figure C-7: Validation mapping of surveyed debris line (red circles) and estimated inundation extents from storm-tide plus wave runup (including setup) elevation at 1-year ARI (yellow) for Whangaparapara. MSL elevation also shown (purple) and location of photo below (blue). Note inundation extents are for sea flooding only. Modelling excludes other processes which may locally affect sea levels such as river flows and wave overtopping flows. [Aerial photograph: Auckland Council GIS, Coordinate system: NZ Transverse Mercator 2000].



Figure C-8: Survey photo at Whangaparapara showing debris (sticks, logs) above rocky beach. [Date: 16/7/2019 1:34 pm, Credit: M. Allis (NIWA)].

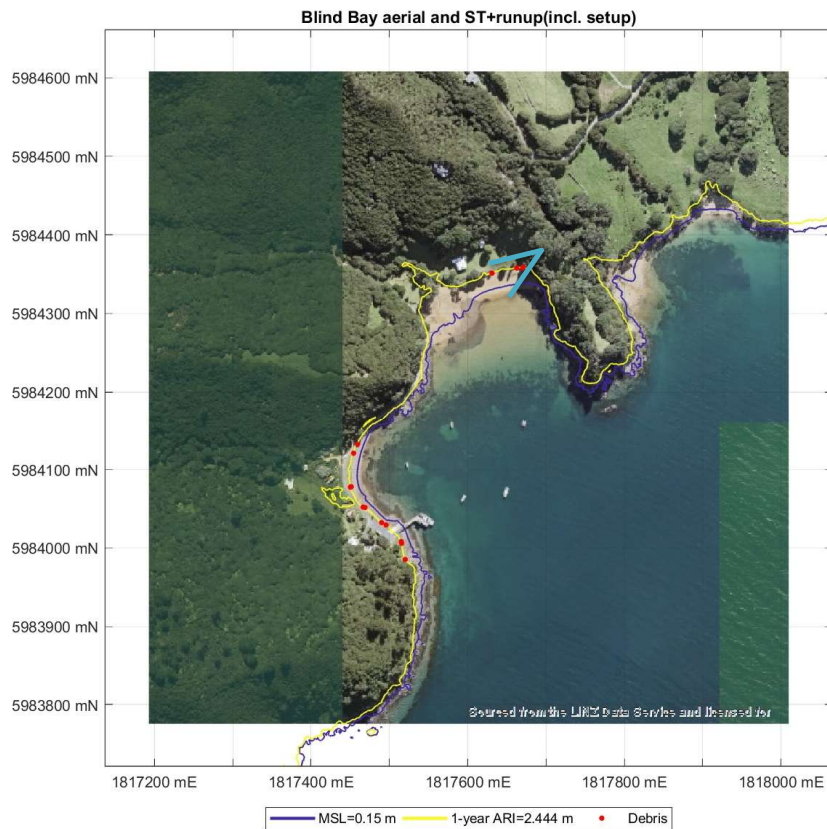


Figure C-9: Validation mapping of surveyed debris line (red circles) and estimated inundation extents from storm-tide plus wave runoff (including setup) elevation at 1-year ARI (yellow) for Blind Bay. MSL elevation also shown (purple) and location of photo below (blue). Note inundation extents are for sea flooding only. Modelling excludes other processes which may locally affect sea levels such as river flows and wave overtopping flows. [Aerial photograph: Auckland Council GIS, Coordinate system: NZ Transverse Mercator 2000].



Figure C-10: Survey photo at Blind Bay showing stranded seaweed (on sand) and small debris (sticks, dried seaweed) within grasses (centre right). [Date: 16/7/2019 11:13 am, Credit: M. Allis (NIWA)].

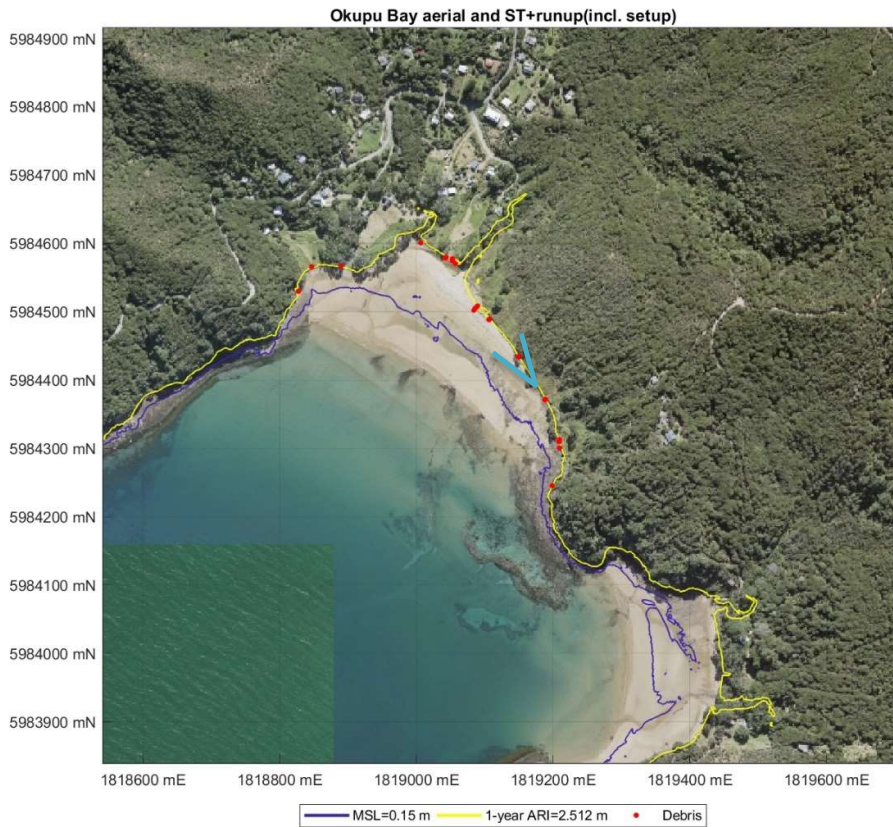


Figure C-11: Validation mapping of surveyed debris line (red circles) and estimated inundation extents from storm-tide plus wave runup (including setup) elevation at 1-year ARI (yellow) for Okupu Bay. MSL elevation also shown (purple) and location of photo below (blue). Note inundation extents are for sea flooding only. Modelling excludes other processes which may locally affect sea level such as river flows and wave overtopping flows. [Aerial photograph: Auckland Council GIS, Coordinate system: NZ Transverse Mercator 2000].



Figure C-12: Survey photo at Okupu Beach showing stranded seaweed (on sand) and small debris (sticks, dried seaweed) within grasses (centre right). [Date: 16/7/2019 9:18 am, Credit: M. Allis (NIWA)].

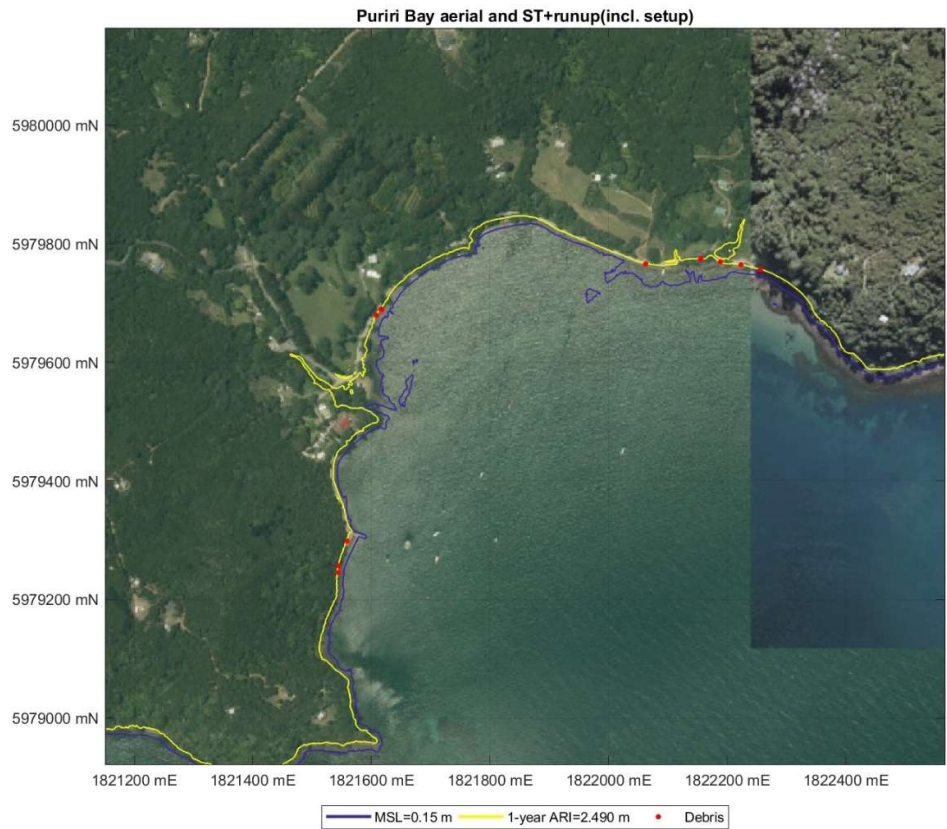


Figure C-13: Validation mapping of surveyed debris line (red circles) and estimated inundation extents from storm-tide plus wave runup (including setup) elevation at 1-year ARI (yellow) for Puriri Bay. MSL elevation also shown (Yellow). Note inundation extents are for sea flooding only. Modelling excludes other processes which may locally affect sea levels such as river flows and wave overtopping flows. [Aerial photograph: Auckland Council GIS, Coordinate system: NZ Transverse Mercator 2000].

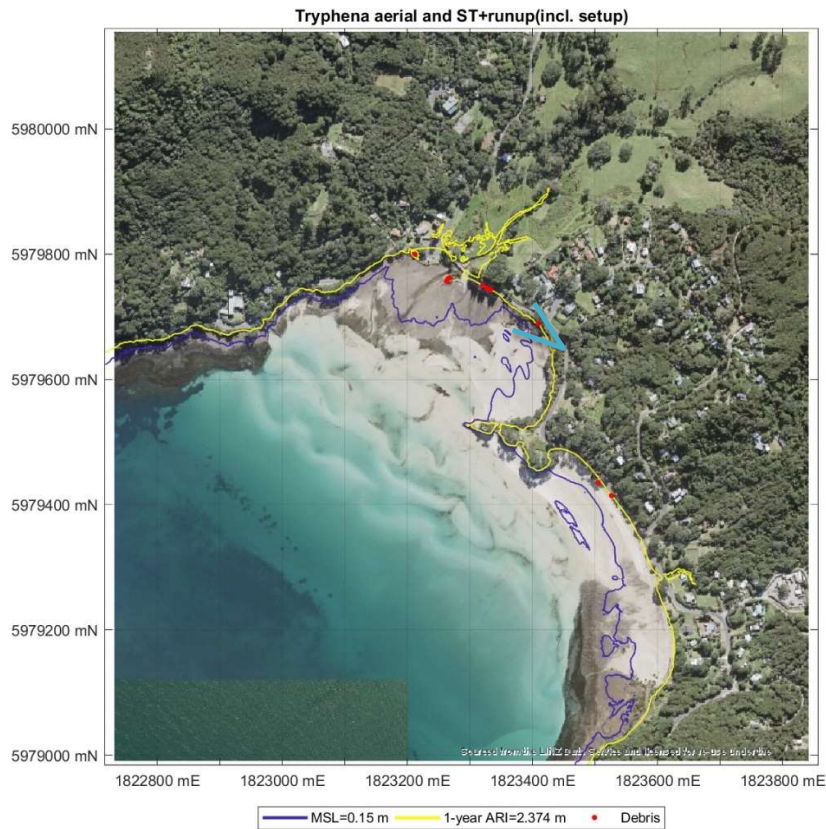


Figure C-14: Validation mapping of surveyed debris line (red circles) and estimated inundation extents from storm-tide plus wave runup (including setup) elevation at 1-year ARI (yellow) for Tryphena. MSL elevation also shown (purple) and photograph location (blue). Note inundation extents are for sea flooding only. Modelling excludes other processes which may locally affect sea levels such as river flows and wave overtopping flows. [Aerial photograph: Auckland Council GIS, Coordinate system: NZ Transverse Mercator 2000].



Figure C-15: Survey photo at Tryphena showing stranded seaweed and small debris (sticks, dried seaweed) at base of cliff (centre right). [Date: 15/7/2019 1:25 pm, credit: M. Allis (NIWA)].

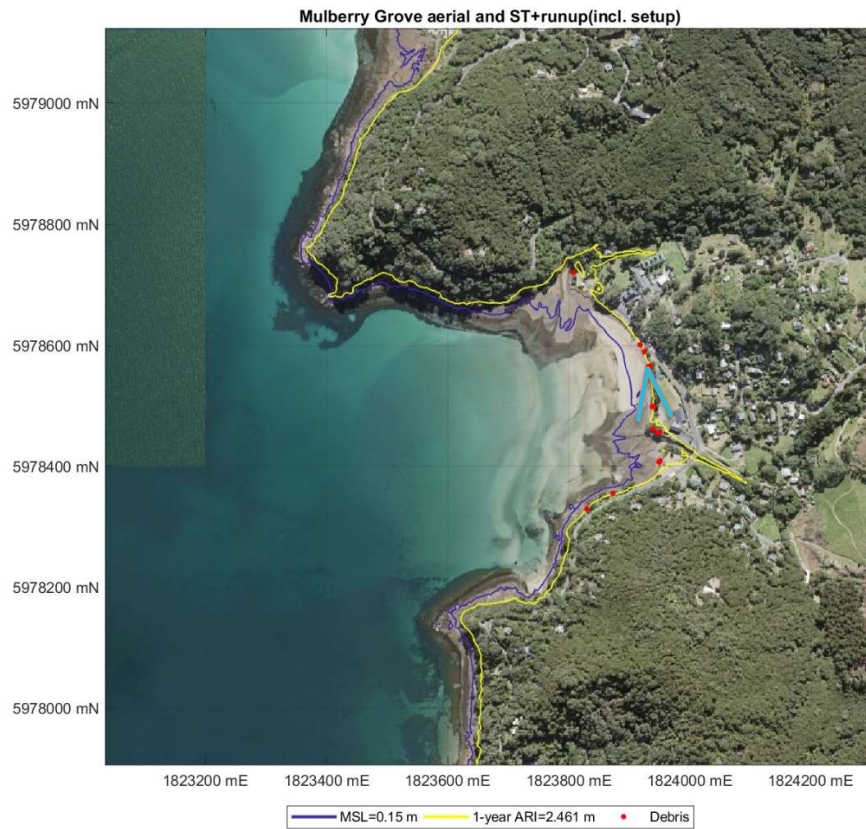


Figure C-16: Validation mapping of surveyed debris line (red circles) and estimated inundation extents from storm-tide plus wave runup (including setup) elevation at 1-year ARI (yellow) for Mulberry Grove. MSL elevation also shown (purple) and location of photograph below (blue). Note inundation extents are for sea flooding only. Modelling excludes other processes which may locally affect sea levels such as river flows and wave overtopping flows. [Aerial photograph: Auckland Council GIS, Coordinate system: NZ Transverse Mercator 2000].



Figure C-17: Survey photo at Mulberry Grove showing stranded seaweed and small debris (sticks, dried seaweed) within grasses (centre left). [Date: 15/7/2019 11:20 am, Credit: R. Ovenden (NIWA)].

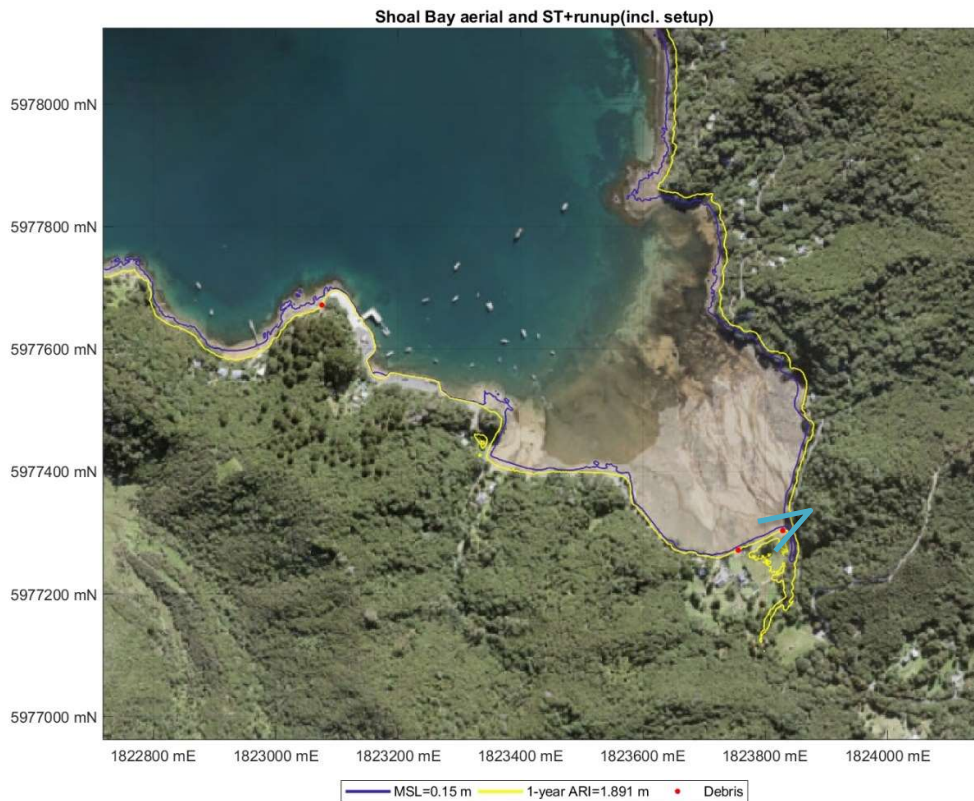


Figure C-18: Validation mapping of surveyed debris line (red and blue circles) and estimated inundation extents from storm-tide plus wave runup (including setup) elevation at 1-year ARI (yellow) for Shoal Bay. MSL elevation also shown (purple) and location of photograph below (blue). Note inundation extents are for sea flooding only. Modelling excludes other processes which may locally affect sea levels such as river flows and wave overtopping flows. [Aerial photograph: Auckland Council GIS, Coordinate system: NZ Transverse Mercator 2000].



Figure C-19: Survey photo at Shoal Bay showing stranded seaweed and small debris (sticks, dried seaweed) at base of grass causeway (centre left). [Date: 15/7/2019 1:25 pm, Credit: M. Allis (NIWA)].



Figure C-20: Validation mapping of surveyed debris line (red circles) and estimated inundation extents from storm-tide plus wave runup (including setup) elevation at 1-year ARI (yellow) for Oruawharo Bay. 5MSL elevation also shown (purple) and location of photograph below (blue). Note the yellow line appears faint on the white beach surface (annotation). Wave runup elevation contour extend inland around low-lying swamp areas (see annotations). Modelling excludes other processes which may locally affect sea levels such as river flows and wave overtopping flows. [Aerial photograph: Auckland Council GIS, Coordinate system: NZ Transverse Mercator 2000].



Figure C-21: Survey photo at Oruawhoro Bay showing stranded seaweed and small debris (sticks, dried seaweed) within vegetation and at base foredune (lower left). [Date: 15/7/2019 11:16 am, Credit: R. Ovenden (NIWA)].



Figure C-22: Validation mapping of surveyed debris line (red and blue circles) and estimated inundation extents from storm-tide plus wave runup (including setup) elevation at 1-year ARI (yellow) for Kaitoke Beach. MSL elevation also shown (Purple) and location of photograph (blue). Note inundation extents are for sea flooding only. Modelling excludes other processes which may locally affect sea levels such as river flows and wave overtopping flows. [Aerial photograph: Auckland Council GIS, Coordinate system: NZ Transverse Mercator 2000].



Figure C-23: Survey photo at Kaitoke Beach showing stranded seaweed and small debris (sticks, dried seaweed) within vegetation and at base foredune. [Date: 18/7/2019 1:26 pm, Credit: M. Allis (NIWA)].

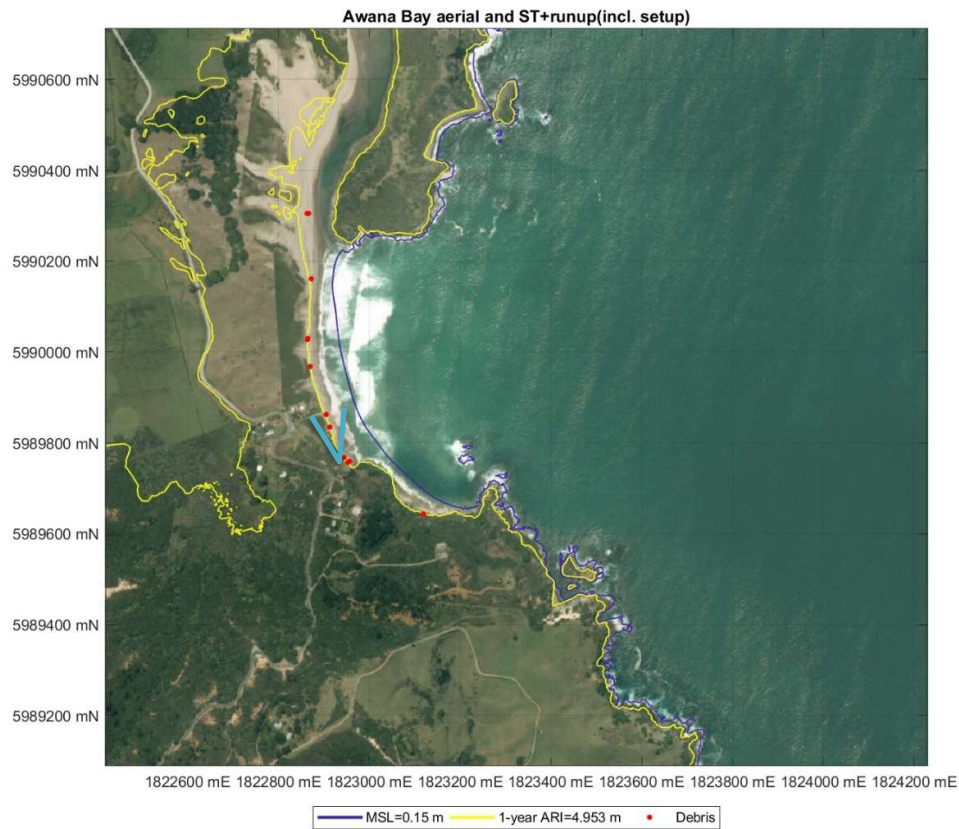


Figure C-24: Validation mapping of surveyed debris line (red circles) and estimated inundation extents from storm-tide plus wave runup (including setup) elevation at 1-year ARI (yellow) for Awana Bay. 5-year ARI elevation also shown (Yellow). Note inundation extents are for sea flooding only. Modelling excludes other processes which may locally affect sea levels such as river flows and wave overtopping flows. [Aerial photograph: Auckland Council GIS, Coordinate system: NZ Transverse Mercator 2000].



Figure C-25: Awana beach showing seaweeds scattered along beach face and some debris below vegetation line below toe of vegetated but steep foredune. [Date: 16/7/2019 4:16 pm, Credit: R. Ovenden (NIWA)].

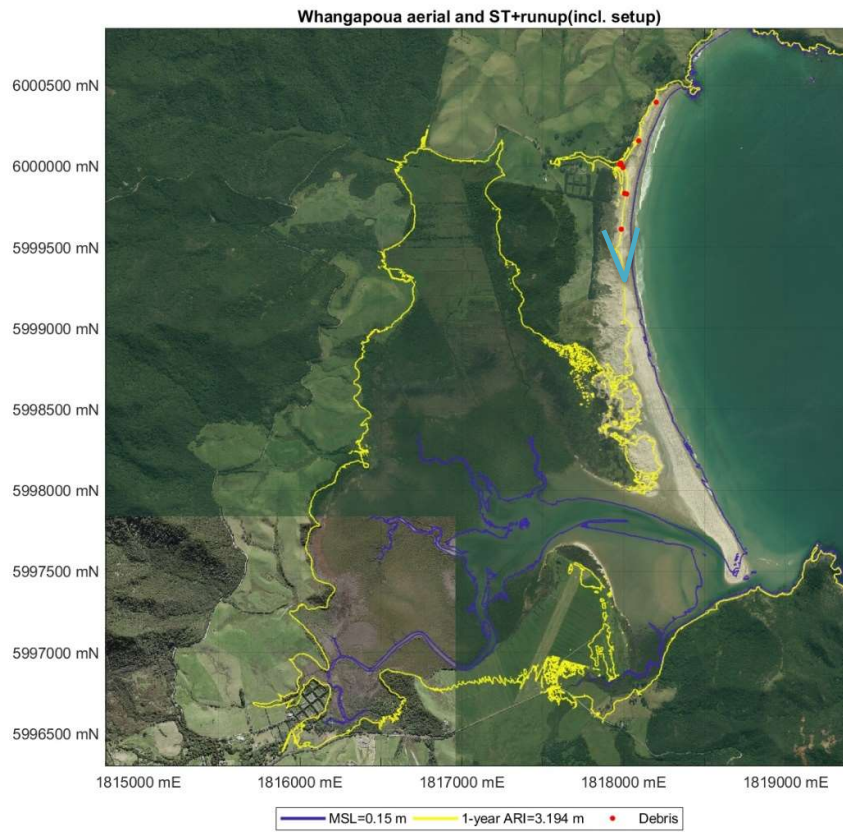


Figure C-26: Validation mapping of surveyed debris line (red circles) and estimated inundation extents from storm-tide plus wave runup (including setup) elevation at 1-year ARI (yellow) for Whangapoua. MSL elevation also shown (purple) and location of photograph below (Blue). Note inundation extents are for sea flooding only. Modelling excludes other processes which may locally affect sea levels such as river flows and wave overtopping flows. [Aerial photograph: Auckland Council GIS, Coordinate system: NZ Transverse Mercator 2000].



Figure C-27: Whangapoua beach showing seaweeds scattered along beach face and some debris. [Date: 17/7/2019 11:20 am, Credit: R. Ovenden (NIWA)].



Part 4: Technical Report: Parakai/Helensville
Coastal Flood Inundation,
DHI 2020



Technical Report: Parakai/Helensville Coastal Flood Inundation

Numerical Modelling



This report has been prepared under the DHI Business Management System certified by Bureau Veritas to comply with ISO 9001 (Quality Management)

ISO 9001
Management System Certification

BUREAU VERITAS
Certification Denmark A/S



Technical Report: Parakai/Helensville Coastal Flood Inundation

Numerical Modelling

Prepared for Auckland Council
Represented by Natasha Carpenter



| | |
|-----------------|-----------------|
| Project manager | Benjamin Tuckey |
| Project number | 44801405 |
| Approval date | 14/02/20 |
| Revision | Final 2.0 |
| Classification | Open |



CONTENTS

| | | |
|----------|---|-----------|
| 1 | Technical Summary | 1 |
| 2 | Introduction | 2 |
| 2.1 | Co-ordinate System and Vertical Datum | 3 |
| 3 | Model Set Up | 4 |
| 4 | Model Calibration and Validation | 7 |
| 4.1 | Model Calibration | 7 |
| 4.2 | Model Validation | 8 |
| 5 | Design Scenarios | 10 |
| 5.1 | Storm Surge Boundary Generation | 10 |
| 5.2 | Elevated River Flow Input | 12 |
| 6 | Simulation Results..... | 13 |
| 7 | Summary..... | 16 |
| 8 | References..... | 17 |

1 Technical Summary

DHI were commissioned by Auckland Council to predict coastal inundation water levels for the Parakai/Helensville floodplain resulting from coastal storm surge.

Simulations were undertaken with a calibrated hydrodynamic model to assess peak flood inundation levels and depths for the following average recurrence interval (ARI) scenarios based on the findings of an extreme sea-level analysis by NIWA:

1. 5 year ARI;
2. 20 year ARI;
3. 50 year ARI;
4. 50 year ARI with +0.5 m sea level rise included;
5. 50 year ARI with +1 m sea level rise included;
6. 50 year ARI with +2 m sea level rise included;
7. 100 year ARI;
8. 100 year ARI with +0.5 m sea level rise included; and
9. 100 year ARI with +1 m sea level rise included; and
10. 100 year ARI with +2 m sea level rise included.

As a sensitivity test, the 50 year ARI coastal storm surge event was simulated with a 50 year ARI flood event for Kaipara River included.

For each of the modelled scenarios, raster based data was provided to Auckland Council of maximum elevation and maximum water depth. The resultant coastal inundation extents are being mapped by Stantec and will be provided on Auckland Councils online geodatabase 'Geomaps'.

2 Introduction

Predictions for coastal inundation water levels for the Parakai/Helensville floodplain have previously been derived by NIWA (2013) from a hydrodynamic modelling analysis of coastal storm surge elevations resulting from storm tides and wave set-up around the coastline of the Auckland region. The results from the hydrodynamic model were spatially interpolated along the coastline and intersected with a digital elevation model of the land surface to produce the static inundation water levels.

One of the key assumptions with this type of approach is that the floodplain storage volumes (in the coastal land area and/or rivers) are small compared to the volume changes being considered in the main body of water. When this is the case, there will be no significant changes in inundation levels between the main water body and the inundated land, therefore the floodplain can be excluded from the hydrodynamic modelling.

In 2014, Auckland Council commissioned DHI to carry out an initial assessment to investigate the effect of this assumption on predicted inundation levels at a particular site of interest, Parakai/Helensville on the Kaipara River (DHI, 2014). The assessment indicated that lower peak flood inundation levels were expected when accounting for the dynamic inundation of the floodplain in this area. It was determined that none of the work to date, suitably assessed this and so Auckland Council commissioned NIWA to undertake an extreme sea-level analysis at Helensville to determine the probability of extreme sea-level elevations (NIWA, 2016). NIWA then commissioned DHI to simulate the flood inundation associated with these coastal storm surges using a model including the floodplain (NIWA and DHI, 2016).

DHI utilised an existing two-dimensional hydrodynamic model of Kaipara Harbour developed for Rodney District Council, to predict extreme water levels in the Kaipara Harbour and to provide downstream water level boundary conditions for the Kaipara River flood model (DHI, 2006) and assess dilutions from proposed upgrade of Helensville wastewater treatment plant (DHI, 2009). The floodplain bathymetry for the area of interest was generated from 2006 LiDAR data.

The model was calibrated (based on observed water levels at the Helensville tide gauge) for a significant storm-tide event that occurred in September 2005. The model was then validated for an event that occurred in June 2012. With the calibrated model, DHI then assessed peak flood inundation levels due to coastal storm surge for selected scenarios.

Auckland Council have commissioned DHI to update the hydrodynamic model with the floodplain bathymetry generated from 2016 LiDAR data. The model resolution was increased for a number of areas within the model as part of this process.

The model was validated (based on observed water levels at the Helensville tide gauge) for the significant storm-tide events that occurred in September 2005 and June 2012. With the updated model, DHI then assessed peak flood inundation levels due to coastal storm surge for the following scenarios:

1. 5 year ARI;
2. 20 year ARI;
3. 50 year ARI;
4. 50 year ARI with +0.5 m sea level rise included;
5. 50 year ARI with +1 m sea level rise included;
6. 50 year ARI with +2 m sea level rise included;

7. 100 year ARI;
8. 100 year ARI with +0.5 m sea level rise included; and
9. 100 year ARI with +1 m sea level rise included; and
10. 100 year ARI with +2 m sea level rise included.

A sensitivity test was also undertaken to investigate the joint probability of elevated river flows (50 year ARI flood event) combining with 50 year ARI coastal storm surge within the southern Kaipara Harbour, to assess the impact that elevated river flows will have on sea level inundation within the southern Kaipara Harbour.

Consistent with DHI and NIWA (2016) the stop banks surrounding the Parakai/Helensville floodplain have not been included in the model. Auckland Council has requested these structure be excluded from the model given their dynamic nature and potential for change over time. It should be noted that for the sea level rise scenarios, the stop banks would have been overtopped anyway.

2.1 Co-ordinate System and Vertical Datum

For this study, all data is presented using the New Zealand Transverse Mercator projection (NZTM) and the vertical datum is Auckland vertical datum 1946.

3 Model Set Up

An existing MIKE 21 Flexible Mesh (FM) two dimensional hydrodynamic model of the Kaipara Harbour and Parakai/Helensville floodplain was updated with 2016 LiDAR data provided by Auckland Council. The bathymetry for the southern part of the harbour and floodplain is shown in Figure 3-1.

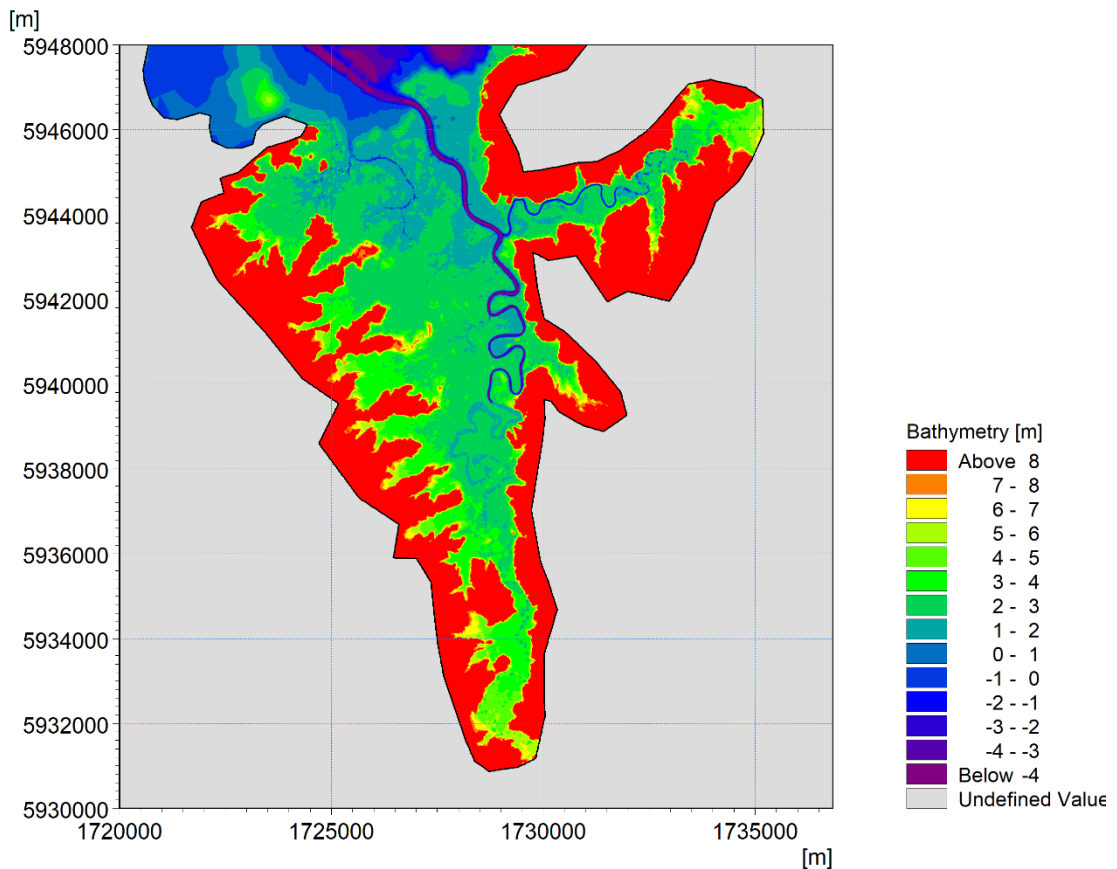


Figure 3-1 Model bathymetry and extent for southern part of Kaipara Harbour and associated floodplain. Depths are shown relative to Auckland vertical datum (1946).

The hydrodynamic model mesh was constructed with a horizontal resolution (varying from approximately 25 to 1000 m² for floodplain) deemed (by DHI) to accurately simulate coastal-storm inundation over the Parakai/Helensville floodplain, while still maintaining efficient and realistic model run-times.

Significant obstructions to flood flow in the floodplain that were resolved by the LiDAR, (e.g. roads) were well represented in the model bathymetry. An example of how Parkhurst Road was represented in the model mesh is presented in Figure 3-2. To further ensure the road was sufficiently resolved, the road was also included as a dike in the model set up, with the crest levels extracted from the LiDAR data.

Council has identified approximately 41 locations where there are culverts/bridges that flow into the harbour, but these have all got flap gates, so these were not included in the model. One exception is 239 Parkhurst Rd where there is 450 mm and 900 mm diameter culverts with no

flap gates. These have been included in the model with invert levels approximately 1.5 m below the road crest level.

There are other locations (e.g. KiwiRail culverts) that Auckland Council do not have sufficient information for to include in the analysis. This is an accepted limitation of the inundation assessment.

The majority of the stop banks protecting the Parakai/Helensville floodplain from the river and harbour, were not well resolved by the LiDAR. Therefore stopbanks were not included in the model at the request of Auckland Council. However it should be noted that for the sea level rise scenarios, the stop banks would have been overtopped anyway.

For the calibration/validation simulations a second model was developed which did not include any floodplain. This is because without stop banks included in the model, there would be significant inundation of the floodplain predicted to occur, when in reality the flow would remain mostly constrained with the harbour and rivers.

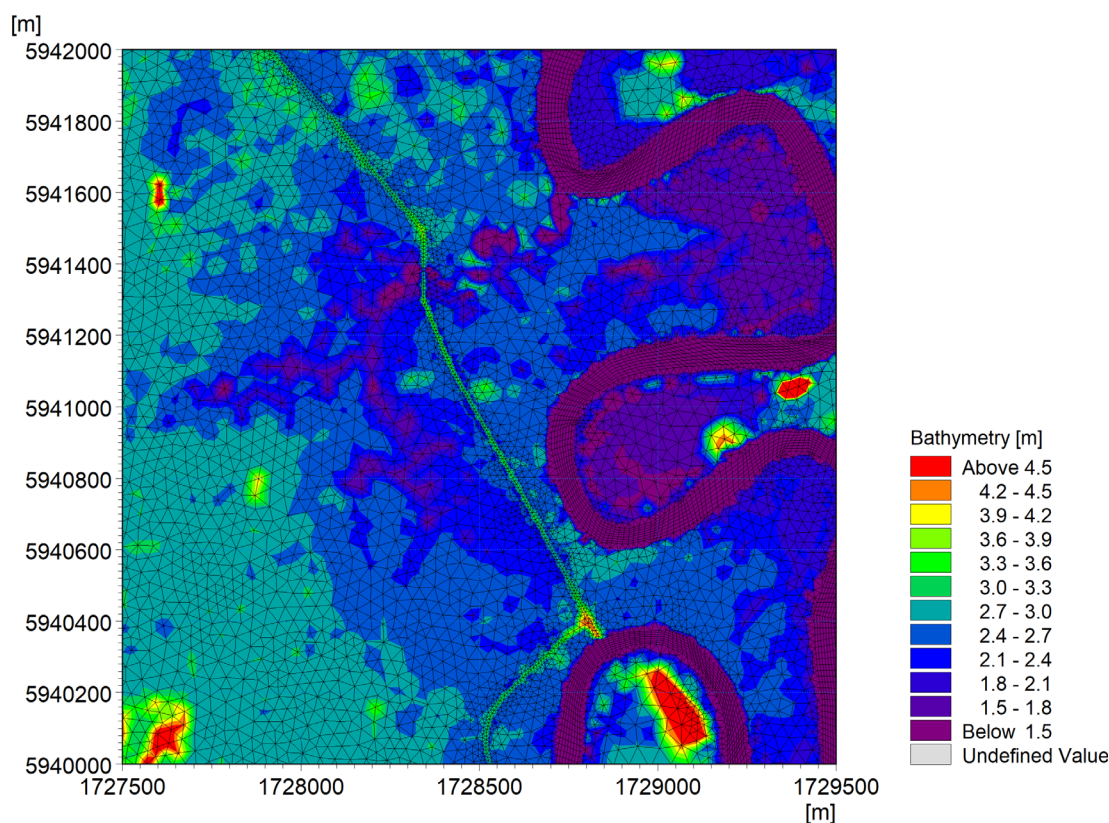


Figure 3-2 Parkhurst Road representation in model mesh. Depths are shown relative to Auckland vertical datum (1946).

No river flows (i.e. Kaipara and Kaukapakapa Rivers) were included in the model set up, since previous work indicated that river flows do not have a significant effect on sea level inundation within the southern Kaipara Harbour (DHI, 2006). This assumption was investigated through a sensitivity test as a part of this study (see Section 6).

Observed water levels from Pouto Point for the period 2001 to 2013 were provided by NIWA and have been utilised as boundary condition, with a shift of minus 55 mins to account for the time for the tide to propagate from the open ocean boundary to Pouto Point tide gauge.

A varying bed roughness map (Manning number M) was generated for the floodplain based on land use characteristics for the area (LCDB2). This is a method that DHI have successfully used for other types of flood assessment studies for Auckland Council. The land use GIS layer was used to derive a resistance map for the MIKE 21 model extent. A spatially varying resistance map was generated by mapping land uses types to various hydraulic resistances (Manning number M) based on experience and accepted use in the industry. The adopted mapping is shown in Table 3-1.

Table 3-1 Land use codes with associated resistance Manning number. Note table is sorted from highest to lowest roughness (smallest to highest Manning Number).

| Description (LCDB2) | Land Use Code | Manning Number (M) |
|-------------------------------------|---------------|--------------------|
| Pine Forest - Closed Canopy | 66 | 8 |
| Manuka and or Kanuka | 52 | 8 |
| Pine Forest - Open Canopy | 65 | 8 |
| Indigenous Forest | 69 | 8 |
| Orchard and Other Perennial Crops | 32 | 8 |
| Vineyard | 31 | 8 |
| Broadleaved Indigenous Hardwoods | 54 | 8 |
| Other Exotic Forest | 67 | 8 |
| Gorse and or Broom | 51 | 8 |
| Afforestation (imaged, post LCDB 1) | 63 | 8 |
| Deciduous Hardwoods | 68 | 8 |
| Major Shelterbelts | 61 | 8 |
| Afforestation (not imaged) | 62 | 8 |
| Forest Harvested | 64 | 8 |
| Built-up Area | 1 | 10 |
| Transport Infrastructure | 5 | 10 |
| Fresh Water Vegetation | 41 | 10 |
| Saline Vegetation | 45 | 10 |
| Mangroves | 70 | 10 |
| High Producing Exotic Grassland | 40 | 20 |
| Short-rotation Cropland | 30 | 20 |
| Surface Mine | 3 | 20 |
| Low Producing Grassland | 41 | 20 |
| Mixed Exotic Shrubland | 56 | 20 |
| Flaxland | 47 | 20 |
| Urban Parkland / Open Space | 2 | 30 |
| River | 21 | 50 |
| River and Lakeshore Gravel and Rock | 11 | 50 |
| Lake and Pond | 20 | 50 |

4 Model Calibration and Validation

The model was calibrated against observed water levels at the Helensville tide gauge (provided by NIWA) for a significant storm-tide event that occurred in September 2005. The model was then validated for an event that occurred in June 2012.

4.1 Model Calibration

On 18th September 2005 at approximately 11:30 pm, a peak water level of 2.83 m was observed at the Helensville tide gauge (see Figure 4-1). This event was selected for calibrating the hydrodynamic model.

Observed water level from the tide gauges at Helensville and Pouto Point were analysed to separate the tidal and non-tidal components of the water level time series. The tidal and non-tidal components of the Helensville water level data (along with the observed water levels at Helensville) and the non-tidal component for the Pouto Point water level data are presented in Figure 4-1.

Overall the non-tidal components (which can be considered mostly the storm surge component of the observed water levels) at the two locations are similar. However between 12 pm to 6 pm on 18th September 2005, there is an increase in the non-tidal component of the water level of approximately 0.5 m at Helensville compared to Pouto Point. This increase in non-tidal water level at Helensville may have been wind or wave generated.

It was outside the scope of the study to represent these types of localised effects so periods when there are significant differences in non-tidal water levels between the two sites will not be accurately modelled at the Helensville site.

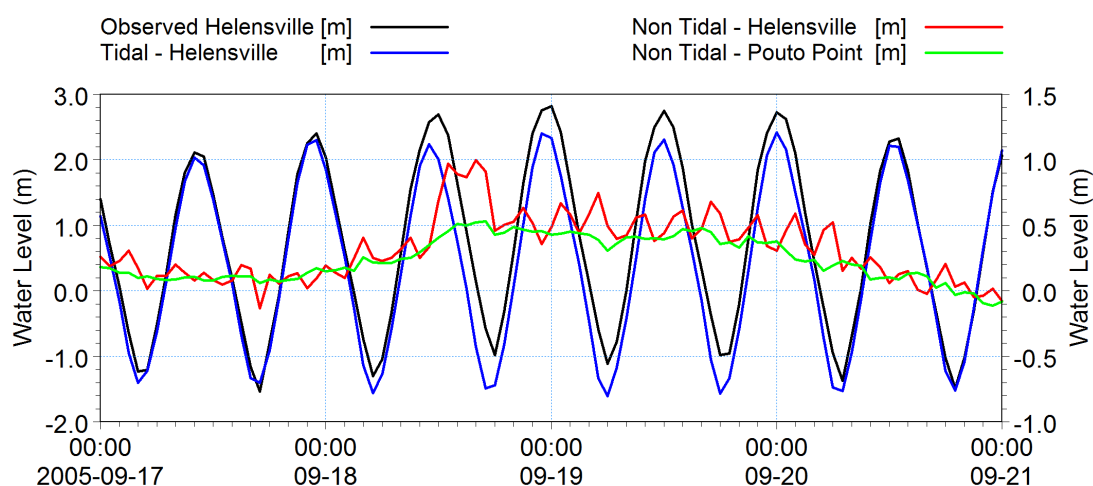


Figure 4-1 Tidal analysis of observed data from the Helensville and Pouto Point Tide gauges for 2005 calibration event. Observed Helensville water levels and tidal component of Helensville water levels (left y-axis) and non-tidal component of Helensville and Pouto Point water levels (right y-axis)

The comparison of the observed and predicted water levels for the 18th September 2005 event at the Helensville tide gauge is presented in Figure 4-2. The calibrated model was able to match the observed high water levels within 6 cm. For this reason the model was deemed to be suitably calibrated for the purposes of this study. As expected the model does not match the peak for the midday high tide of the 18th September, since there was a non-tidal associated increase in water levels at Helensville at this time, which the model was not set up to reproduce.

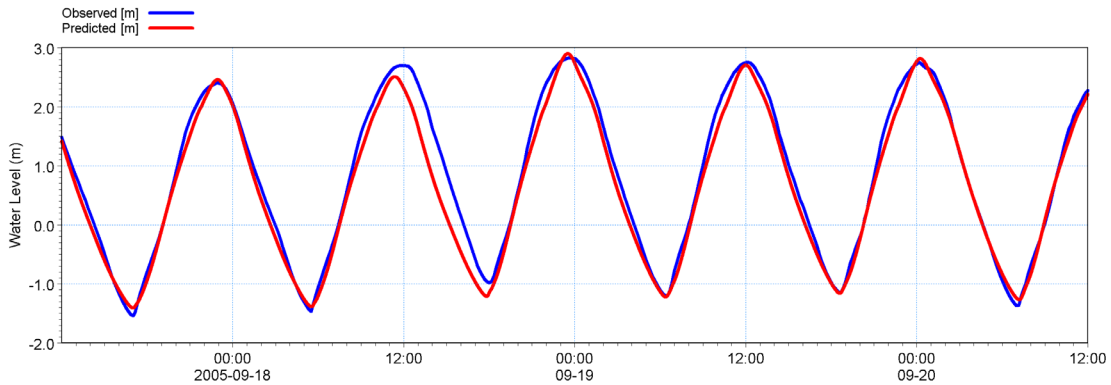


Figure 4-2 Comparison of observed and predicted water levels at Helensville tide gauge for September 2005 calibration event.

4.2 Model Validation

On 7th June 2012 at approximately 1:00 am, a peak water level of 2.72 m was observed at the Helensville tide gauge (see Figure 4-3). This event was selected for validating the calibrated hydrodynamic model.

The tidal and non-tidal components of the Helensville water level data (along with the observed water levels at Helensville) and the non-tidal component for the Pouto Point water level data are presented in Figure 4-3. The non-tidal components of the observed water levels at both Pouto Point and Helensville tide gauges are very similar, therefore this was considered a good event for validating the model.

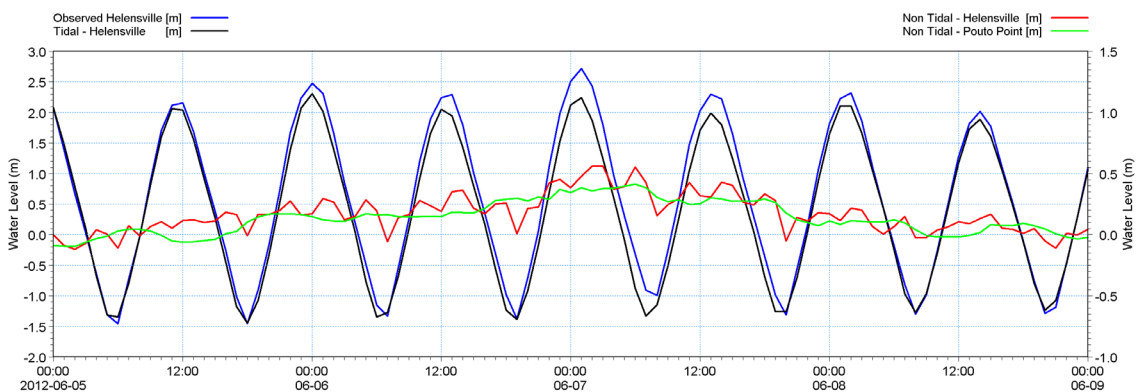


Figure 4-3 Tidal analysis of Helensville and Pouto Point Tide gauges for validation event. Observed Helensville water levels and tidal component of Helensville water levels (left y-axis) and non-tidal component of Helensville and Pouto Point water levels (right y-axis)

The comparison of the observed and predicted water levels for the 7th June 2012 event at the Helensville tide gauge is presented in Figure 4-4. The calibrated model was able to match the observed high water levels within 5 cm. The good agreement for the validation event further supported that the model was suitably calibrated and that the model is suitable for predicting coastal inundation of the Parakai/Helensville floodplain.

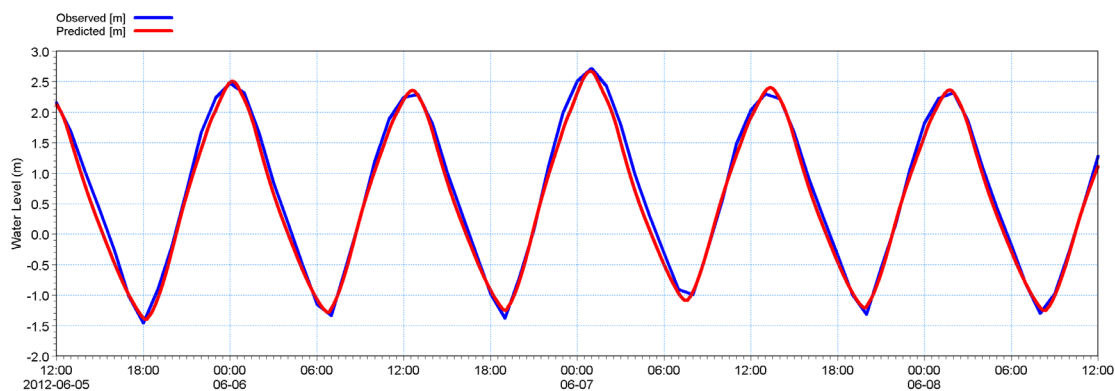


Figure 4-4 Comparison of observed and predicted water levels at Helensville tide gauge for June 2012 validation event

5 Design Scenarios

This section outlines the simulations that were undertaken to assess peak flood inundation levels for the Parakai/Helensville floodplain due to a number of coastal storm surge scenarios with and without sea level rise. The scenarios simulated were as follows:

1. 5 year ARI;
2. 20 year ARI;
3. 50 year ARI;
4. 50 year ARI with +0.5 m sea level rise included;
5. 50 year ARI with +1 m sea level rise included;
6. 50 year ARI with +2 m sea level rise included;
7. 100 year ARI;
8. 100 year ARI with +0.5 m sea level rise included; and
9. 100 year ARI with +1 m sea level rise included; and
10. 100 year ARI with +2 m sea level rise included.

A sensitivity test was also undertaken to investigate the impact that elevated river flows will have on sea level inundation within the southern Kaipara Harbour. This simulation was a 50 year ARI coastal storm surge event coinciding with a 50 year ARI flow for the Kaipara River with a peak flow of 305 m³/s. This event is noted to have a high joint probability of occurrence, with the two events having low to mild interdependency (NIWA 2018).

NIWA (2016) calculated the 5, 20, 50 and 100 year ARI coastal storm surge peak levels for the Helensville tide gauge, which are presented in Table 5-1.

Table 5-1 Summary of ARI coastal storm surge peak levels for the Helensville tide gauge (AVD-46).

| ARI | Sea Level (m) |
|-----|---------------|
| 5 | 2.82 |
| 20 | 2.97 |
| 50 | 3.08 |
| 100 | 3.18 |

5.1 Storm Surge Boundary Generation

For the design scenarios, a 48 hour duration storm surge (based on a sech^2 relationship) was generated, with the peak of the surge coincident with the high water of a spring tide.

The storm surge (y_{ss}) was generated using the following sech^2 relationship:

$$y_{ss} = a_{ss} \operatorname{sech}^2 k(t - t_0)$$

where a_{ss} = amplitude of the storm surge;

t_0 = time of the peak;

k = frequency defined by:

$$k = \frac{3}{n_d}$$

where n_d = number of days either side of peak when y_{ss} falls to $a_{ss}/100$.

The amplitude of the storm surge was calculated such that at the Helensville tide gauge location, the required extreme water level (i.e. for 100 year ARI, 3.18 m) was achieved for a simulation which did not include the floodplain.

As an example, the boundary condition generated to obtain the peak water level for the 100 year ARI, is presented in Figure 5-1. For this scenario, the peak water level for the boundary condition is 2.72 m.

For sea level rise scenarios, the boundary condition was then shifted by +0.5 m, +1 m or +2 m.

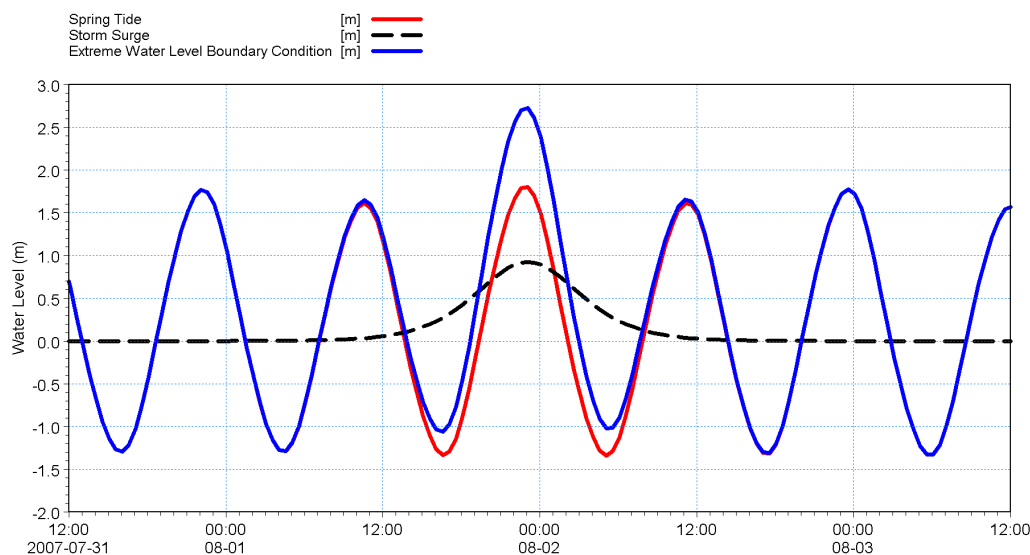


Figure 5-1 100 year ARI extreme water level open ocean boundary condition, including spring tide and storm surge components (red and black dashed lines are added together to give the solid blue line).

5.2 Elevated River Flow Input

Auckland Council provided the flow hydrograph for the 50 year ARI event for Kaipara River. The flow time series for this event is presented in Figure 5-2 and has a peak flow of 305 m³/s.

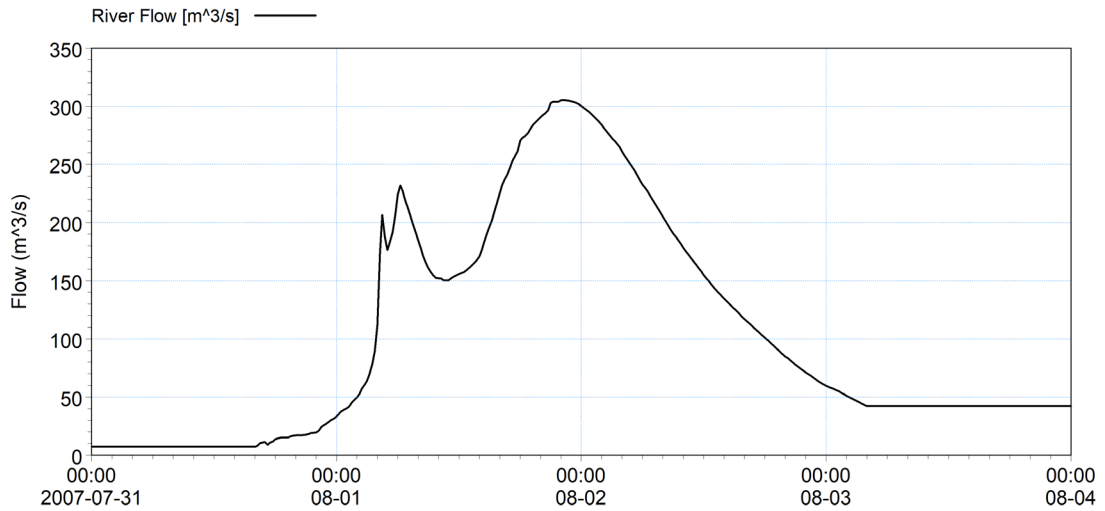


Figure 5-2 Auckland Council provided hydrograph for 50 Year ARI flood event for Kaipara River.

6 Simulation Results

For each of the simulated scenarios, 10 m x 10 m resolution rasters of maximum water depth and maximum water level were provided to Auckland Council.

For all scenarios, peak water levels at the locations indicated in Figure 6-1 are provided in Table 6-1.

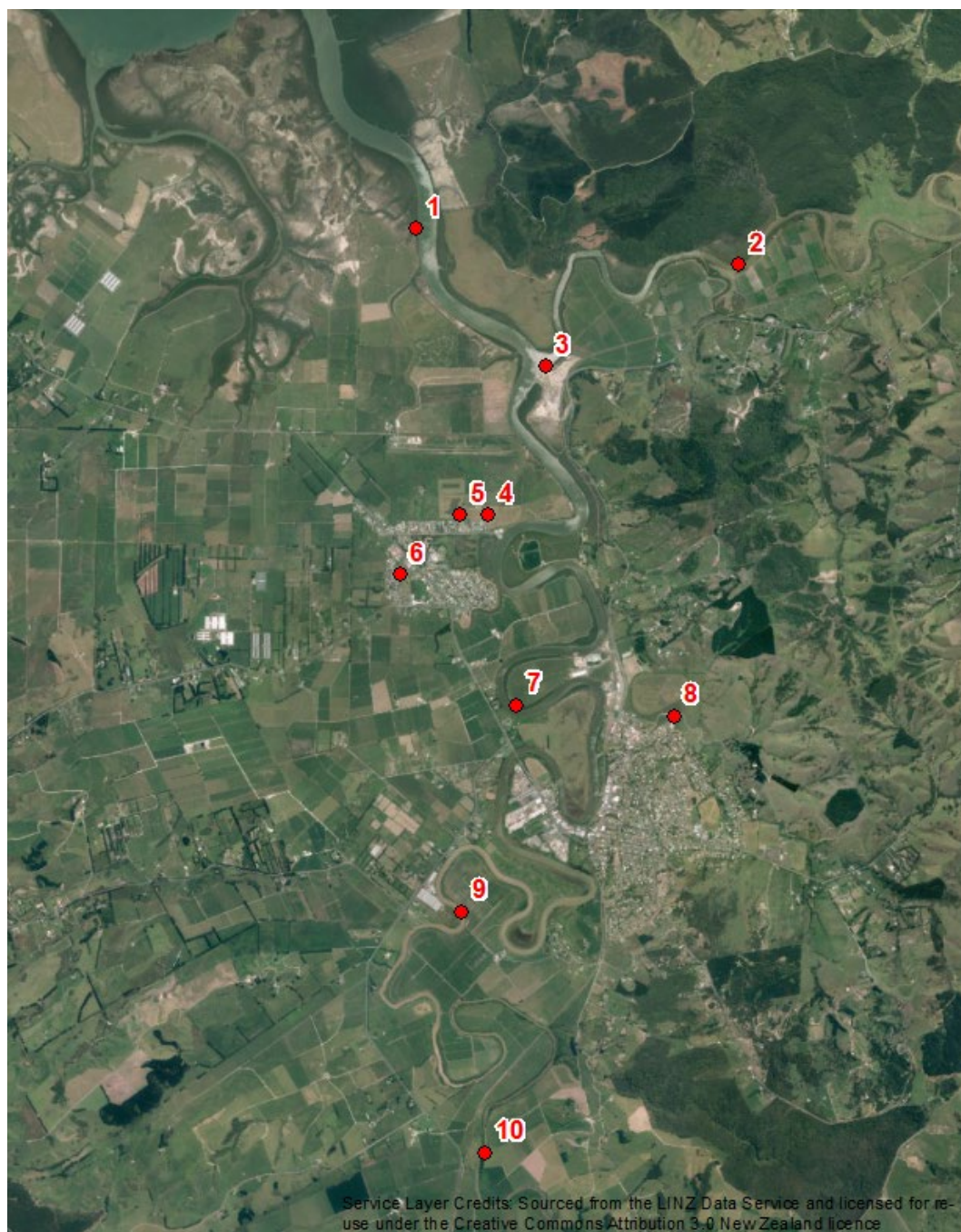


Figure 6-1 Locations where peak water levels for scenarios extracted.

Table 6-1 Predicted extreme water levels at selected locations (see Figure 6-1) for all scenarios. Water levels are relative to AVD-46.

| Site Number | Easting (NZTM) | Northing (NZTM) | Peak Water Level (m) | | | | | | | | | | |
|-------------|----------------|-----------------|----------------------|-------------|-------------|-------------------------|-----------------------|-----------------------|--------------|--------------------------|------------------------|------------------------|---------------------------------|
| | | | Scenario | | | | | | | | | | |
| | | | 5 Year ARI | 20 Year ARI | 50 Year ARI | 50 Year ARI + 0.5 m SLR | 50 Year ARI + 1 m SLR | 50 Year ARI + 2 m SLR | 100 Year ARI | 100 Year ARI + 0.5 m SLR | 100 Year ARI + 1 m SLR | 100 Year ARI + 2 m SLR | 50 Year ARI + 50 Year ARI Flood |
| 1 | 1728041 | 5944559 | 2.75 | 2.88 | 2.98 | 3.41 | 3.86 | 4.76 | 3.06 | 3.51 | 3.95 | 4.86 | 3.03 |
| 2 | 1730647 | 5944268 | 2.66 | 2.77 | 2.86 | 3.31 | 3.73 | 4.66 | 2.94 | 3.40 | 3.81 | 4.76 | 2.95 |
| 3 | 1729086 | 5943448 | 2.72 | 2.84 | 2.93 | 3.38 | 3.80 | 4.71 | 3.01 | 3.47 | 3.89 | 4.81 | 3.02 |
| 4 | 1728623 | 5942244 | 2.69 | 2.82 | 2.91 | 3.35 | 3.71 | 4.62 | 2.99 | 3.43 | 3.79 | 4.72 | 3.04 |
| 5 | 1728399 | 5942244 | 2.66 | 2.81 | 2.91 | 3.35 | 3.72 | 4.63 | 2.99 | 3.43 | 3.79 | 4.73 | 3.03 |
| 6 | 1727909 | 5941768 | N/A | N/A | N/A | 3.04 | 3.57 | 4.58 | N/A | 3.17 | 3.67 | 4.68 | N/A |
| 7 | 1728848 | 5940709 | 2.68 | 2.78 | 2.85 | 3.24 | 3.53 | 4.47 | 2.93 | 3.30 | 3.61 | 4.57 | 3.07 |
| 8 | 1730120 | 5940620 | 2.51 | 2.57 | 2.62 | 2.97 | 3.52 | 4.48 | 2.64 | 3.09 | 3.6 | 4.58 | 2.85 |
| 9 | 1728412 | 5939042 | 2.28 | 2.48 | 2.61 | 2.94 | 3.34 | 4.33 | 2.69 | 2.97 | 3.42 | 4.43 | 3.10 |
| 10 | 1728597 | 5937098 | N/A | N/A | N/A | 2.59 | 3.11 | 4.29 | N/A | 2.65 | 3.21 | 4.40 | 2.98 |

* N/A – no inundation

The difference between the maximum water level for the 50 year ARI coastal storm surge with and without the 50 year ARI flood flow in the Kaipara River is presented in Figure 6-2.

While the sea level inundation within the southern Kaipara Harbour is not impacted by the elevated river flow as suggested by previous work (DHI, 2006), there is actually an increase in water levels for the Parakai/Helensville floodplain of up to approximately 0.4 m, while there are even larger increases in water level further upstream. This indicates that the role of river floods coinciding with coastal storm surge needs to be considered further in future work. However it can be concluded that normal river flows will not have a significant impact on water levels from inundation of the floodplain from coastal storm surge.

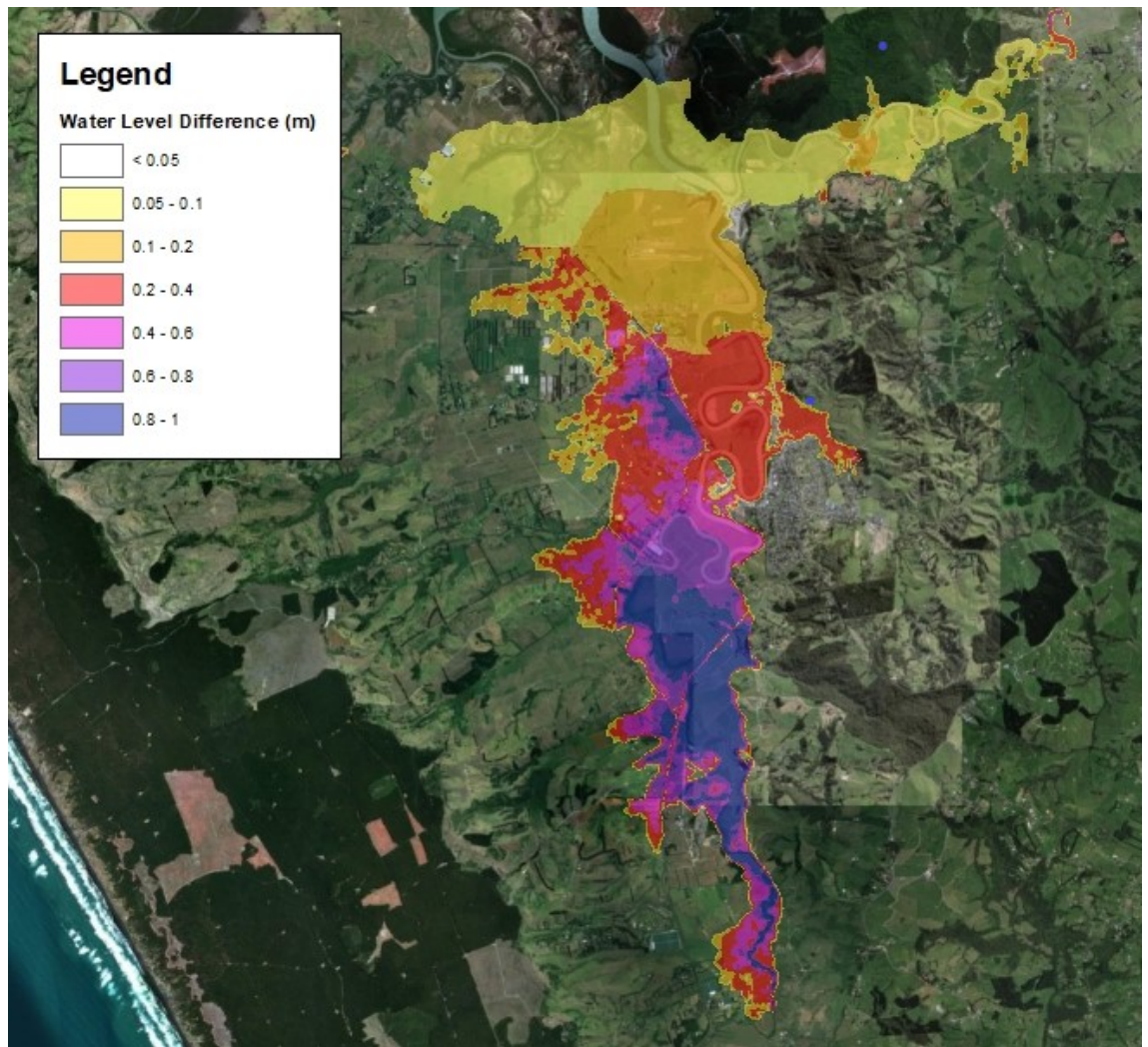


Figure 6-2 Maximum water level difference for the 50 year ARI coastal storm surge event with and without the 50 year ARI flood flow in the Kaipara River.

7 Summary

DHI were commissioned by Auckland Council to provide predictions of coastal inundation water levels for a number of coastal storm surge scenarios. NIWA have undertaken an extreme sea-level analysis at Helensville to determine the probability of extreme sea-level elevations, while DHI have simulated the flood inundation of the Parakai/Helensville floodplain associated with these coastal storm surge levels using a hydrodynamic model.

DHI utilised an existing hydrodynamic model of the southern Kaipara Harbour and Parakai/Helensville floodplain, however it was updated with 2016 LiDAR data.

The hydrodynamic model was calibrated against observed water levels at the Helensville tide gauge for a significant storm-tide event that occurred in September 2005. The model was then validated for an event that occurred in June 2012. A good agreement was obtained between observed and predicted water levels at Helensville for both the calibration and validation events, therefore the model was deemed suitable for predicting coastal inundation of the Parakai/Helensville floodplain.

Simulations were undertaken with the calibrated model to assess peak flood inundation levels due to coastal storm surge for the following scenarios:

1. 5 year ARI;
2. 20 year ARI;
3. 50 year ARI;
4. 50 year ARI with +0.5 m sea level rise included;
5. 50 year ARI with +1 m sea level rise included;
6. 50 year ARI with +2 m sea level rise included;
7. 100 year ARI;
8. 100 year ARI with +0.5 m sea level rise included; and
9. 100 year ARI with +1 m sea level rise included; and
10. 100 year ARI with +2 m sea level rise included.

Rasters of the maximum water level and water depth for the Parakai/Helensville floodplain have been provided for these scenarios. The coastal inundation extents are being mapped by Stantec and will be provided on Auckland Councils online geodatabase 'Geomaps'.

When comparing the 50 year ARI coastal storm surge scenario with and without 50 year ARI flood event in Kaipara River, an increase in water levels for the Parakai/Helensville floodplain of up to approximately 0.4 m was predicted to occur. There are even larger increases in water level further upstream.

8 References

DHI (2006). *Determination of Water levels in Kaipara Harbour, Kaipara Harbour Hydrodynamic Modelling*. Report prepared for Rodney District Council. DHI ref. 50044. August 2006.

DHI (2009). *Helensville Wastewater Treatment Plant Dilution Modelling*. Report prepared for Rodney District Council. DHI ref 50107. April 2009.

DHI (2014). *Rough Order Assessment of Inclusion of Floodplain Storage Volumes on Predicted Extreme Water Levels at Parakai*. Technical Memo prepared for Auckland Council. December 2014.

NIWA (2013). *Coastal Inundation by storm-tides and waves in the Auckland region*. Report prepared for Auckland Council. NIWA ref. HAM2013-059. September 2013.

NIWA (2016). *Coastal-storm inundation in the Auckland Region – supplementary information*. Report prepared for Auckland Council. NIWA ref. HAM2016-015. March 2016.

NIWA and DHI (2016). *Coastal inundation by storm-tides and waves in the Auckland region*. Prepared by the National Institute for Water and Atmospheric Research, NIWA and DHI Ltd for Auckland Council. Auckland Council technical report, TR2016/017.

NIWA (2018). *Joint probability analysis of rainfall and sea level records in Auckland*. NIWA, Hamilton.